Developmentally regulated proteolysis of cytoplasmic polyA polymerase GLD-2

Dissertation
zur Erlangung des
Doktorgrades der Naturwissenschaften (Dr. rer. nat.)

der

Naturwissenschaftlichen Fakultät I – Biowissenschaften –

der Martin-Luther-Universität
Halle-Wittenberg,

vorgelegt

von
Herrn Oyewale, Tosin

geb. am 12.08.1987 in Odeomu, Nigeria

Gutachter:

1. Prof. Dr. Christian R. Eckmann

2. Prof. Dr. Stefan Hüttelmaier

3. PD Dr. Roland Dosch

Tag der Verteidigung: March 8th, 2021

Summary

During an initial phase of transcriptional repression, embryonic germ cell development primarily depends on maternally donated RNA-regulatory proteins and their mRNA targets. However, to put the zygotic genome in charge, these maternal germline-intrinsic factors must be eventually terminated. While numerous works have addressed how the expression of mRNA regulators is controlled during post-embryonic germ cell development, little is known about how their expression is terminated in embryonic primordial germ cells (PGCs). In studying the developmental regulation of the cytoplasmic polyA polymerase, GLD-2, a prime example of a maternally donated mRNA regulator whose expression ceases upon birth of both PGCs in *C. elegans*, this work found that the proteasome regulates the turnover of GLD-2 cytoPAP in PGCs. Moreover, it identified GRIF-1, a TRIM32-related putative ring finger domain-containing ubiquitin ligase as a GLD-2 turnover factor in PGCs. Importantly, upon compromising *grif-1's* functions by RNAi or CRISPR-induced loss-of-function mutations, these embryos produced animals with a mortal germline phenotype: despite maintaining their identity and proliferative capacity across a few generations, germ cells eventually lose their proliferating capacity and undergo cell death during postembryonic development. Furthermore, this work revealed a Nanos-based pathway which act redundantly with GRIF-1 to ensure turnover of maternal transcripts in PGCs and postembryonic survival of germ cells. GRIF-1 indirectly promotes maternal transcript clearance by promoting GLD-2 turnover in a highly developmentally regulated manner. Together, the collected data describe molecular pathways and mechanisms via which regulated protein turnover of GLD-2 cytoPAP promotes maternal-to-zygotic transition in PGCs.

Zusammenfassung

Während der initialen Phase der transkriptionellen Repression in der Embryogenese hängt die Entwicklung der embryonalen Keimzellen hauptsächlich von maternalen RNA-regulatorischen Proteinen und den von diesen regulierten mRNAs ab. Wird die transkriptionelle Aktivität durch das zygotische Genom übernommen, müssen diese maternalen intrinsischen Faktoren in den Keimzellen letztendlich terminiert werden.

Während eine Vielzahl von Arbeiten sich damit beschäftigten, wie die Expression von mRNA- Regulatoren während der Entwicklung der postembryonalen Keimzellen kontrolliert wird, ist nur wenig darüber bekannt, wie deren Expression in embryonalen primordialen Keimzellen (primordial germ cells, PGCs) terminiert wird. Durch die Analyse der entwicklungsabhängigen Regulation der zytoplasmatischen PolyA–Polymerase (cytoPAP) GLD-2 als grundlegendes Beispiel für einen maternalen mRNA-Regulator, dessen Expression nach der Etablierung der beiden PGCs in *C. elegans* endet, wurde in dieser Arbeit herausgefunden, dass das Proteasom den Proteinumsatz (Turnover) der GLD-2 cytoPAP in primordialen Keimzellen reguliert. Mit GRIF-1, einer mit der E3 Ubiquitin-Proteinligase TRIM32 verwandten, putativen RING-Finger Domänbesitzenden Ubiquitin-Ligase wurde ein Faktor identifiziert, welcher als Regulator für den GLD-2 Turnover in PGCs fungiert. Dabei ist es bedeutend, dass nach einer Funktionsstörung von *grif-1,* resultierend aus RNAi oder mittels CRISPR induzierten Loss-of-Function Mutationen, aus den Embryos Tiere mit einem *„mortal"* Keimzellenphänotyp entstehen: Trotz der Aufrechterhaltung ihrer Identität und der Proliferationsfähigkeit über einige Generationen verlieren die Keimzellen schließlich ihre Proliferationsfähigkeit und unterliegen dem Zelltod während der postembryonalen Entwicklung. Weiterhin wurde in dieser Arbeit ein Nanos-abhängiger Regulationsweg aufgedeckt, welcher redundant mit GRIF-1 funktioniert und ein Turnover maternaler Transkripte in primordialen Keimzellen sowie das postembryonale Überleben von Keimzellen gewährleistet. GRIF-1 begünstigt entwicklungs-abhängig indirekt die Entfernung maternaler Transkripte durch die Förderung des Turnovers von GLD-2. Zusammenfassend beschreiben die erhaltenen Daten molekulare Mechanismen und Reaktionswege, durch welche der regulierte Turnover der cytoPAP GLD-2 den maternal-zygotischen Übergang (MZT) in primordialen Keimzellen fördert.

Table of Contents

1. Abbreviations

aa:	amino acid
APS:	Ammonium persulfate
bp:	base pairs
BSA:	Bovine serum albumin
cDNA:	Complementary deoxyribonucleic acid
CPB/CPEB:	Cytoplasmic polyadenylation element-binding protein
CRISPR:	Clusters of regularly interspaced short palindromic repeats
crRNA:	CRISPR RNA
CTD:	C-terminal domain
Cy3:	Cyanine 3
cytoPAP:	Cytoplasmic polyA polymerase
DAPI:	4',6-diamidino-2-phenylindole
DNA:	Deoxyribonucleic acid
DTC:	Distal tip cell
DUB:	De-ubiquitinating enzyme (De-ubiquitinase)
E1:	Ubiquitin-activating enzyme
E2:	Ubiquitin-conjugating enzyme
E3:	Ubiquitin ligase
eIF:	Eukaryotic translation initiation factor
FBF:	*fem*-3-binding factor
GFP:	Green fluorescent protein
GLD:	Germline development defective
GLS:	Germline survival defective
gp:	Guinea pig
gt:	Goat
GTP:	Guanosine-5'-triphosphate
H3:	Histone H3
H3K27me3:	Tri-methylated lysine 27 of histone H3
H3K4me:	Methylated lysine 4 of histone H3
H3K4me2:	Di-methylated lysine 4 of histone H3
H3K4me3:	Tri-methylated lysine 4 of histone H3
H4:	Histone H4
H4K8ac:	Acetylated lysine 8 of histone H4
HA:	Hemagglutinin
HDR:	Homology-directed repair
HECT:	Homology to E6-associated protein C terminus

HEPES:	4-(2-hydroxyethyl)-1-piperazineethanesulfonic acid
hr(s):	Hour(s)
IDP:	Intrinsically disordered protein
IDR:	Intrinsically disordered region
IP:	Immunoprecipitation
KH:	K homology
LAP tag:	Localization and affinity purification tag
LB:	Lysogeny broth
mA:	Milliampere
MAPK:	Mitogen-activated protein kinase
MD transcripts:	Maternal degradation transcripts
MES:	Maternal effect sterile
min(s):	Minute(s)
ml:	Milliliter
mo:	Mouse
MosSCI:	Mos1-mediated single copy insertion
MR:	Mitotic region
mRNA:	messenger RNA
Mrt:	Mortal germline
MZT:	Maternal-to-zygotic transition
NaOAC:	Sodium acetate
NC:	Nitrocellulose
NGM:	Nematode growth medium
NHEJ:	Non-homologous end joining
ORF:	Open reading frame
PAA:	Polyacrylamide
PABP:	PolyA binding protein
PAGE:	Polyacrylamide gel electrophoresis
PAP:	PolyA polymerase
PCI:	Phenol: Chloroform: Isopropanol
PCR:	Polymerase chain reaction
PFA:	Paraformaldehyde
PGC:	Primordial germ cell
PIC:	Pre-initiation complex
piRNA:	Piwi-interacting RNA
PMSF:	Phenylmethylsulphonyl fluoride
PRC2:	Polycomb repressive complex 2

pSer2:	Phosphorylated serine 2
pSer5:	Phosphorylated serine 5
PUF:	Pumilio and FBF
PUP:	PolyU polymerase
PVDF:	Polyvinylidene difluoride
PZ:	Proliferative zone
rb:	Rabbit
RBP:	RNA-binding protein
RFP:	Red fluorescent protein
RNA:	Ribonucleic acid
RNAi:	RNA interference
RNP:	Ribonucleoprotein
rpm:	Revolution per minutes
rt:	Rat
RT:	Reverse transcription
S:	Svedberg, sedimentation unit
SD:	Standard deviation
SDS:	Sodium dodecyl sulfate
SEM:	Standard error of the mean
SGP:	Somatic gonad primordium
siRNA:	Small interfering RNA
SRS:	Substrate recognition subunit
ss:	Single stranded
TBE:	Tris-borate-EDTA buffer
TCA:	Trichloroacetic acid
TEMED:	N,N,N',N' Tetramethylethylenediamine
TF:	Transcription factor
TRIM:	Tripartite motif-containing protein
tRNA:	Transfer RNA
TUT/TUTase:	Terminal uridyl transferase
TZ:	Transition zone
Ub:	Ubiquitin
UBC:	Ubiquitin-conjugating enzyme
UPS:	Ubiquitin proteasome system
UTR:	Untranslated region
V:	Voltage
WT:	Wild type

Y2H: Yeast 2-hybrid

ZGA: Zygotic genome activation

β-gal: β-galactosidase

μl: Microliter

2. Introduction

Germ cells are the indispensable link that ensures survival and continuity of sexually reproducing species, from one generation to the next. Additional to this, they also provide the platform to generate and transmit heritable adaptive changes that leads to evolution of species (Lehmann 2012, Lesch and Page 2012). To carry out their functions, germ cells undergo a series of conserved,- as well as species-specific-, biological, genetic, and molecular changes across development. These tasks, which are required from one generation to the next, are broadly categorised into four groups as observed in classical model animals studied to date. The first task is the specification of germ cell fate. The second is maintenance of already specified germ cell fate. The third task is initiation of gametogenesis (meiotic division and differentiation program) that is coupled to sex determination. The fourth task is preparation of already formed gametes to support embryonic events after fertilization (Lesch and Page 2012).

Almost all molecular processes carried out throughout germ cell development are regulated at the posttranscriptional level through the activities of RNA regulators. Since posttranscriptional regulation is pivotal to germ cell development, the activities, abundance and spatiotemporal expression of many RNA regulators are tightly and developmentally regulated to execute proper germ cell development. While several studies have contributed to our understanding of the importance of RNA regulators during postembryonic development (Dahanukar, Walker et al. 1999, Eckmann, Crittenden et al. 2004, Hansen, Wilson-Berry et al. 2004, Kadyrova, Habara et al. 2007, Lai, Singh et al. 2012, Kim, Ha et al. 2015, Kisielnicka, Minasaki et al. 2018), very little is known about how the spatiotemporal expression of RNA regulators is regulated during embryonic germ cell development. Specifically, how is the expression of maternally donated RNA regulatory proteins controlled during embryonic germ cell development? Additionally, how do their developmentally controlled regulation assist germ cell development?

This thesis addressed the problems of how maternal donated RNA regulators and their associated mRNAs are controlled during *C. elegans* primordial germ cell development. Therefore, this introduction aims at giving broad and universal insights into (i) gene expression mechanisms regulating protein abundance, (ii) primordial germ cell (PGC) fate specification and maintenance, (iii) post embryonic germ cell development, and (iv) the maternal to zygotic transition (MZT). Whereas the introduction gives universal insights with examples from several model systems, more focus is placed on *C. elegans* as a model system.

2.1. Regulation of protein abundance and spatiotemporal expression

Multicellular animals build complexity by organising cells into complex structures that perform unique functions. Interestingly, these unique functions are achieved by different cell types despite the fact that all cells within an animal essentially have identical genomic material. For example, brain is made up of neurons capable of transmitting information, while germline is made up of germ cells generating gametes. To achieve these differences, a tight regulation of genetic information dictates cellular output, in terms of protein identity and quantity produced per time, causing even neighbouring cells to carry out distinct activities and tasks. These gene expression regulations are essential for the formation of complexity in multicellular organisms. Protein abundance and spatiotemporal expression is regulated at two major levels; protein synthesis and protein degradation.

2.1.1. Regulation of protein abundance through protein synthesis

The synthesis of cellular proteins involves two major steps: (i) transcription- to produce mRNAs from information stored in the genome, and (ii) translation- to covert the information in mRNAs into proteins. Both steps are spatially separated in eukaryotic cells. Transcription occurs in the nucleus and contributes significantly to the abundance of mRNAs available for translation per time. Translation occurs in the cytoplasm and dictates the abundance of proteins produced per time in the cell (Alberts 2008). Therefore, tight regulation of both transcription and translation is essential for controlling protein synthesis and abundance across development.

2.1.1.1. mRNA, from nucleus to the cytoplasm

Nascent pre-mRNA undergoes several processing and modifications, in part, already initiated during transcription to generate a stable and mature messenger RNA (mRNA) that is capable of serving as template for translation in the cytoplasm (see Figure 2.1.1.1). These includes in the nucleus: splicing, addition of 7-methylguanosine cap to the 5'end and addition of polyA tail to the 3'UTR of the newly synthesized mRNA. The 5' cap and the polyA tail have been demonstrated to be beneficial for many aspects during the lifetime of mRNAs, including export, stability, and translation. Upon export into the cytoplasm, essentially all features of mRNAs can be explored to regulate the translation of mRNAs into proteins.
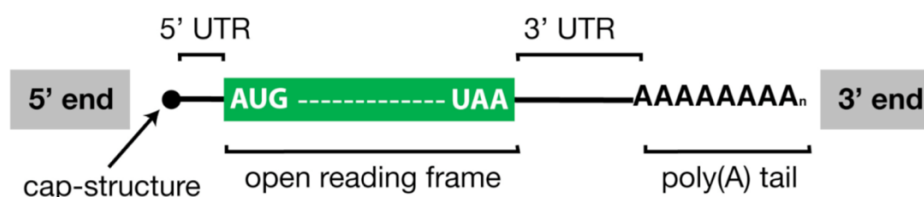
Figure 2.1.1.1. The basic structure of mRNA.

2.1.1.2. Translation and translational regulation

2

mRNAs do not exist as linear naked molecules and a protein coat may force it into a closed-loop structure (see Figure 2.1.1.2). Depending on regulatory state, mRNAs are decorated by RNA-binding proteins (RBPs) to control their stability and localization or when being translated, they are decorated by ribosomes, which are ribonucleoprotein (RNP) structures that are critical for interpretation of mRNA encoded messages (Vicens, Kieft et al. 2018). The 5'cap is bound by the cytoplasmic cap-binding protein, eukaryotic translation initiation factor 4E (eIF4E), which replaces the nuclear cap-binding complex immediately after the first round of translation. In a similar manner, nuclear polyA-binding protein (PABPN) bound to the polyA tail of mRNA is replaced in the cytosol by cytoplasmic polyA-binding protein (PABPC). To achieve a closed-loop structure, the polyA tail comes in proximity with the cap structure in an indirect interaction between PABPC and eIF4E that is mediated by another protein; eukaryotic initiation factor 4G (eIF4G). The formation of this closed-loop structure has been proposed to be important for recruitment of ribosome to mRNA and enhancement of translational efficiency, although, there is emerging body of knowledge challenging this canonical model and suggests that closed-loop enhanced translation may not be universal (reviewed in Vicens, Kieft et al. 2018).
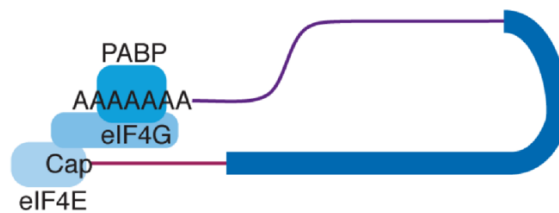
Figure 2.1.1.2. The closed loop structure of mRNA
Image taken and modified from Vicen, Kieft et al. 2018

2.1.1.3. The polyA tail

The polyA tail is one of the features of mRNA that contributes significantly to regulation of a mRNA stability and translatability. PolyA tail length fluctuates throughout mRNA life and as such polyA tail is dynamic. It is originally added in the nucleus by the nuclear polyA polymerase. In the cytoplasm, the polyA tail is subject to additional regulation; de-adenylation and re-adenylation.

PolyA tail trimming is carried out by a class of enzymes known as deadenylases. Trimming often corelates with translational repression and at a critical length, it correlates with mRNA decay. In fact, polyA tail shortening has been proposed to be the rate-limiting step during mRNA decay, which subsequently trigger both 5' to 3' and 3' to 5' degradation of mRNA (Decker and Parker 1993). Several conserved deadenylases exist in eukaryotic cells, although they may display both conserved and distinct functions while regulating aspects of development in different organisms (Goldstrohm and Wickens 2008, Nousch, Techritz et al.

2013). The main deadenylase that removes polyA tail of bulk mRNAs in eukaryotic cells is the CCR4-Not deadenylase complex, consisting of several subunits of distinct functions. NOT-1 (NTL-1 in *C. elegans*) is a scaffolding subunit that interacts with other complex members. Besides this, it also provides docking site for several RBPs. CAF-1 (CCF-1 in *C. elegans*) and CCR4 (also CCR-4 in *C. elegans*) are the subunits that provide catalytic activities to the complex (Goldstrohm and Wickens 2008, Nousch, Techritz et al. 2013).

Intriguingly, to prevent deadenylation-induced repression and mRNA turnover, the length of polyA tail can be re-extended in the cytoplasm by a unique class of enzymes known as cytoplasmic polyA polymerase (cytoPAP) (Eckmann, Rammelt et al. 2011). Since a long polyA tail often correlates, especially in neurons, germ cells, and early embryos, with increased stability and translatability, cytoPAPs positively promote the expression of target mRNAs (see Eckmann, Rammelt et al. 2011 for review).

2.1.1.4. The GLD-2/GLD-3 complex, a paradigm for cytoPAPs

C. elegans GLD-2 (*ce*GLD-2) was the first cytoPAP to be identified (Wang, Eckmann et al. 2002). Since then, paralogues and orthologues have been described in worms and other organisms, respectively. CytoPAPs function in different biological contexts including germ cell development and neuronal function (Wang, Eckmann et al. 2002, Kwak, Drier et al. 2008, Schmid 2008, Sartain, Cui et al. 2011). Unlike the nuclear polyA polymerase, cytoPAPs do not possess any obvious RNA recognition-motif (RRM) that could promote their association with target mRNAs. Consequently, they are envisioned to be recruited to mRNA via interactions with RBPs. Furthermore, as the name implies, cytoPAPs are broadly expressed in the cytoplasm where they promote the expression of target mRNAs. Since cytoPAP are often abundantly distributed, stage-specific association with RBPs might serve a regulatory function to focus their polyadenylation activity to a subset of transcripts at every stage of development (Suh, Jedamzik et al. 2006, Schmid, Kuchler et al. 2009, Nousch, Minasaki et al. 2017).

The domain structure of GLD-2 protein is pivotal to its enzymatic activity. GLD-2 protein belongs to the DNA polymerase beta-like nucleotidyltransferase superfamily. Therefore, GLD-2 has a nucleotidyltransferase domain that is embedded in a larger central domain which forms the catalytic core of GLD-2 cytoPAP (see Figure 2.1.1.4). GLD-2 has an intrinsically disordered region (IDR) in its N-terminal end and while the central domain of GLD-2 is directly involved in polyadenylation activities, the functions of the IDR remains unexplored. GLD-2 IDR and the C-terminal end, which has no identifiable domain, are envisioned to be the interaction surface for either regulatory proteins that may modulate the expression and the activities of GLD-2 cytoPAP or RBPs that may recruit GLD-2 to mRNAs in the cytoplasm. Both possibilities are not mutually exclusive.
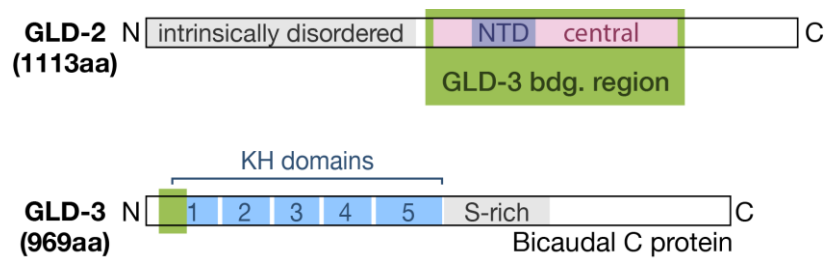
Figure 2.1.1.4. GLD-3 binds and stabilizes the catalytic core of GLD-2.

Linear structure and interaction surfaces of GLD-2 and GLD-3 proteins. GLD-2 contains a Nucleotidyltransferase domain important for polyA tail extension and a N-terminal intrinsically disordered domain. GLD-3 is multi-KH Bicaudal-C homologue. GLD-3 N terminal domain, in green, interacts with the catalytic core of GLD-2.

The *ce*GLD-2 cytoplasmic polyA polymerase is a heterodimeric complex containing two conserved proteins; GLD-2 and GLD-3. They are broadly expressed in the cytosol and localize to germ granules during germline development (Eckmann, Kraemer et al. 2002, Wang, Eckmann et al. 2002). In isolation, either the central domain of GLD-2 or full-length GLD-2 protein has a poor polyA tail extension activities (Nakel, Bonneau et al. 2015). To activate polyadenylation activity, GLD-3, a multi-KH domain-containing protein, interacts with GLD-2 central domain and stabilize its three-dimensional fold thereby significantly improving its catalytic activity. GLD-3 also contribute some positive amino acids into the catalytic cleft of GLD-2 which may stabilize the GLD-2-polyA tail interaction during catalysis (Nakel, Bonneau et al. 2015). Together, GLD-2 and GLD-3 make a functional cytoPAP. Similar to GLD-2 other cytoPAP may rely on other proteins that may act as cofactors to stimulate activity or to provide RNA recognition platforms.

2.1.2. Regulation of protein abundance through protein degradation

In addition to tight regulation of protein synthesis, protein degradation contributes immensely to shaping the abundance and spatiotemporal expression of proteins across development (Hochstrasser 1995, Papaevgeniou and Chondrogianni 2014). This is underscored by many developmental defects and diseases that arise from either mutations that affect protein degradation pathways or mutations that leads to mis-expression of cellular proteins (Extensively reviewed by Hanna, Guerra-Moreno et al. 2019). A good example here is the degradation defect of beta-Catenin, which is an oncoprotein whose levels is constantly kept low by protein degradation. Defects in beta-Catenin degradation cause accumulation and subsequent translocation of beta-Catenin into the nucleus, thereby causing malignant and benign neoplasms through its activity as a transcription factor (Kinzler, Nilbert et al. 1991, Munemitsu, Albert et al. 1995, Sparks, Morin et al. 1998).

Besides its importance for developmental control of protein amounts, protein degradation is also crucial for maintenance of protein quality within every cell, removing

damaged and misfolded proteins. In fact many neurodegenerative diseases are a result of accumulation of undegraded misfolded proteins (Hipp, Park et al. 2014, Labbadia and Morimoto 2015, Hanna, Guerra-Moreno et al. 2019). An unregulated and hyperactive degradation pathway could similarly affect both regulated protein degradation and protein quality control leading to developmental defects and pathologies. For example, excessive degradation of tumor-suppressing protein may lead to cancer and in the same vein, excessive removal of slightly misfolded but otherwise functional protein may be detrimental to development. A single point mutation in cystic fibrosis transmembrane conductance regulator (CFTR), which is a chloride ion channel, slightly affects its folding and delivery to the cell surface due to excessive degradation. Interestingly, cystic fibrosis, a disease caused by this mutation, is treated by drugs that reduce degradation, leading to delivery of the mutated CFTR to the membrane where it is able to perform its functions albeit at a rate slightly lower than wild-type protein (Ward, Omura et al. 1995). Altogether, protein degradation pathways are indispensable to functionality of cellular and developmental systems and therefore, their activities must be tightly regulated for the best output.

To prevent protein misexpression and accumulation of damaged and misfolded proteins, cells have a host of pathways to degrade proteins in a specific manner. The two major protein degradation systems known in cells are lysosomal-mediated degradation and the ubiquitin proteasome systems (UPS) (Papaevgeniou and Chondrogianni 2014). Lysosomes are membrane-bound spherical vesicles and organelles that contain hydrolytic enzymes employed for bulk protein degradation. To achieve lysosomal degradation, autophagosomes internalize cellular proteins and fuse with a lysosome to degrade their content. Initially, autophagy, a process by which autophagosomes are formed, was thought to degrade protein in a nonspecific manner, however, more evidences have been emerging to demonstrate that autophagy is a highly regulated process and that proteins are selectively targeted to autophagosome in a highly specific and regulated manner. During *C. elegans* embryogenesis for example, germ granule-associated components are selectively and specifically degraded by autophagy in somatic cells through their interaction with SEPA-1, a component of autophagy pathway in *C. elegans* (Zhang, Yan et al. 2009, Kaushik and Cuervo 2012). In contrast to autophagy whose regulation we are just beginning to understand, the UPS has been studied extensively in several model systems.

2.1.2.1. The ubiquitin proteasome system and ubiquitination

The proteasome is a multi-subunit protein complex that degrades most of cellular proteins (Papaevgeniou and Chondrogianni 2014). Similar to lysosomal degradation, the proteasome has both regulatory and quality control functions. A target protein to be degraded is covalently modified with ubiquitin, which is subsequently recognized by the proteasome as

a mark for degradation. Therefore, this molecular pathway of degradation is termed the Ubiquitin-Proteasome System (UPS). It is often difficult to reveal proteasome functions due to its far-reaching degradative capacity to remove many proteins, whose turnover is critical for cellular functions, at every particular stage. Therefore, when analyzing mutants of proteasome factors, late functions are often masked by earlier ones and those late functions can only be revealed through systematic approaches: for example, by performing knockdown experiment at a particular stage of interest instead of analyzing mutants. Alternatively, when possible, chemical inhibitor such as MG132 can also be used to inhibit the proteasome (Orsborn, Li et al. 2007)

Although there seems to be some species-specific subtle differences, the proteasome is a huge protein complex, comprising of nearly 66 subunits and sedimentation constant of approximately 26S. Based on the arrangement of its subunits, it is made up of two major parts. The first part is a chamber-like core where proteolysis occurs, known as the 20S proteasome. The second part is made up of two equally sized 19S regulatory complexes that caps the chamber-like core at both ends (see Figure 2.1.2.1 for structure of 26S proteasome). These 19S proteasomes bind, unfold, and translocate ubiquitinated target substrate into the core chamber where it is degraded into small peptides, ranging from 3 to 30 amino acids. The small peptides are released into the cytosol and are cleaved further into amino acids by the activity of cytosolic endopeptidases (Kisselev, Akopian et al. 1998, Pickart and Cohen 2004, Saric, Graef et al. 2004).

The number of ubiquitin chain on target substrate required by proteasome for degradation may also vary. Most studies have suggested that for a target protein to be recognized and degraded by the 26S proteasome, the minimal length of attached ubiquitin chain should be 4, however, in some cases, mono-ubiquitinated target proteins are also accepted (Thrower, Hoffman et al. 2000, Shabek, Herman-Bachinsky et al. 2012). In fact, recent but still few data suggest that proteasome may even degrade protein targets, in exceptional cases, in a ubiquitin independent manner (Asher, Lotem et al. 2002, Asher, Tsvetkov et al. 2005, Tsvetkov, Reuven et al. 2010, Erales and Coffino 2014, Sanchez-Lanzas and Castano 2014). A common theme that seems to allow ubiquitin-independent degradations by the proteasome is the presence of one or several intrinsically disordered regions in target proteins and examples of proteins degraded in this manner include p53, p21, c-Jun and alpha-synuclein. For a detailed review, see Erales and Coffin 2014.
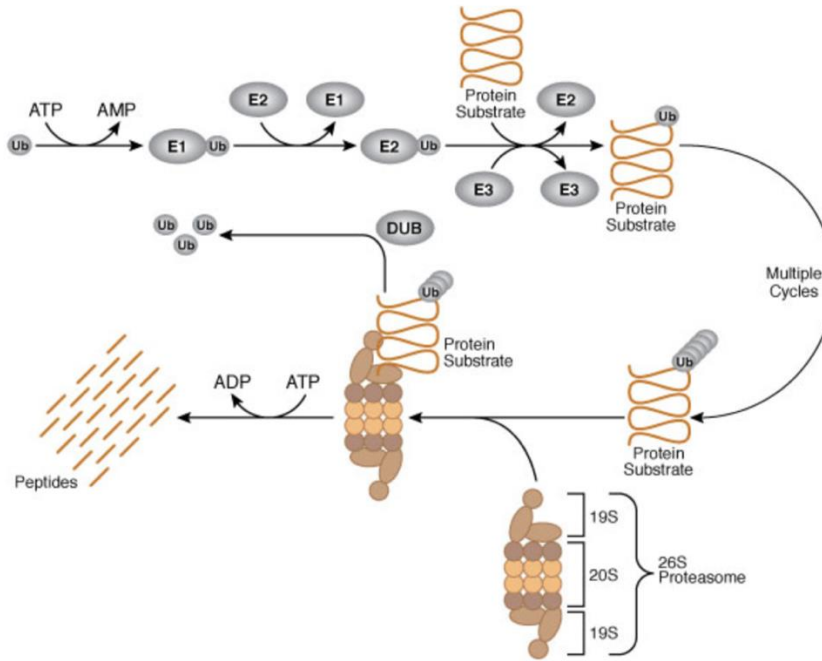
Figure 2.1.2.1. Ubiquitin Proteasome System (UPS): molecular mechanism of ubiquitination leading to protein degradation by the proteasome.

Cartoon depiction of ubiquitination reaction followed by protein degradation via the proteasome. Ubiquitination occurs in a sequence of reactions involving attachment of ubiquitin molecules to target protein by three main enzymes: E1, E2 and E3. Subsequently, ubiquitinated proteins are bound and degraded by the proteasome. Ub= ubiquitin. DUB= deubiquitinating enzymes (or deubiquitinases). See main text for explanation. Figure adapted from https://media.cellsignal.com/www/pdfs/science/pathways/Ubiquitin_Proteasome.pdf

Ubiquitin is a highly conserved polypeptide with 76 amino acids. For the attachment of the first ubiquitin moiety to a target protein, the COOH group of the C-terminal glycine of ubiquitin is covalently linked in an isopeptide bond to an amino group in the side chain of a lysine present in target protein. The covalent attachment of ubiquitin to a target protein occurs is a series of reactions by the concerted activities of three enzymes; ubiquitin-activating enzyme E1, ubiquitin-conjugating enzyme E2, and ubiquitin ligase E3 (or E3 ubiquitin ligase). To this end, the ubiquitin-activating enzyme E1 forms a thiolester bond with the C-terminal end of ubiquitin in an energy-dependent reaction that requires the hydrolysis of ATP. In the next step, the already activated ubiquitin forms another thiolester bond with ubiquitin-conjugating enzyme E2. The last enzyme, E3 ubiquitin ligase interacts with both E2 and the target substrate and facilitates the transfer of ubiquitin to the target substrate (see Figure 2.1.2.1). These steps are repeated multiple times to generate a polyubiquitin chain on a target protein. After the attachment of the first ubiquitin, subsequent ones are attached through an isopeptide bond formed between glycine 76 and lysine 48 (Gly-76-Lys-48 isopeptide bond). Although, lysine 48 linkage is the most predominant linkage for protein degradation through the UPS, other lysine linkages, such as lysine 6, 11, 27, and 29 linkages, have also been observed to trigger proteolysis through UPS. However, lysine 63

linkage does not induce protein degradation but instead works as part of signaling cascades to induce endocytosis, DNA repair, and translation (Pickart 1997, Thrower, Hoffman et al. 2000, Alberts 2008). In exceptional cases in which E2 and E3 enzymes are inefficient in generating a long poly-ubiquitin chain, ubiquitin assembly factor E4 may be used to considerably extend the ubiquitin chain seeded by the E2-E3 complex (Koegl, Hoppe et al. 1999).

2.1.2.2. E3 ubiquitin ligases

E3 ligases are the enzymes that bring specificity to protein degradation through UPS. In *C. elegans,* just one E1 enzyme and twenty-two E2 enzymes are encoded in its genome. By contrast, there are over 150 E3 ligases (Jones, Crowe et al. 2002). This type of distribution is not peculiar to *C. elegans* but seems to be rather the norm than exception in eukaryotic cells. For instance, the human genome also encodes just two E1 enzymes, approximately thirty E2 enzymes, and over 600 E3 ligases (Komander 2009, Berndsen and Wolberger 2014, Weber, Polo et al. 2019). As a vast majority of cellular proteins are degraded through the UPS, the high number of E3 reflects their function to specifically select many cellular proteins for degradation. In this selection system, a single protein may be recognized by one or multiple E3 ligases at any developmental stage and conversely, a single E3 ligase may recognize one or multiple proteins at any developmental stage. Regardless, E3 ligases bring specificity to the UPS.

There exist two major class of E3 ligases: Homologous to the E6-AP carboxyl terminus (HECT) domain-containing and Really interesting gene (RING) domain-containing E3 ligases. This classification is primarily based on how they facilitate ubiquitin transfer from E2 to target protein and sequence similarities. As the name implies, HECT domain E3 ligases contain a catalytic HECT domain, which is often located in their C-terminal end. Based on the composition and organization of additional domains, HECT domain ligases can be further divided into different sub families. In any case, all HECT ligases invariably interact with E2 and (Ying, Huang et al. 2011) form a thiolester bond with ubiquitin before subsequently transferring the ubiquitin to target proteins (Verdecia, Joazeiro et al. 2003, Passmore and Barford 2004), recently reviewed in Weber, Pol et al. 2019. By contrast, RING domain E3 ligases do not form any thiolester bond with ubiquitin. Instead, they interact with both E2 and target substrate and facilitate a direct transfer of ubiquitin from E2 to target protein (Metzger, Pruneda et al. 2014). Depending on the number of proteins required for their E3 ligase activities, RING domain E3 ligases are further classified into single subunit (monomeric) or multi subunit (multimeric) RING domain E3 ligases (Metzger, Hristova et al. 2012, Metzger, Pruneda et al. 2014).

2.1.2.3. Single subunit RING domain E3 ligases

The RING domain is a zinc finger fold of about 40 to 60 amino acids that coordinates two zinc ions primarily by the interactions between key cysteine and histidine amino acids (Ying, Huang et al. 2011). Like for most zinc finger domains, a RING finger domain was originally thought to be primarily important for DNA binding, however, accumulated data over the years have shown a RING domain to adopt a unique fold that is atypical of canonical zinc finger domains, mediating protein-proteins interaction instead. While a few RING domain-containing proteins may perform other specialized activities, most act as E3 ubiquitin ligases. Single subunit RING domain E3 ligases are capable of protein ubiquitination as a single protein. This is in contrast to many multi-subunit or multimeric RING domain ligases, which require one or two RING domain-containing proteins to act as adaptors to recognize target proteins as part of a relatively large ligase complex (reviewed in Metzger, Pruneda et al. 2014).

Many of the single subunit RING domain E3 ligases belong to the conserved superfamily of Tripartite motif-containing (TRIM) proteins. As the name implies, TRIM proteins are identified based on the invariant presence of three domains: a N-terminal RING domain, followed by one or two B Box domains (a B Box domain is also a zinc finger domain) which is followed by a coiled coil domain. These three domains are together referred to as the RBCC motif (or domain) and they have been implicated in ubiquitin ligase activity of many TRIM proteins with the RING domain being the major domain that confers ubiquitin ligase activities (see Ozato, Shin et al. 2008, Hatakeyama 2017, and van Gent, Sparrer et al. 2018 for review on TRIMs, their structure and biological functions).

In majority of TRIM proteins, one or more domains which are unique to each TRIM protein subfamily are located C-terminally of the RBCC domain where they either support the ubiquitination activity of the RBCC of TRIM protein or are involved in a completely different molecular activity (see Figure 2.1.2.3 for domain organization of TRIM proteins). For example, the C-terminal SPRY domain of TRIM25 subfamily mediates an interaction with its ubiquitination substrate, while the C-terminal end of the TRIM32 subfamily has several NHL (NCL-1, HT2A and LIN-41) repeats that bind Argonaute (Ago-1). As demonstrated in several organism including human, mouse and fruit fly, the binding of NHL domain of TRIM32 influences *let-7* microRNA levels, independently of TRIM32 ubiquitination activities, which in turn regulate the levels of *let-7* mRNA targets. Therefore, TRIM32 regulates gene expression through its RBCC-driven ubiquitin ligase activity, which promotes the turnover of many target proteins. This includes but is not limited to c-Myc, ABI2, Actin, Dysbindin and Piasy. At the same time TRIM32 regulates microRNA activities independently of its E3 ligase activity

through its NHL repeats (Kudryashova, Kudryashov et al. 2005, Gack, Shin et al. 2007, Kano, Miyajima et al. 2008, Ozato, Shin et al. 2008, Locke, Tinsley et al. 2009, Schwamborn, Berezikov et al. 2009, Borlepawar, Rangrez et al. 2017, Hatakeyama 2017, van Gent, Sparrer et al. 2018).
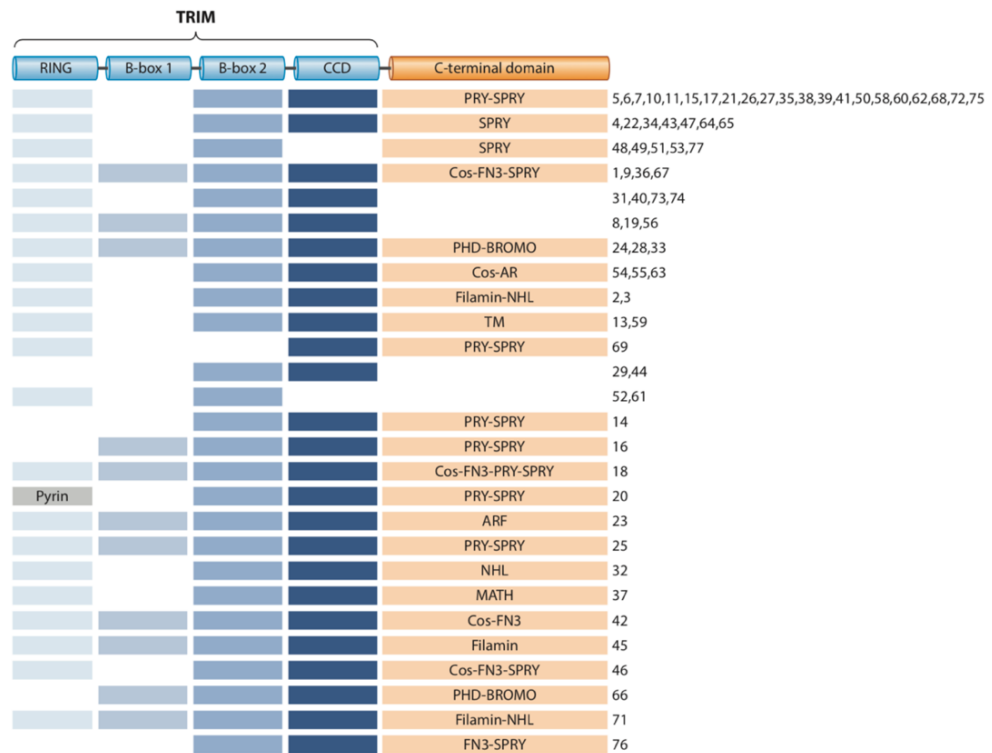
Figure 2.1.2.3. Domain structure of TRIM proteins.

The cartoon image showing the domain organisation of TRIM proteins. It highlights the N-terminal RBCC motifs and the varying C-terminal domains. The numbers on the right denotes the identity of each TRIM subfamily member. The position of RING domain is replaced with Pyrin doman in TRIM20. Many proteins with pyrin domain are importants for inducing inflamation. Image taken from van Gent, Sparrer et al. 2018.

Although TRIM proteins are capable of ubiquitination as a single protein, some TRIM proteins act as homodimers while others form heterodimeric complexes with other single subunit RING domain proteins. Homodimerization of TRIM proteins is often mediated by coiled coil domains, although exceptions have been observed (Li, Yeung et al. 2011, Streich, Ronchi et al. 2013, Li, Wu et al. 2014, Sanchez, Okreglicka et al. 2014, Yudina, Roa et al. 2015, Koliopoulos, Esposito et al. 2016, Watanabe and Hatakeyama 2017). Additionally, most TRIM proteins display E3 ligase activities to promote proteasomal degradation, although recent studies suggest that TRIM-dependent ubiquitination may also promote autophagic degradation of target proteins. For example, during viral infection in human cells, TRIM23 promotes auto-ubiquitination of its ADP-ribosylation factor (ARF) domain. This auto-ubiquitination triggers the GTPase activity of the ARF domain that is required for induction of autophagy to act as defense system against viral infections (Sparrer, Gableske et al. 2017,

Sparrer and Gack 2018). Moreover, other TRIMs do not have E3 ligase activities but instead promote other molecular activities such as SUMOylation and transcription activation as a transcription factor (further discussed in van Gent, Sparrer et al. 2018).

2.1.2.4. UPS is important for many aspects of development including germ cell development

In *C. elegans,* similar to other systems, mutations in genes encoding core proteasome factors and/or RNAi mediated knockdown of core proteasome factors affect almost every aspect of development including embryogenesis, larvae development and postembryonic germ cell development (Gonczy, Echeverri et al. 2000, Takahashi, Iwasaki et al. 2002, Kamath, Fraser et al. 2003, Kahn, Rea et al. 2008, Kisielnicka, Minasaki et al. 2018). Therefore, coupled to translational control of gene expression that regulate the time of protein synthesis, especially in germ cells, proteasome may support translational control to achieve a fine-tuned spatiotemporal protein expression. While, especially during postembryonic germ cell development, the biological functions of several ubiquitin conjugating enzyme (Jones, Crowe et al. 2002, Fay, Large et al. 2003, Schulze, Altmann et al. 2003) and several multimeric RING domain E3 ligases such as the cullin-based complexes have been revealed (Feng, Zhong et al. 1999, Liu, Vasudevan et al. 2004, Sonneville and Gonczy 2004, Starostina, Lim et al. 2007, Merlet, Burger et al. 2010, Starostina, Simpliciano et al. 2010, Burger, Merlet et al. 2013, Kisielnicka, Minasaki et al. 2018), very little is known about the function of TRIM proteins in both embryonic and post embryonic germ cell development. It would be interesting, in future, to unravel more molecular mechanisms of regulated protein degradation by TRIM proteins during development and relevance of such regulations.

2.2. Primordial germ cell development; specification of fate and maintenance

Germ cells maintain survival of species in a cyclical manner- germ cells are set aside in the embryo as PGCs, PGCs produce an entire germline tissue that produces gametes, gametes then form a totipotent zygote, the first cell in embryogenesis. To ensure continuity of this cycle, in successive generations, the newly formed zygote must quickly establish or specify a new lineage of germ cells and it must be maintained until sexual maturity in adulthood. Although there have been two major modes of germ cell specification described, which are preformation and induction modes (Extavour and Akam 2003, Marlow 2015), specification of germ cells is completely unique in all animals in terms of complexity, timing, biology, and identity of molecules required for germ cell specification. One major common factor accompanying germ cell specification is that a special cytoplasm called the germ plasm must first exist or be generated and/or inducced (see Magnusdottir and Surani 2014,

Marlow 2015, Whittle and Extavour 2017, for more details). Therefore, it is imperative to take a close look at the nature of germ plasm and its composition before germ cell specification and maintenance is discussed.

2.2.1. Germ plasm

The germ cell-determining cytoplasm is known as germ plasm. Germ plasm consist of many regulatory factors, most of which are either RNA-binding or RNA-modifying proteins that are together essential for germ cell specification and development. These factors form protein-protein and protein-RNA interaction networks that aggregate to form electron dense complexes known as germ granules (Eddy 1975). Germ plasm have been proposed to be important for several aspects of germ cell development especially during embryogenesis, including but not limited to (i) transport and localization of germline enriched RNAs, (ii) local translation of maternal mRNA that may be distributed throughout developing embryo, (iii) protection of these mRNAs from degradative mechanisms which clears them out in somatic cells, (iv) transcriptional silencing prior to germ cell specification, and (v) migration of specified germ cells to future somatic gonad (Bashirullah, Cooperstock et al. 2001, Johnstone and Lasko 2001, Starz-Gaiano and Lehmann 2001, Blackwell 2004).

2.2.1.1 Germ granules

Germ granules are evolutionary conserved component of germ plasm made up of a plethora of associating ribonucleoprotein complexes (RNPs) which, like in several other types of granules, form interactions through protein-protein, protein-RNA and RNA-RNA affinities (Voronina, Seydoux et al. 2011). Using electron microscopy, germ granules have been observed to appear as electron dense, organelle like, compact fibrillar aggregates without any surrounding membrane. Germ granules are identified by different nomenclatures in different organisms. For example, in mice germ granules are known are nuage and in *C. elegans,* germ granules are referred to as P granules (Voronina, Seydoux et al. 2011). Germ granules of all studied organisms often contain germ cell-specific proteins and RNAs that are required for germ cell development and a vast majority of these proteins are RNA-regulatory, RNA-binding and RNA-modifying proteins or enzymes that are crucial for posttranscriptional gene expression regulation, leading to the hypothesis that germ granules may be site of posttranscriptional gene expression regulation. (Eddy 1975, Guraya 1979, Strome and Wood 1982, Voronina, Seydoux et al. 2011).

Whereas the function of germ plasm during germ cell development remains undisputable, the functions of germ granules have been highly speculative in nature and hence are highly debated. Most of the functions often associated with germ granules are

revealed either through mutation or knockdown of factors that associate with germ granules in germ plasm (Voronina, Seydoux et al. 2011).

For a long time, germ granules have been proposed to be crucial to germ cell specification. For example, in *D. melanogaster,* mutations in Oskar, a protein that is enriched on germ granules, lead to a loss of germ plasm and germ cells. Conversely, ectopic expression of Oskar leads to establishment of germ granules, germ plasm, and germ cells at ectopic sites during embryogenesis (Ephrussi and Lehmann 1992). Similar to Oskar, mutations in Bulky ball, a germ granule-enriched protein factor, lead to loss of germ plasm and germ cells during zebrafish embryogenesis (Bontems, Stein et al. 2009). Loss of Nanos, a conserved germ granule-associated protein family that is broadly expressed in germ cells of many organisms, leads germ cell death in *C. elegans, D. melanogaster* and mouse (Tsuda, Sasaoka et al. 2003, Voronina, Seydoux et al. 2011). All these examples indicate that many factors associated with germ granules are crucial to germ cell specification and development. However, it is often difficult to tease apart germ granule-dependent functions of these components from germ granule-independent ones.

2.2.1.2. P granules

P granules are donated as parts of maternal germ plasm into the embryo where they experience constant asymmetric partitioning into germ cell precursors- the P lineage. In *C. elegans,* starting from the P0 zygote, a cascade of asymmetric cell divisions generate 4 posteriorly localized germ cell precursors- P1, P2, P3 and P4, and their respective somatic sister blastomeres- AB, EMS, C and D. P4 is born around 24-cell stage and around 28-cell stage, at the onset of gastrulation, P4 is internalized into the developing embryo. Once internalized, between 80-cell and 100-cell stage, P4 divides symmetrically to give rise to Z2 and Z3. Although, P4 is essentially the first germline restricted founder cell, Z2 and Z3 are regarded as the primordial germ cells (see Figure 2.2.1.2.) (Sulston, Schierenberg et al. 1983, Chihara and Nance 2012).

The process of asymmetric P granule partitioning to the P lineage is initiated in the 1-cell embryo (also called P0). It involves a process of highly dynamic granule disassembly in the anterior cytoplasm that give rise to somatic precursors and rapid assembly in the posterior cytoplasm that give rise to germ cell precursors. Unlike in immature postembryonic germ cells where they are predominantly perinuclear, P granules remain distributed in the cytoplasm from the 1-cell embryo until approximately the 16-cell stage. Afterwards, the majority of P granules becomes progressively attached to the nuclear envelope and by 24-cell stage they become exclusively perinuclear in germ cell lineage. This perinuclear form is maintained as the predominant form throughout germline development until detachment

again during oocyte maturation (Hird, Paulsen et al. 1996, Brangwynne, Eckmann et al. 2009, Gallo, Wang et al. 2010).
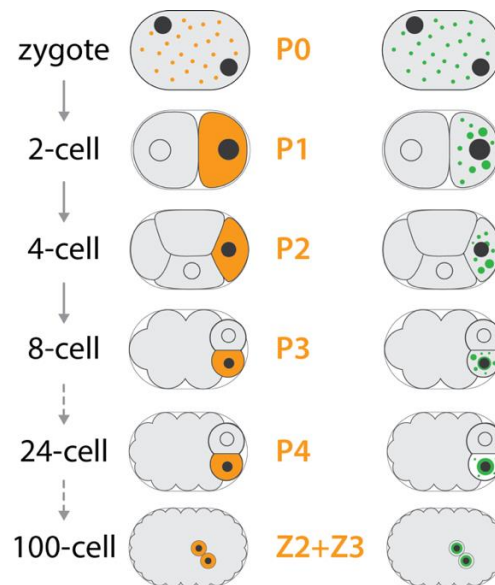
Figure 2.2.1.2. Primordial germ cells are formed through cascades of asymmetric division and P granules are segregated with germ cell lineage.

Carton display of *C. elegans* embryo. The left column describes the developmental stages. Middle columns in orange display position and the identity of each germ cell precursor during embryogenesis. Right column in green show segregation and localization of P granules which follow germ cell fate very tightly.

2.2.2. Germ cell specification

Germ cell specification is one of the earliest events during embryogenesis in most animals. This process has been studied in several organisms and two modes of specification have been identified so far: preformation and induction modes. In the preformation mode, germ plasm is inherited from oocytes. The preformation mode is employed by many organisms, including *D. melanogaster, C. elegans* and *Xenopus laevis.* By contrast, in the induction mode, germ plasm is not inherited from the oocyte. Instead, germ plasm is stimulated to form during early embryogenesis. Most mammalians specify germ cells through induction (Extavour and Akam 2003, Magnusdottir and Surani 2014, Marlow 2015, Whittle and Extavour 2017).

2.2.2.1. Germ cell fate specification by preformation

In this mode of specification, the newly fertilized embryo inherits germ plasm from the oocyte and segregates it into a cell lineage fated to give rise to PGCs. For example, in *Drosophila melanogaster,* germ plasm is assembled in the posterior end of the developing egg and some of the materials required for germ cell determination are supplied by nurse cells. During the multi-nucleated proliferative stage of early embryogenesis, about five to six nuclei migrate to the posterior germ plasm to become pole cells which give rise to primordial germ cells. Therefore, the germ plasm does not intermingle with soma until primordial germ

cell are born. Intriguingly, ectopic transfer of the posterior germ plasm into the anterior end of embryos generated ectopic primordial germ cells at the anterior end of the embryos, arguing that the germ plasm is not only correlative but also instructive and deterministic of germ cell fate specification. As earlier mentioned, just a single protein, Oskar, is sufficient to assemble germ plasm at ectopic sites (Illmensee and Mahowald 1974, Ephrussi and Lehmann 1992).

Despite the fact that *C. elegans* also undergo preformative mode of germ cell specification, several events and mechanisms are in contrast to primordial germ cell specification in *D. melanogaster.* In *C. elegans,* the maternal germ plasm that contains many germ cell determinants, both in the cytosol and on P granules, are asymmetrically segregated with the P lineage. Unlike in *D. melanogaster* in which a pole plasm is secluded from soma from early embryogenesis, in *C. elegans,* the germ plasm intermingles with somatic fate and each cell division gives rise to cells fated for soma and germ cell. Another major difference compared to *D. melanogaster* is that ectopic transfer of posterior germ plasm into anterior end does not induce germ cells arguing that early germ plasm is required for fate specification but no sufficient to induce it at ectopic sites (Schierenberg 1988). By extension, no single protein has been identified that is sufficient to induce germ plasm formation, although several proteins have been identified which are necessary for germ cell fate specification, all of which are maternally donated by the oocyte and segregate with P lineage. The observation that ectopic transfer of germ plasm and ectopic expression of germ plasm proteins was not sufficient to induce germ plasm would later be explained, in part, by the discovery of *mex-5* and *mex-6* (Schubert, Lin et al. 2000)*.* MEX-5 and MEX-6 proteins localize to the anterior end of cytoplasm during an asymmetric cell division and promote disassembly of P granules. Additionally, upon completion of an asymmetric cell division, some residual germ plasm RNAs, proteins and P granules are inherited by the somatic sister cell. However, these residual germ plasm proteins and enriched RNAs are quickly cleared out in somatic sister cells in a MEX-5/6-dependent manner (Schubert, Lin et al. 2000). Therefore, whereas, both *D. melanogaster* and *C. elegans* have inherited mode of germ cell specification, specific details of biological and molecular mechanisms are unique.

2.2.2.2. Common themes of germ cell specification

Although, there are many species-specific developmental events that culminate into PGC specification, several common themes emerged. Two of these themes that are relevant to this thesis are repression of transcription and epigenetic regulation (Nakamura and Seydoux 2008, Lesch and Page 2012).

2.2.2.2.1. Transcriptional repression

Transcriptional repression seems to be a pertinent requirement for germ cell specification. It has been observed in all studied organism, regardless of clade or mode of germ cell specification. However, the scale and the timing of transcriptional repression during germ cell specification may be organism specific and dependent on the mode-of-specification. For example, most organisms with preformed mode of specification experience global transcriptional repression. This is initiated already during oogenesis and continues into embryogenesis until germ cell fate specification is complete (Nakamura and Seydoux 2008). By contrast, in organisms using an induction mode such as mice, global zygotic transcription is activated very early in embryogenesis but the genome becomes repressed again in specific cells induced to become germ cells (Jukam, Shariati et al. 2017).

During *C. elegans* embryogenesis, global transcription is achieved by the activities of two highly similar and redundant proteins, OMA-1 and OMA-2, until the 2-cell stage. OMA proteins interact with and sequester TATA-binding protein associated factor 4 (TAF-4) in the cytoplasm. TAF-4 is one of the key components of the pre-initiation complex of RNA polymerase II (pol II). OMA proteins therefore prevent formation of pre-initiation complex, thereby inhibiting all pol II-dependent transcriptional activities (Walker, Rothman et al. 2001, Guven-Ozkan, Nishi et al. 2008). In 2-cell embryos, the OMA proteins are removed by protein degradation (see Figure 2.2.2.2.1) (Guven-Ozkan, Nishi et al. 2008, Wang and Seydoux 2013). Subsequently, the mode of transcriptional repression in germ cells is switched from OMA-based repression to PIE-1-based transcriptional repression (see Figure 2.2.2.2.1) (Guven-Ozkan, Nishi et al. 2008, Guven-Ozkan, Robertson et al. 2010, Ewen-Campen, Donoughe et al. 2013). This allows for the first wave of zygotic transcription in soma at 4-cell stage, while transcription is continuously repressed in germ cell lineage until the birth of PGCs (Guven-Ozkan, Nishi et al. 2008, Wang and Seydoux 2013).

PIE-1 (Pharynx and Intestine in Excess) is a zinc finger protein that is expressed in all embryonic germ cell precursors. Concomitant with the birth of primordial germ cells, PIE-1 protein expression is terminated. In germ cell precursors, PIE-1 shuttles between the cytoplasm and nucleus to inhibits global transcription starting from P2 onwards. To this end, it inhibits the phosphorylation of serine 2 (Ser2) and serine 5 (Ser5) of the carboxyl terminal domain (CTD) of pol II (Mello, Schubert et al. 1996, Batchelder, Dunn et al. 1999, Ewen-Campen, Donoughe et al. 2013). In the nucleus, PIE-1 uses a domain that resembles the CTD of pol II to interact with PTEFb, a kinase complex required for phosphorylation of CTD of pol II, thereby blocking its kinase activity. Interestingly, removal of the PIE-1 domain that resembles CTD of pol II in worms only led to precocious appearance of phosphorylated Ser2 (pSer2) but not phosphorylated Ser5 (pSer5) in germ cell precursors. This argues that PIE-1 uses an additional and yet to be identified redundant mechanism for blocking Ser5

phosphorylation (Batchelder, Dunn et al. 1999, Ghosh and Seydoux 2008, Wang and Seydoux 2013).
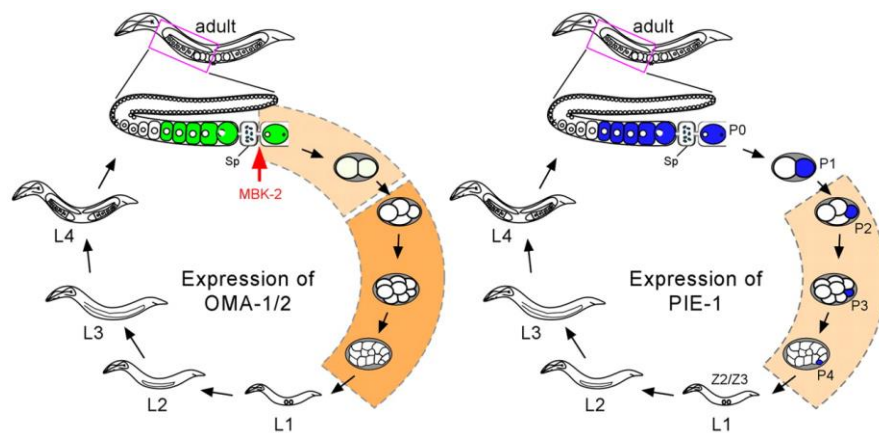
Figure 2.2.2.2.1. Expression and transcription repression function of two OMA proteins versus PIE-1

The expression of both OMA proteins and PIE-1 are initiated during oogenesis. At fertilization phosphorylation by MBK-2 kinase activates the transcriptional repression activities of OMA proteins. OMA proteins repress transcription until they are degraded in 2 cell-stage. PIE-1 repression activity is initiated in P2 until division of P4 to give rise to PGCs. Image take from Guven-Ozkan, Robertson et al. 2010

The transcriptional repression activity of PIE-1 is required for germ cell fate specification. In *pie-1* mutants, P2 germ cell precursors lose germ cell fate and adopt the fate of its somatic sister cell instead, generating dead embryos with excess pharyngeal and intestinal cells; hence the name Pharynx and Intestine in Excess (*pie-1*) (Mello, Draper et al. 1992, Mello, Schubert et al. 1996, Ewen-Campen, Donoughe et al. 2013). This observation led to initial speculations that transcriptional repression, during germ cell specification may serve to temporarily inhibit initiation of somatic programs in the early germ cell precursors to protect their plasticity until the germ cell fate becomes completely established (Nakamura and Seydoux 2008, Saitou and Yamaji 2012, Strome and Updike 2015).

Similar to the germ cell precursors in *C. elegans,* pole cells of *D. melanogaster* are transcriptionally quiescent. Interestingly, the mechanism of global transcriptional repression in *Drosophila* is highly similar to the PIE-1-based mechanism. To achieve global transcriptional repression, polar granular component (PGC), a protein component of the maternally inherited germ plasm, interacts with the PTEFb kinase complex, preventing its association with pol II. (Hanyu-Nakamura, Sonobe-Nojima et al. 2008, Lesch and Page 2012). So far, no obvious sequence similarities have been seen between PIE-1 and PGC protein (Batchelder, Dunn et al. 1999, Hanyu-Nakamura, Sonobe-Nojima et al. 2008), suggesting that these similar mechanisms may be independently derived during evolution. In mice, during the process of germ cell specification, BMP-4 activates the expression of Prdm1 and Prdm14, which are both required redundantly for the specification of germ cells.

Prdm1/14-positive cells have been observed to undergo strong but selective transcriptional repression of somatic program yet allowing the transcription of germ cell determining factors. Therefore, regardless of mode of specification, repression of transcription is essential during germ cell fate specification.

2.2.2.2.2. Epigenetic regulation of chromatin

Another common theme during germ cell specification, which is not far removed from transcriptional repression, is epigenetic regulation of chromatin. In *C. elegans,* global transcription is repressed by OMA proteins from P0 to P2 and PIE-1 from P2 to P4. Although these P cells are under transcriptional repression, the chromatin of germ cell precursors is relaxed and expresses epigenetic modifications that correlates with transcriptional activation. These marks include di- methylated lysine 4 and tri-methylated lysine 4 of histone H3 (H3K4me2 and H3K4me3) (Schaner, Deshpande et al. 2003). This suggests that although global transcription is repressed through inhibition of pol II, the chromatin is primed for transcriptional activities. The chromatin of germ cell precursors may, therefore, be primed for transcription to assist sister somatic blastomeres kick-start somatic gene expression programs, immediately upon completion of an asymmetric cell division.

In *C. elegans,* global transcriptional repression through inhibition of pol II activity is replaced with chromatin regulation during gastrulation of P4 (Schaner, Deshpande et al. 2003). Several events have been observed during the switch to chromatin regulation. The chromatin of P4 germ cell precursor becomes condensed and compact. A gradual reduction in PIE-1 protein levels culminates in a complete loss upon PGC birth. Furthermore, in nascent wild-type PGCs, upon PIE-1 protein degradation, there is also a corresponding appearance of pSer2 and pSer5 of pol II. In addition to these, other major epigenetic changes occur in nascent PGCs. For example, histone modifications such as di- and tri-methylated lysine 4 of histone H3 (H3K4me2 and H3K4e3) and acetylated lysine 8 of histone H4 (H4K8ac), which are strongly associated with active chromatin become reduced in PGCs. By contrast, modification such as tri-methylated lysine 27 of histone H3 (H3K27me3) that is strongly associated with repressed chromatin becomes upregulated in nascent PGCs (See Figure 2.2.1) (Schaner, Deshpande et al. 2003, Bender, Cao et al. 2004). All these changes suggest that PIE-1-based global transcriptional repression is replaced by chromatin mode of transcriptional repression. Due to these changes, nascent PGCs do not undergo major transcriptional activity until hatching. In fact, only a handful of genes including *xnd-1, nos-1, pgl-1, rec-8* and *htp-3,* have been shown to be zygotically transcribed in embryonic PGCs (Kawasaki, Shim et al. 1998, Subramaniam and Seydoux 1999, Spencer, Zeller et al. 2011, Mainpal, Nance et al. 2015). Importantly, a switch from PIE-1-based repression to chromatin repression has implication for PGC development (see section 2.2.3).

A very similar but not identical scenario occurs in *D. melanogaster.* Unlike *C. elegans,* only a basal expression of H3K4me2 and H3K4me3 is detectable in pole cells prior to gastrulation and expression stays low during gastrulation of pole cells to the mid-gut (Schaner, Deshpande et al. 2003). This suggest that during early embryogenesis, the chromatin of pole cells is not transcriptional competent. Unlike *C. elegans,* soma is completely separated in *D.* melanogaster from the first sets of cell divisions and therefore a requirement of chromatin transcriptional competence may not be necessary in pole cells. Additionally, similar to PIE-1 degradation in *C. elegans,* PGC protein is degraded during gastrulation of pole cells to the mid-gut and pSer2 and pSer5 of pol II concomitantly appear. Although Ser2 of RNA pol II becomes hyperphosphorylated after PGC protein turnover, no transcriptional output is detected at this stage (Schaner, Deshpande et al. 2003, Santos and Lehmann 2004). Onset of transcription in germ cell coincides with the appearance of H3K4me2 and H3K4me3 during migration into somatic gonad precursors (Schaner, Deshpande et al. 2003). Therefore, several aspects of chromatin regulations are similar in worms and flies and presumably many other organisms*.*

2.2.3. Maintenance of germ cell fate in primordial germ cells

Once primordial germ cells have been formed, they undergo several germ cell-specific biological and molecular programs that are imperative for germline development and for preservation of germ cell immortality across many generations. These include: (i) Germ cells must maintain the already established germ cell fate. (ii) Germ cells maintain pluripotency whilst being committed to a single lineage. (iii) In some animals, especially those that specify germ cells through preformation, PGCs initiate clearance of maternal gene expression products to establish a zygotic program. In many animals, all of these molecular changes occur during migration of PGCs to colonise to somatic gonad. More importantly, they are carried out in preparation for proliferation of PGCs. Two of the molecular changes in primordial germ cells that are relevant for this thesis are discussed below.

2.2.3.1 Maintenance of already established chromatin regulation and establishment of new ones in PGCs.

Many of the chromatin changes in PGCs mentioned above are initiated prior to their formation. It is noteworthy to state that although they precede PGC formation, many are not required for PGC specification but are majorly important to form a landscape which is to be maintained in PGC for a successful germline development. A good example is the switch from pol II-dependent transcriptional repression to epigenetic regulation of transcription in worms and flies (Lesch and Page 2012). Lysine-specific demethylase 1 (LSD-1) is a histone demethylase required for the removal of methyl groups from methylated lysines of histone

H3, typically, lysine 4 and lysine 9. In *C. elegans*, mutation in the LSD-1 orthologue, *spr-5,* leads to progressive loss of fertility across generations (termed Mortal germline phenotype, *Mrt*) as a result of prolonged expression of H3K4me2 mark in primordial germ cells. This argues that erasure of H3K4me2 histone modification by SPR-5 is not required for PGC specification per se but important to allow reprograming of PGCs to re-establish and maintain immortality of germ cells (Katz, Edwards et al. 2009). Similarly, in *D. melanogaster,* mutation in suppressor of variegation 3-3 (Su(var)3-3), which is the *Drosophila* homologue of LSD-1 and *spr-5* histone demethylase also leads to elevated levels of H3K4me2 modification and eventual germ cell death (Rudolph, Yonezawa et al. 2007).

As summarized in Figure 2.2.3.1, some other histone modifications are either added, erased, maintained, or increased in Z2 and Z3 of *C. elegans*. While we have some knowledge about the activity and importance of these modification (Van Wynsberghe and Maine 2013), very little is known about how they are regulated.

Histone modification	P1-P4 (embryo)	Z2/Z3 (embryo)	Z2/Z3 (fed L1)	Transcriptional state of associated chromatin
H3K4me2/me3	present	absent	present	activated
H4K8ac	present	absent	present	activated
H4K16ac	present	present	present	activated
H3K9/K14ac2	present	present	present	activated
H3K27me2	present	absent	N/D	repressed
H3K27me3	present	present	N/D	repressed
H3K9me3	absent	absent	N/D	repressed

Figure 2.2.3.1. Germline epigenetic landscape is remodeled in *C. elegans* PGCs.
Table showing histone modifications during early embryonic germline development and the coupled state of chromatin associated with individual modification as determined in *C. elegans*. N/D = not determined. Table is taken and adapted from WormBook: (http://www.wormbook.org/chapters/www_germlinechromatin/germlinechromatin.html)

In general, epigenetic regulation of chromatin is a universal system in germ cells to continuously express select genes to maintain the already established germ cell fate and to assist development of PGCs. In all, loss of genes required for maintenance of the epigenetic landscape in PGCs and preservation of germ cell fate often cause either of these three phenotypes: (i) a mortal germline phenotype in which fertility is lost over many generations (Katz, Edwards et al. 2009); (ii) the occurrence of germline survival defects (Capowski, Martin et al. 1991, Paulsen, Capowski et al. 1995, Katz, Edwards et al. 2009, Mainpal, Nance et al. 2015); or occasionally, (iii) trans-differentiation of germ cells into other cells, usually, neurons (Holdeman, Nehrt et al. 1998, Korf, Fan et al. 1998, Bender, Cao et al. 2004). In some instances, a combination of these three is observed (Capowski, Martin et al. 1991, Holdeman, Nehrt et al. 1998, Korf, Fan et al. 1998). Therefore, PGC expressed epigenetic

regulators are required for maintenance of germ cell identity, germ cell immortality and germline survival.

2.2.3.2. Clearance of maternal factors and activation of the zygotic genome

After their specification, PGCs clear out maternal gene products and transition in a systematic manner into the zygotic program by activating the transcription of genes required for germ cell development. Although ample amounts of data exist to describe the molecular mechanisms of maternal transcripts clearance in soma, very little is known about how the expression of maternal transcripts and their associated regulatory protein factors is terminated in PGCs (Simonelig 2012). One common observation in many animals is that the maternal program is significantly delayed in germ cells compared to soma during early embryogenesis, presumably a necessity for germ cell specification and maintenance in many animals (Siddiqui, Li et al. 2012, Simonelig 2012). This makes sense, given that transcriptional repression in is delayed in germ cells compared to soma and is required for germ cell specification. The molecular mechanisms that assist clearance of maternal gene expression products in PGCs remain elusive and its relevance is further discussed under section 2.4.2, by comparing the where maternal-to-zygotic transition (MZT) in soma and germ cells.

2.2.4. Migration, proliferation and development of primordial germ cells

In most analyzed animal models including fruit fly, zebrafish and mouse, PGCs migrate to colonize the somatic gonad (Warrior 1994, Moore, Broihier et al. 1998, Weidinger, Wolke et al. 2002, Richardson and Lehmann 2010). This is reversed in *C. elegans.* P4 germ cell primordium is born in the posterior end of the developing embryo around 24-cell stage. The expression of adhesion protein HMR/E-cadherin is triggered by a yet to be understood post-transcriptional mechanism. HMR/E-cadherin thus facilitates attachment to endodermal cells which assists the internalization of P4 connected to endodermal cells during gastrulation (Chihara and Nance 2012).

After division of P4, resultant PGCs are still affected by endodermal cells, which help to reduce the size of the quiescent PGCs by cannibalistic digestion of projecting lobes of Z2 and Z3 (Abdu, Maniscalco et al. 2016). In addition to cannibalistic remodeling, PGCs undergo cell cycle arrest in the G2 phase and remain mitotically quiescent throughout embryogenesis. Towards the end of the first half of embryogenesis, two somatic gonad precursor cells (SGPs) migrate towards both primordial germ cells, Z2 and Z3, and wrap around them forming the nascent 4-cell gonad primordium (McIntyre and Nance 2020). The wrapping of PGCs by SGPs has been demonstrated to be important for maintenance of quiescence in PGCs during the remaining part of embryogenesis. It also protects PGCs by

limiting the cannibalistic remodeling activities of endodermal cells to engulfment of PGC lobes but not the entire cells (McIntyre and Nance 2020). At hatching, the L1 larvae is born with the already formed gonad primordium consisting of two SGPs (Z1 and Z4), two PGCs (Z2 and Z3) and a basal membrane. PGCs and the SGPs remain mitotically quiescent until the middle of the first larvae stage after which they initiate rapid proliferation, forming the entire germline tissue and somatic gonad of an adult animal, respectively.

2.3. Postembryonic germline development in *C. elegans* hermaphrodite

A naturally occurring population of *C. elegans* is made up of self-fertile hermaphrodites and males. Wild-type males make sperm throughout adult development and occur less frequently as they are produced spontaneously at a rate of one in every five hundred in self propagating population under laboratory conditions. By contrast, hermaphrodites are somatically females but they are capable, temporarily, of sperm production in the last larvae stage before switching to continuous oogenesis throughout adulthood. Sperm is stored in spermatheca which is then used for fertilization of oocyte. The germline is therefore built in a systematic manner from the first larvae stage to support this complex biology.

2.3.1. Postembryonic germline development: germline proliferation and differentiation

To form the hermaphrodite germline which supports self-fertility, primordial germ cells must successfully undergo proliferation and correct execution of germ-cell-specific programs in a stage-dependent manner. An overview of postembryonic germ cell development is given in Figure 2.3.1.
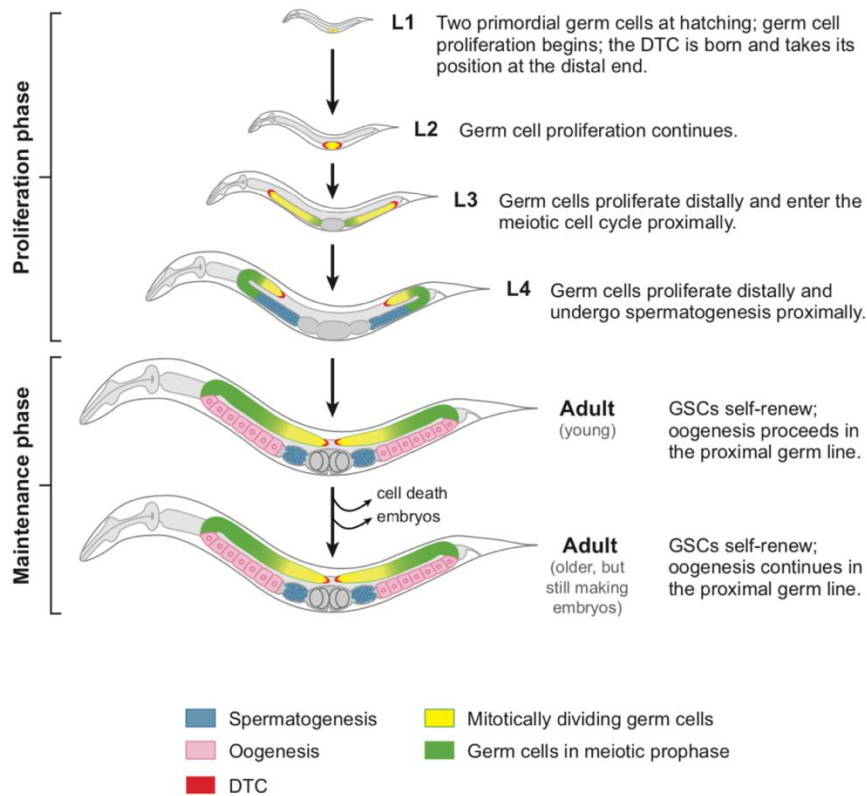
Figure 2.3.1. Postembryonic germline development in *C. elegans.*
Figure was taken from Kimble and Crittenden 2007. DTC is distal tip cell.

At hatching, the initiation of PGC proliferation depends on availability of nutritional sources. In the absence of food, both the SGPs and PGCs arrest indefinitely. Upon food signal, Z2 and Z3 begin to proliferate at exponential rate in the first two larval stages; L1 and L2. In the third larval stage; L3, while proliferation is still taking place, some of the germ cells initiate differentiation (Hirsh, Oppenheim et al. 1976, Kimble and Hirsh 1979, Kimble and White 1981).

Proliferating and differentiating germ cell nuclei exist in a syncytial cytoplasm. Although the cytoplasm of PGC seems to be connected by a cytoplasmic bridge from the onset of their birth during embryogenesis, a prominent cytoplasmic syncytium in which the cytoplasm is shared by many germ cell nuclei is not established until the second larval stage. Despite the syncytium, germ cells do not undergo synchronous proliferation during larvae development or differentiation in adults. The level of autonomy displayed by germ cell nuclei may be a reflection of a partial enclosure by an incomplete cell membrane that is formed around individual germ cell nucleus (Hirsh, Oppenheim et al. 1976). The somatic gonad has been shown to support germline development in several ways including supporting germline tissue architecture, proliferation, differentiation and maintenance of meiotic program in adult animals

In L3 animals, the most proximally located germ cells adjacent to the spermatheca exit the proliferating germ cell pool, initiate meiosis and differentiate according to the male program. Approximately 40 germ cells will undergo both meiotic divisions (meiosis I and II) coupled to spermatogenesis to provide an adult self-fertile hermaphrodite with a total of approximately 320 sperm. Upon transition into adulthood, spermatogenesis ceases in young adults and remaining germ cell switch from sperm production to oogenesis. By adulthood the germ line consists of approximately 2000 mitotically dividing and differentiating germ cells. In adulthood, the exponential growth of the germline tissue ceases and switches into maintenance mode to sustain the population of already produced germ cells. Throughout the reproductive life of adult hermaphrodite, germ cells will continue to produce oocytes. (Hirsh, Oppenheim et al. 1976, Kimble and Hirsh 1979, Kimble and White 1981). In adults, fully formed gonad is two U-shape structure which are connected by two adjacent completely formed spermatheca and a centrally located uterus. The spermatheca is a sac-like structure with two valves on both ends and store the mature amoeboid sperm (Hirsh, Oppenheim et al. 1976, Hubbard and Greenstein 2005, Kimble and Crittenden 2007). In essence the two PGCs give rise to the entire germline population; each filling one of the two gonadal arms.

2.3.3. Postembryonic germline development in individuals: germline survival

Apoptosis promotes programmed cell death, which is important for development in many organisms. In *C. elegans,* physiological apoptosis contributes to embryogenesis and adult germline development. In fact, to support oogenesis, physiological apoptosis removes between 50 % and 80 % of germ cells during differentiation at the bend region of the germline corresponding to pachytene exit (Gumienny, Lambie et al. 1999, Fox, Vought et al. 2011). The physiological programmed germ cell death is regulated by the conserved core apoptotic genes *ced-4* and *ced-3* (Seshagiri and Miller 1997). *ced-3* encodes for a cysteine protease or caspase that is important for all known apoptosis related events in *C. elegans* (Seshagiri and Miller 1997). CED-3 protein activates or inactivates a good number of substrates. CED-4 protein acts upstream of CED-3, activating and enhancing CED-3 apoptotic activities (Seshagiri and Miller 1997, Spector, Desnoyers et al. 1997).

Besides physiological apoptosis, which is important for germ cell differentiation program, apoptosis also assist maintenance of adult germline tissue by removing cell with compromised genomic integrity during gametogenesis. Similar to physiological apoptosis, DNA damage-induced apoptosis often takes place at pachytene exist, although the molecular lesion leading to cell death may have occurred earlier during DNA replication in the distal proliferative region. However, many of these genomic errors occur during pachytene stage due to double strand breaks that allow exchange of genomic materials between homologous chromosome (Navarro, Shim et al. 2001). DNA damage-induced cell

death can be exacerbated by genotoxic stress such as exposure to genotoxic chemicals, irradiation, oxidative stress and infection. It is also exacerbated by mutations in genes controlling genome integrity (Gartner, Milstein et al. 2000). In fact, germ cell death is a common feature of phenotype arising from mutations in genes that are important for maintaining genome integrity in germ cells (Smelick and Ahmed 2005). Germ cell death caused by DNA damage is usually morphologically indistinguishable from physiological apoptosis and is regulated by the core apoptotic genes *ced-3* and *ced-4* and additional gene such as EGL-1, a worm specific protein. This suggest that DNA-damage induced apoptosis is regulated through additional pathways

Aberrative germ cell death is not limited to adult germline tissue. Excessive germ cell death may also occur during larval development, leading to loss of all germ cells in the gonad by adulthood a phenotype known as Germline survival defective (Gls). Surprisingly, postembryonic germline survival is often dictated by maternally expressed genes. One good example is *gld-3*. GLD-3 modulates the activities of RNA regulators to influence several aspects of germ cell development. Intriguingly, loss of maternal but not zygotic *gld-3* affects germline survival during larvae development; germ cells in *gld-3* animals are able to undergo proliferation in the first two larval stages but In the third larval stage, proliferation ceases and germ cells begin to undergo cell death and by adulthood, generating a gonad that is completely devoid of germ cells (Eckmann, Kraemer et al. 2002). Interestingly, removal of *ced-3* has no effect on *gld-3*-induced germ cell death, suggesting that this cell death may be independent of canonical apoptotic pathways (Eckmann, Kraemer et al. 2002, Rybarska, Harterink et al. 2009). The cell death pathway that removes germ cells during larvae development remains unknown. Similarly, the molecular mechanisms by which GLD-3 complexes promote survival of the germ line are just emerging (Eckmann, Kraemer et al. 2002, Rybarska, Harterink et al. 2009).

Postembryonic germline survival is also promoted in *C. elegans* by orthologs of *D. melanogaster* Nanos. Together, NOS-1 and NOS-2, two of three *C. elegans* Nanos family members are redundantly required for postembryonic germline survival by promoting clearance of maternal transcripts in PGCs. Several aspects of *nos-1* and *nos-2* functions resemble those of *Drosophila* Nanos. In *D. melanogaster,* Nanos forms a complex with the RNA-binding protein Pumilio to repress the expression of target mRNAs by recruiting the CCR4-Not complex to trim the polyA tail of bound mRNAs (Asaoka-Taguchi, Yamada et al. 1999). *C. elegans* Pumilio protein orthologues are called PUF (Pumilio and FEM-3-binding factor) proteins. The activity of *C. elegans pufs* were tested for their requirement in the regulation of germline survival. Interestingly, similar to *nos-1* and *nos-2,* maternal PUF proteins also contribute to survival of the germline: simultaneous knockdown of five of the eleven Pumilio orthologs that are expressed in *C. elegans* led to germline survival phenotype

(Subramaniam and Seydoux 1999, Lee, Lu et al. 2017). This suggests that during *C. elegans* embryogenesis, similar to *Drosophila,* maternal NOS proteins may form complexes with PUF proteins to regulate gene expression.

Several other germ cell components expressed in the embryonic P lineage are maternally required for survival of the germ line. These include GLS-1 and GLD-4, two components of a GLD-4 cytoPAP complex, which modulate several aspects of germline development (Schmid 2008, Rybarska, Harterink et al. 2009, Schmid, Kuchler et al. 2009, Millonigg, Minasaki et al. 2014). Other good examples are MEG (maternal effect germ-cell defective) proteins. *meg-1* and *meg-2* are expressed in embryonic P lineage and are degraded concomitant with PGC birth. Both genes are redundantly required for post embryonic germ cell proliferation and germline survival through a yet to be identified molecular mechanism (Leacock and Reinke 2008, Kapelle and Reinke 2011). Several genes expressed in PGCs required for maintenance of PGC epigenetic landscape and preservation of germ cell fate display germline survival phenotype, such as members of the polycomb repressive complex 2 (PRC2) (Capowski, Martin et al. 1991, Holdeman, Nehrt et al. 1998, Korf, Fan et al. 1998). In all, despite the fact that a few genes have been identified, our understanding of germline survival and molecular events and/or mechanisms that cause associated pathologies are very limited.

Several common themes that strongly correlate with germline survival phenotypes are emerging. (1) All genes known to regulate survival of the germline are expressed during embryonic germ cell development. Some are exclusively expressed in the embryo and others are not. When their expression is not be limited to embryogenesis, as in the case of GLD-3, GLD-4 and GLS-1, only maternal but not zygotic activity seems to contribute to regulation of postembryonic germline survival. (2) Although loss of these genes may occasionally affect embryogenesis, their loss often has no effect on PGC specification. They only affect PGC development after their specification. (3) In all cases, germ cell death is unaffected by the loss of *ced-3* or *ced-4,* suggesting that cell death is either completely independent of apoptosis or triggers alternative pathways of cell death, such as necrosis. (4) In all cases, PGCs are born with P granules. However, as PGCs proliferate, there is either a loss of P granule integrity, in which P granule components are present but do not assemble into granules, or a complete loss of P granules and its components is observed (Subramaniam and Seydoux 1999, Eckmann, Kraemer et al. 2002, Ciosk, DePalma et al. 2006, Leacock and Reinke 2008, Rybarska, Harterink et al. 2009, Kapelle and Reinke 2011, Updike, Knutson et al. 2014, Mainpal, Nance et al. 2015). All these observations indicate strong phenotypic similarities when the activity of any of itemized gene is missing.

2.3.4. Postembryonic germline development across generations: germline immortality

While soma may tolerate a background level of genomic alteration, there is a strong selective pressure on germ cell to maintain accurate genomic information. Due to this dichotomy, germ cells seem to have evolved germ cell-specific mechanisms to limit passage of deleterious changes and mutations to successive generations (Smelick and Ahmed 2005). Therefore, perturbation of pathways that regulate genome integrity may cause transgenerational accumulation of deleterious gene expression changes and/or genomic alterations leading to transgenerational sterility phenotype. Therefore, the mortal germline phenotype (*Mrt*) describes a progressive loss of fertility across generations (Ahmed and Hodgkin 2000). This definition neither emphasize associated germ cell-specific phenotypes nor link the phenotype to a specific gene category.

To date, loss of three major categories of genes have been shown to display a mortal germline phenotype. (1) Genes that are important for regulating DNA damage checkpoints and genome integrity, such as RAD-1-type telomerase, *mrt-2* (Ahmed and Hodgkin 2000) and checkpoint clamp protein, *hus-1* (Hofmann, Milstein et al. 2002). (2) Genes that are important for addition, removal, or interpretation of epigenetic modifications that may be required for maintenance of the epigenetic landscape in germ cells. Their activities may be effected either during PGC development such as lysine demethylase, *spr-5* (Katz, Edwards et al. 2009) or during postembryonic germ cell development, such as methyl transferases, *met-2* and *set-32* (Lev, Seroussi et al. 2017, Spracklin, Fields et al. 2017, Woodhouse, Buchmann et al. 2018). (3) Genes that are involved in production, regulation, or maintenance of small RNAs during *C. elegans* germline development, such as *prg-1, hrde-1, henn-1* and some *nrde* and *rsd* genes (Buckley, Burkhart et al. 2012, Svendsen, Reed et al. 2019, Weiser and Kim 2019). These categories of gene are not mutually exclusive in their regulatory mechanism of action and activities via which they promote germ cell immortality. For example, small RNAs have been shown to regulate the chromatin landscape in germ cells and *met-2* transgenerational sterility is also dependent on the HRDE-1 pathway (Lev, Seroussi et al. 2017, Weiser and Kim 2019). Additionally, piRNAs are important for maintenance of genomic integrity by preventing transposon-mediated DNA damage, suggesting a strong network of complex interaction among the three listed categories of genes.

Several typical germ cell aberrations have been associated with *Mrt* phenotype. These phenotypes include increased DNA damage (Ahmed and Hodgkin 2000, Grabowski, Svrzikapa et al. 2005), proliferation defects (Ahmed and Hodgkin 2000, Li and Maine 2018), germ cell death (Sakaguchi, Sarkies et al. 2014, Li and Maine 2018) and differentiation defects in sperm and oocytes (Conine, Moresco et al. 2013, Sakaguchi, Sarkies et al. 2014, Li and Maine 2018). In some cases, both sperm and oocytes are affected and in others, especially spermatogenesis is sensitive to germ cell immortality. In the later scenario,

progressive loss of fertility will be a consequence of reduced number of functioning sperm or total number of sperm set aside in self-fertilizing hermaphrodites across generations (Conine, Moresco et al. 2013, Sakaguchi, Sarkies et al. 2014, Johnston, Krizus et al. 2017).

Molecular mechanisms that promote germ cell immortality are not exhausted by these three gene categories. Ahmed and Hodgkin 2000 observed that not all the sixteen genes recovered from the mortal germline screen have obvious or direct function in maintaining genome integrity (Ahmed and Hodgkin 2000). Besides this study, other studies have shown the requirement of RNA regulators and RBPs in regulating germ cell immortality (Johnston, Krizus et al. 2017, Li and Maine 2018). Emerging studies may identify and demystify new pathways that regulate germ cell immortality.

2.3.5. Germ cell immortality versus germline survival

These two terms are often interchangeably used in the literature. Survival of the germline at every generation seems to be an obvious prerequisite to maintain immortality of germ cells across many generations. However, as mentioned above, phenotypes that affects germ cell immortality may not necessarily affect germline survival. As these two terms describe similar but not identical phenotypes and are used distinctively in this thesis, there is the need to expatiate and make their relatedness and differences obvious.

The mortal germline phenotype manifest as a gradual loss of fertility across generations. It may be associated with molecular defects such as increased DNA damage, aberrant expression of small RNAs, changes in chromatin epigenetic landscape, transcriptional changes. It may also be associated with several biological defects including proliferation defect, differentiation defects, transdifferentiating and cell death. Cell death due to mortal germline phenotype is often but not always dependent on the apoptotic pathway. Also, germ cell death may be initiated at any stage of development and it may affect a small proportion of germ cells within the germline tissue. Furthermore, all the molecular and biological defects are a result of activities of genes or molecular changes that could occur at any stage of germ cell development and are not specifically associated with activities of genes during embryonic germ cell development (Ahmed and Hodgkin 2000, Buckley, Burkhart et al. 2012, Svendsen, Reed et al. 2019, Weiser and Kim 2019).

By contrast, the germline survival phenotype is a defect that occurs to the germline tissue of a developing individual; a germ cells death that is initiated during larvae development resulting in almost complete or complete loss of all germ cells within the gonad by adulthood. This cell death always occurs independently of *ced-3* and *ced-4*-dependent apoptotic pathways. Lastly, it arises as result of loss of activity of germ cell-intrinsic factors activity during embryonic germ cell development; either in the P lineage or in PGCs

(Subramaniam and Seydoux 1999, Eckmann, Kraemer et al. 2002, Leacock and Reinke 2008, Kapelle and Reinke 2011, Mainpal, Nance et al. 2015, Lee, Lu et al. 2017).

2.4. The Maternal-to-Zygotic Transition (MZT) in germ cells

Newly fertilized zygote develops initially under transcriptional repression and rely on its maternal load (Tadros and Lipshitz 2009, Schulz and Harrison 2019). Primarily, oocyte-derived RNA-regulatory proteins and their mRNA targets govern early development. In later stages, a transition from maternally controlled to zygotically controlled gene expression program is required. This switch in gene expression regulation is termed maternal-to-zygotic transition (MZT) (Tadros and Lipshitz 2009, Schulz and Harrison 2019). While, many studies already addressed the mechanisms of MZT in soma, so far, only a handful of studies addressed MZT in germ cells. Therefore, to get full perspective of molecular principles that guide MZT in germ cells, a look into soma is necessitated.

2.4.1. MZT: lessons from soma

In all studied organisms, two major events have been observed to take place during MZT. The first event is the turnover of maternally donated gene expression products; proteins and mRNAs, and the second event is zygotic genome activation (ZGA). ZGA occur in waves; transcription is first initiated in a small scale and later in large scale (see Figure 2.4.1). The small-scale transcription in which only a small fraction of genomic loci is transcribed is known as minor ZGA while the global scale transcription is known as major ZGA. Termination of maternal program is important for a successful transition into zygotic program. Maternal load consists of both maternal mRNA and associated regulatory proteins. Interestingly, while only a few studies have addressed molecular mechanisms of how specific maternal proteins are degraded in early embryos, there exists many genome-wide studies addressing the scale, timing and dynamics of how maternal transcripts are degraded during embryogenesis (Baugh, Hill et al. 2003, Hamatani, Carter et al. 2004, De Renzis, Elemento et al. 2007, Tadros, Goldman et al. 2007, Thomsen, Anders et al. 2010).

Many initial studies on molecular mechanisms of how maternal transcripts are terminated during MZT were conducted in *D. melanogaster* and some of these findings hold true for several other organism. (i) maternal transcript destabilization occurs in waves and (ii) two major pathways control maternal transcript clearance. One pathway is maternally controlled and it is responsible for the removal of majority of maternally loaded transcripts and a second pathway is zygotically induced upon activation of the genome (De Renzis, Elemento et al. 2007, Tadros, Goldman et al. 2007, Tadros and Lipshitz 2009).

Smaug protein promotes the clearance of majority of maternal transcripts through maternal pathway. Smaug binds to Smaug response elements (SREs) in the 3'UTR of

maternal mRNAs. Upon binding, Smaug recruits the CCR4-Not deadenylase complex that promotes trimming and destabilization of more than two-third of total maternally loaded transcripts in the first 3 hours of embryogenesis (Semotok, Cooperstock et al. 2005, Tadros, Goldman et al. 2007). How the expression and activity of Smaug protein is controlled during MZT for the best possible outcome is unknown. In addition, maternally induced piRNAs promote turnover of maternal transcripts in Smaug-dependent and Smaug-independent manner. Aubergine, one of the PIWI family of Argonautes in *Drosophila melanogaster,* interacts with maternal transcripts in a piRNAs-dependent manner. Aubergine additionally interacts with Smaug and CCR4-Not complex thereby promoting transcript clearance in a Smaug-dependent manner. Moreover, Aubergine-piRNAs complex also promotes transcript clearance in a second mechanism which is independent of Smaug activities. piRNAs in Aubergine-piRNAs complex form incomplete base pairing with maternal transcript and promote endonuclease cleavage of maternal transcript at the site of interaction (Nishida, Saito et al. 2007, Rouget, Papin et al. 2010, Dufourt, Bontonou et al. 2017).

The zygotic pathways of maternal transcript clearance kicks in immediately after zygotic genome activation. In *D. melanogaster*, the expression of microRNA-309 (miR-309) cluster is triggered after transcription is activated in a Smaug-dependent manner. miR-309 cluster subsequently promotes the turnover of only about 15 % of all maternal transcripts degraded through zygotic clearance pathway (Bushati, Stark et al. 2008, Benoit, He et al. 2009, Tadros and Lipshitz 2009). Hence, other factors, such as microRNAs exist as part of zygotic clearance pathway. (Bushati, Stark et al. 2008, Tadros and Lipshitz 2009). Similar mechanisms have been observed in *X. laevis* (frog) (Paillard, Omilli et al. 1998, Detivaud, Pascreau et al. 2003, Graindorge, Le Tonqueze et al. 2008, Lund, Liu et al. 2009) and *D. rerio* (Zebrafish) (Giraldez, Mishima et al. 2006, Ferg, Sanges et al. 2007, Bazzini, Lee et al. 2012, Zhao, Wang et al. 2017).
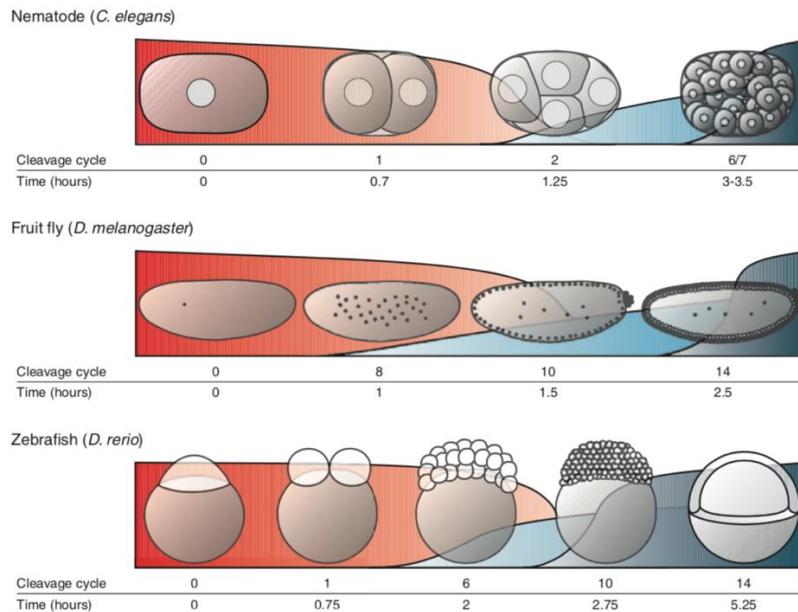
Figure 2.4.1. Maternal-to-zygotic transition: mRNA clearance and transcription activation.

Scheme showing the scale, timing and dynamics of MZT in different organism. Red is maternal transcript clearance and blue is zygotic genome active: light blue is the minor wave of transcription (minor ZGA) and deep blue is full scale zygotic genome transcription (major ZGA). Taken from Tadros and Lipshitz 2009.

In *C. elegans,* several RBPs and/or RNA regulators have been shown to promote either repression or turnover of a maternal transcripts in early embryos in a manner that is gene-specific or somatic blastomere lineage specific, for example, MEX-5 and MEX-6 (Gallo, Munro et al. 2008). Whether microRNAs regulate maternal transcript turnover in *C. elegans* is yet to be determined. Regardless, the trend observed so far is that most maternally-induced transcript clearance is carried out by RBPs (Paillard, Omilli et al. 1998, Ferg, Sanges et al. 2007, Zhao, Wang et al. 2017) and zygotically-induced transcript clearance is mediated by miRNA (Giraldez, Mishima et al. 2006, Lund, Liu et al. 2009). How the activity and expression of these maternal RBPs is regulated during MZT remain elusive?

RNA regulators ensure maternal transcript clearance through deadenylation. It is envisaged that the expression and activities of the maternal proteins must also be tightly regulated to avoid dysregulation of MZT. For example, the expression of Smaug protein is tightly linked to MZT. Its expression is terminated in soma at approximately 3 hours into embryogenesis concomitant with termination of maternal transcripts. Smaug might be developmentally regulated during MZT to avoid Smaug mediated turnover of zygotically-produced transcripts that may bear SREs. This suggest that a tight developmental regulation of activity and expression of RBPs and RNA regulators involved in MZT may be crucial. The molecular mechanisms that promotes regulated turnover of RNA regulators during MZT is unexplored in any system.

2.4.2. MZT: soma versus germ line

Strikingly, in many systems, maternal gene program is often unique in embryonic germ cell lineage compared to soma. In soma, maternal gene program does not perdure for a long period into embryogenesis before transition is made in a gradual manner into zygotically controlled gene expression program. By contrast, maternal gene program perdure for a significantly longer time in germ cell lineage compared to soma (Seydoux and Fire 1994, Bashirullah, Halsell et al. 1999, Bergsten and Gavis 1999, Dahanukar, Walker et al. 1999, Bashirullah, Cooperstock et al. 2001, Koprunner, Thisse et al. 2001, Tadros, Houston et al. 2003, Lecuyer, Yoshida et al. 2007). Unlike soma, the molecular mechanisms that regulate MZT in germ cell remain elusive. A perduring maternal gene expression program may be required for fate specification in germ cell lineage which continuously experience transcriptional repression until formation of primordial germ cells. This suggest that many maternal mRNA and regulatory proteins experience differential protective regulation in germ cell lineage until PGC formation.

A good example is Smaug-mediated maternal transcript turnover in *D. melanogaster* in which hundreds of Smaug target maternal transcripts are unaffected by Smaug-mediated degradation in primordial germ cell precursors or pole cells. In soma, all Smaug-dependent maternal transcripts are destabilized by 3 hours into embryogenesis. By contrast, in germ cell lineage, hundreds of maternal transcripts bearing Smaug response element (SRE) are stable in germ cell lineage. Surprisingly, Smaug expression is not excluded from developing germ cell. In fact, while its expression is terminated in soma at approximately 3 hours into embryogenesis, its expression perdures until after 7 hours. Smaug is only degraded in PGCs after 7 hours. By extension, this observation suggests that germ cells have protective mechanisms that is able to overcome all pathways of transcript degradation until germ cell specification (Bashirullah, Halsell et al. 1999, Dahanukar, Walker et al. 1999, Lecuyer, Yoshida et al. 2007, Siddiqui, Li et al. 2012). Importantly, it also suggests that the expression of Smaug and presumably other RNA regulators must be tightly controlled by regulated protein turnover to achieve a successful MZT. For example, continued expression of RNA regulators that control maternal mRNA degradation in PGCs may perturb zygotic program by interfering with the expression of zygotically produced transcripts.

In *C. elegans,* maternal mRNAs and RNA regulators are also differentially regulated in soma compared to germ cell lineage. Maternal mRNAs are quickly degraded in soma but persist in germ cell lineage (Seydoux and Fire 1994, Baugh, Hill et al. 2003, Osborne Nishimura, Zhang et al. 2015). Concomitant with minor ZGA, many maternal RNA-regulatory germ plasm proteins are selectively degraded in soma but not in germ cells (Eckmann, Kraemer et al. 2002, Wang, Eckmann et al. 2002, Elewa, Shirayama et al. 2015). These trends clearly show that the expression of both maternal mRNAs and regulatory proteins

must be tightly regulated by degradation to undergo successful transition into zygotic program. While RNA turnover mechanisms have been extensively studied in soma and modestly in germ cell lineage, details and relevance of turnover of RBPs and RNA modifying enzymes remain unexplored.

As a result of these observations, three compelling and broad questions become obvious. (i) What molecular mechanisms protect germline-enriched transcripts and associated regulatory proteins from early maternal degradation to allow further perdurance of maternal program in germ cells compared to soma? (ii) How are maternal mRNAs in germ cells eventually released from these protective mechanisms to allow a clean transition into zygotic program or better put, how is maternal program eventually terminated in germ cells? (iii) Importantly, what molecular mechanisms regulate turnover of RNA regulators such as RBPs and RNA-modifying enzymes during MZT and what is the relevance of these developmental regulation? This thesis addressed these questions by focusing on the impact of developmental regulation of *ce*GLD-2 cytoPAP expression during maternal-to-zygotic transition in the embryonic germ cell lineage.

2.5. Regulation of GLD-2 cytoPAP during early embryogenesis in *C. elegans*

The GLD-2/GLD-3 cytoPAP complex is broadly donated as part of maternally donated gene expression products for a broad regulation of the maternal transcriptome. Disruptions of either *gld-2* or *gld-3* expression through RNAi-mediated knockdown leads to arrest or lethality during early embryogenesis. This suggest that the polyadenylation activities of GLD-2/GLD-3 cytoPAP may be important for embryogenesis (Eckmann, Kraemer et al. 2002, Wang, Eckmann et al. 2002, Elewa, Shirayama et al. 2015, Osborne Nishimura, Zhang et al. 2015). GLD-2 cytoPAP has been shown to be required for polyadenylation of maternal transcripts during oocyte maturation in several model organisms including worm, fruit fly, frog and mice (Barnard, Ryan et al. 2004, Rouhana, Wang et al. 2005, Kim and Richter 2006, Nakanishi, Kubota et al. 2006, Benoit, Papin et al. 2008, Cui, Sackton et al. 2008, Cui, Sartain et al. 2013, Dufourt, Bontonou et al. 2017). However, the specific roles of GLD-2 cytoPAP in protecting a broad spectrum of maternal transcripts during early embryogenesis and especially in embryonic germ cell lineage remain unknown.

Strikingly, the GLD-2/GLD-3 cytoPAP complex has a dynamic embryonic expression pattern. Maternally deposited GLD-2 and GLD-3 are cytosolic and also enriched on P granules during early embryogenesis. During mitosis of P cells, GLD-2 cytoPAP is asymmetrically partitioned into the posterior cytoplasm. As a result of this, resultant posteriorly localized germ cell precursors inherit a high level of GLD-2 cytoPAP while a residual amount is inherited by anterior somatic sister cells. The residual GLD-2 cytoPAP is gradually cleared out in the somatic sister cells. By contrast, GLD-2 expression is enriched in

germ cell lineage. GLD-2 cytoPAP expression ceases upon the birth of PGCs (see Figure 2.5.1) (Eckmann, Kraemer et al. 2002, Wang, Eckmann et al. 2002). This shows that expression of GLD-2 cytoPAP strongly correlates with transcriptional repression and maternal phase of gene expression (see Figure 2.5.2). Therefore, maternal GLD-2 cytoPAP complex may be expressed in germ cell lineage during early embryogenesis and may be a key germ cell-intrinsic factor that protects maternal transcripts through polyadenylation activities. This may enhance stability and/or abundance of maternal transcripts until MZT. Hence, GLD-2 may contribute to a delayed maternal program in germ cells. More importantly, developmentally regulated GLD-2 turnover in PGCs may be a key mechanism to facilitate maternal transcript turnover and hence MZT in PGCs.
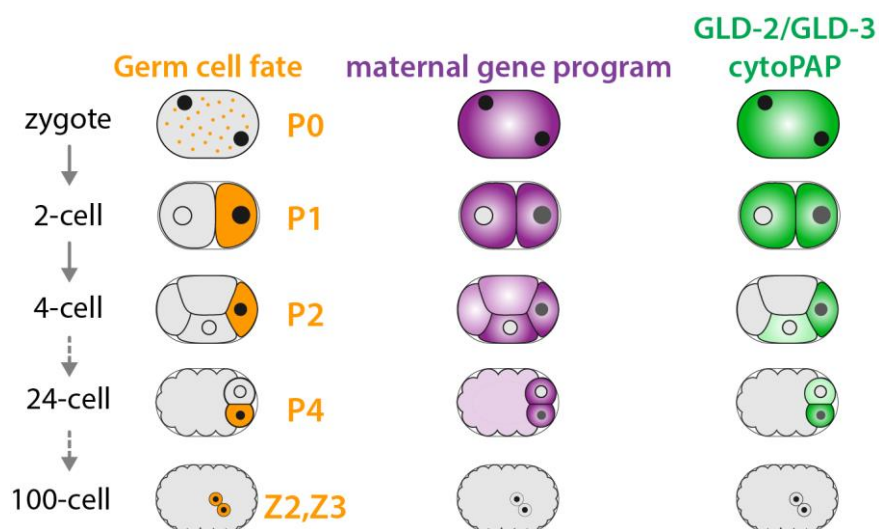
Figure 2.5.1. GLD-2 cytoPAP has a highly dynamic embryonic expression pattern that correlates with maternal gene expression program.

Cartoon images of germ cell fate during embryonic development (orange), the pattern of many maternal transcripts during early embryogenesis (purple) and the distribution of GLD-2 cytoPAP (green). GLD-2 and GLD-3 are abundantly expressed in cells that are yet to clear maternal transcripts and are transcriptionally repressed.

2.6. Aim of the thesis

Early embryonic development occurs under transcriptional repression and therefore to assist early embryonic development, the oocyte donates gene expression products in form of mRNAs and associated regulatory proteins, which direct subsequent development through posttranscriptional gene expression control. However, to put the zygotic genome in charge, these maternal factors must be eventually terminated. While numerous works have addressed how RNA-regulatory proteins regulate MZT, little is known about how the expression of RNA regulators themselves are regulated to achieve a wholesome transition into zygotic program.

In *C. elegans,* the GLD-2/GLD-3 cytoPAP complex is maternally donated into the embryo where it presumably regulates posttranscription gene expression programs critical for soma and germ line development. As GLD-2 cytoPAP expression becomes quickly terminated concomitant with MZT in soma, it remains restricted to germline lineage, which experiences continued transcriptional repression, arguing that GLD-2 cytoPAP activity may be distinctively and differentially required to prolong maternal program in germ cells. Interestingly, similar to soma, GLD-2 expression is terminated in PGCs just prior to ZGA, suggesting a time resolved expression of GLD-2 may also be required for a termination of their maternal program to allow a clean transition into zygotic program.

This study aims to understand the molecular mechanisms that drive maternal GLD-2 cytoPAP degradation. An extension of this objective is the determination of the identity of factors that promote the developmentally regulated turnover of GLD-2 cytoPAP. Furthermore, through interaction studies, this study aims to determine the regions in GLD-2 that facilitates its targeting for protein degradation. As GLD-2 cytoPAP is a positive regulator of gene expression, one of the critical objectives of this project is to determine the molecular and biological relevance of GLD-2 turnover.

3. Materials and Methods

3.1. Chemicals, Reagents, and Inhibitors

3.1.1. Chemicals

- Agarose (Invitrogen #16500-500)
- Albumin (ROTH #8076.3).
- CloneJet PCR cloning Kit (Thermo Fisher Scientific #K1231).
- 4',6-diamidino-2-phenylindole (DAPI, SERVA #18860).
- Enhance chemiluminescence (ECL, Promega #0000265789/90).
- Ethidium bromide (SERVA)
- Glycerol (VWR Chemicals #24388.295)
- Phenol:chloroform:isoamylalcohol (PCI, ROTH #A1561).
- Sodium dodecyl sulphate (SDS, ROTH #0183.3).
- Tetramethylethylenediamine (TEMED, Sigma #T9281s).
- Trichloro acetic acid (TCA, MERCK #1.00807.1000).
- Triton X-100 (TX-100, SERVA #3725.2).
- TRIZOL (Invitrogen #15596026)
- Tween-20 (Tw20, SERVA #37470.01).
- Vectashield mounting solution (Vector laboratories #H-1000).

3.1.2. Protease inhibitors

- Benzamide (SERVA: Benzamidine.HCl hydrate, MW- 156.6 g/mol): stock concentration is 1 M in ddH_2O, final concentration is 2 mM.
- Complete protease inhibitors (with or without EDTA, Roche): for 25x stock, one tablet is dissolved in 2 ml of ddH_2O.
- Leupeptin (SERVA): stock concentration is 1 mg/ml, final concentration is 1 µg/ml.
- Pefabloc (SERVA): stock concentration is 100 mg/ml in ddH_2O, final concentration is 0.1 mg/ml.
- Pepstatin A (SERVA): stock concentration is 1 mg/ml in 100 % ethanol, final concentration is 1 µg/ml.
- PMSF (Roche): stock concentration is 100 mM in ethanol, final concentration is 1 mM.

3.1.3. Phosphatase inhibitors

- Beta-glycerolphosphate: (glycerol 2-phosphate hydrate disodium salt, Sigma): stock concentration is 0.5 M in ddH_2O, final concentration is 20 mM.
- Sodium fluoride (NaF, Sigma): stock concentration is 0.5 M in ddH_2O, final concentration is 1 mM.

3.2. Solutions and Media

Universal

- 1x Phosphate-buffered saline (PBS): 2.7 mM KCl, 137 mM NaCl, 2 mM KH_2PO_4, 10 mM Na_2HPO_4.

Worms

- Bleach solution (for harvesting embryos): 800 parts of water, 1 part of 5M NaOH (MERCK #1.06498.1000), 1 part of sodium hypochlorite (Merck, 6-14 % active chlorine).

- Egg buffer (for PGC isolation): 25 mM HEPES-KOH (ROTH #9105.3) (pH 7.3), 118 mM NaCl, 48 mM KCl, 2 mM $CaCl_2$, 2 mM $MgCl_2$, osmolarity was adjusted with osmometer to 340±5 mOsm.
- M9 Buffer: 22 mM Na_2HPO_4, 22 mM KH_2PO_4, 1mM $MgSO_4$, 85 mM NaCl.
- PBSB (for immunostaining): 1x PBS, 0.5% BSA.
- PK buffer (for genotyping): 50 mM KCl, 10 mM Tris-HCl (pH 8.3), 2.5 mM $MgCl_2$, 0.45 % Tween-20, 0.01 % gelatin.

Yeasts

- Z-buffer: 60 mM Na_2HPO_4, 40 mM NaH_2PO_4 (adjusted to pH 7), 10 mM KCl, 1 mM $MgSO_4$, 25 µg/ml X-Gal (bromo-chloro-indolyl-galactopyranoside)

Nucleic acids

- 5x TBE buffer: 89 mM boric acid, 89 mM TRIS-HCl, 2mM EDTA.
- 10x MOPS (pH 7.0): 200 mM MOPS (ROTH #6979.3), 50 mM NaOAc (SERVA #3957.2), 10 mM EDTA (ROTH #X986.2).
- 10x DNA loading dye: 0.25 % xylene cyanol, 0.25 % bromophenol blue, 50 % glycerol.
- 10x RNA loading buffer ("Orange G"): 0.25 % (w/v) Orange G, 50 % glycerol, 10 mM EDTA (pH 8.0). sterile filtered and stored at room temperature.
- Isopropanol (Chemsolute)
- Trizol: 9.5g Guanidiniumthiocyanate (ROTH, #0017.1), Ammoniumthiocyanate (ROTH, #4477.1), 3.5 ml sodium acetate solution (3M, pH5.0 SERVA, #39572.01), 5 ml glycerol, 48 ml phenol (Roti-Aqua-Phenol fuer RNA-Isolierung, pH 4.5, ROTH, A980.2) and 43.5 ml DEPC-treated ddH_2O. Stored at 4°C in the dark.

Proteins

- 1x SDS-PAGE running buffer: 3.02 g/l Tris base, 14.2 g/l glycine, 1 g/l SDS.
- 2x SDS sample buffer: 2 ml of 1M Tris-HCl (pH 6.8), 1.6 ml SDS (10 %), 4.6 ml glycerol (50 %), 0.4 ml bromophenol blue (0.5 %), 0.4 ml β-mercaptoethanol (SERVA #39563.01).
- Antibody stripping solution: 0.5 % SDS, 2% acetic acid.
- B70 Buffer (for co-immunoprecipitation): 50 mM HEPES-KOH (pH 7.4), 1mM NaF, 70mM KAc, 5 mM Mg(OAc)$_2$, 20 mM β-glycerol phosphate, 0.1 % Triton X-100, 10 % glycerol. HEPES-KOH was only added after autoclaving of the solution of remaining components.
- Blotting Buffer: 14.411 g/l glycine and 3.082 g/l Tris base.
- Borate Buffer: 200 mM Borate (ROTH #5935.1)
- Coomassie Brilliant Blue: 1g Coomassie Brilliant Blue R: 250 ml methanol, 50 ml acetic acid, 200 ml water.
- Coomassie destaining solution: 2 ml acetic acid (100 %), 45 ml methanol (100 %), 45 ml water.
- PBST: 1x PBS, 0.05 % Tween-20.
- Polyacrylamide stacking gel mix: 213.5 ml ddH_2O, 25 ml 40 % Acrylamide/Bis (37.5:1), 31.5 ml 1M Tris (pH 6.8) and 2.5 ml 10 % SDS; stored at 4°C.

Media

- LB medium: 1 % (w/v) NaCl, 1 % (w/v) tryptone, 0.5 % (w/v) yeast extract, adjusted to pH 7.0 and autoclaved.

- SOC medium: 0.5 g/l NaCl, 20 mM glucose, 5 g/l yeast extract, 20 g/l bacto tryptone, 2.5 ml/l of 1M KCl, adjusted to pH 7.0 and autoclaved. Before use, 5ml/l of 2M MgSO$_4$ and 5 ml/l of 2M MgCl$_2$ were added.
- Yeast synthetic defined (SD) drop out media: 1.3 g/l dropout mix, 2 g/l adenine (SERVA #10739), 5 g/l (NH$_4$)$_2$SO$_4$, 1.7 g/l Yeast Nitrogen Base (YNB), 100 ml of 20 % glucose.
- YPD media: 20 g/l bacto peptone, 20 g/l glucose, 5 g/l yeast extract, 0.05 g/l adenine.

3.3. Bacterial and yeast strains

- *Escherichia coli* OP50: uracil auxotroph, standard feeding bacteria for nematode propagation.
- *E. coli* DH5α (cloning): F$^-$ *endA1 glnV44 thi-1 recA1 relA1 gyrA96 deoR nupG purB20* φ80d*lacZ*ΔM15 Δ(*lacZYA-argF*)U169, hsdR17(rK^-mK^+), λ$^-$
- *E coli* XL1-Blue (cloning): endA1 gyrA96(nal^R) thi-1 recA1 relA1 lac glnV44 F'[::Tn10 proAB$^+$ lacI^q Δ(lacZ)M15] hsdR17(rK^- mK^+).
- *E. coli* HT115 (RNAi feeding): F-, mcrA, mcrB, IN (rrnD-rrnE)1, λ-, rnc14::Tn10 (DE3 lysogen: lacUV5 promoter -T7 polymerase) (IPTG-inducible T7 polymerase) (RNase III minus). The Tn10 transposon interrupting the rnc14 gene carries a tetracycline resistance gene.
- *Saccharomyces cerevisiae* L40: *MATa his3Δ200 trp1-901 leu2-3112 ade2 LYS::(4lexAop-HIS3) URA3::(8lexAop-LacZ)GAL4.*

3.4. DNA work

3.4.1. Miniprep

To prepare plasmid DNA, the *Wizard Plus SV Minipreps DNA Purification System* (Promega, #A1460) was used according to the manufacturer's instructions.

3.4.2. Analytical or diagnostic restriction digest of plasmid DNA

To determine the identity of a plasmid, a test digest was performed: 800 ng DNA, 0.2 µl restriction enzyme (20 U/µl, NEB), 2 µl 10x digestion buffer and water to reach 20 µl were mixed, spun down and incubated for 1 hour at 37°C.

2 µl 10x DNA-loading dye were added to the reaction and 5 – 10 µl were analyzed on a 0.8 % - 1.5 % agarose gel. 200 ng of undigested DNA were always loaded as a control.

3.4.3. Agarose gel analysis

The appropriate amount of agarose was dissolved in 1x TBE buffer by boiling using the microwave. For example, 1 g agarose in 100 ml TBE for a 1 % gel. When the solution cooled to a temperature of about 50-60°C, 1 µl ethidium bromide per 100 ml was added and the gel was poured into horizontal gel casting stand. Samples mixed with 10x DNA loading dye were run for 30 min (or longer when required) at constant 120 V and maximum of 200 mA.

3.4.4. Phenol chloroform purification of DNA

To 500 µl DNA were added: 15 µl of 1M Tris-HCl (pH 7.5) and 400 µl PCI. The two phases were mixed vigorously. Phases were separated by centrifugation for 5 min, 13,000 rpm at room temperature. The upper phase was taken to a new tube and 350 µl CI were added. This was mixed and centrifuged at 13,000 rpm for 5 min at room temperature. The last step was repeated once more and supernatant was recovered into a fresh tube.

3.4.4.1. Precipitation of DNA

To precipitate the DNA, 1/10 of the resulting volume of 3M NaOAc (pH 5.2) and 2.5 times the volume of 100 % ethanol were added, mixed well and incubated at -20°C for at least one hour. The DNA was pelleted for 15 min at 13,000 rpm and 4°C. The supernatant was removed using a drawn out glass pipette. The pellet was washed with 1 ml cold 75 % ethanol. After centrifugation for 5 min at 4°C and 13,000 rpm the supernatant was removed using a drawn out glass pasteur pipette. The pellet was air-dried and resuspended in water.

3.4.5. DNA sample sequencing

A sequencing reaction was composed of 1 µl of 5X buffer, 1 µl of DNA, 1 µl of 4 µM primer (see list of primers in Appendix 7.2), 0.5 µl of enzyme-nucleotide mixture (BigDye, Life Technology #66102), and volume was adjusted to 10 µl with water

PCR program (Biometra thermocycler, Analytikjena)

1. 95°C for 15 seconds
2. 95°C for 40 seconds
3. 50°C for 40 seconds
4. 62°C for 4 minutes
5. go to step 2. 40 times
6. Room temperature forever

10 µl of water was added to each tube after PCR and transferred to 1.7 ml tubes. DNA was precipitated with standard protocol with slight adjustment (see section 3.4.4.1 Precipitation of DNA). Samples were centrifuges immediately at full speed for 30 minutes and washed with 200 µl of 70 % ethanol. After a centrifugation for 5 minutes at full speed, supernatant (70 % ethanol) was discarded and samples were dried for 15 min with open lid at 37°C before submission to in house capillary sequencing (3130xl Genetic Analyzer, Applied Biosystems, Hitachi).

3.4.6. Transformation of bacterial cells

For electro-competent cells, 100 µl of -80°C-frozen XL1-Blue electro-competent cells were thawed on ice, 900 µl ice-cold water was added and gently mixed by pipetting. 1 µl Miniprep DNA (1:500 dilution) was pipetted into a cuvette. 100 µl diluted bacteria were added on top. Cells were incubated on ice for 5 to 10 minutes and then electroporated at 2.4 V. Immediately after electroporation 900 µl pre-warmed SOC medium was added, the solution was transferred to a fresh 1.7 ml tube and shaken for 1 hour at 37°C; 50 µl were plated on an agar plates containing the required antibiotics. The remaining 950 µl were spun 2 min at 4000 rpm. The bacterial pellet was resuspended in 50 µl LB medium and spread on an additional plate. All plates were incubated over night at 37°C.

For chemical competent cells, 100 µl of -80°C-frozen DH5α chemical competent cells were thawed on ice and added to 1 µl Miniprep DNA (1:500 dilution) or 5 µl of a column-purified ligation. Cells and DNA were gently mixed by flicking the bottom of tubes. Subsequently, cells were incubated on ice for 5 to 10 minutes and then placed for 45 seconds in 42°C for heat shock. Immediately thereafter, tubes were placed on ice for 5 minutes. 900 µl of pre-warmed SOC medium was added and shaken for 1 hour at 37°C. Cells were plated as described above.

3.4.7. Making glycerol stock of bacterial cultures

500 µl LB medium containing the appropriate antibiotic was inoculated with a single bacterial colony. The culture was grown for 8 hours at 220 rpm and 37°C. 500 µl of the culture was mixed with 500 µl of 40 % sterile glycerol by vortexing. Cells were frozen immediately at -80°C.

3.5. RNA work
3.5.1. RNA extraction

To extract total RNA, worm samples were frozen in liquid nitrogen. 200 µl Trizol was added was added approximately 5 µl of hand-picked worms and 500 µl Trizol to a pellet of approximately 1 million isolated PGCs and shaken in a thermoshaker (Eppendorf) for 10 minutes at 65°C at 1400 rpm. 1/5 volume of chloroform was added and shaken vigorously by hand for about 15 seconds. Samples were kept at room temperature for about 3 minutes to allow phase separation, then centrifuged at full speed for about 15 min at 4°C. The supernatant was carefully taken to a new 1.7 ml tube and RNA was precipitated with equal volume of 100 % isopropanol for approximately 10 min. The tubes were subsequently centrifuged at full speed for 15 min at 4°C and pellets were washed twice with 1 ml of 75 % ethanol, each time centrifuged at full speed for 5 minutes at 4°C. The 75 % ethanol was removed completely and pelleted RNA was briefly dried at room temperature (not more than 5 minutes). Samples were resuspended in 10 to 20 µl of water.

3.5.2. Denaturing agarose gel electrophoresis
3.5.2.1. Preparation of RNA sample for denaturing agarose gel analysis

Per sample the following reagents were assembled freshly before running the samples: 12.5 µl of deionized Formamide, 4.3 µl of 37 % Formaldehyde, 2.5 µl of 10x MOPS, 2.5 µl RNA loading buffer ("Orange G"), 0.5 µl 1 % ethidium bromide (SERVA) and 3 µl RNA or an RNA pellet and with extra 3 µl ddH$_2$O. After assembly, the 1.7 ml tubes were racked three times to mix, spun down, heated at 96°C for 2 min in a heating block, again racked three times, spun down and samples were loaded immediately.

3.5.2.2. Gel casting and electrophoresis

Using a flamed spoon, 0.5 g agarose were weighed into an autoclaved conical flask containing a flamed stir bar. 50 ml of sterile ddH$_2$O was added. Agarose was dissolved by heating in a microwave. The solution was stirred for about 10 min and cooled to about 60°C. While stirring, 5.85 ml 10x MOPS and 1.75 ml of 37 % Formaldehyde were added. The mixture was poured into a horizontal gel casting stand. A loaded gel was run in 1x MOPS at constant 90 V and maximum 200 mA for 90 min.

3.5.3. cDNA generation by reverse transcription

Total RNA was denatured exactly three minutes at 96°C and put on ice water immediately. The cooled sample was spun down and divided into a RT+ and a RT- sample. The reverse transcription reaction was performed according to RevertAid premium manual using components of the RevertAid premium kit (Thermo Fisher Scientific #K1622)

The following reaction was assembled on ice in 0.2 ml PCR tubes:

Components	RT+ sample	RT- sample
5x RT Buffer	4 µl	4 µl
Primers (100 pmol)	1 µl	1 µl
dNTPs (10 mM)	1 µl	1 µl
RiboLock RNAse inhibitor (20U)	0.5 µl	0.5 µl
ddH$_2$O	up to 20 µl	up to 20 µl
Total RNA template	1 pg - 5 µg	1 pg - 5 µg
Revert Aid Reverse transcriptase (200 U/µl)	1 µl	-

When oligo dT anchor primers were used, reactions were incubated for 30 minutes at 50°C. When random hexamer primers were used, reactions were first incubated for 10 minutes at 25°C followed by incubation for 30 min at 50°C. Reactions were terminated by heating for 5 min at 58°C.

3.5.4. Quantitative reverse transcription PCR (qRT-PCR)

For quantitative analysis of the expression level of transcripts, quantitative reverse transcription PCR was performed on a CFX Connect Real-Time PCR detection system (BioRad) using SYBR green to detect the PCR products. The following reagents were assembled in 96 well plates (Thermofast96 non skirted, Abgene #AB-0600): 2 µl template and 8 µl master mix. 8 µl of master mix was composed of 5 µl absolute SYBR green mix (ThermoFisher #AB-1166/B) and 3 µl primer pairs. 96 well plate was sealed with Ultraclear cap strips (Abgene #AB-0866)

The following PCR program was run:

1. 95°C for 15 minutes
2. 95°C for 30 seconds
2. 60°C for 1 minute
4. 72°C for 30 seconds
5. go to step 2. 40 times
6. 95°C for 1 minute 60°C for 30 seconds
7. 96°C for 30 seconds

3.6. Protein work

3.6.1. Polyacrylamide gel electrophoresis (PAGE)

SDS-polyacrylamide gel electrophoresis (SDS-PAGE) was carried out for the analysis of protein extracts (Details of protein extract preparations can be found in section 3.7.2 for yeast and section 3.8.5 for worm; embryos and adult worms). SDS-polyacrylamide gels were prepared using the PROTEAN-minigel system (BioRad).

For a 10 % gel, 1.75 ml of distilled water, 1.88 ml of 1M Tris-HCl (pH8.8), 1.25 ml of 40 % Acrylamide, 50 µl of 10 % SDS, 40 µl of TEMED (Sigma #T9281), and 10 µl of Ammonium sulphate (APS) (ROTH #7869.1) were gently mixed together. Upon addition of TEMED and APS, gels were poured immediately. 100 % Isopropanol was gently added as a top layer. Once solidified, isopropanol was removed, a 4 % PAA stacking gel was poured on top and a comb was inserted. Gels were run in 1x SDS-PAGE running buffer at 25 mA per gel and a maximum of 200 V for 1 hour.

3.6.2. Western blotting

Resolved proteins were transferred and immobilized on a nitrocellulose membrane by Western blotting using the Mini-Trans-Blot Cell system (BioRad). BA 85 Nitrocellulose (NC) membranes (Millipore, GE health care) were soaked in ddH$_2$O. Subsequently, the NC membrane and filter papers (Whatman, #3030917) were soaked briefly in 1x blotting buffer.

A PAA gel was then overlaid with a NC membrane and both were sandwiched between filter papers. The assembly was placed in a cassette and blotted in a cold room or on ice at 400 mA and maximum of 180 V for two hours.

3.6.3. Immunodetection of blotted proteins

For detection of blotted proteins, nitrocellulose membranes were blocked with 5 % milk diluted in PBST for 15 minutes at room temperature. Primary antibodies (Appendix 7.1) were added for overnight incubation in 0.5 % milk in PBST. However, for GRIF-1 antibodies which were used as supernatants or as highly concentrated purified antibody, to avoid unspecific background signal, the primary antibodies were used in 5 % milk in PBST. Primary antibody incubation was often performed overnight at $4^{o}C$ and in extremely rare cases for three to four hours at room temperature. After primary antibody incubation, membranes were washed three times for 5 minutes each with PBST on a rocking benchtop shaker. Thereafter, membranes were incubated with horseradish peroxidase-linked secondary antibodies diluted at 1 to 20,000 in 0.5 % milk in PBST for one hour at room temperature. Membranes were then washed again as described before and proteins were detected and visualized in the dark with chemiluminescent substrates (ECL, Promega #0000265789/90) and detected by X-ray film.

3.6.4. Re-probing of nitrocellulose membranes

Membranes were washed in PBST twice in PBST for 5 min each. Membranes were carefully placed inside a 50 ml Falcon tube filled with stripping solution (2 % acetic acid, 0.5 % SDS) and incubated at $55^{o}C$ for 30 min. Subsequently, membranes were rinsed with distilled water to removed excess stripping solution and then incubated and washed on a shaking platform three times 10 min each with distilled water. Membranes were subsequently washed with PBST for a minimum duration of 30 min. Membranes were re-probed immediately or stored at $4^{o}C$ for later use. To re-probe membranes, they were again blocked with 5 % milk in PBST and primary antibodies were applied as described in section 3.6.3

All primary antibodies used for western blotting are summarized in Appendix 7.1.
Secondary antibodies:
HRP-conjugated anti-mouse, anti-rabbit or anti-guinea pig secondary antibodies (Jackson Laboratories) were applied at a dilution of either 1:20,000 or 1:40,000 in 0.5 % milk in PBST.

3.6.5. Coomassie staining

After electrophoresis, when required, gels were stained with Coomassie Brillant Blue solution, with gentle agitation at room temperature for 2 hours. Subsequently, gels were de-

stained in the Coomassie destaining solution for 1 hour, washed briefly with tap water, placed in a plastic sleeve and scanned.

3.7. Yeast work

3.7.1. Transformation of yeast

Yeast colonies expressing proteins whose interactions are to be tested were generated through transformation according to (Gietz and Woods 2002). L40 reporter yeast strain is streaked out on a YPD agar plate and incubated at 30°C. From this plate, 20 ml YPD media was inoculated and grown overnight at 30°C. The next day, the culture was used for transformation at a concentration of 5×10^{6} cells/ml. Yeast was grown to optical density 600 (OD600) of less than 1 usually 0.7 and the yeast cells were harvested at 300 rpm for 5 minutes and washed with 25 ml of ddH_2O. Afterwards, the yeast cells were pelleted, resuspended in 1 ml of 0.1 M lithium acetate (LiAc) (AppliChem #A3478), and transferred to 1.7 ml tube, and harvested in the 1.7 ml tube by spinning down at 15000 rcf for 15 seconds, supernatant was discarded and cells were gently resuspended in 400 µl of 0.1 M LiAc. The suspension was distributed equally into ten 1.7 ml tubes for individual transformation. Cells were harvested as before and the supernatant was discarded. 326 µl of transformation mixture containing 36 µl of 1 M LiAc, 240 µl of 50 % PEG and 40 µl of denatured 2 mg/ml salmon sperm DNA was added to each tube. Before salmon sperm DNA was added, it was boiled at 96°C for 5 minutes and then immediately chilled on ice. Thereafter, the combinations of two plasmids to be transformed into the yeast cells was added at a total concentration of 200-500 ng each in 34 µl of water to generate a single transformation DNA mix. Each tube which contained a yeast pellet and 400 µl of transformation mix was then vortexed, racked vigorously, and incubated at 30°C for 25 minutes. Transformation of DNA was then induced by a heat shock at 42°C for 25 minutes. Afterwards, the yeast cells were collected by spinning at 4000 rpm for just 15 seconds and subsequently resuspended in 0.5 ml of ddH_2O. 100 µl of the cell suspension was plated on synthetic double drop out agar plates (SD-Leu-Trp) to select for transformation with pACT(-2) and pLex(kn2) plasmids. The rest of cell suspension was harvested and plated in 100 µl of water as a precaution for poor transformation. The plates were incubated at 30°C for growth of transformed colonies. The colonies were then used in a beta-galactosidase (blue-white) Y2H assay.

3.7.2. Beta-galactosidase (blue-white) Yeast 2-Hybrid assay

For blue-white beta-galactosidase assay, using hand-held P200 tip, yeast colonies were streaked out on nitrocellulose (NC) membrane placed on drop out agar plate and on a

replica drop out agar plate without NC membrane. The plates were incubated overnight at room temperature. In the morning of the second day, a chromatography paper is soaked in 1.6 ml of X-gal-containing Z-buffer placed in the lid of an empty petri dish. NC membrane was removed from agar with forceps and dipped. After 15 seconds, NC membrane was pulled out and placed on a molecular bench for thawing at room temperature. Subsequently, NC membrane was transferred onto soaked chromatography paper as earlier described. The petri dish is closed and wrapped with parafilm and incubated at 37 ^{o}C until an intense blue color is observed for the positive control (and possibly other test samples). Image of color development is taken every hour. When chromatography paper becomes dry, additional Z buffer was added. Experiments were terminated before the negative controls become blue.

3.7.3. Determination of protein expression after Yeast 2-Hybrid assay

To test whether proteins are expressed in yeasts, colonies to be tested (from replica plates) were inoculated into 10 ml of selective drop-out media at 30°C. The next day, OD600 of cells were checked to be certain it was below 1.5, otherwise, the cells were diluted to OD of 0.4 and grown again. Then a total of 4 OD units was harvested and used for protein extraction. To this end, cells were harvested at 4000 rpm for 5 min and placed on ice. The cells were washed with 1 ml of 20 % trichloro acetic acid (TCA) and then transferred to 1.7 ml tubes. These suspensions were pelleted at full speed for 1 min and the supernatant were discarded. At this point, pellet was either kept at -20°C for later or the extraction process was completed immediately. After resuspension in 200 µl of 20 % TCA, 200 µl of glass beads (Sigma) were added and the slurry was vortexed twice of for 30 seconds each and twice 10 min in bead beater. Samples were collected at the bottom of the tube with a brief spin of less than 5 seconds and the supernatant were saved using long-nosed tips. The extraction process was repeated using 200 µl of 5 % TCA and supernatant of the second extraction was combined with that of 20 % TCA. The proteins were precipitated from the supernatant by gentle centrifugation; 3000 rpm, 10 minutes at room temperature. Supernatants were discarded and 200 µl of 2x SDS sample buffer were added immediately and resuspended by shaking in thermoshaker for 10 minutes at 95°C. Materials that were not dissolved were pelleted by centrifugation at 3000 rpm for 10 minutes at room temperature. Supernatant were saved to new tubes and 10 to 15 µl were analyzed by SDS PAGE-western blot. The remaining extract were stored at -20°C and used later if required. Detection of Gal4 fusions were done with HA-specific monoclonal antibodies, or antibodies to protein of interest. LexA fusion proteins were detected by LexA-specific antibody, or antibodies to proteins of interest (see Appendix 7.1).

3.8. Worms work

All nematode strains were handled according to standard procedures (Brenner 1974). Except otherwise stated in a particular experiment, worms were grown and maintained on NGM plates seeded with *E. coli* OP50 at 20°C. In all experiments, Bristol N2 was used as wild type. All worm experiments were carried out at 20°C unless otherwise stated. Furthermore, all phenotypes were analyzed 24 hours past mid-L4 at 20°C and 18 to 20 hours past mid-L4 at 25°C. All crosses were performed according to Brenner, 1974.

3.8.1. Genotyping of worm strains

To genotype mutations in any particular locus, PCR was used on DNA material obtained after proteinase K (PK) treatment. PK treatment was carried out by treating each worm with 0.2 U/µl PK enzyme in 8 µl PK buffer for 75 min at 60°C. 2µl of obtained DNA solution was used as template in PCR reactions. In some cases, nested PCR was performed by using 0.5 µl of the first PCR reaction as a template in the second reaction. PCR was performed in Biometra thermocycler (Analytikjena). Upon completion of PCR, 5 to 10 µl of the reactions were analyzed by agarose gel electrophoresis (see section 3.4.3). All primers used for genotyping are summarized in Appendix 7.2.

The standard PCR reaction mixes included:
- water 13.55 µl
- 10x PCR buffer- 2 µl
- forward primer (10 µM)- 1 µl
- reverse primer (10 µM)- 1 µl
- dNTPs (10 mM)- 0.4 µl
- Taq/Pfu polymerase – 0.05 µl
- Template DNA- 2 µl

PCR program

Reaction conditions		
steps	Temperature ^{o}C	time
1	95	4 min
2	95	50 seconds
3	56	45 seconds
4	72	2 min
5	Go to 2, 34 times	
6	72	7 min
7	20	20 seconds
8	end	

3.8.2. Genomic engineering and transgenesis

Except for two strains, *grif-1(ok1610)* and *grif-1(tm2559),* obtained from *C elegans* deletion consortium, all genomic mutations in *grif-1* locus were generated using the CRISPR/Cas9 technique (Ran, Hsu et al. 2013) (see the below section). To express transgenes of choice, the Mos-1-mediated Single Copy Insertion (MosSCI) genome engineering technique was used (Zeiser, Frokjaer-Jensen et al. 2011). Double and triple mutants were generated by crosses. Strains and how they were generated is summarized in Appendix 7.3.

3.8.2.1. RNP-based CRISPR/Cas9 genomic engineering

CRISPR/Cas9 is a genetic engineering technique that allows for quick and robust modifications of genome of an organism. It is an adaptation of bacterial defense system which employs Cas9 enzyme as endonuclease and a guide RNA for targeting unit. To this end, RNP mixes containing purified Cas9, guide RNAs, and when required, repair templates (see below for more details) were injected into wild-type worms. To produce guide RNAs, DNA sequences of single guide RNAs (sgRNAs) were clone into the pDR274 plasmid, replacing the existing sequence of a zebrafish sgRNA (Hwang, Fu et al. 2013). After cloning, a DNA template sequence of approximately 300 bp for *in vitro* transcription was generated using primers CE5255 and CE5256. Prior to column purification, the original plasmid template was digested using DpnI (NEB). Subsequently, the guide RNA was *in vitro* transcribed for 2 hours at $37^{o}C$ and the resultant RNA was purified using phenol-chloroform extraction, ethanol precipitation (see section 3.4.4) and then resuspended in 10 µl of ddH_2O.

In vitro transcription reaction

- 4 µl 5X transcription buffer (Ambion)
- 2 µl DTT (100mM)
- 0.5 µl RNAsin ribonuclease inhibitor (Thermo Fisher Scientific)
- 4 µl rNTP mix (10mM) (Fermentas)
- 1 µl DNA template (1 µg/µl)
- 1 µl T7 phage RNA polymerase (Ambion)
- 7.5 µl nuclease free H_2O

RNP mixture for injection

- 1-2 µg purified sgRNA
- 1 µl repair template (10 µM)
- 0.5 µl Cas9 buffer 10x (150mM NaCl, 200mM Hepes-KOH (pH 7.5))
- 0.5 µl Cas9 endonuclease enzyme (5 µg/µl) (MPI-CBG protein facility)
- Volume adjusted to 5 µl with H_2O

Mixture was incubated at room temperature for 5 minutes before injection.

The assembled RNP mixes were injected into the gonads of young adult hermaphrodites. F1 worms were screened for the desired mutation using genotyping PCR (see section 3.8.1). To make screening easier, a co-CRISPR strategy was employed to determine the success of injection and the activity of Cas9 (Paix, Wang et al. 2014). In this strategy, a second marker sgRNA was generated for the *dpy-10* gene. The mixture for *dpy-10* sgRNA and sgRNA of choice were combined before injection. Concomitant injection of both sgRNAs caused mutation at *dpy-10* locus leading to *Dpy* phenotypes (Roller, Dumpy and Dumpy-Roller) and mutation of locus of choice. Visual inspection to see *dpy-10* phenotypes were performed and plates with high percentage of rollers were screened with PCR for genomic changes of choice at desired locus. Upon identification of the worm carrying the correct desired modification, a worm which is wild type in *dpy-10* locus segregated by heterozygote roller mother carrying the desired modification is selected.

Appendix 7.4 summarizes the guides and repair templates that were used to generate desired changes in *grif-1* locus.

3.8.2.2. Identification and confirmation of genomic changes

All changes at the genomic locus of *grif-1,* including those generated by CRISPR/Cas9 and those obtained from external sources, were confirmed by sequencing corresponding PCR amplicons (see Appendix 7.2 for list of primers and section 3.4.5. for sequencing).

Additionally, total RNA was extracted from *ok1610* and *tm2559* (see section 3.5.1. RNA extraction), converted to cDNA (see section 3.5.3. cDNA generation by reverse transcription), cloned into the pJet1.2 plasmid according to manufacturer's instructions (Thermo Fisher Scientific, CloneJet PCR cloning Kit) and sequenced (see section 3.4.5. Sequencing). All clones of *tm2559* cDNA produced identical sequences, which were used for a theorical prediction. *ok1610* contains a deletion that affects exon-intron junction. Of the 6 clones that were sequenced, 4 were identical while the remaining two had unique sequences affected in the exon-intron junction. This suggests that although splicing at this junction may be affected by the deletion, one transcript is still predominantly produced. The theoretical prediction of GRIF^{ok1610} is based on this transcript.

3.8.2.3. Transgenesis by MosSCI

Ectopic expression of *grif-1,* establishment of transgenic strains expressing *grif-1 3'UTR* translational reporter, and those expressing either full-length or N-terminally truncated GLD-2 protein were all achieved through MosSCI transgenesis technique (Frokjaer-Jensen, Davis et al. 2012). To this end, EG6699 *unc-119* animals were injected with a mix of six plasmids that are important to surveil the injection procedure and to select for transgene integration at defined locus on linkage group II (LG II) (see below for injection mix). Next, animals were singled into individual plates and kept at 25°C until starvation, which typically takes about a week and half. Moving worms are an indication of successful experiment, as *unc-119* is reintroduced together with the desired transgene. Plates containing moving worms were heat shocked at 34°C for 4 hours to induce expression of *peel-1;* a toxic gene. This heat shock selectively kills worms carrying an extrachromosomal array made of concatemerized plasmids. After recovery at 25°C for about 4 hours, plates were screened for moving worms that do not express co-injections markers (Table 1). Movers were singled and their progenies were analyzed with PCR for the integration of construct of choice into MosSCI locus on LGII using the following primer combinations: CE3376 and CE2640 for primary PCR and CE4314 and CE2634 for secondary PCR. A PCR product of approximately

1.5 kb is expected in transgenic worms while no product is expected from non-transgenic worms

Plasmid	Description	Purpose	Concentration in mix
pCFJ601	Peft-3::transposase	Transposase enzyme	50 ng/µl
pGH8	Prab-3::mCherry	pan-neuronal marker	10 ng/µl
pMA122	Phsp::peel-1	Selection	10 ng/µl
pCFJ90	Pmyo-2:: mCherry	Pharynx muscle marker	2.5 ng/µl
pCFJ104	Pmyo-3:: mCherry	Body muscle marker	5 ng/µl
pNJ derivatives	Targeting construct	Desired transgene unc-119 rescue	10 – 50 ng/µl

Table 1. Injection mix used for MosSCI mediated transgenesis

3.8.3. RNAi-mediated knockdown experiments

RNAi constructs were made from cDNA or genomic DNA of *grif-1, nos-2,* and *ntl-9* via PCR and cloned into pL4440 (see Appendix 7.2 for list of primers). Correct insertion was analyzed by restriction digestion and sequencing (see section 3.4. for miniprep, restriction digest analysis, and sequencing). Newly cloned constructs and those that already existed in the lab such as *pbs-6, pas-5, lgg-1* (Kisielnicka, Minasaki et al. 2018), and *gld-2* (Wang, Eckmann et al. 2002) were then transformed into HT115 *E. coli* bacterial strain. Bacteria were grown overnight on NGM plates containing tetracycline and ampicillin (15 µg/µl and 50 µg/µl, respectively). Single colonies were selected and grown overnight in 20 ml of ampicillin-containing LB media. After overnight growth, bacteria were harvested in 50 ml tubes, spun down at 3800 rpm for 8 minutes, washed in 20 ml LB and resuspended in 2 ml of ampicillin-containing LB. To induce dsRNA production, 1mM Isopropyl-beta-D-thiogalactopyranoside (IPTG) was added to samples and incubated at room temperature in the dark for 1 hour. Bacteria were then spotted onto NGM plates containing 25 µg/ml of carbenicillin and 1 mM IPTG.

For *grif-1, lgg-1, nos-2,* and *ntl-9* knockdown, RNAi was initiated from L1 stage. F1 were either analyzed during embryogenesis for changes in protein expression or allowed to grow to adulthood for sterility analysis and analysis of associated germline phenotypes. For *pbs-6, pas-5* and *gld-2* RNAi, young adults were treated with RNAi. F1 were either analyzed during embryogenesis for changes in protein expression or allowed to grow to adulthood for sterility analysis.

3.8.4. Analysis of fertility and fecundity
3.8.4.1. Determination of brood size

To determine the brood size of any genotype, L4 hermaphrodite animals were individually transferred on separate plates. They were moved every 24 hours to new plates (for *grif-1,* F2 descendants of heterozygotes were analyzed). The sired embryos from which

the mother had just been removed were given another 24 hours to hatch. After 24 hours, the hatched larvae were counted as living progenies, the unhatched embryo were counted as dead embryos and a sum of the two from four days was taken as the total brood size of the mother.

3.8.4.2. Brood size of transgenerational analysis at 25°C

For determination of brood size during transgenerational assay (see Figure 4.6.1.1). Wild-type or F2 *grif-1* adults grown at 20 degree centigrade were dissolved with bleach solution to harvest embryos. Harvested embryos were then allowed to hatch into L1 animals in M9 buffer. Synchronised L1 population were then spotted into OP50-seeded NGM plates incubated at 25-degree centigrade. The spotted animals were regarded at P0 in this experiment. Brood sizes were determined at each generation as above.

3.8.4.3. Determination of sterility

To determine the percentage of sterility in F1 progenies, P0 mutant or RNAi-treated mothers were singled on OP50 or RNAi plates, respectively. Mothers were allowed to lay progenies (F1) and shifted to new plates every 24 hour. The sired F1 progenies were analyzed at adulthood. F1 adults with no embryo in the uterus were scored as sterile, while those containing at least a single embryo in the uterus were scored as fertile.

3.8.5. Preparation of animals for western blot experiments
3.8.5.1. Embryo protein sample

To obtain embryonic samples for robust detection of GRIF-1 proteins in immunoblotting, a minimum of 2000 embryos was required, preferably more. Therefore, embryos harvested from several 6 cm or two 10 cm NGM plates filled with a lot of gravid adults by washing with M9 buffer and transferred into 1.7 ml or 15 ml tubes, respectively. Thereafter, to harvest embryos from the mixed populations, the samples were treated with bleach solution for 5 minutes with vigorous shaking. Mild treatment with bleach solution selectively dissolves animals with soft tissue; larvae and adults, and leaves embryo intact. The recovered embryos were transferred into several 1.7 ml tubes generating a pellet of approximately 100 µl each, when working with 10 cm NGM plates, and washed three times with M9. For each wash, 1 ml of M9 buffer is added to embryos per tube. Embryos were resuspended by shaking and pelleted at 2000 rpm for 1 min. After a minimum of three washes with M9, embryos were pelleted, supernatant completely removed, and the pellet snap frozen in liquid nitrogen. 2X SDS sample buffer was added to the embryos at a ratio of 100 embryos/µl. Protein samples were boiled at 96°C for five minutes and further sonicated in a water-bath sonicator (Bandelin) that is heated to 80°C for 10 minutes. Samples were

centrifuged at 15000 rpm for 1 min to generate a pellet of non-dissolvable materials. Supernatants were loaded on gel and analyzed with western blots (see section 3.6.1).

3.8.5.2. Adult worm protein sample

For adult worm samples, depending on the expression levels of protein of choice, either 30 or 60 adult worms (usually 24 hours past mid-L4 at 20°C) were hand-picked under dissecting microscope and placed inside 100 µl of M9 buffer. The 1.7 ml tube containing worms and M9 buffer was then centrifuged at 1000 rpm for 10 seconds and placed on ice immediately afterwards to collect the worms at the bottom of the tube. The supernatant was carefully removed and another 100 µl of M9 was added to wash the worms. After two washes, the supernatant was aspirated to a minimum of approximately 10 µl of M9. The tubes were then placed in liquid nitrogen to snap freeze the sample. 15 µl of boiled 2x SDS sample buffer was then added to the tubes, boiled afterwards for 5 min at 96°C, and sonicated in water bath as described for embryos. Samples were centrifuged at 15000 rpm for 1 min to generate a pellet of non-dissolvable materials. Supernatants were loaded on gel and analyzed with western blots (see section 3.6.1).

3.8.6. Immunofluorescence analysis of embryos

To isolate embryos for immunofluorescence staining, typically 35 gravid mothers are placed into 8 µl of M9 on a coverslip (Menzel Gläser) and cut open around the vulva. The wiggly worms then released their embryos and the coverslip was transferred to standard microscope glass slide (Marienfeld), which had been coated with poly-lysine. The glass slide was immediately placed pre-cooled metal plate (on dry ice) for minimum of 15 minutes to freeze crack the egg shell on dry ice (Strome and Wood 1982, Duerr 2013). Thereafter, coverslips were removed and glass sides with freeze-cracked embryos were gently submerged for 10 minutes in dry ice-cold 100 % methanol (-20°C also works). After 10 minutes, the samples were transferred to into 100 % acetone at the same temperature as methanol for permeabilization for 5 minutes. Samples were removed from acetone and kept for 3 to 5 minutes at room temperature as an optional step. Then, to rehydrate the samples, they were submerged into 1xPBS for 5 minutes and subsequently blocked with PBSB (PBS + 0.5 % BSA) for 30 minutes at room temperature or longer at 4°C in a humidified chamber. Primary antibodies, which were diluted with PBSB, were applied overnight at 4°C. The next day, samples were washed three times with 100 µl PBSB and samples were then incubated with secondary antibodies which were diluted in PBSB. Samples were then washed again three times as before and mounted in 8 µl of Vectashield antifade medium (Vector laboratories). Slides were dried in dark for about 10 minutes at room temperature and sealed on three sides with transparent nail polish.

In most immunofluorescent experiments, PGL-1 intensity was used as a positive control for correct localization and tissue penetration. Axiovision Software (Zeiss) was used for acquisition of wide-field images on an Imager M1 microscope (Zeiss). Images were processed in Photoshop CS6 (Adobe) and labelled in Illustrator CS6 (Adobe).

All primary antibodies used for western blotting are summarized in Appendix 7.5.
Secondary antibodies:
Cy5-, Cy3- or FITC-conjugated AffiniPure donkey anti-rabbit, -mouse or -guinea pig IgG antibodies (Jackdon Laboratories) were used as secondary antibody. They were applied at a dilution of 1:1000 (final concentration of 0.75 µg/ml) from a stock solution of 0.75 mg/ml.

3.8.7. Large scale worm culture to harvest embryos and worms for large scale experiments

Since some of the experiments performed in this study such as co-immunoprecipitation and isolation of PGCs from embryos were done on a relatively large scale, lots of embryos had to be produced to get adequate amount of materials for such experiments.

To this end, four freshly starved 6 cm worm plates were washed with 4 ml of M9 buffer into 1.7 ml tubes. Worms were either placed on ice for about 5 min to allow them to settle or worms were pelleted at 1000 rpm for 1 min. After removing supernatant, were worms were combined into a single tube and resuspended in total of 1 ml of M9 buffer. 100 µl of worm suspension in M9 buffer were spotted on 10 cm NGM plates seeded with OP50 bacteria. These plates were placed at 20°C and allowed to grow until a vast majority of the worms were gravid adults, this usually take approximately 4 to 6 days, depending on the age and density of worms on the initial 4 plates. During this period, the plates were checked every day to assess the overall quality of the ongoing experiment and from the 4th day onward, special attention was placed on the food status on the plates. To avoid starvation, which has a strong impact on the gene expression program of worms, more OP50 bacteria were added to plates on which worms were running low on food and allowed to dry under laminal flow hood. When a vast majority of animals reached adulthood, worms were harvested by adding M9 to each plates and worms were pipetted into 15 ml tubes. The worms were collected at the bottom of the tube by centrifugation into at 1000 rpm for 2 minutes. Afterwards the worms were washed with 12 ml of M9 buffer and pelleted by centrifugation at 1000 rpm for 2 minutes. This washing was performed about two to three times to remove residual OP50 bacteria. Thereafter, to harvest embryos from the mixed populations, the samples were treated with bleach solution for 5 minutes with vigorous shaking. The recovered embryos were washed 3 times (washing was described before) and hatched overnight in M9 solution to get a synchronized population of L1 larvae. Synchronized

L1 larvae were distributed on new set of seeded 10 cm NGM plates at the rate of 8000 L1 larvae per plates and grown as before to adulthood. Upon reaching adulthood, the embryos produced were harvested again as described before and at this point further treatment was dependent on the application of the harvested embryos whether it is for co-immunoprecipitation or PGC isolation.

For co-immunoprecipitation, the previously washed embryos were additionally washed 2 times with B70 buffer and eventually resuspended in equal volume of B70 buffer and dripped into liquid nitrogen to form pearls. Pearls were recovered from liquid nitrogen using a sieve. Recovered pearls were used immediately or stored in appropriate tube for later co-immunoprecipitation experiment. For PGC isolation to get RNA for sequencing experiments which required *nos-2* RNAi, the L1 from the first bleaching were distributed on *nos-2* RNAi plates and grown at 25°C until adulthood. Upon reaching adulthood, recovered embryos were washed three times in M9 buffer and additionally washed in the 15 ml tubes with egg buffer and then pelleted embryos were transferred into 1.7 ml tubes for further treatment (see PGC isolation). For co-immunoprecipitation experiment in which young adult or L4 were used, the synchronized L1 larvae were grown to L4 or young adults as required and harvested and frozen as described before for embryos.

3.9. Co-Immunoprecipitation (co-IP) experiments

Co-IP experiment were performed according to Jedamzik and Eckmann, 2009 (Jedamzik and Eckmann 2009). All steps of co-immunoprecipitation, except for coupling of antibodies to protein G, were performed at 4°C and using B70 buffer. Briefly, 25 µl of Protein G-coated DynaBeads (Invitrogen) slurry were used per antibody pulldown. DynaBeads were washed several times and equilibrated with B70. A total of 10 µg of monoclonal antibodies were incubated with DynaBeads at 4°C overnight. The next day, bound antibodies were crossed-linked to protein G using 25 mM dimethyl pimelimidate (DMP, Sigma #D8388-5G) dissolved in 200 mM borate buffer for 30 min at room temperature and blocked in 100 mM ethanolamine (pH 8.2) for 2 hours. Afterwards, the cross-linked antibodies were washed four times with ice cold B70 buffer and then kept at 4°C.

In the meantime, embryos samples were prepared for co-immunoprecipitation experiment. To prepare protein samples, frozen embryo or worm pearls (see section 3.8.7) were minced in a bead mill (Retsch) to break them open. The generated powder was collected into tubes and resuspended in B70 buffer containing protease inhibitors including 2 mM Benzamidine, 1 mM DTT, 1 µg/ml pepstatin A, 1 mM PMSF, 1 µg/µl leupeptin, 0.1 mg/ml pefabloc, 1X complete protease inhibitor cocktail with EDTA (Roche). The protein samples were then centrifuged at 12000 rpm, for 15 minutes at 4°C. The supernatant protein extracts were collected and filtered with S+S Whatman Puradisc FP 30mm syringe filter (0.45 µm

pore size, GE Healthcare #10462100) and then applied to the Dynabeads cross-linked with antibodies and incubated for 1 hour at 4°C. For experiments that required RNAse treatment, 5 µg of RNAse A (Jena Bioscience #EN-173L) was added halfway through the incubation. After 1 hour, beads were collected with magnet and samples were washed three times with B70 buffer. A fourth wash was done on a rotating wheel for 5 minutes. Beads were finally collected and purified proteins were eluted in 2x SDS sample buffer. All stages of the co-immunoprecipitation procedure, including input samples, flow through (unbound fractions) and eluates were analyzed with western blotting (see section 3.6.1). All antibodies used for co-IP are summarized in Appendix 7.6.

3.10. Isolation of PGCs for FACs

PGC were isolated according to methods developed by Sangaletti and Bianchi, 2013, with slight modifications introduced by Lee et al., 2017. Briefly, after harvesting, embryos were treated with egg buffer-diluted chitinase (4 U/ml, Sigma #C6137) for a maximum of 1 hour at room temperature on a rotating wheel moving at 9 rpm. At about 30 minutes into chitinase treatment, 10 µl of embryos suspension were examined under dissecting microscope to determine the efficiency of chitin shell digestion; well digest embryos look swollen with no visible chitin shell. This is repeated every 5 minutes until more than 80 % of embryos have been digested which usually takes place at around 40 to 55 minutes into chitinase treatment. To increase efficiency, the maximum number of embryos placed into 1.7 ml tube is 1 million embryos. Thereafter, the chitinase-digested embryos were gently pelleted at 900g for three minutes at 4°C and the supernatant was removed and discarded. Subsequently, the embryos were treated with trypsinase solution (accumix solution, innovative cell technologies, AM105, used at 1:3 dilution in egg buffer) for five minutes to cause cell to cell detachment. During this treatment, the embryos were gently pipetted again the wall of the 1.7 ml tube to facilitate the detachment process and the recovered cells were then pelleted at 900g for three minutes at 4°C. Pelleted cells were gently resuspended in ice cold egg buffer and FACS sorted in collaboration with Tony Gutschner (Medical faculty, Martin Luther University, Halle).

4. Results

4.1. GLD-2/GLD-3 cytoPAP complex turnover in PGCs might be regulated by Ubiquitin Proteasome System and not the autophagy system

The GLD-2 cytoPAP complex experiences protein turnover concomitant with the birth of PGCs. Regulated turnover of cellular proteins is promoted by two major protein degradation pathways; the ubiquitin proteasome system and autophagy-mediated degradation (Papaevgeniou and Chondrogianni 2014).

4.1.1. Proteasome activity is important for embryogenesis and germ cell development
4.1.1.1. Experimental set up and condition for knockdown of proteasome factors

The Ubiquitin Proteasome System (UPS) is essential for many aspects in development (Gonczy, Echeverri et al. 2000, Takahashi, Iwasaki et al. 2002, Kamath, Fraser et al. 2003, Kahn, Rea et al. 2008, Kisielnicka, Minasaki et al. 2018). Therefore, an efficient RNAi-mediated knockdown of core proteasome factors may lead to 1-cell embryonic arrest, which will make it very difficult to reveal late stage embryonic functions of proteasome. Therefore, to assess whether the ubiquitin proteasome system promotes turnover of the GLD-2 cytoPAP complex in primordial germ cells, a partial RNAi-mediated knockdown of two proteasome core subunits, *pas-5* and *pbs-6,* was performed*.*

To achieve a partial knockdown, young adult wild-type animals were fed with *pas-5* and *pbs-6* double stranded RNA-producing bacteria that were diluted with control bacteria expressing empty constructs only. This step allows for double stranded RNA to be loaded into oocytes, yet letting some of the embryos produced to complete embryogenesis, which is roughly 800 minutes post fertilization. This will allow for the analysis of GLD-2 turnover which occurs concomitantly with the birth of PGCs at approximately 200 to 250 minutes into embryogenesis.

Time course experiments were performed to ascertain which experimental time point permits knockdown of *pas-5* and *pbs-6* and yet allows embryos to develop to the stage of PGC birth with no or very mild defects. Since PAS-5 and PBS-6 antibodies were not available to monitor knockdown efficiency during the experiments, the effectiveness of RNAi-mediated knockdown was gauged by analysing the number of embryos that hatched after different hours of feeding wild-type hermaphrodites with bacteria expressing double stranded RNA to *pas-5* and *pbs-6*. For both *pas-5* and *pbs-6* RNAi, from 18 hours of feeding RNAi onward, *pas-5* and *pbs-6* knockdown led to approximately 100 % embryonic lethality. This preliminary observation suggests that both *pas-5* and *pbs-6* RNAi are highly effective and that to carry out a detailed analysis of GLD-2 turnover in PGC, a time point before 18 hours should be chosen. Therefore, based on this preliminary experiment, a 14-16 hour window in which only a percentage of embryos experience lethality was selected for a detailed analysis

as shown in the scheme of experiment (Figure 4.1.1A). The detailed analysis performed includes determination of percentage of embryos that hatched into larvae, analysis of which percentage of those larvae developed into fertile adults and lastly, analysis of percentage of embryos in which stabilizing GLD-2 cytoPAP expression was extended into their PGCs.

4.1.1.2. Partial knockdown of *pas-5* and *pbs-6* affects embryogenesis slightly

To demonstrate efficiency of RNAi knockdown at the selected window, percentage of embryos that hatched into larvae was estimated (Figure 4.1.1B). As explained earlier, an ideal situation is to reduce proteasome function to the extent that a reasonably good percentage of embryos complete embryogenesis without overt defects. After feeding bacteria expressing *pas-5* and *pbs-6* double stranded RNA to young adults for 14 hours, 100 animals were transferred to OP50 plates to lay embryos for 2 hours before the mothers were removed from the plates (Figure 4.1.1A). The embryos laid on these new OP50 plates were analysed after 24hours by counting the number of larvae and dead embryos on the plates (Figure 4.1.1B). In control animals, greater than 99 % (n=2949) of embryos hatched into larvae. By contrast, only approximately 29 % (n=2288) and 21 % (n=2168) of *pas-5(RNAi)* and *pbs-6(RNAi)* embryos hatched into larvae, respectively (Figure 4.1.1B). The stage at which embryonic lethality occurs varied considerably (data not shown). This result shows that mild knockdown *pas-5* and *pbs-6* leads to partial embryonic lethality.

4.1.1.3. Some *pbs-6* and *pas-5* RNAi embryos are fertile as adults

Any turnover defect of maternal proteins due to *pas-5* and *pbs-6* RNAi might be because PGCs have lost germ cell character and therefore accumulate molecular phenotypes that are indirect consequences of *pas-5* and *pbs-6* RNAi. It was therefore important to analyse the ability of PGCs that experienced *pas-5* and *pbs-6* RNAi during embryogenesis to support fertility when these embryos developed into adult hermaphrodites. As even partial knockdown of *pas-5* and *pbs-6* leads to embryonic lethality, and to avoid further knockdown due to continued exposure to feeding RNAi, hatched larvae were grown on regular OP50 bacteria and analysed as adults (Figure 4.1.1A).

Although fed on OP50 bacteria, the hatched larvae still displayed somatic phenotypes during development. These somatic phenotypes were not analysed in detail but included delayed larvae development, larvae arrest and some protruding vulva in adult animals. Resultant adult animals were analysed for fertility such that animals producing at least single embryo was judged as fertile (Figure 4.1.1C). In control animals, all analysed F1 progenies were fertile (n=200). By contrast, *pas-5(RNAi)* and *pbs-6(RNAi)* F1 progenies displayed reduced fertility; approximately 63 % (n=195) and 45 % (n=101), respectively (Figure 4.1.1C). Therefore, a partial knockdown of *pas-5* and *pbs-6* induces a reduction of fertility in

F1 progenies, indicating that the knockdown does not lead to complete loss of germ cell fate in PGCs during embryogenesis and thus allows for the analyses of GLD-2 cytoPAP expression in proteasome-compromised PGCs.

A

move 100 adults to OP50
to lay embryos for 2hrs
(remove adults after 2hrs)

score F1:
% living progeny
(see panel B)

score % fertility
at adulthood
(see panel C)

+24hrs

+3days

adults (P0) $\xrightarrow[\text{14hrs}]{\text{RNAi}}$ adults (P0)

adults (P0) $\xrightarrow[\text{+1hr}]{}$ Collect F1 embryos for IF analysis (t=15 hrs RNAi)

B

C
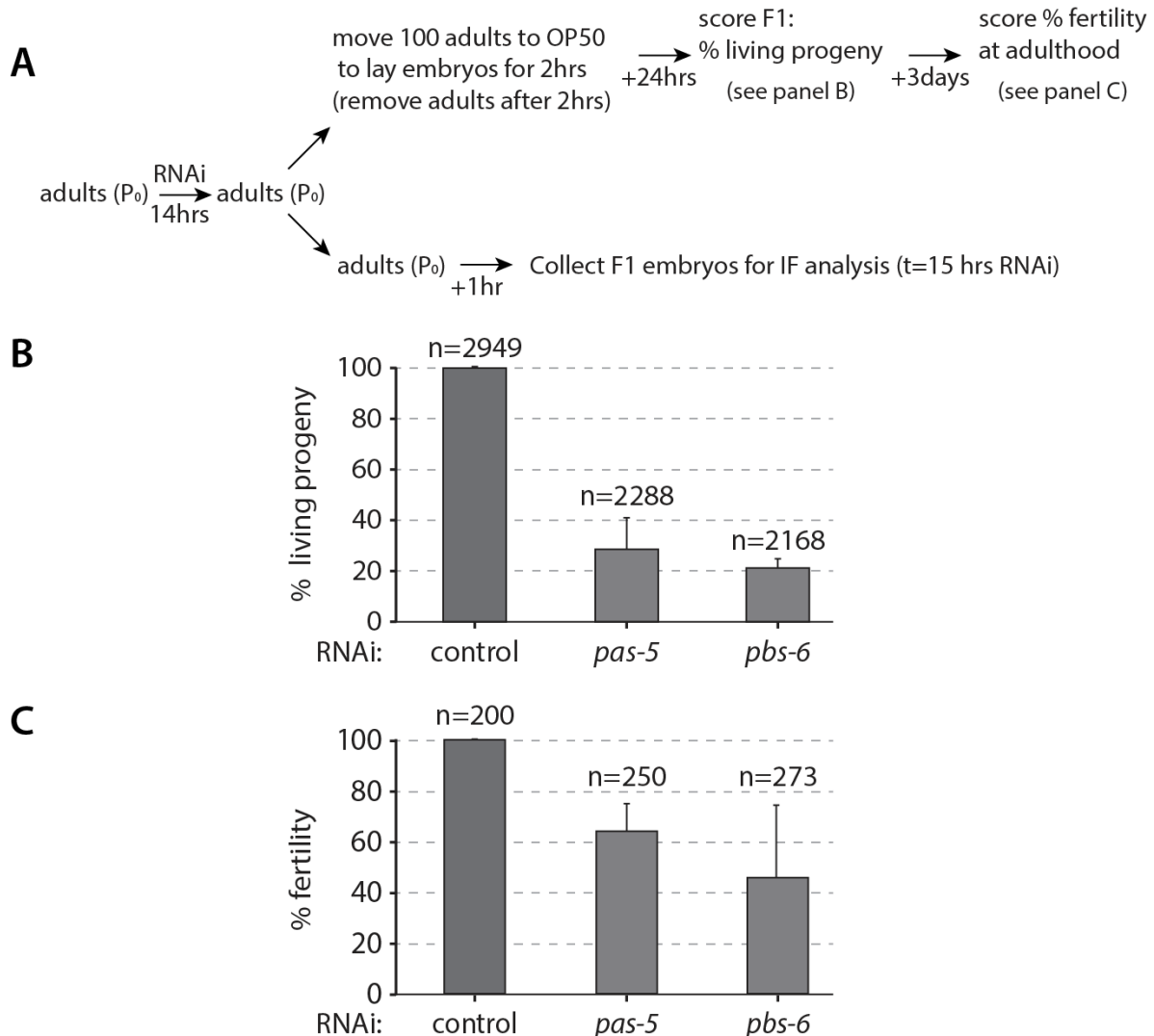
Figure 4.1.1. Knockdown of *pas-5* and *pbs-6* affects embryogenesis and germ cell development.

(A) Scheme of experimental workflow to mildly reduce proteasome expression in embryos (see main text for detailed explanation). (B) A bar graph showing the percentage of embryos that hatched into larvae after RNAi-mediated knockdown of the proteasome subunits *pas-5* and *pbs-6*. (C) A bar graph showing the percentage fertility of hatched embryos, from (B), after they reached adulthood. Adults with no embryo in the uterus were scored as sterile, while those containing at least a single embryo in the uterus were scored as fertile. Bar charts show mean (± Std. Dev). On average, 68 % (n=864) of *pas-5(RNAi)* and 56 % (n=618) of *pbs-6(RNAi)* F1 animals arrested as larvae (data not shown).

4.1.2. Extended GLD-2/GLD-3 complex expression in proteasome-compromised PGCs

To test whether the proteasome influences the stability of GLD-2 cytoPAP complex in PGCs, immunofluorescent analysis of GLD-2 and GLD-3 protein levels were performed in *pas-5(RNAi)* and *pbs-6(RNAi)* embryos (Figure 4.1.2). Germ cells were revealed by staining

for the expression of the constitutive P granule component, PGL-1(Kawasaki, Shim et al. 1998). Embryos were analysed between two developmental time frames: the 100-cell stage, when PGC are newly born, and the approximately 500-cell stage, when the embryo is bean shaped.

Similar to wild type, PGCs of control(RNAi) embryos were PGL-1 positive while GLD-2 and GLD-3 proteins were not detectable in PGCs of all analysed embryos (n=90). However, in *pas-5* or *pbs-6* knockdown embryos, unlike control RNAi, GLD-2 and GLD-3 proteins were robustly detected in PGCs of embryos passed the 100-cell stage; 93 % (n=118) and 96 % (n=75), respectively (Figure 4.1.2 A and B).
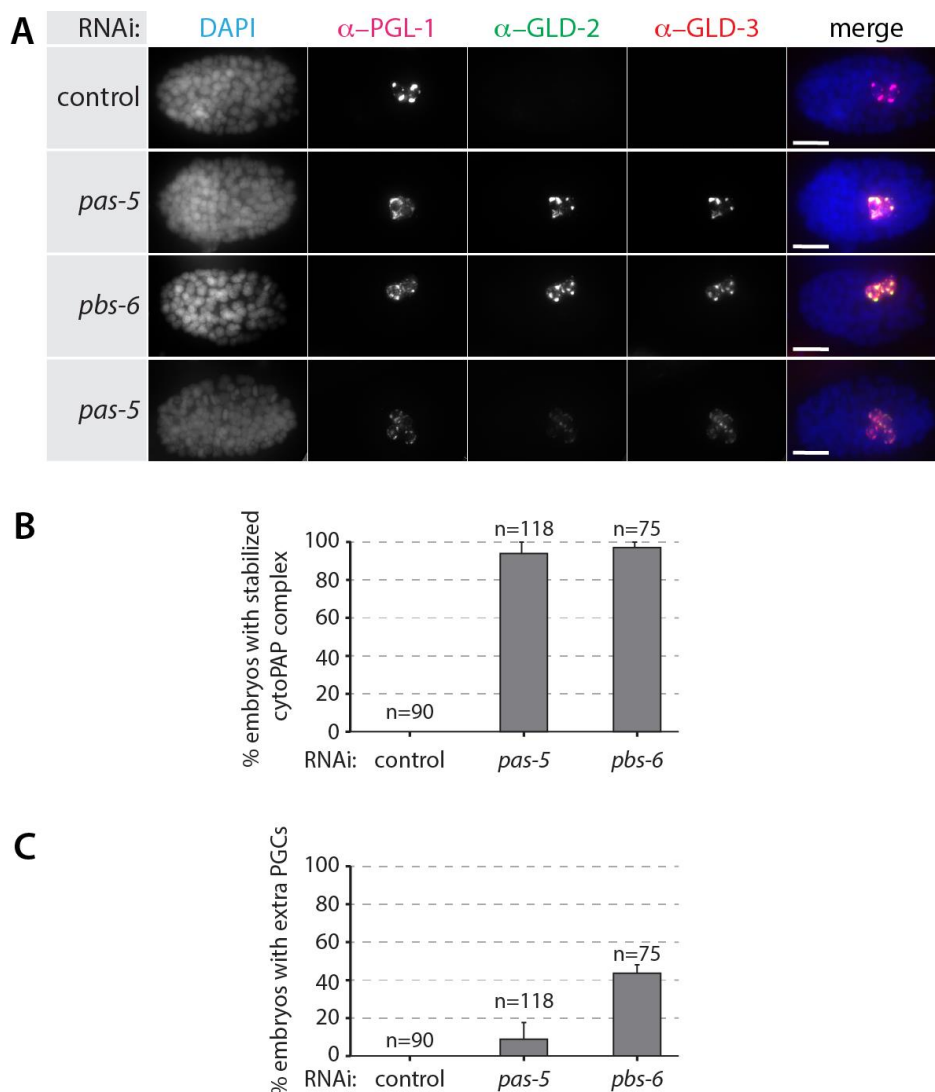
Figure 4.1.2. PGCs maintain GLD-2 cytoPAP complex expression upon *pas-5* or *pbs-6* knockdown.

(A) Fluorescent images of wild-type embryos, treated with control, *pas-5* and *pbs-6* RNAi, immunostained for PGL-1, GLD-2 and GLD-3, and stained with DAPI for chromatin. Merge is blend of all channels. Bottom row shows *pas-5(RNAi)* embryos with more two PGCs. Scale bar is 10 μM. (B) Bar graph showing the percentage of embryos displaying continued expression of GLD-2 and GLD-3 in PGCs after 15 hours of RNAi treatment. (C) Bar graph showing the percentage of embryos displaying extra PGC phenotype in control, *pas-5* or *pbs 6* RNAi.

4.1.2.1. Extra PGCs arise in proteasome-compromised embryos

While analysing the effect of *pas-5* and *pbs*-6 knockdown on GLD-2 cytoPAP expression in PGCs, a peculiar effect on the germ cell lineage was observed. In wild type embryos, the germ cell precursor P4 is born around the 24-cell stage at its posterior end. P4 gastrulates into the middle of an embryo and divides around the 100-cell stage to give rise to the two primordial germ cells, Z2 and Z3. In control RNAi, as in wild type, two PGL-1 expressing primordial germ cells were detected (Figure 4.1.2A and C). However, in *pas-5(RNAi)* or *pbs-6(RNAi)* embryos consisting of more than one hundred cells, two populations of embryos were identified. The first group of embryos had two PGL-1-positive cells in the middle of embryos just like in control RNAi, whereas the second group of embryo had more than two PGL-1-positive cells. They were often four in number, but six cells have been occasionally observed as well. Furthermore, these PGL-1-positive cells expressed GLD-2 and GLD-3, suggesting that extra PGC were generated in these embryos (Figure 4.1.2A, bottom row and Figure 4.1.2C). To further confirm whether these multiple cells have germline character, the *pas-5(RNAi)* and *pbs-6(RNAi)* embryos were immunostained with anti-GLH-1 antibodies; GLH-1 is another protein exclusively expressed in the germ cell lineage and often used to identify primordial germ cells (Gruidl, Smith et al. 1996, Kuznicki, Smith et al. 2000, Updike, Knutson et al. 2014). As these multiple cells also expressed GLH-1 protein (data not shown), these data suggest that embryos with compromised proteasome activity produce additional primordial germ cells.

In wild-type embryos, both PGCs are arrested at the G2 phase of cell division until the end of embryogenesis (Schaner, Deshpande et al. 2003, Wang and Seydoux 2013, Mainpal, Nance et al. 2015). After hatching, in the presence of food, Z2 and Z3 undergo rapid proliferation beginning from the L1 larvae stage, ultimately forming the entire germline tissue in an adult animal. In *pas-5(RNAi)* or *pbs-6(RNAi)* embryos, extra primordial germ cells might arise during embryogenesis because Z2 and Z3 exited G2 cell cycle arrest and underwent additional divisions. Alternatively, more than one germ cell precursor might have been specified at earlier stages during embryogenesis and they then gave rise to an increase in PGC number. In fact, to support the later possibilities, more than one germ cell precursors, have been occasionally observed in the posterior end of embryo containing less than forty cells. This may indicate that some somatic sister cells adopted germ cell fate. As these embryos with two or three germ cell precursors were not the same ones whose PGCs were analysed later in development, it is not possible to distinguish between these two scenarios. Further analysis needs to be carried out, such as, staining for loss of descendants of somatic sister cells, or checking the DNA of the primordial germ cells to determine if they exited the

expected G2 arrest leading to extra division, or making a time lapse videos of *pas-5(RNAi)* and *pbs-6(RNAi)* embryos. Nonetheless, these data support the conclusion that proteasome activity is important for termination of GLD-2 and GLD-3 protein expression in PGCs and for germ cell development.

4.1.3. Autophagy does not regulate GLD-2 cytoPAP abundance in primordial germ cells

The UPS is not the only pathway that promotes protein degradation. In addition to the proteasome, many cytoplasmic proteins are degraded by autophagy through lysosomal degradation systems (Nakatogawa 2007, Nakatogawa, Ichimura et al. 2007, Zhang, Yan et al. 2009, Kaushik and Cuervo 2012). Therefore, it was imperative to analyse whether the abundance of GLD-2 cytoPAP complex is regulated by autophagy. To this end, expression of GLD-2 protein was analysed upon compromising *lgg-1* expression by RNAi-mediated knockdown; *lgg-1* is the ortholog of yeast autophagy protein atg8 (Zhang, Yan et al. 2009, Palmisano and Melendez 2016).

In *C. elegans*, perturbation of *lgg-1* does not lead to severe developmental defects (Zhang, Yan et al. 2009). To test a potential influence of autophagy on GLD-2 expression, synchronised wild-type L1 animals were raised to adulthood on either *lgg-1* or control RNAi feeding bacteria. Gravid adults were dissected to collect embryos that were then analysed by immunofluorescence for GLD-2 expression in PGCs. Since there was no antibody available to monitor the knockdown efficiency of *lgg-1,* the activity of autophagy was monitored as a read out of knockdown efficiency. The turnover of PGL-1, a known target of autophagy in embryonic somatic cells, was monitored using PGL-1-specific antibodies in immunofluorescent experiments and simultaneously, PGL-1 expression was also used to mark germ cells as autophagy does not affect PGL-1 expression in the embryonic germ cell lineage (Zhang, Yan et al. 2009).

In control RNAi, PGL-1 was detectable almost exclusively in the entire embryonic germ cell lineage, and it was enriched on P granules while GLD-2 and GLD-3 proteins were not detectable anymore in PGCs. In *lgg-1* RNAi, PGL-1 expression and localization to the germ cell lineage is comparable to control RNAi. However, unlike in control RNAi, ectopic PGL-1-positive granules, which were smaller than P granules, were observed in somatic cells of *lgg-1* RNAi embryos (Figure 4.1.3). This observation indicates that *lgg-1* RNAi led to reduced autophagy functions, causing previously reported turnover defect of PGL-1 in somatic cells. Importantly, as in control RNAi, the expression of GLD-2 and GLD-3 proteins were still terminated in PGCs of *lgg-1* RNAi, arguing that autophagy or lysosomal degradation likely does not promote the turnover of GLD-2 cytoPAP complex in PGCs (Figure 4.1.3).

RNAi:	DAPI	α–PGL-1	α–GLD-2	α–GLD-3	merge
control					
lgg-1					
pas-5					
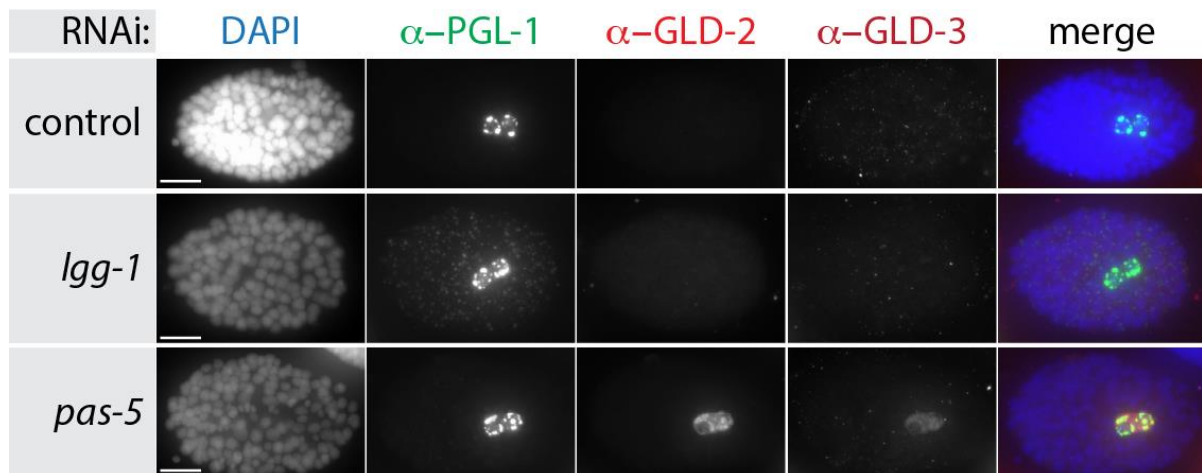
Figure 4.1.3. GLD-2 cytoPAP expression remains unaffected upon *lgg-1* knockdown.

Immunofluorescent images of embryos that experienced control RNAi (top row), *lgg-1* RNAi (middle row) and *pas-5* RNAi (bottom row). Embryos were stained for DAPI to mark chromatin in order display the embryonic stage (left column); PGL-1, a P granule protein in germ cells (middle-left column); GLD-2 (centre column) and GLD-3 (middle-right column). The merge of all channels is displayed in the right column. Scale bar is 10 μM. While PGL-1 expression remains unaffected in either *pas-5* or control RNAi, PGL-1 positive granules are clearly visible in somatic cells of *lgg-1(RNAi)* embryos. GLD-2 and GLD-3 proteins are not detectable in PGCs of control and *lgg-1* RNAi. As documented in Figure 4.1.2, *pas-5* RNAi led to extension of GLD-2 and GLD-3 expression in PGCs.

Taken together, these data suggest that autophagy might not be a major regulatory pathway for the turnover of at least a subset of maternal proteins, including GLD-2 and GLD-3, whose degradation is initiated in P4 and completed in PGCs. The observed continued expression of GLD-2 and GLD-3, when proteasome function is compromised strongly suggests that proteasome might be the most predominant pathway that removes most maternal proteins in PGCs to assist, presumably, maternal-to-zygotic transition in PGCs.

4.2. Identification and characterization of the potential regulator of GLD-2 stability

The proteasome degrades a vast number of proteins across development (Erales and Coffino 2014, Papaevgeniou and Chondrogianni 2014). A major mechanism by which the proteasome determines protein substrate is by recognition of a polyubiquitin side chain which is attached to target proteins. Therefore, the attachment of a ubiquitin chain serves as a selective process for protein degradation. This posttranslational modification is carried out by a diverse family of proteins, which collectively referred to as E3 ubiquitin ligases (Passmore and Barford 2004, Metzger, Hristova et al. 2012, Metzger, Pruneda et al. 2014, Papaevgeniou and Chondrogianni 2014, Weber, Polo et al. 2019). Therefore, the observation in embryos that the proteasome may promote a reduction of GLD-2 cytoPAP in PGCs alludes to the fact that there might exist at least one E3 ubiquitin ligase or E3 ligase complex that targets GLD-2 protein for poly-ubiquitination and subsequently for proteasome-mediated degradation.

4.2.1. A yeast two-hybrid (Y2H) screen identified GRIF-1 as a potential regulator of GLD-2 turnover

To identify the E3 ubiquitin ligase or ligase complex that regulates the turnover of GLD-2 cytoPAP complex in PGCs, a Y2H screen was performed by Anu Bhargava, a former student of the lab, using full-length GLD-2 as bait. Among several potential GLD-2 interactors the prominent candidate Y51F10.2 stood out; as it encoded an uncharacterised RING-domain containing protein. As Y51F10.2 had not been described or named before and based on the presence of RING domain and its interaction with GLD-2, it was named GLD-2-interacting RING Finger protein 1 (GRIF-1) (Figure 4.2.1A). GRIF-1 protein has 305 amino acids and has a predicted size of approximately 35.5 kDa (Figure 4.2.1A).

4.2.1.1. GRIF-1 is a RING finger domain-containing putative ubiquitin ligase

N-terminal RING (Really Interesting New Genes) domain is a characteristic signature of Tripartite motif-containing proteins (TRIMs). However, in TRIMs, the N-terminal RING domain is usually followed by a B-Box domain, which is another zinc finger domain, one or two coiled coil (CC) domains and at least another domain that varies in different TRIM proteins (Ozato, Shin et al. 2008, Hatakeyama 2017, Jaworska, Wlodarczyk et al. 2020). For example, in the TRIM32 protein family, the C-terminal portion of the protein contain several NHL repeats (named after NCL-1, HT2A and LIN-41) which are important for mRNA regulation through microRNA; the RING, B-Box, and coiled coil domains are important for E3 ubiquitin ligase activity (Kudryashova, Kudryashov et al. 2005, Kano, Miyajima et al. 2008, Kudryashova, Wu et al. 2009, Locke, Tinsley et al. 2009, Schwamborn, Berezikov et al. 2009, Mokhonova, Avliyakulov et al. 2015). While several protein databases identified GRIF-

1 as TRIM32 related, only the N-terminal RING domain is annotated and displayed by these databases (e.g Wormbase). Therefore, a detail analysis was carried out to potentially identify other TRIM domains in GRIF-1. Multiple sequence alignments were carried out with TRIM32 from human, mouse and zebrafish using Clustal Omega program (Figure 4.2.1A, B and C). Based on sequence similarity of key amino acids important for the formation of zinc finger domains and their position, these alignments revealed a single RING domain and identified an additional zinc finger domain closely related to a B-Box domain in other TRIM32 proteins (Figure 4.2.1 A, B and C). Notably, there are stretches of amino acids in both RING and B-Box domains, which are absent in three other TRIM32 proteins assessed in the multiple sequence alignment and compared to other TRIM32 family members (Figure 4.2.1B and C). These amino acid stretches may form loops to optimize the GRIF-1 zinc finger domains for target-specific protein-protein interaction(s).

Coiled coils are bundles of two or more alpha helices that wind around each other to form supercoiled helical structures. They are present in many TRIM proteins serving as platform for protein interaction and for self-assembly. The presence of coiled coil in any protein can be predicted using bioinformatic tools. Here, the program COILS (version 2.2) was used to predict coiled coils on 14, 21 and 28 amino acid windows. This means that to predict the propensity of a protein sequence to fold into a coiled coil domain, the program will compare proteins of interest, using a string of either 14 or 21 or 28 amino acids, with other proteins known to have coiled coil domain. According to the program algorithm, the most reliable windows are window 21 and 28. In window 21 and 28, COILS successfully predicted the presence of two coiled coil domains in the C-terminal end of GRIF-1 immediately after the B-Box domain (Figure 4.2.1D).

Just like TRIM32, GRIF-1 has RING, B-Box and coiled coil domains. However, unlike TRIM32, GRIF-1 lacks all NHL repeats or any other recognisable domain after the coiled coil domains. Since, GRIF-1 is devoid of the C-terminal NHL repeats important in TRIM32 for mRNA regulation through microRNAs (Schwamborn, Berezikov et al. 2009), its unique architecture strongly suggests that GRIF-1 might be exclusively a E3 ubiquitin protein ligase.

Figure 4.2.1. GRIF-1 is a TRIM32-related putative E3 ubiquitin ligase.

(A) The domain architecture of GRIF-1 and its closest human ortholog, TRIM32. GRIF-1 lacks the NHL repeats required in TRIM32 for RNA regulation. (B and C) Respective multiple sequence alignments of the RING and B-Box domain of GRIF-1 (UniProt entry Q8WTJ8), and TRIM32 from zebrafish (*Dr,* UniProt entry A8WGA9), mouse (*Mm,* UniProt entry Q8CH72) and human (*Hs,* UniProt entry Q13049). Red arrows points to key amino acids important for zinc finger formation, C (cysteine) and H (histidine). Amino acid sequence conservation is highlighted in the bottom line; full stop (.) indicates similar amino acids, semicolon (:) indicates highly similar amino acids and asterisk (*) indicates conserved or identical amino acids. Multiple sequence alignment was carried out using Clustal Omega program. (D) The probability that GRIF-1 has coiled coil domains was predicted using the program COILs (version 2.2). COILS searches with strings of 14, 21 or 28 amino acid with its output displayed in respective windows. The font style and size of the output have been changed. As predicted in window 21 and 28 of COILS, GRIF-1 has two putative coiled coil domains (see main text for details).

4.2.2. Several mutations were generated in *grif-1* locus using the CRISPR/Cas9 system

According to wormbase, the *grif-1* genomic locus is located on chromosome I and situated at genetic position -12.39 ± 0.000 cM. Excluding the promoter and the 3'UTR, from start to stop codon, the genomic sequence is predicted to consist of 5 exons and 4 introns and spans approximately 5.2 kilobases in length.

Figure 4.2.2. Genomic organization and mutations of the *grif-1* locus and corresponding protein products.

(A) Genomic locus of *grif-1* in wild type and mutants. *tm2559* and *ok1610* alleles were isolated by EMS mutagenesis and obtained from *C. elegans'* deletion consortia. All other alleles were generated using the CRISPR/Cas9 system. *ef35* and *ok1610ef40* alleles were generated by introducing a premature stop codon (TGA) into the first exon of *grif-1* in wild type and *ok1610,* respectively. *ef32* is an allele in which a large portion of the *grif-1* locus was deleted. Red vertical lines in *ef32* represent many random bases inserted into the locus. *ef38* and *ef36* are alleles carrying additional sequence string that encodes for a duplicated FLAG epitope tag (2xFLAG tag) insert either at the N- or C-termini of the wild-type locus, respectively. (B) The theoretical protein predictions from wild-type locus and mutants' loci corresponding to (A). The red colour in GRIF[tm2559] is a new sequence introduced due to the out-of-frame deletion.

To study the function of *grif-1*, two deletion mutants were obtained from two *C. elegans* deletion consortia. *grif-1(tm2559)* contains an out-of-frame deletion that removes 151bp in the 4th exon of *grif-1* while *grif-1(ok1610)* contains a deletion of 1016bp, affecting exon 4 and intron 4 (Figure 4.2.2). These genomic lesions were confirmed in this work during the course of various experiments. Based on further molecular analysis of *tm2559* and *ok1610* mutant alleles, both strains produce truncated versions of GRIF-1 protein and do not

represent protein null alleles (see section 3.2.5). Therefore, additional efforts were made to generate *grif-1* mutant alleles that are likely genetic null alleles and produce no functional GRIF-1 protein products.

Using CRISPR/Cas9-mediated genome engineering techniques, several other genomic changes were introduced into the locus, generating additional mutant and transgenic alleles. *ef32* contains a large out-of-frame deletion introduced into *grif-1* locus with many random bases inserted into the locus, presumably during the repair process. *ef35* and *ok1610ef40* have a premature stop codon almost immediately downstream of cognate start codon in exon 1 of wild-type and *ok1610 grif-1* locus. *ef38* and *ef36* have sequence coding for a duplicated FLAG peptide inserted at the 5'and 3' end of the GRIF-1 encoding open reading frame (Figure 4.2.2). Together, these alleles serve as tools for the analysis of *grif-1* function.

4.2.3. Several antibodies raised against GRIF-1 protein recognize GRIF-1 specifically in different applications

To further characterize GRIF-1 protein expression and function, several attempts were made to raise both monoclonal and polyclonal antibodies specific to GRIF-1. To raise monoclonal antibodies in mice, full-length GRIF-1 was expressed in a heterologous bacterial system as a fusion protein containing 6xHis::SUMO::GRIF-1::GFP. The fusion protein was then purified under denaturing conditions and used as an antigen to immunize mice. After several pre-screening selection steps, the supernatant from immortalized cells were eventually screened for activity against GRIF-1 in immunoblots, derived from yeast protein extract containing either LexA or LexA::GRIF-1 fusion protein.

An exemplary western blot of five (representative) hybridoma clone supernatants is shown in Figure 4.2.3. All five hybridoma clones (CV26, CV28, CV30, CV31 and CV33) secreted antibodies recognised a band of approximately 55 kDa in lanes loaded with lexA::GRIF-1 yeast lysate, which is the expected size of lexA::GRIF-1, but detected no band in lanes loaded with lexA only yeast lysates (Figure 4.2.3). These observations suggest that each clone produces antibodies that recognise GRIF-1 protein specifically from yeast extract. Monoclonal antibody CV28 (mAbCV28) detected another band that is higher than the expected size and additionally detected in lexA only control lane arguing that this is an unspecific signal. In all, several other clones were recovered that specifically recognise GRIF-1 heterologously expressed in yeast (data not shown). And together, they could be grouped into two categories; those that recognised GRIF-1 specifically without any additional unspecific background band in yeast and those that cross-react with yeast proteins in addition to GRIF-1.
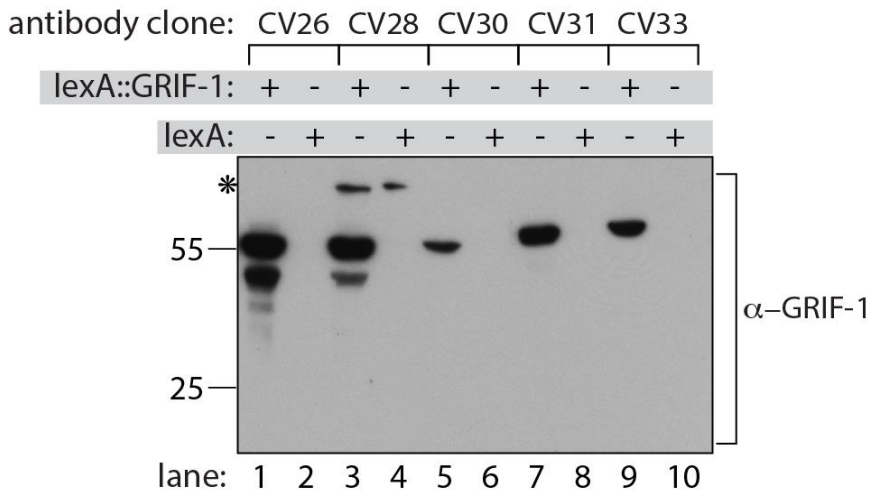
Figure 4.2.3. Hybridoma clones secret antibodies that cross-react specifically with GRIF-1 protein expressed in a heterologous system.

Immunoblot of yeast lysates used to analysed the cross-reactivity of antibodies secreted by hybridoma clones. All displayed antibodies detected LexA::GRIF-1 of the expected size but not LexA, suggesting cross reactivity to GRIF-1. CV28 detected an additional protein band unrelated to GRIF-1 (lane 3 and 4). Asterisk (*) shows unspecific background signal.

4.2.4. Monoclonal antibody epitopes map to different domains of GRIF-1

Full-length GRIF-1 protein was used to immunize mice to generate GRIF-1-specific monoclonal antibodies. This means that epitopes recognised in full-length GRIF-1 by these monoclonal antibodies might be distributed across the sequence space of GRIF-1. However, knowledge of the individual epitope will be valuable for interpretations of future experiments. To map epitopes recognised by GRIF1-specific antibodies, further immunoblotting experiments were carried out using yeast protein lysates containing LexA-GRIF-1 fusion protein derivatives.

Exemplary immunoblots are shown in Figure 4.2.4A. mAb CU33 recognised protein bands of expected sizes to all fragments containing the B-Box domain but failed to recognise any protein band lacking the B-Box domain. These observations argue that this antibody binds to an epitope residing in or near the B-Box domain of GRIF-1; between amino acid 77 and 172 (Figure 4.2.4A). Several other antibodies that were positive for GRIF-1 in the first selection step were mapped in a similar manner and the results are summarised in a graphical display in Figure 4.2.4B.
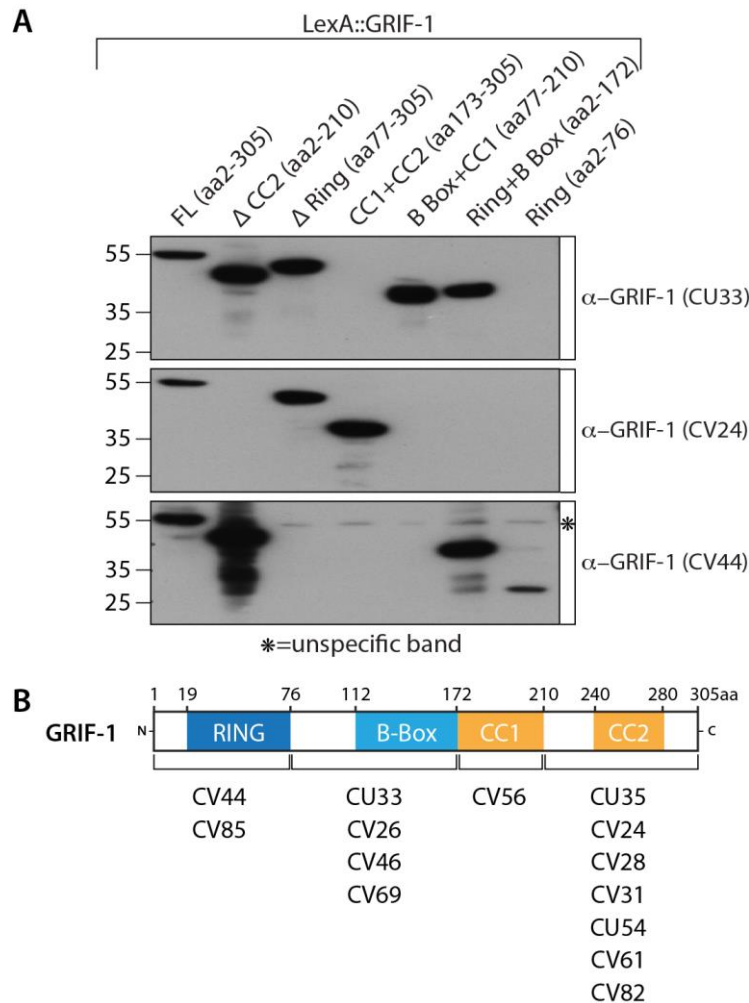
Figure 4.2.4. Epitopes mapping of anti-GRIF-1 specific monoclonal antibodies.

(A) Representative images of immunoblots used to map the regions in GRIF-1 that contains epitopes recognised by GRIF-1 monoclonal antibodies. Epitope of mAb CU33 resides in or near the B-Box domain of GRIF-1, Epitope of mAb CV24 in or near the CC2 domain, and Epitope of mAb CV44 in or near the RING domain area of GRIF-1 protein. Asterisk (*) shows unspecific background signal. (B) A visual display of GRIF-1 domains showing the number of epitopes that are mapped to each domain. More epitopes are mapped to the C-terminal end containing coiled coil 2 domain than any other domain or region of the GRIF-1 protein.

4.2.5. Characterization of GRIF-1 antibodies using endogenous worm proteins

Using *C. elegans* proteins, additional tests were carried out to determine antibody suitability in western blot, immunofluorescence, and pulldown experiments. Whilst determining the specificity of these antibodies, *grif-1* mutants were concomitantly characterised using immunoblotting experiments. To this end, several independent embryo extracts were prepared from wild type, *grif-1* loss-of-function and epitope-tagged mutant alleles. The extracts were then analysed in western blotting experiments using GRIF-1 monoclonal antibodies and blots were also probed for DYN-1, a *C. elegans* orthologue of human dynamin proteins, as a loading control.

4.2.5.1. Western blotting and *grif-1* mutants

Based on theoretical analysis from WormBase, the wild-type *grif-1* locus is predicted to produce a protein of approximately 35.5 kDa in size. Insertion of a duplicated FLAG (2XFLAG) peptide sequence is expected to increase the size of GRIF-1 by approximately 2 kDa. *ok1610* and *tm2559* mutant alleles are expected to produce truncated GRIF-1 proteins, *ok1610ef40* and *ef35* mutant alleles are predicted to produce only the first 10 amino acids while while *ef32* is predicted to produce the first 17 amino acids (see Figure 4.2.2). In an exemplary western blot using embryonic protein extract shown in Figure 4.2.5.1, GRIF-1 monoclonal antibodies recognised a protein band of approximately 38 kDa in *ef38,* corresponding to the expected size of 2XFLAG tagged *grif-1* (Figure 4.2.5.1). They also recognised a protein band of approximately 36 kDa in wild type which is the expected size of full-length GRIF-1 protein and a 29 kDa protein band in *ok1610* which is the predicted size of truncated GRIF-1 protein in *ok1610.* By contrast, no protein band was detected in *ef32, ok1610ef40,* and *ef35.* These results suggest that GRIF-1 monoclonal antibodies mAb CU35 and mAb CV44 recognize GRIF-1 specifically from embryo extracts. Of all monoclonal antibodies tested, 3 clones were recovered that are usable in western blotting experiments when using worm extracts. Taken together, monoclonal GRIF-1 antibodies specifically recognise GRIF-1 in western blotting experiments.

Besides the specificity of the tested antibodies, other important inferences can made from the western blotting experiments. First, the results suggest that a single protein form of approximately 36 kDa is produced by wild-type *grif-1* locus, at least during embryogenesis. Second, *ok1610* allele still robustly expresses truncated GRIF-1 protein and therefore is not a protein null. Third, GRIF-1 protein is not detected in either CRISPR/Cas9 generated *grif*-1 mutant alleles; *ef32, ef35* or *ok1610ef40,* and each is therefore most likely a protein null allele. It is noteworthy to mention that the expected truncated protein in *tm2559* has never been detected by western blot but it is often detected with extremely weak signals by immunofluorescence (see Figure 4.2.8B). This could be as a result of a likely increased instability of the truncated protein. Alternatively, truncated protein may be heavily modified and the antibody epitope is no longer recognised. Whatever the reason, it is not unlikely that no protein is produced from the truncated transcript, which was fairly robustly detected in cDNA analysis (data not shown). These observations suggest that *grif-1(tm2559)* is not a protein null but instead a very strong loss-of-function allele, producing very low levels of truncated GRIF-1 protein. Taken together, different genomic alterations affect GRIF-1 protein production differently, ranging from robust expression of truncated protein in *ok1610* to extremely weak expression of truncated protein in *tm2559,* and to undetectable expression of GRIF-1 in allele generated by CRISPR/Cas9. Therefore, using CRISPR/Cas9-mediated

genome engineering technique, several protein null *grif-1* alleles were successfully generated and several monoclonal antibodies are specific to GRIF-1.
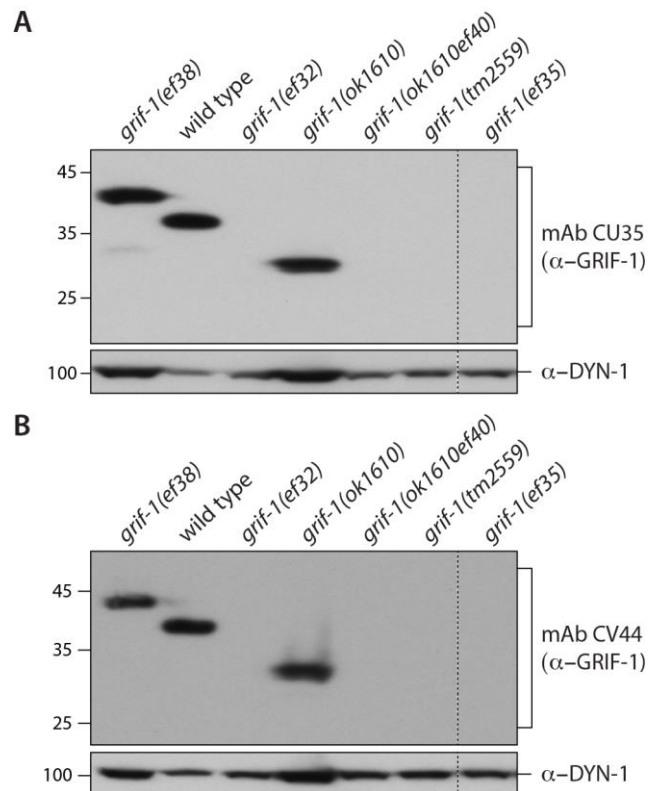
Figure 4.2.5.1. GRIF-1 monoclonal antibodies recognise GRIF-1 specifically from embryo extracts.

GRIF-1 monoclonal antibodies secreted by (A) hybridoma clone CU35 and (B) hybridoma clone CV 44 were used to probe a protein blot containing embryo extracts from *ef38*, wild type and *grif-1* mutants (see Figure 4.2.2). The same blot was stripped and re-probed with anti-DYN-1 antibody.

4.2.5.2. Further characterization of GRIF-1 antibodies in other applications

GRIF-1 antibodies were further tested for GRIF-1 specific activity in immunofluorescence experiments and several antibodies were recovered that specifically detected GRIF-1 in immunofluorescence experiments (see Figure 4.2.7 that describe GRIF-1 embryonic expression). Lastly, some were also tested for co-immunoprecipitation applications, either as a single antibody or when combined to form antibody mix. Several antibodies were identified that could enrich for GRIF-1 in co-immunoprecipitation experiments (Figure 4.3.4 and data not shown). In conclusion, GRIF-1 specific antibodies were successfully generated and they are suitable for different applications.

4.2.6. GRIF-1 expression is restricted to embryogenesis

A pertinent question at this point was to determine the developmental and spatiotemporal expression pattern of GRIF-1 protein. To this end, protein extracts were prepared from every stage of worm development from embryos to adults and were used in a western blot. To test for somatic expression of GRIF-1 protein, extracts were additionally

prepared from temperature sensitive *glp-4(bn2)* adult animals that contain very few germ cells in their gonads. Lastly, *grif-1* mutants were used as specificity controls. The immunoblots prepared from these extracts were first probed with GRIF-1-specific antibodies and then with a tubulin-specific antibody, to provide a loading control (Figure 4.2.6).
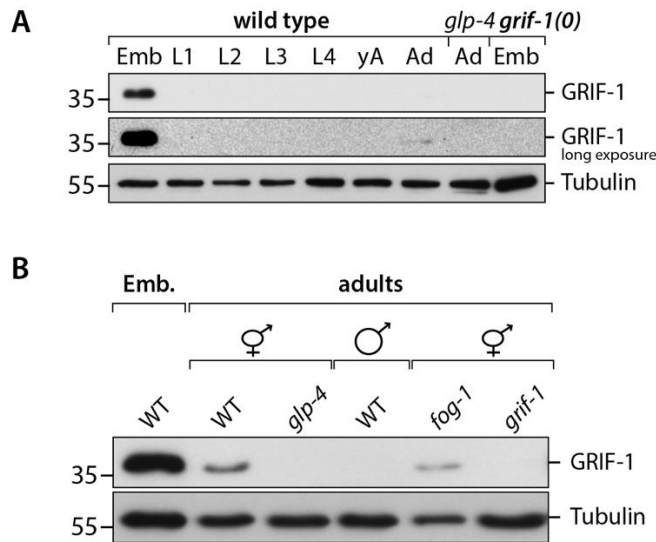
Figure 4.2.6. GRIF-1 is predominantly expressed in embryos.

(A) Immunodetection of extracts of different developmental stages. Emb= embryos, L= larvae, yA= young adults, and Ad= adults. *grif-1(tm2559)* embryos were used as specificity control. Temperature sensitive *glp-4(bn2)* animals lack a developed germline and serve as a test for somatic expression of GRIF-1. Blot was probed with mAb CU35 GRIF-1 antibody and tubulin was used as loading control. A longer exposure is given to reveal a weak GRIF-1 signal from wild-type adults. (B) Immunoblotting experiment to determine the source of GRIF-1 signal in adults. Extracts were prepared from wild-type embryos and adult hermaphrodites, *glp-4(bn2)* animals, wild-type males, *fog-1(q785)* and *grif-1* mutants. Blot was probed with mAb CU35 GRIF-1 antibody, and tubulin antibody.

A protein band of approximately 36 kDa, the expected size of GRIF-1, was predominantly detected in embryo extracts; it was basically undetectable from all larvae stages and barely detected in adults with embryos (Figure 4.2.6A). Furthermore, the protein band is not detected in *glp-4(bn2)* mutants arguing that the weak signal from adults is most likely not due to somatic cells. Importantly, no protein band was detectable from *grif-1* mutant embryos extracts*,* suggesting the antibody used recognised GRIF-1 specifically (Figure 4.2.A). Together, these observation shows that GRIF-1 is predominantly expressed during embryogenesis.

The weak GRIF-1 signal detected in adults might be either from *in utero* embryos, sperm, oocytes or immature germ cells. To ascertain the source of this weak adult signal, another western blot was carried out. In addition to extracts from embryos, wild-type and *glp-4(bn2)* adult hermaphrodite, protein extracts were made from adult males, to test for GRIF-1 expression in sperm, and *fog-1(q785)* adult female, which produce only oocytes but not sperm, to test for GRIF-1 expression in oocytes. Lastly, extracts were also prepared from adult *grif-1* mutants to ascertain specificity (Figure 4.2.6B). In wild type, GRIF-1 was

predominantly detected from embryo extracts and weakly detected in hermaphrodite or female adults. It was absent in *glp-4(bn2)* and *grif-1(tm2559)* adults. Moreover, GRIF-1 was not detected in males, arguing that the signal in hermaphrodites is most likely not coming from sperm. The GRIF signal in *fog-1* mutants suggests that oocytes contribute to the GRIF-1 signal in adults. However, this does not exclude a likely contribution of *in utero* embryos in wild-type. Together, these western blot experiments suggest that GRIF-1 is predominantly expressed during embryogenesis and extremely weak levels may be detectable in oocytes.

4.2.7. GRIF-1 is specifically expressed in embryonic germ cells

In order to determine the spatiotemporal expression of GRIF-1 during embryogenesis, immunofluorescent analysis was carried out on wild-type embryos, using anti-GRIF-1 monoclonal antibodies and *grif-1* mutants as specificity control. Several monoclonal antibodies were used in immunofluorescent analyses. Additionally, the germ cell lineage was distinguished from somatic lineages by the expression of the constitutive P granule component, PGL-1 (Figure 4.2.7).
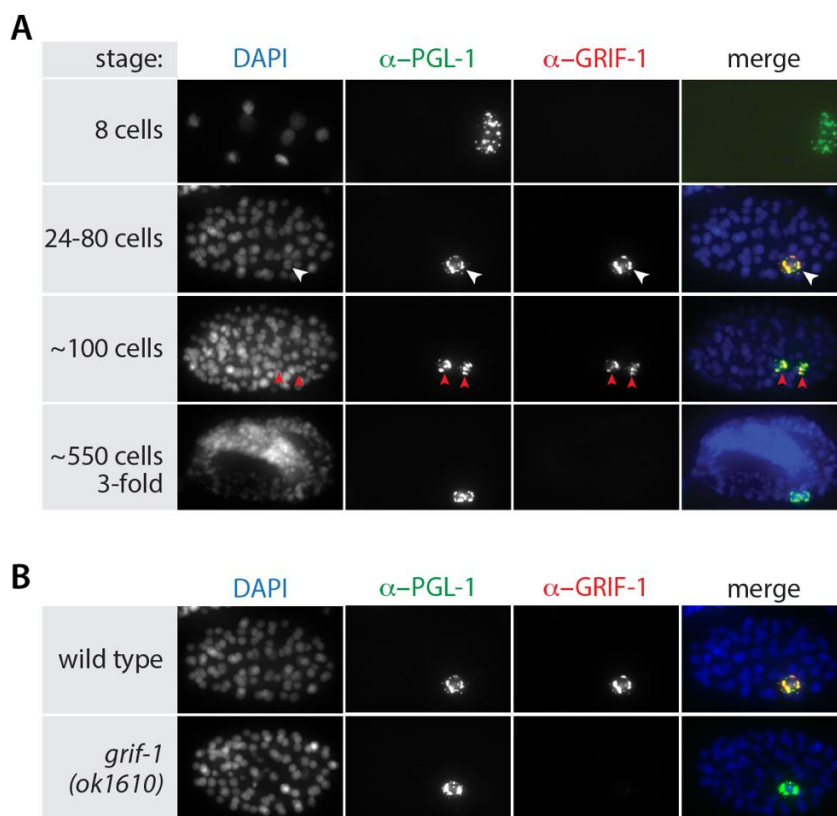
Figure 4.2.7. GRIF-1 is specifically expressed in the embryonic germ cell lineage.

(A) Immunofluorescent images of different embryonic stages of wild-type embryos stained for chromatin (DAPI, left column), P granules (PGL-1, middle-left column), and GRIF-1 (anti-GRIF-1 mAb CU35, middle-right column). GRIF-1 is detectable in P4 (white arrowhead) and primordial germ cells; Z2 and Z3 (double red arrowheads). (B) Immunofluorescent images of wildtype (top row) and *grif-1(ok1610)* embryos (bottom row) stained for chromatin (DAPI, left column), P granules (PGL-1, middle-left column), and GRIF-1 (anti-GRIF-1 mAb CU35, middle-right column). The merge of all

channels is shown on the right column. mAb CU35 detected a strong signal in wild type but not *ok1610.*

Intriguingly, GRIF was not detected in somatic cells throughout embryogenesis indicating that the expression is likely germ cell specific (Figure 4.2.7A). Surprisingly, GRIF-1 was also not detected in germ cell precursors of 1-cell to 23-cell stage embryos. GRIF-1 protein, however, first became detectable around 24-cell stage in germ cell primordium P4 and localises exclusively to P granules (Figure 4.2.7A). Initially, GRIF-1 protein amounts remain high in primordial germ cells Z2 and Z3 until they drop gradually to undetectable levels in PGCs just prior to 3-fold stage of embryogenesis. The specificity of the antibody and several other monoclonal antibodies used in immunofluorescent experiments was determined by comparing expression of GRIF-1 in wild type to *grif-1* mutants (Figure 4.2.7B). While a robust GRIF-1 signal was detectable in germ cell primordium, P4, of wild-type embryos, an extremely week signal of GRIF-1 protein is detected in *grif-1(ok1610)* demonstrating the specificity of the antibody (Figure 4.2.7B). Several other monoclonal antibodies that detected GRIF-1 specifically were recovered.
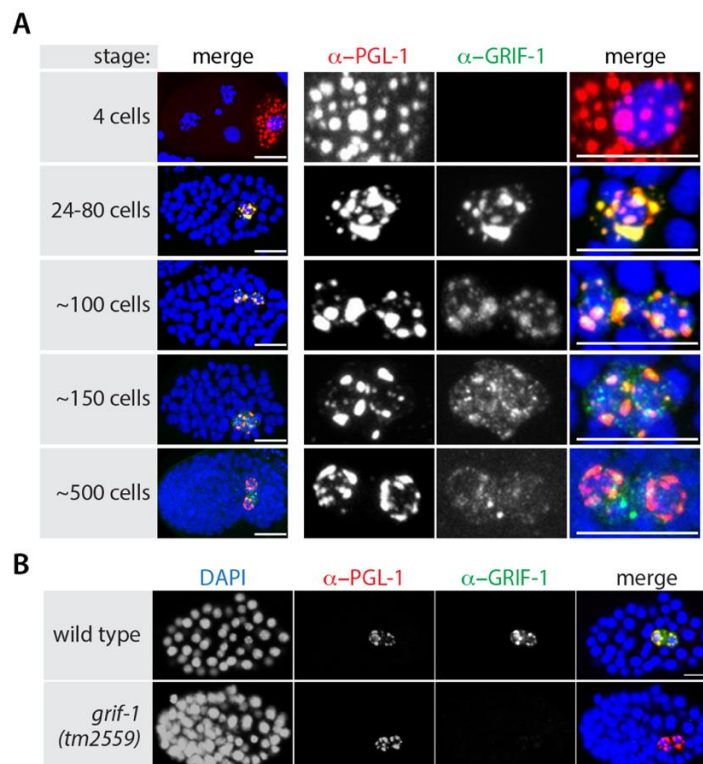
Figure 4.2.8. GRIF-1 has a highly dynamic expression pattern in PGCs.

(A) Confocal immunofluorescent images of wild-type embryos of different developmental stages stained for chromatin (DAPI, in blue), PGL-1 (in red) and GRIF-1 (in green) (left column). Next to each developmental stage, are blow ups focusing on the germ cell lineage. The close up of PGCs in embryos of approximately 500 cells (bottom row) was rotated 90 degrees in clockwise direction for display. PGL-1 expression was used as penetration control and to mark PGCs. Note, GRIF-1 is dissociated from P granules in primordial germ cells from around 150 cell stage onwards (see main text for details). Scale bar is 10 μM. (B) Confocal immunofluorescent images of approximately 100-cell stage embryos stained for chromatin (left column), PGL-1 (middle-left column) and GRIF-1 (middle-

right column). Polyclonal anti-GRIF-1 antibody (rb333043) detected a strong signal in wild type but an extremely weak and background signal in *tm2559.* Scale bar is 10 μM.

To confirm GRIF-1 expression using different tools, full-length GRIF-1 purified by Sebastian Vogt, a former student of the lab, was used to immunise rabbits to raise polyclonal anti-GRIF-1 sera. Two positive sera were recovered; rb332095 and rb333043. GRIF-1 specific antibodies were affinity purified from rb333043 sera and used in immunofluorescence to confirm GRIF-1 expression. Polyclonal anti-GRIF-1(rb333043) antibodies reveal identical expression pattern as monoclonal antibodies (Figure 4.2.8A). The specificity of the polyclonal antibody was assessed by comparing wild-type embryos to *grif-1(tm2559)*. While a strong and robust signal was detected in wild type, an extremely weak background signal was detected in *tm2559* demonstrating the specificity of the polyclonal antibody (Figure 4.2.8B).

Additionally, regardless of the GRIF-1 antibody used to analyse GRIF-1 expression during embryogenesis, on close examination, GRIF-1 was observed to dissociate slowly from PGL-1 associated granules in PGCs as embryogenesis progresses, and eventually forms distinct puncta in the cytosol that are almost completely free of P granules by 500-cell stage of embryogenesis (Figure 4.2.8A). Taken together, GRIF-1 is a germ cell intrinsic factor, localises to P granules, and has a very narrow and yet highly dynamic expression pattern during germ cell development. In summary, this section reveals that the TRIM protein, GRIF-1 is expressed in the right cells at the right time to potentially act as a regulator of GLD-2 stability. Moreover, several tools were established here that allow for the study of expression and function of GRIF-1 protein. These tools include multiple *grif-1* alleles, as well as monoclonal and polyclonal antibodies to GRIF-1.

4.3. GRIF-1 interacts with GLD-2 and regulates GLD-2 cytoPAP expression in PGCs

Above data demonstrate that GRIF-1 is a unique TRIM32 ubiquitin ligase-related protein with a highly dynamic, exceedingly regulated and very restricted protein expression pattern during embryonic germ cell development. These observations strongly suggest GRIF-1 may interact with GLD-2 and promote its regulated turnover as a E3 ubiquitin ligase in primordial germ cells. This section describes experiments carried out to: (i) confirm GRIF-1 and GLD-2 interaction, (ii) map the interaction sites between GRIF-1 and GLD-2, and (iii) determine whether GRIF-1 promotes GLD-2 turnover in PGCs.

4.3.1. GRIF-1 specifically interacts with GLD-2 in yeast two-hybrid tests

GRIF-1 was identified as a GLD-2-interacting protein in a Y2H screen. Therefore, further Y2H tests were carried out to recapitulate the outcome of the yeast two-hybrid screen and more importantly, to map the interaction region between GRIF-1 and GLD-2.

In a Y2H system, two fusion proteins reconstitute a functional transcription factor which triggers the expression of a reporter gene. In the Y2H system used, one protein was fused to the activation domain of yeast Gal4 while the second protein was fused to the DNA-binding domain of the bacterial LexA repressor. A physical association between the two proteins of choice will trigger expression of a reporter gene, and in this case, beta galactosidase (β-gal). The expression of β-gal is then monitored by its ability to convert the colour-less substrate, X-gal, to a blue product. Therefore, during a Y2H test, a change in the colour of a yeast colony, from white to blue, is an indication that interaction most likely occurred.

DB fusion LexA::	AD fusion GAL4::	galactosidase	% Blue (n)
GLD-2 (FL)	GLD-3L		95 (60)
GLD-2 (FL)	none		0 (60)
GLD-2 (FL)	GRIF-1(FL)		85.3 (75)
none	GRIF-1(FL)		0 (30)

Figure 4.3.1. GRIF-1 binds GLD-2 specifically in Y2H tests.

Beta-galactosidase activity of yeast cells co-expressing indicated fusion proteins. Blue colour indicates a potential interaction. Next to the Beta-galactosidase assay is the percentage of colonies that were blue and the total number of colonies tested (n) is in bracket.

To recapitulate the interaction between GLD-2 and GRIF-1, full-length GLD-2 was fused to the LexA DNA-binding domain while a hybrid of full-length GRIF-1 was generated with Gal4 activation domain (Figure 4.3.1). GLD-3 was fused to Gal4 as a positive control for GLD-2 interaction since the interaction between GLD-3 and GLD-2 had been reported before

(Eckmann, Crittenden et al. 2004). Furthermore, LexA::GLD-2 co-expressed with GAL4 only and GAL4::GRIF-1 co-expressed with LexA only were used, respectively, as a negative controls to test whether GLD-2 and GRIF-1 by themselves could cause a background autoactivation of reporter gene.

Consistent with previous findings (Eckmann, Crittenden et al. 2004), almost all yeast colonies that co-expressed GLD-2 and GLD-3 turned blue (95 %, n=60) (figure 4.3.1). By contrast, none of the yeast colonies co-expressing GLD-2 and Gal4-AD turned blue, suggesting that LexA::GLD-2 by itself is unable to induce the expression of β-gal reporter gene. Importantly, majority of yeast colonies co-expressing LexA::GLD-2 and Gal4::GRIF-1 fusion turned blue (85 %, n=75), confirming and strengthening the Y2H screen data that GLD-2 interacts with GRIF-1 in yeast. Lastly, no blue colour was observed in any of the yeast colonies co-expressing LexA only with Gal4::GRIF-1, also suggesting that GRIF-1 is unable to stimulate the expression of β-gal by itself (Figure 4.3.1). Together, these data show that GRIF-1 binds GLD-2 specifically in Y2H assay.

4.3.2. The intrinsically disordered region of GLD-2 specifically interacts with GRIF-1

To determine which part of GLD-2 cytoPAP is important for the interaction with GRIF protein, several truncations were generated in GLD-2 and fused to LexA DNA-binding domain and co-expressed with Gal4::GRIF-1 full length. In this experiment, full-length GLD-2 was used as positive control and negative controls were as before.

As observed in previous experiment (Figure 4.3.1), yeast colonies that co-expressed full-length GLD-2 with full-length GRIF-1 were blue (Figure 4.3.2A). None of the yeast colonies expressing N-terminal truncations that lack the intrinsic disordered region of GLD-2 turned blue (Figure 4.3.2A). This suggests that neither the central part of GLD-2 that contains the catalytical domain nor the C-terminal end of GLD-2 is required for an interaction with GRIF-1. Intriguingly, all truncations that contain the intrinsically disordered region of GLD-2 (aa 1-334) turned blue (Figure 4.3.2A). To ascertain the expression of all tested fusion proteins, western blot analyses were carried out using yeast extracts of analysed colonies. All the tested combinations were detected, arguing that white coloured yeasts are not due to a lack of expression (Figure 4.3.2B). These observations altogether show that the N-terminal intrinsically disordered region of GLD-2 is required and sufficient for interaction with GRIF-1 in Y2H assays.
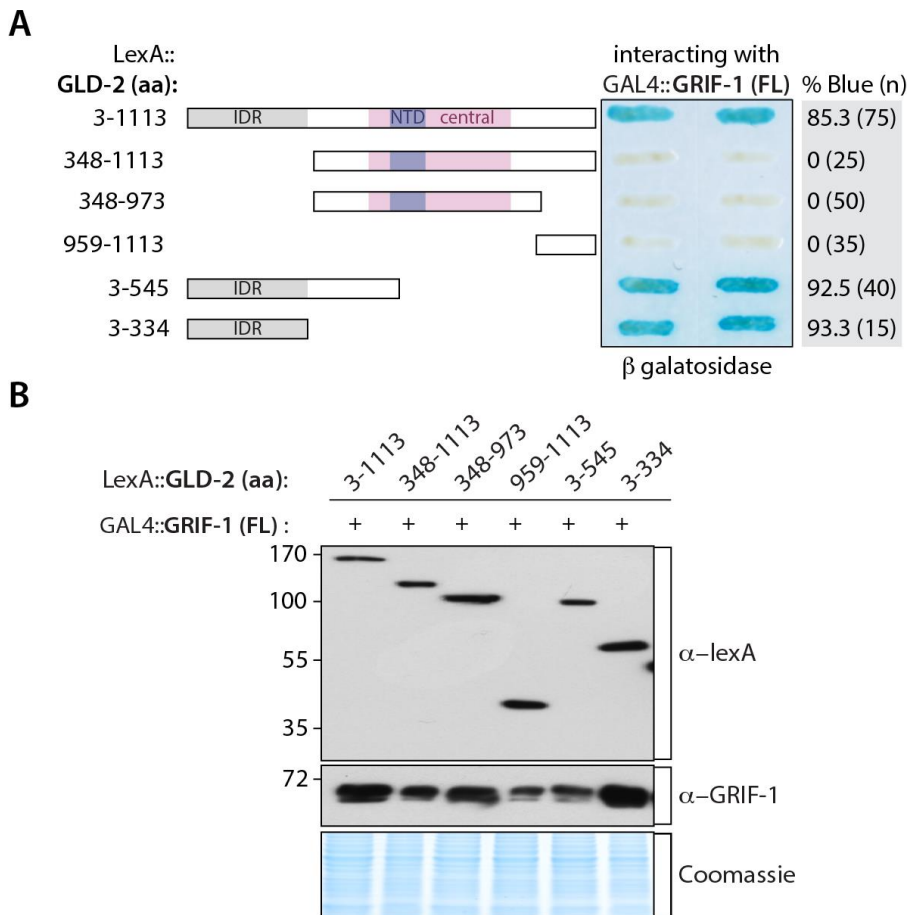
Figure 4.3.2. The N-terminal portion of GLD-2 is required for interaction with GRIF-1 in Y2H test.

(A) Beta-galactosidase activity in yeasts co-expressing GAL4::GRIF-1 full-length fusion protein and different truncations of GLD-2 fused with LexA DNA-binding domain. A blue colour indicates that an interaction may have occurred. Next to the Beta-galactosidase assay is analysis of percentage of colonies that were blue and the total number of colonies tested is in bracket as n. (B) Immunoblots of yeast extracts corresponding to (A) and probed with anti-LexA to determine GLD-2 levels (top blot) and anti-GRIF antibodies to determine expression of GRIF-1 (lower blot). The lowest panel is an image of acrylamide gel stained with Coomassie. It contains the total protein from yeast extract which is a loading control.

4.3.3. All GRIF-1 domains are cooperatively required to interact with GLD-2

In a converse experiment to determine which part of GRIF-1 is required for GLD-2 binding in yeast, several truncations of GRIF-1 protein were generated and fused to the Gal4 transcriptional activation domain. GRIF-1 truncations were co-expressed with LexA::GLD-2 full-length fusions. However, unlike in GLD-2 protein in which an unambiguous domain that interact with GRIF-1 was identified, a rather complex picture emerged during experiments to determine a single GLD-2 interacting surface in GRIF-1 (Figure 4.3.3).
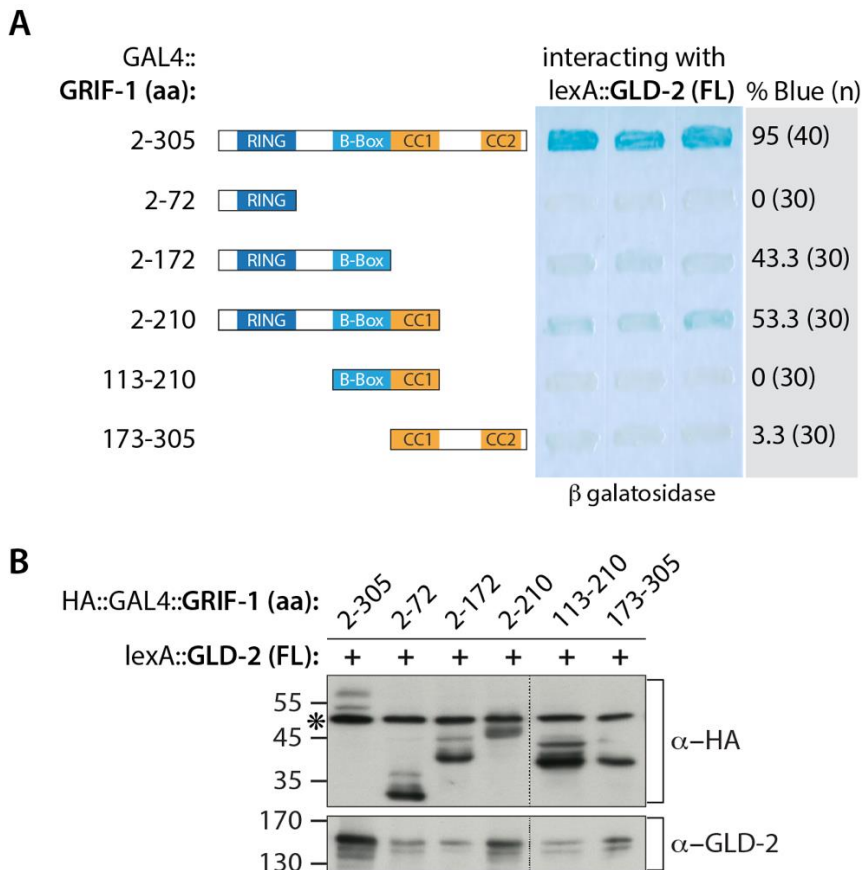
Figure 4.3.3. All GRIF-1 domains are essential for optimal interaction with GLD-2 in Y2H test.

(A) Beta-galactosidase activity of yeasts co-expressing indicated fusion proteins. Blue colour indicates potential interaction. (B) Immunoblot of yeast extracts corresponding to (A) to ascertain that all combinations of fusion proteins were expressed. The blot was probed with anti-HA antibody to determine expression of GRIF-1 (top blot) and probed with anti-GLD-2 to determine GLD-2 levels (bottom blot). Asterisk (*) shows unrelated background signal.

As observed above in Y2H assays, yeast colonies expressing full-length of both GRIF-1 and GLD-2 proteins showed a high likelihood of interaction between GLD-2 and GRIF-1; as they turned blue in most cases (Figure 4.3.3A). However, none of the yeasts co-expressing any of GRIF-1 truncations with full-length GLD-2 gave rise to intense blue colour comparable to GRIF-1 full length in the first 3 to 4 hours of blue-white assay (Figure 4.3.3A). This suggest that removal of any part of GRIF-1 perturbs its interaction with GLD-2.

Noteworthy, after 4 hours of assay, yeast colonies expressing fusions that lack either one or two of GRIF-1's coiled coil domains developed extremely weak blue colour even when negative controls were clearly white (Figure 4.3.3A). By contrast, none of yeast colonies co-expressing GRIF-1 truncation containing either RING alone, B-Box with coiled coil 1 or both coiled coil domains turned blue. Importantly, protein expression level differences could not explain these observations as GRIF-1 truncations were robustly detected in western blot analysis carried out to test the expression of fusion proteins encoded by all constructs (Figure 4.3.3B). These results suggest that, although the contribution of the coiled coil domain may be little compared to others, all GRIF-1 domains are important for GLD-2

interaction in Y2H tests. Additionally, it may also suggest that for optimal interaction with GLD-2, full-length GRIF-1 must adopt a critical conformation that is important for its interaction domain to make contact with GLD-2. Removal of any part of GRIF-1 may perturb this conformation.

4.3.4. GLD-2 and GRIF-1 form a protein complex in embryonic extracts

An interaction between GLD-2 cytoPAP and its potential turnover factor, GRIF-1, in yeast suggests that the two proteins may also interact *in vivo*. Therefore, to determine if GRIF-1 forms a complex with GLD-2 in worm, protein co-immunoprecipation (co-IP) experiments were performed from wild-type embryonic extracts using monoclonal antibodies against GRIF-1 and red fluorescent protein (RFP). The later serves as a background control for unspecific binding to the bead material and IgG.

Due to the very restricted expression pattern of GRIF-1 protein during early embryogenesis, only a small percentage of embryos, in every harvested population, is expected to contain GRIF-1 protein. Moreover, even in those embryos that express GRIF-1, only one cell (P4) or two cells (Z2/Z3) express GRIF-1 protein, depending on the stage of their development. Therefore, protein extracts for co-IP experiments will have to be made from a very high number of embryos and per experiment an average of 2 to 4 million embryos were used to generate a single co-IP extract. Upon completion of pulldown, Co-IP materials were analysed by western blotting. 5 % of input and unbound fractions and 50 % of eluate materials were loaded on polyacrylamide gel and analyzed with western blot (Figure 4.3.4).
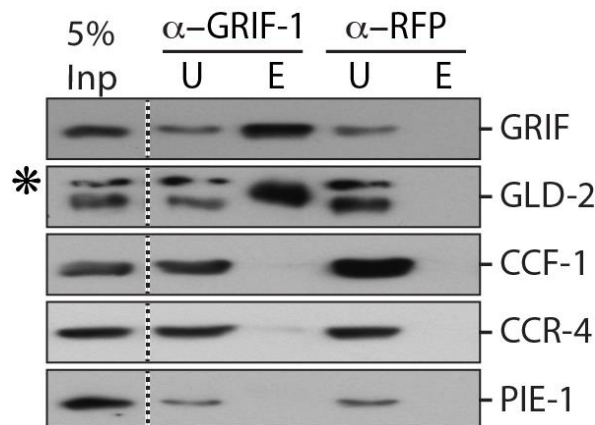
Figure 4.3.4. GLD-2 is enriched in GRIF-1 pulldown from embryonic extracts

Immunoblot of co-immunoprecipitation experiments using monoclonal GRIF-1 antibodies to pull GRIF-1 protein from embryonic extracts and anti-RFP antibodies as background control and probed with several antibodies recognising GRIF-1, GLD-2, CCF-1, CCR-4 and PIE-1. 5 % of the input material (Inp), 5 % of the supernatants or unbound fractions (U), and 50 % of eluate materials (E), were analysed with immunoblotting. Asterisk (*) shows unspecific background signal. GRIF-1 pull down was performed with a mixture of 4 monoclonal antibodies (see materials and methods). Individual use of these antibodies gives similar results. To reduce a likely turnover activity of GRIF-1, a metalloenzyme, protease inhibitors containing EDTA were used in these co-IP experiments.

GRIF-1 and GLD-2 were detected in input fraction as well as in the unbound fractions of both GRIF-1 and RFP pulldown experiment. Importantly both proteins were also detected in GRIF-1 but not in RFP pulldown, suggesting that GLD-2 and GRIF-1 enrichment was specific and it is not due to stickiness of either GRIF-1 or GLD-2 to IgG or bead material during the experiment (Figure 4.3.4). Furthermore, to control for specificity in GRIF-1 pulldown materials, several other RNA regulators expressed in embryonic germ cells were tested for enrichment. These included transcription and mRNA regulator, PIE-1, and the two catalytic subunits of the CCR4-Not deadenylase complex, CCF-1 and CCR-4. None of these three proteins were enriched in either GRIF-1 or RFP pulldown (Figure 4.3.4). These observations suggest that GLD-2 associates with GRIF-1 in embryo extracts and the two proteins most likely associate with each other *in vivo.*

4.3.5. GRIF-1 colocalizes with GLD-2 protein on P granules

The interaction of GRIF-1 and GLD-2 in both Y2H assay and co-IP experiments strongly suggests that the two proteins also interact *in* vivo during embryogenesis. Furthermore, the previously observed localization of GRIF-1 to P granule in the P4 germ cell precursor (Figure 4.2.7 and 4.2.8) suggests that GRIF-1 may interact with GLD-2 within P granules. This hypothesis predicts that GRIF-1 should co-localise with GLD-2 on P granule in P4 germ cell precursor. To test this hypothesis, an immunofluorescent experiment was carried out in which wild-type embryos were probed with antibodies specific to GLD-2, GRIF-1 and PGL-1 proteins. PGL-1 expression was used as penetration control, to identify germ cells and ultimately, P granules (Figure 4.3.5).
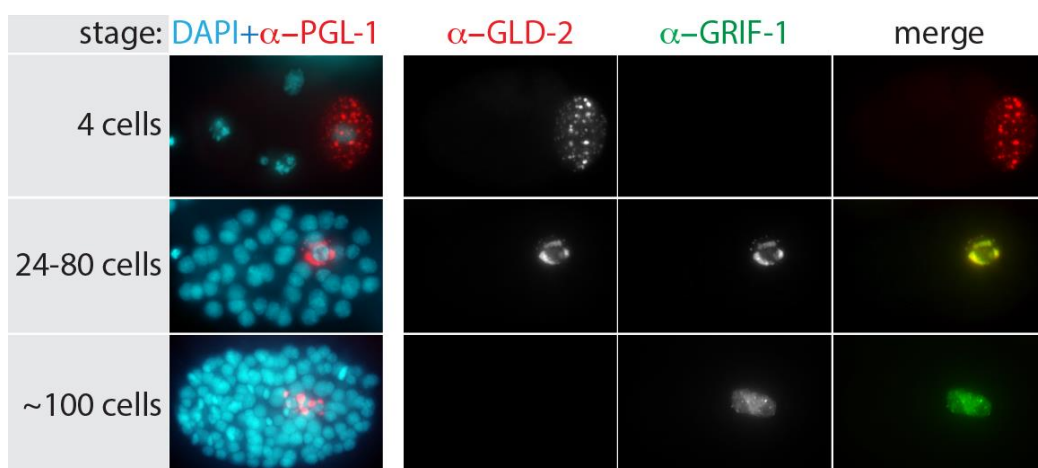
Figure 4.3.5. GRIF-1 colocalises with GLD-2 on P granules.

Immunofluorescent images of different developmental stages of wild-type embryos stained for PGL-1 and chromatin (left column). Next to left column, from left to right column, are column showing the same embryos probed for GLD-2 (Rhodamin channel), GRIF-1 (FITC channel), and merge of both GLD-2 and GRIF-1 (red and green, respectively).

In this immunofluorescent analysis to determine a likely colocalization between GRIF-1 and GLD-2 on P granules, PGL-1 was detected in the entire embryonic germ cell lineage and almost exclusively enriched on P granules (Figure 4.3.1) (Kawasaki, Shim et al. 1998, Kawasaki, Amiri et al. 2004). In contrast to PGL-1, GLD-2 was initially detected in the cytoplasm of embryonic germ cell precursors in 1-cell to approximately 80-cell stage embryos where it is both cytosolic and enriched on P granules. GLD-2 protein expression ceases once primordial germ cells are born at around 100-cell stage of embryogenesis (Wang, Eckmann et al. 2002 and Figure 4.3.5). Conversely, yet consistent with previous data (Figure 4.2.7 and 3.2.8), GRIF-1 was not detectable in early embryos but became detectable in germ cell precursor P4 of approximately 24-cell to 80-cell stage embryos where it is almost exclusively localised to P granules. Focusing on germ cell primordium P4 of every observed embryo, GRIF-1 and GLD-2 shows a striking co-localization on P granules. GRIF-1 expression continued into PGCs where it is less granular and more diffusely cytosolic (Figure 4.3.5). This experiment shows that GRIF-1 strongly co-localises with GLD-2. Furthermore, it reveals that disappearance of GLD-2 in PGCs strongly correlates with the dissociation of GRIF-1 from P granules.

4.3.6. GRIF-1 promotes turnover of GLD-2 protein in primordial germ cells

The expression of the TRIM32-related protein, GRIF-1, is activated in P4 at a time that shortly precedes loss of GLD-2 expression. Additionally, GRIF-1 interact with GLD-2 from embryo extracts and co-localise with GLD-2 on P granules. Hence, GRIF-1 may promote the turnover of GLD-2 cytoPAP in primordial germ cells. To address this possibility, the expression of GLD-2 cytoPAP was analysed in PGCs of various *grif-1* mutants.

grif-1 mutants are maintained as heterozygotes over a balancer chromosome (hT2g) and since *grif-1* is a maternal gene, the effect of *grif-1* loss would be observed in F2 homozygote *grif-1* embryos. Therefore, to analyse GLD-2 expression in the primordial germ cells of these F2 embryos, gravid F1 homozygote *grif-1* animals were dissected to extrude F2 embryos. The embryos were then analysed for GLD-2 cytoPAP expression in an immunocytochemistry experiment alongside wild-type embryos as control. To control for equal antibody penetration and to mark germ cells, embryos were co-stained with anti-PGL-1 antibodies in additional to anti-GLD-2 and anti-GLD-3 antibodies. In this experiment, PGL-1 was detected and localised to P granule in PGCs of wild-type embryos (Figure 4.3.6). In wild type, during embryogenesis, GLD-3 has similar, if not identical, expression pattern to GLD-2 (Eckmann, Kraemer et al. 2002, Wang, Eckmann et al. 2002). Therefore, as expected, both GLD-2 and GLD-3 were not detectable in PGCs of wild-type embryos (Figure 4.3.6). Similar to wild type, PGL-1 expression was detectable in PGCs of all *grif-1* embryos analysed. Intriguingly and in contrast to wild type, GLD-2 and GLD-3 proteins were robustly observed in

nascent PGCs, from 100-cell stage to the end of embryogenesis, of all analysed *grif-1* mutant embryos (Figure 4.3.6). This observation demonstrates that GRIF-1 promotes the turnover of GLD-2/GLD-3 cytoPAP complex in PGCs.

Interestingly, in *grif-1* embryos, the levels of both GLD-2 and GLD-3 proteins only stay high and are enriched on P granules until approximately 500-cell stage (or more specifically comma stage). However, from comma stage onwards, they were observed to dissociate from P granular into more diffuse cytosolic localization in PGCs until hatching. This change in localization was accompanied with what appeared to be a gradual reduction in the levels of both GLD-2 and GLD-3, and although reduced, both proteins were still detectable at hatching (data not shown). Importantly, similar results were obtained when the expression of *grif-1* was reduced by RNAi-mediated knockdown (data not shown). Together, these results suggest that GRIF-1 promotes correct timing of GLD-2 turnover in PGCs. It also suggests that additional factor(s) may act with GRIF-1 to efficiently terminate GLD-2 cytoPAP expression in PGCs. Alternatively, this gradual reduction in the levels of GLD-2 and GLD-3 in *grif-1* mutants may be due to general instability of the proteins that is independent of the stage of development.
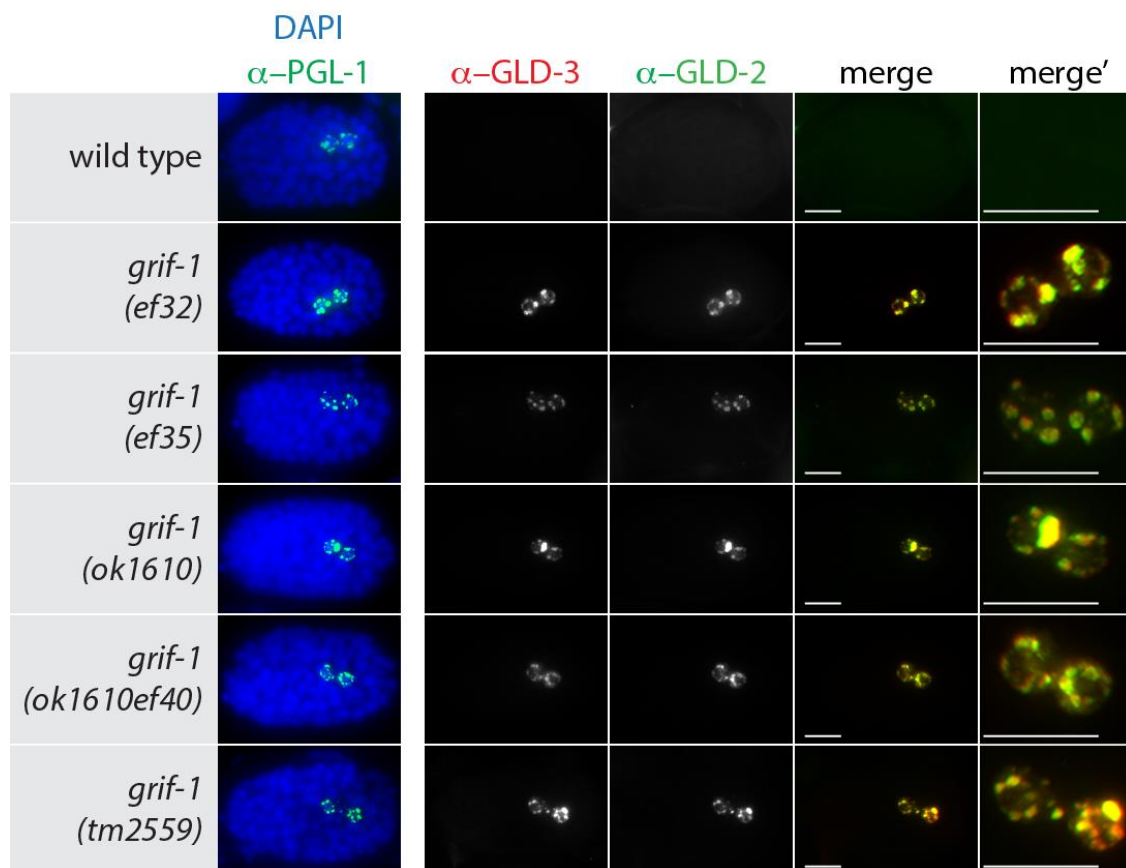
Figure 4.3.6. Expression of GLD-2 and GLD-3 proteins is extended into PGCs in *grif-1* mutants

Immunofluorescent images of wild-type (top row) and *grif-1* mutant embryos (second to bottom row) stained for chromatin, in blue, and PGL-1, in green (left column). The next three columns, from left to right, display GLD-3 in grey scale, GLD-2 in grey scale, and merge image of the GLD-3 and GLD-2

channels in colour (red and green, respectively). The right column labelled as merge' is a blow up of the merge images focusing on PGCs. Scale bar is 10 μM.

4.3.7. The expression of at least two other maternal proteins are extended in *grif-1* mutants

The protein expression of several other maternal proteins are terminated concomitant with the birth of PGCs in wild-type embryos. This includes RNA regulators PIE-1, POS-1, SPN-4, MEG-1, MEG-2, MEG-3 and MEG-4 (Mello, Schubert et al. 1996, Tabara, Hill et al. 1999, Leacock and Reinke 2008, Wang, Smith et al. 2014). The observation that GRIF-1 promotes the turnover of GLD-2 and GLD-3 proteins in PGCs begs the question whether GRIF-1 promotes the turnover of other maternal proteins in PGCs.
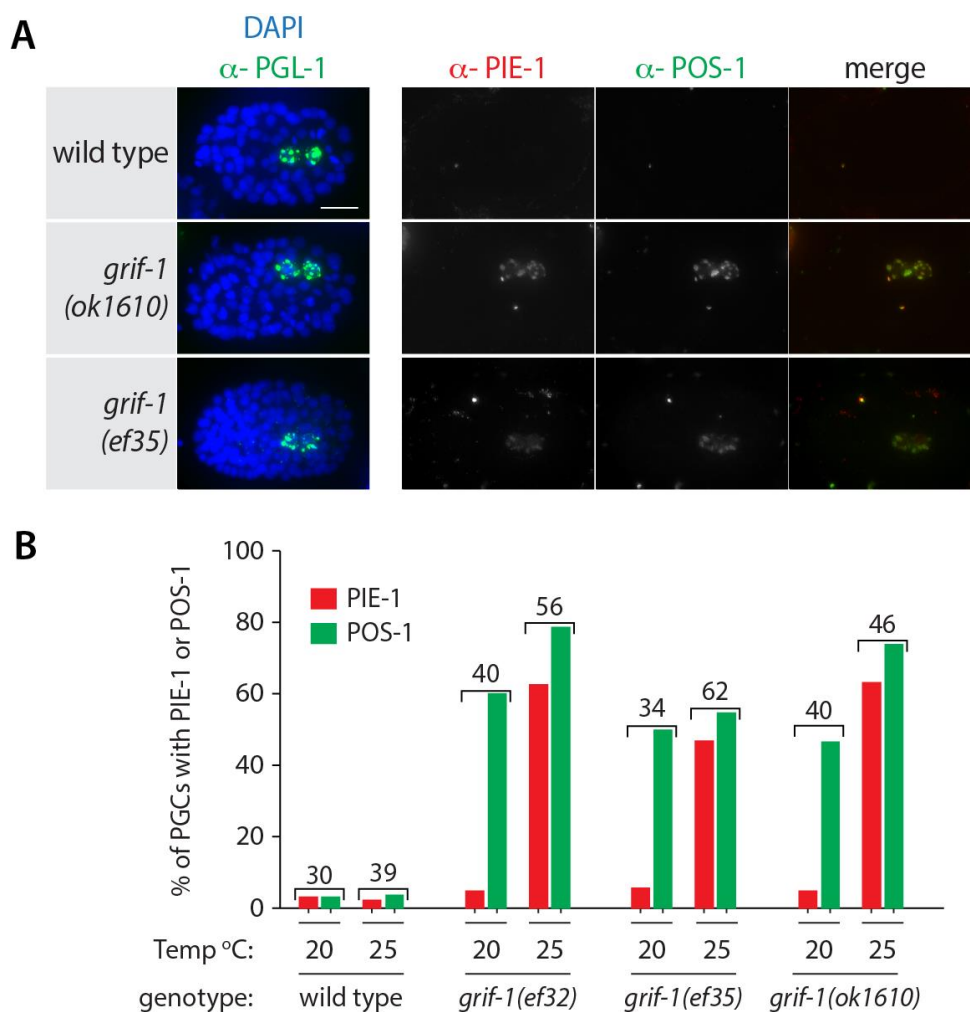
Figure 4.3.7. PIE-1 and POS-1 expression is transiently extended in *grif-1* mutants.

(A) Immunofluorescent images of approximately 100-cell stage embryos of indicated genotypes stained for chromatin in blue and PGL-1, in green (left column). The next three columns, from left to right, display PIE-1 in Cy3 channel, POS-1 in FITC channel, and merge image of POS-1 and PIE-1 in colour (green and red respectively). Scale bar is 10 μM. (B) A bar chart showing the percentage of embryos of indicated genotypes with extended expression of either PIE-1 or POS-1 proteins in PGCs. Only embryos between 100-cell and 300-cell stage were analysed. The number above the bar charts are the number of embryos analysed.

To address whether the turnover of other maternal proteins is promoted by GRIF-1, additional immunofluorescent experiments were performed on *grif-1* mutants using antibodies specific to PIE-1 and POS-1. Antibodies or other recourses to other maternal proteins were unfortunately not available. In this experiment, PGL-1 was robustly detected in the PGCs of wild type and *grif-1* embryos (Figure 4.3.7A). Interestingly, while PIE-1 and POS-1 were not detected in PGCs of wild-type embryos, the expression of either protein was detected in PGCs of *grif-1* embryos (Figure 4.3.7A). However, several observations were made about PIE-1 and POS-1 expression in *grif-1* mutants that differed from those observed for GLD-2 and GLD-3 proteins. Firstly, unlike GLD-2 and GLD-3 which were prolonged in the PGCs of all embryos of *grif-1* mutants, only a subset of embryos was detected with prolonged PIE-1 and POS-1 expression; at 20°C, more embryos stabilised POS-1 than PIE-1 while at 25°C, both were stabilized in almost equal number of embryos (Figure 4.3.7B). Secondly, in contrast to GLD-2 and GLD-3 which were prolonged throughout embryogenesis with gradual but marginal loss in expression, PIE-1 was only detected from 100-cell stage until ~150-cell stage while POS-1 was detected until ~300-cell stage, after which the expression of either protein is no longer detectable (data not shown). Together, these results show that the expression of PIE-1 and POS-1 are only transiently prolonged in *grif-1* mutants. PIE-1 does not co-purify with GRIF-1 in pulldown experiments (Figure 4.3.4), suggesting that GRIF-1 may not directly regulate PIE-1 and presumably, POS-1 too. However, determination of whether prolonged expression of PIE-1 and POS-1 is an indirect downstream consequence of its activity on GLD-2 cytoPAP will require additional experiments. A likely dependence of extended expression of these two maternal proteins on GLD-2 is further expatiated (see Discussion, section 5.3).

4.4. Ectopic expression of GRIF-1 leads to lower levels of GLD-2 in adult germ cells

GRIF-1 is predominantly expressed in embryonic germ cells and promotes the turnover of GLD-2 and GLD-3 proteins in PGCs. An attractive hypothesis is that GRIF-1 is a ubiquitin ligase that polyubiquitinates GLD-2 to target it for proteasome degradation and when ectopically expressed at any other stage of germ cell development, GRIF-1 might also induce a reduction in GLD-2 amounts, provided that other necessary molecular machineries are available. An extension of this hypothesis is that, biological defects might arise due to reduced levels of GLD-2 cytoPAP complex. This section describes experiments carried out to analyse GLD-2 expression and possible downstream defects in germ cells that ectopically express GRIF-1.

4.4.1. Forced postembryonic germline expression of GRIF-1

To ectopically express GRIF-1 in the postembryonic germ line, several steps were taken. The genomic locus of *grif-1* contains only a small proportion of coding exonic sequences but large intronic sequences. To put this in perspective, the ORF is 918 bases while the locus, from start codon to stop codon and excluding any upstream regulatory sequence and the 3'UTR is approximately 5.2kb in length (Figure 4.4.1A). These large introns made amplifying the entire sequence from genomic DNA very difficult. Unfortunately, the complete cDNA of *grif-1* was not a great option as the presence of introns is known to facilitate the expression of transgenes (Jo and Choi 2015, Shaul 2017). To circumvent this bottleneck in the process of generating a *grif-1* transgene, the *grif-1* locus was re-engineered; the first three exons were amplified from genomic sequence and was fused to the last two exons derived from cDNA. This generated a single piece of DNA containing all five exons with only the first two introns (Figure 4.4.1B).

To express GRIF-1 throughout the germline, at all stages of development, a germline-specific promoter and a 3'UTR which drives protein expression at all stages of germ cell development were required. *mex-5* promoter is a germline-specific promoter while *tbb-2* 3'UTR drives protein expression at all developmental stages. Therefore, the newly generated piece of *grif-1* DNA, alongside with *mex-5* promoter and tubulin 3'UTR (*tbb-2* 3'UTR) were subsequently cloned into a single construct through multi-site gateway system (Zeiser, Frokjaer-Jensen et al. 2011). A control construct encoding a presumed inactive GRIF-1 protein was generated; a point mutation in which a key cysteine amino acid was replaced with alanine was introduced into the RING domain of GRIF-1 to reduce its potential ligase activity (Figure 4.4.1C). Therefore, either *grif-1* transgene is expected to drive GRIF-1 protein expression at all stages of germ cell development. Using Mos-1-mediated Single Copy insertion (MosSCI) transgenesis methods, these transgenes were inserted into the genome.

Two independent lines of strains were generated and analysed for each construct to ensure reproducibility (Figure 4.4.1C).
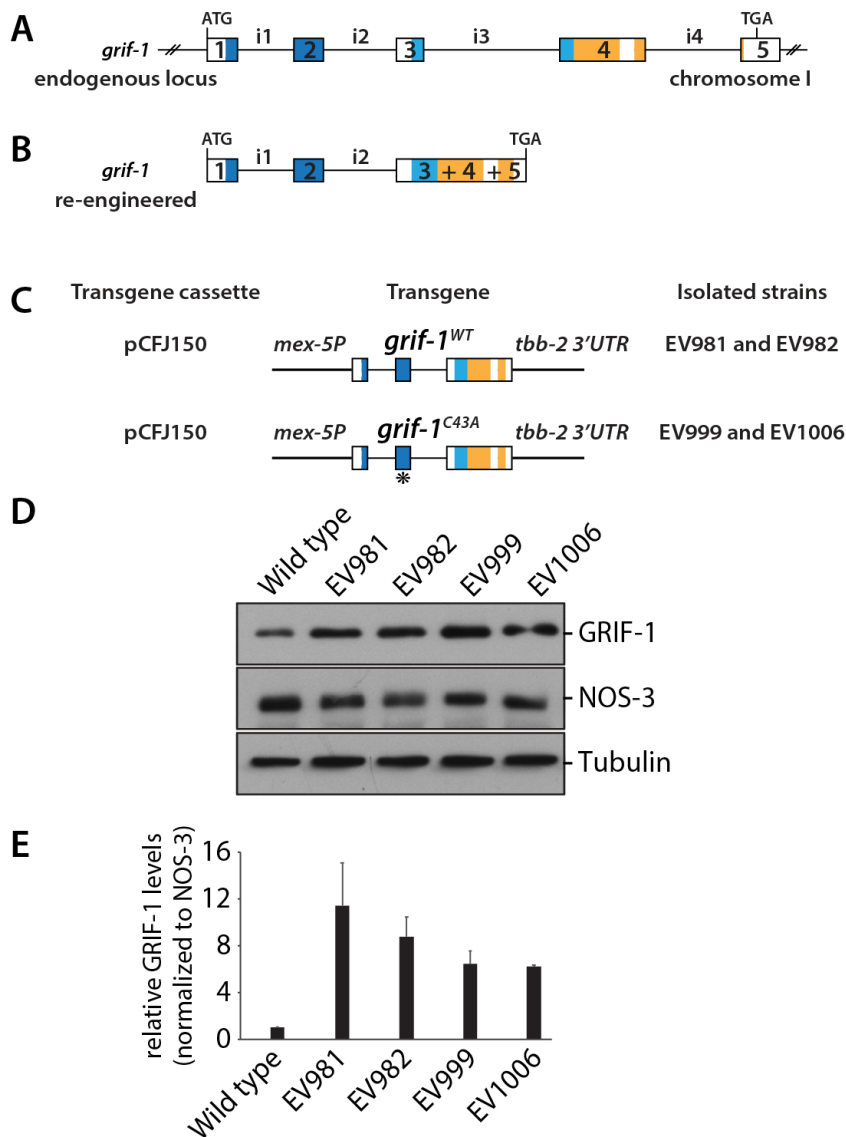
Figure 4.4.1. Generation of transgenic animals expressing GRIF-1 from a *mex-5* promoter and tubulin 3' UTR.

Graphical display of (A) wild-type endogenous *grif-1* genomic locus on chromosome I and (B) re-engineered for integration on chromosome II (see detail in main text). (C) Wild-type or RING mutant copy of *grif-1* transgene from multi-gateway assembled transgenic constructs from (B), driven by *mex-5* promoter and *tbb-2* 3' UTR, used for ectopic expression of GRIF-1 protein. Display in C is not drawn to scale. Asterisk marks the position of C43A point mutation in the re-engineered locus. Using already established Mos-1-mediated Single copy Insertion (MosSCI) transgenesis technique, the transgenes were inserted into chromosome II. Two independent lines were generated per transgenic constructs. Strain names were given as EV numbers. (D) Immunoblot of wild type (N2) and strains expression *grif-1* transgenes. NOS-3 and Tubulin serve as loading control. (E) Quantification of GRIF-1 from several blots (Four replicates for WT, EV981 and 982. Two replicates for EV999 and EV1006). GRIF-1 levels were normalized to NOS-3 levels. Error bars= standard deviation.

To determine whether the generated strains express transgenic GRIF-1, protein extracts were prepared from randomly selected one-day-old adult animals and were

subjected to western blotting experiments. GRIF-1 protein band was weakly detected in wild-type adult animals as expected in animals with embryos. By contrast, a more robust GRIF-1 protein band signal was detected in all transgenic strains expressing either wild-type or mutant GRIF-1 (Figure 4.4.1D). Tubulin protein which is both expressed in somatic as well as in the germ line of adult animals was used as loading control to estimate total protein loaded on gel. Therefore, immunoblots were probed with tubulin-specific antibodies. Tubulin was detected to almost equal levels in all strains (Figure 4.4.1D).

mex-5 promoter specifically drives expression in the germ line. Since GRIF-1 transgenes are expected to be specifically expressed in germ cells but not in soma, a protein which is expressed specifically in the germ line but not somatic cell may help to quantify the amount of germline material loaded into a lane. Therefore, the expression level of NOS-3, a protein expressed through the germ line, was determined using a NOS-3-specific antibody. NOS-3 protein was robustly detected in wild-type animals as expected. However, NOS-3 protein levels seem to be slightly lower in strains ectopically expressing wild-type GRIF-1 but not mutant GRIF-1 transgene. Differences in germ cell number may account for these expression variations. Nonetheless, the GRIF-1 amounts were normalized to the expression levels of NOS-3 in all the strains to determine the relative abundance of GRIF-1 that is expressed in germ cells (Figure 4.4.1E). The relative abundance of GRIF-1, normalised to NOS-3 levels, revealed that transgene driven *grif-1* produced moderately high levels of GRIF-1 protein in the germ line (Figure 4.4.1E). Together, these observations suggest that *mex-5* promoter and *tbb-2* 3'UTR driven *grif-1* transgene successfully promote detectable expression levels of GRIF-1 in the germ line.

4.4.2. Ectopic germline expression of GRIF-1 leads to reduced GLD-2 levels in adults

GRIF-1 promotes turnover of GLD-2 cytoPAP in PGCs during embryogenesis. Hence, ectopically expressed GRIF-1 may also promote GLD-2 turnover in the adult germline tissue. Therefore, to test for a likely reduction in GLD-2 and maybe also GLD-3 levels due to ectopic expression of GRIF-1 protein, immunoblots from protein extract of various strains were probed with GLD-2 and GLD-3 specific antibodies (Figure 4.4.2).

GLD-2 protein band was robustly detected in wild type (Figure 4.4.2). However, unlike in wild-type animals, GLD-2 protein levels were significantly reduced in transgenic strains ectopically expressing GRIF-1^{WT}. Interestingly, almost wild-type GLD-2 levels were detected in transgenic strains ectopically expressing GRIF-1^{C43A}, arguing that the mutated RING finger perturbed GRIF-1's function and the reduced GLD-2 levels seen in transgenic strains ectopically expressing GRIF-1^{WT} is due to RING dependent GRIF-1 activity (Figure 4.4.2). The two isoforms of GLD-3 proteins were robustly detected in wild-type animals. In contrast to GLD-2, normalised GLD-3 levels remain unchanged in transgenic strains ectopically

expressing either GRIF-1^{WT} or GRIF-1^{C43A} (Figure 4.4.2). Together, these results suggest that ectopically expressing wild-type but not mutant GRIF-1 leads to reduced levels of GLD-2. The results further demonstrate that GRIF-1 activity is dependent of its RING domain and a point mutation in the domain is sufficient to reduce GRIF-1 function.
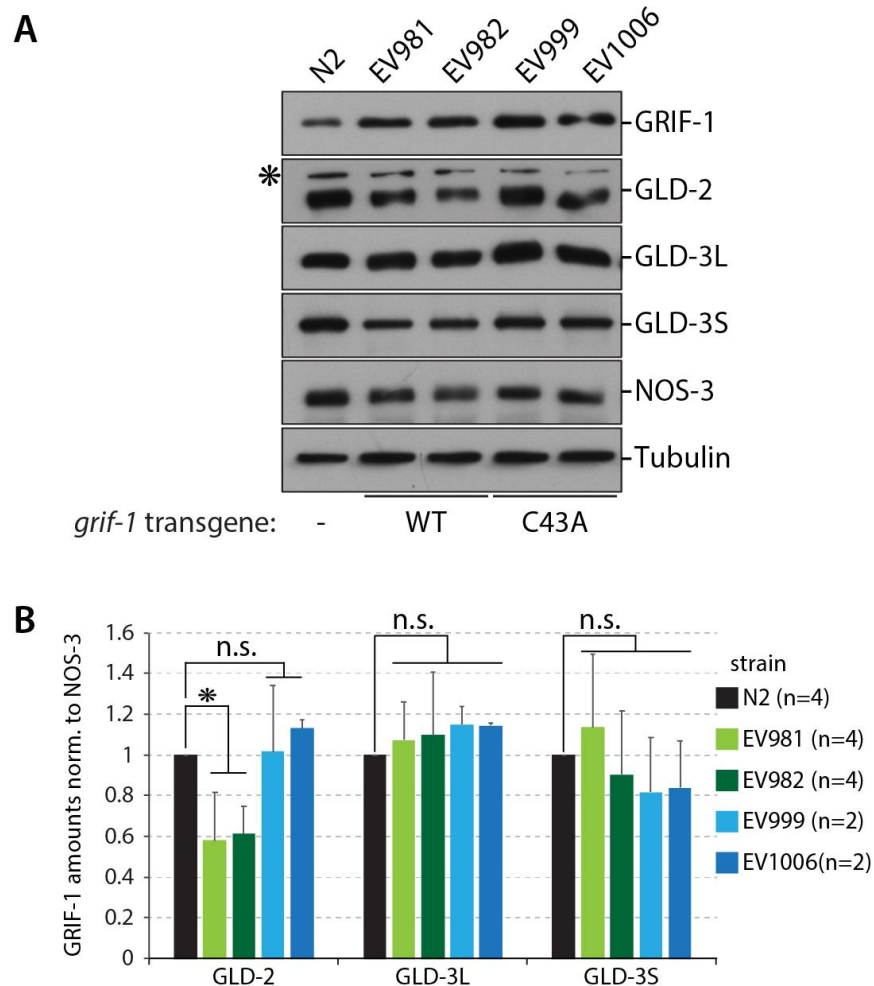
Figure 4.4.2. Lower GLD-2 levels upon ectopic expression of GRIF-1.

(A) Immunoblots of wild type (N2) and *grif-1* transgenic strains probed with antibodies against GRIF-1, GLD-2, GLD-3, NOS-3, and Tubulin. Asterisk (*) shows unspecific background signal. (B) Bar chart showing the relative levels of GLD-2 and GLD-3 isoforms corresponding to (A). Levels were normalised to NOS-3. Bar chart shows mean value (±SD). Significance was calculated by student's t-test: *= $p<0.05$, n.s.= not significant. n is the number of replicates performed.

4.4.3. Ectopically expressed GRIF-1 copurify with GLD-2

If the observed reduction of GLD-2 abundance in the germ line of strains ectopically expressing wild-type GRIF-1 were due to the presumed E3 ubiquitin ligase activity of GRIF-1 and not an alternative mechanism, several conditions may apply. GRIF-1 should interact with GLD-2 in an RNA-independent manner, incubation of extracts containing both proteins in sufficient amount should lead to observable GLD-2 degradation and modified or ubiquitinated GLD-2 should be identifiable either through western blot or mass spectrometry. These

possible outcomes were explored to gain further insights into the molecular mechanisms by which GRIF-1 promotes GLD-2 turnover.
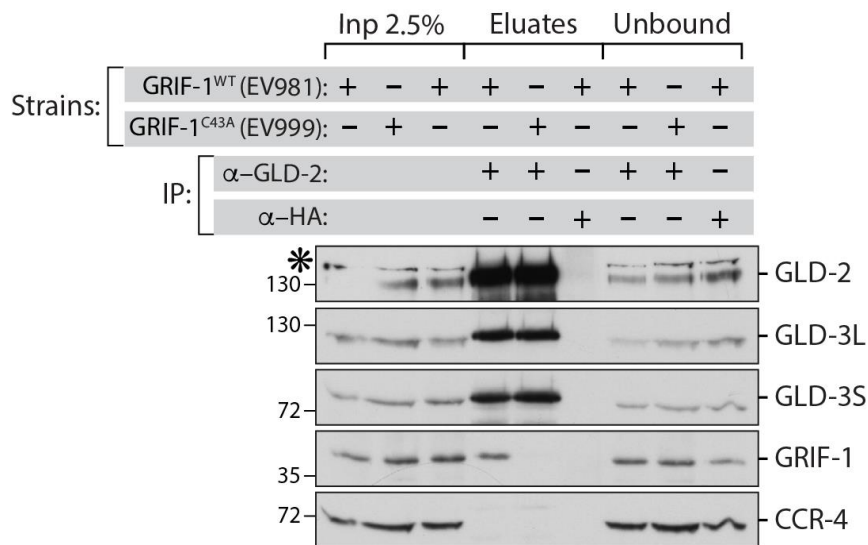
Figure 4.4.3.1. Ectopically expressed GRIF-1 interacts with GLD-2 in a RING domain-dependent manner.

Immunoblots of anti-GLD-2 and anti-HA co-IP experiments from transgenic strains ectopically expressing GRIF-1^{WT} (EV981) or GRIF-1^{C43A} (EV999) were probed with monoclonal antibodies specific to GLD-2, GLD-3, GRIF-1, and the deadenylase, CCR-4. Both isoforms of GLD-3 were detected. Asterisk (*) shows unspecific background signal. 2.5 % of Input (Inp), unbound fractions and 50 % of eluates were analysed.

To determine whether ectopically expressed GRIF-1 may form a complex with GLD-2 in the germ line, co-immunoprecipitations were performed from strains ectopically expressing either wild-type or mutant GRIF-1 using GLD-2-specific monoclonal antibodies. As a specificity and background precipitation control, a monoclonal anti-HA antibody was used in combination on the same protein extract. The materials were analysed with western blot and immunoprobed with monoclonal antibodies specific to GLD-2, GLD-3 and GRIF-1. To avoid any contribution of endogenous embryonic wild-type GRIF-1 in strain ectopically expressing mutant GRIF-1, which may complicate interpretation of results, protein extracts for co-immunoprecipitations were prepared from a synchronised population of animals consisting of L4 larvae and young adult hermaphrodites, avoiding embryo-carrying adult hermaphrodites.

By comparing input and eluate materials, GLD-2 protein was enriched in eluates of anti-GLD-2 pulldown from both strains expressing either wild type or mutant GRIF-1. Importantly, GLD-2 was not detected in eluates of anti-HA arguing that GLD-2 was specifically enriched with GLD-2 antibody without background interactions due to IgGs or bead materials (Figure 4.4.3.1). Furthermore, both isoforms of GLD-3 protein, a confirmed direct interaction partner of GLD-2, were robustly detected in eluates of GLD-2 but not in eluates of anti-HA, arguing that ectopic expression of either wild-type or mutant GRIF-1 does not perturb the GLD-2 and GLD-3 interaction (Figure 4.4.3.1).

Intriguingly, GRIF-1 was observed to be enriched in GLD-2 precipitation of extracts that were produced from transgenic strain ectopically expressing GRIF-1^{WT} but not GRIF-1^{C43A} despite the fact that both GRIF-1^{WT} and GRIF-1^{C43A} were detectable to similar amounts in inputs and GLD-2 is enriched to similar amounts in eluates of both strains (Figure 4.4.3.1). An extremely weak signal of GRIF-1^{C43A} is detectable in immunoblots after a very long exposure (data not shown). This significantly reduced enrichment of GRIF-1^{C43A} was consistently observed in several co-immunoprecipitation experiments, arguing that reduced enrichment in pulldown was not due to experimental artefacts (n=3, Figure 4.4.3.1 and data not shown). As an additional control, immunoblots were probed with anti-CCR-4 antibodies. CCR4 is one of the catalytic subunits of the CCR4-Not deadenylase complex. Although detected in input materials, CCR-4 was not enriched in eluates of either GLD-2 or HA pulldown, suggesting that GLD-2 antibody specifically enriched for GLD-2-interacting proteins and not all germline proteins. These observations suggest that ectopically expressed GRIF-1 interact with GLD-2 in a RING-dependent manner, supporting earlier results from yeast two-hybrid tests that suggest that all domains of GRIF-1 work cooperatively for an optimal interaction with GLD-2.

To determine whether interaction of germline expressed GRIF-1 with GLD-2 is RNA dependent, co-immunoprecipitation experiments were repeated using protein extract from transgenic strain expressing GRIF-1^{WT} alone which was either treated or untreated with RNAse A. GLD-2 was observed to be enriched in the eluates of GLD-2 pulldown but not RFP pull down (Figure 4.4.3.2). As observed before, GLD-3 isoforms and GRIF-1 were also enriched in GLD-2 pulldown but not RFP pulldown and enrichment of GRIF-1 was unaffected by treatment with RNAse A (Figure 4.4.3.2). By contrast, several other proteins, including CCF-1, CCR-4 and LAF-1 which were investigated as additional specificity control were not enriched in GLD-2 pulldown (Figure 4.4.3.2). These observations suggest that GRIF-1 interact with GLD-2 in RNA-independent manner.

During the course of the above experiment, shorter products of GLD-2 were often observed in eluates of transgenic strains ectopically expressing GRIF-1^{WT} (See white arrowheads in Figure 4.4.3.2). Although the abundance of these likely degradation products varies from experiment to experiment, they were always specific for GLD-2 protein and not observed with other analysed proteins. Additionally, they were only observed in eluates but not in input or unbound fractions, suggesting a correlation of the degradation products with local high concentrations of GRIF-1 and GLD-2 and that modified GLD-2 may be degraded by proteasome in the extracts. Importantly, when the experiment was repeated in the presence of wild-type strain lacking a transgene (i.e. N2), degradation products of GLD-2 were observed in transgenic strains expressing GRIF-1^{WT} but not wild-type strains lacking

GRIF-1 transgene (data not shown). However, this last experiment was performed once and additional experiments are required for clarity.
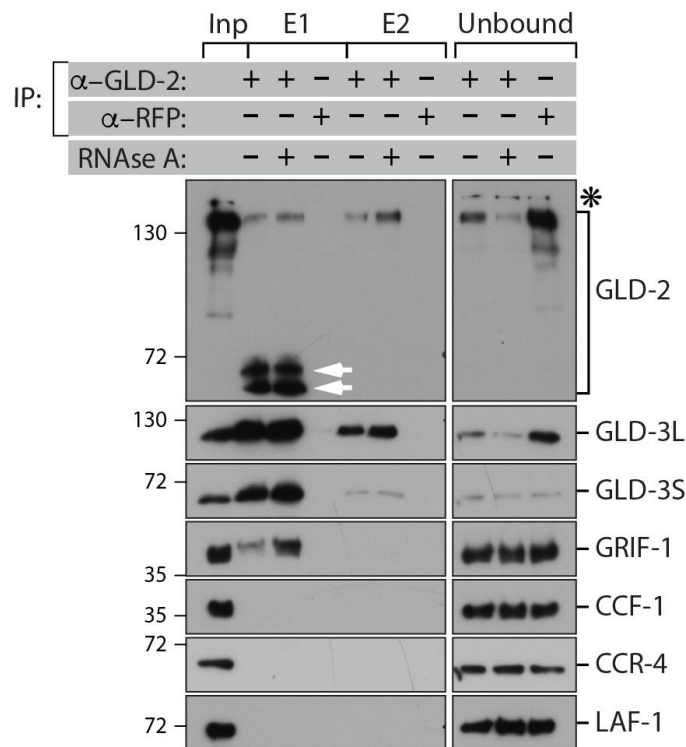
Figure 4.4.3.2. The interaction of ectopically expressed GRIF-1 with GLD-2 is independent of RNA.

Immunoblots of anti-GLD-2 and anti-RFP co-IP experiments from the EV981 transgenic strain that ectopically expresses GRIF-1^{WT} either RNAse A treated or untreated. Blots were probed with antibodies specific to GLD-2, GLD-3, GRIF-1, CCF-1, CCR-4, and LAF-1. Proteins were eluted under mild (E1) and stringent conditions (E2). 5 % of input (Inp), unbound fractions and 50 % of eluates were analysed. White arrowheads indicate possible degradation products of GLD-2 which were detected in the eluates of GLD-2 pulldown. Asterisk (*) shows unspecific background signal. To allow GRIF-1 activity as a presumed metalloenzyme, EDTA-free inhibitors were used in this experiment.

Together, these observations suggest that GRIF-1 interacts with GLD-2 in an RNA independent manner. Additionally, the results suggest that, given a high local concentration, GRIF-1 may promote degradation of GLD-2 protein in extracts. Hence, a more robust ectopic expression of GRIF-1 would most likely lead to almost complete *in vivo* degradation of GLD-2 protein in adult germline tissue.

4.4.4. Ectopic GRIF-1 expression leads to fertility defects

In wild-type animals, GRIF-1 is only expressed in a brief window during embryonic germline development. Therefore, an ectopic expression of GRIF-1 protein throughout all stages of germ cell development might lead to germ cell defects due to reduced GLD-2 expression levels or other potential unknown targets. Since GLD-2 levels were only reduced to approximately half of its wild-type amounts; although strong variability in transgene

expression is expected from animal to animal as immunoblots only revealed levels of combined population of animals, a highly penetrant *gld-2* null phenotype was not expected. To begin to analyse germ cell defects associated with ectopic expression of GRIF-1, fecundity of wild-type adult animals as well as transgenic adult animals expressing either GRIF-1[WT] or GRIF-1[C43A] was initially analysed at 20°C and later at 25°C.

At 20°C, wild-type animals produce on average approximately 340 embryos. By contrast, strains expressing wild-type GRIF-1 transgenes produced significantly reduced number of progenies (data not shown). Interestingly, sterile animals were observed with a rough estimate of 2-5 % and these sterile animals often displayed two major germline phenotypes when examined with Nomarski microscopy (data not shown). In the first category, animals accumulated diplotene-like germ cells in the proximal region of their gonads and their gonads were extended compared to wild-type animals, a phenotype similar to those of *gld-2(0)* animals. In the second category, animals had gonads that are significantly smaller than in wild type. These shrunken gonads appeared to contain fewer and occasionally, no clearly identifiable germ cells, indicating either a strong germ cell proliferation defect or germline survival defect. Although those defects were not further analysed in detail, these phenotypes were not observed in transgenic strains ectopically expressing GRIF-1[C43A].

strain:	N2	EV981	EV982	EV999	EV1006
grif-1 transgene:	-	WT	WT	C43A	C43A
grif-1 genomic locus:	+	+	+	+	+
n:	1550	3990	2580	1945	1750
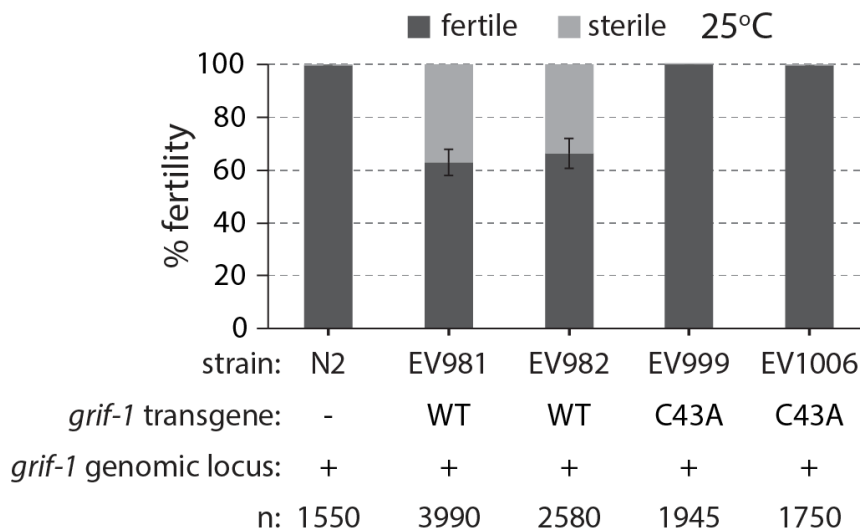
Figure 4.4.4.1. Ectopic expression of GRIF-1 in the germline leads to sterility.

A bar chart display of percentage fertility in wild type (N2) and strains ectopically expressing wild-type GRIF-1; EV981 and EV982 and those expressing mutant GRIF-1; EV999 and 1006. All strains were allowed to acclimatise at elevated temperature for two generations before analysis was carried out. Bar chart shows mean (± SEM).

The low frequency of these phenotype may be because transgenic GRIF-1 is expressed only at moderately high levels leading to incomplete turnover of targets. Therefore, strains were raised at elevated temperature of 25°C since elevated temperature is

known to reveal otherwise hidden phenotypes due to heat stress sensitivity (Schisa 2019). Moreover, increased temperature is also known to strongly promote transgene expression (Strome, Powers et al. 2001). Upon shift to elevated temperature as adults, animals were allowed to acclimatise to this temperature for two generations before the fecundity of resulting F2 adult worms was analysed again.

All analysed wild-type adult worms were fertile (>99 %, n=1550) (Figure 4.4.4.1). In contrast to wild type, a reduced number of transgenic animals ectopically expressing GRIF-1^{WT} were fertile (EV981: 63 %, n=3990; EV982 66 %, n=2580) and the remaining worms were sterile. Importantly, similar to wild type, all transgenic strains ectopically expressing GRIF-1^{C43A} were fertile (EV999: >99 %, n=1945; EV1006: >99 %, n=1750); in very rare cases during maintenance of these strains, one or two sterile animals were occasionally observed on a plate.

Some of the transgenic animals ectopically expressing GRIF-1^{WT} were fertile. To determine whether ectopic GRIF-1 expression also affected the germ line of fertile worms, brood sizes were determined and analysed for the number of living progenies and dead embryos. Since only fertile worms were of interest in this study, sterile worms were excluded from the analysis.

At 25°C, wild type produced approximately 212 embryos on average (n=15). Almost all of which hatched to produce living progenies with an insignificant number of dead embryos observed (Figure 4.4.4.2). By contrast, transgenic strains ectopically expressing GRIF-1^{WT} had a reduced brood size compared to wild type; EV981 produced 140 embryos on average (n=43) while EV982 produced 143 embryos on average (n=45) (Figure 4.4.4.2). Moreover, less than half of each brood hatched to produce living progenies and the remaining embryos either arrested or died during embryogenesis (Figure 4.4.4.2). Importantly, point mutation in RING domain did not induce these phenotypes and its brood size and number of living progenies were similar to wild type (Figure 4.4.4.2).

Together, these observations suggest that ectopic expression of GRIF-1 protein causes different levels of phenotype severity ranging from reduction in fecundity to complete loss of fecundity or sterility presumably due to variation in the expression levels of *grif-1* transgene in individual animals. Embryonic lethality may be a consequence of ectopic GRIF-1 activity either during gametogenesis or early embryogenesis where it would be otherwise absent in wild type. Notably, all induced phenotypes are dependent on the RING domain of GRIF-1. The occasional appearance of sterile animals in transgenic strains ectopically expressing GRIF-1^{C43A} shows that although a point mutation of a key amino acid in the RING domain significantly reduced GRIF-1 function, the mutation didn't completely abolish it. Alternatively, the phenotypes may represent transgene related but GRIF-1 independent activities. Nonetheless, the penetrance of this phenotype is not statistically significant.
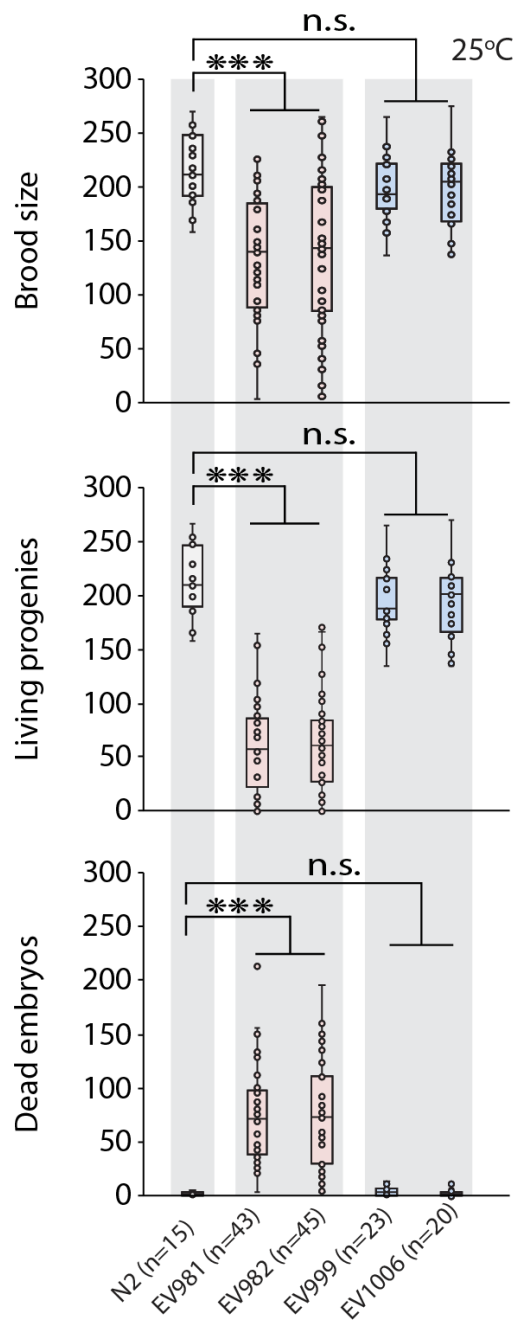
Figure 4.4.4.2. Fertile animals of GRIF-1 transgenic strains display reduced brood size.

Box plots showing the distribution of brood size (top), living progenies (middle) and dead embryos (bottom) of wild type and transgenic strains ectopically expressing GRIF-1^{WT}; EV981 and EV982, or GRIF-1^{C43A}; EV999 and EV1006. All strains were allowed to acclimatise at 25°C for two generation before analysis and sterile worms were excluded from this analysis. n is the number of analysed mothers. ***- P<0.001 Student's T-test. n.s= not significant

Each stage of meiosis and germ cell differentiation programs is characterized by distinct chromatin morphology which is easily revealed by immunofluorescent stanning using 4',6-diamidino-2-phenylindole (DAPI), a fluorescent stain that binds to DNA. To determine which germline defects were associated with sterility in strains ectopically expressing GRIF-

1^{WT} at elevated temperature, adult animals were stained with DAPI and visualized under fluorescent microscope (Figure 4.4.4.3).

In wild-type animals, the distal end of gonad contains mitotically dividing germ cells, which extend further proximally to about 20-cell diameter and this region is referred to as the proliferative or progenitor zone. The cells in this zone display a relaxed and diffusive chromatin with a ring-like appearance due to a centrally located and poorly DAPI stained nucleolus. Further proximally, germ cells exit the progenitor zone into a region known as the transition zone. Here, germ cells start meiotic prophase, undergoing the initial stages of leptotene and zygotene and the nucleolus becomes asymmetrically localised to one side of the nucleus, giving the chromatin a characteristic crescent-shape morphology. Further proximally, cells enter the pachytene stage in which a more condensed chromatin redistributes across the nuclear periphery and the nucleolus becomes re-centered. The condensed chromosome bivalents form thick threads of chromatin in the nucleus. In the bend region of the gonad, upon pachytene exit into diplotene, homologous chromosomes condense further, and bivalents become more visible and distinguishable. In the last stage of meiotic prophase I, termed diakinesis, the chromatin becomes fully condensed and six bivalents, held together by chiasmata, become visible. As germ cells begin to exit pachytene, meiotic program becomes coupled to germ cell growth with germ cells reaching a significant size by diakinesis. Female germ cells arrest as diakinetic oocytes in the proximal end of the gonad. The process of ovulation resumes meiosis and fertilization may occur by mature sperms (Kimble and Crittenden 2007).

Transgenic strains ectopically expressing GRIF-1^{C43A} have superficially normal gonads with germ cell organization that is similar to wild-type animals (Figure 4.4.4.3A). By contrast, strains ectopically expressing GRIF-1^{WT} display a plethora of germline phenotypes at elevated temperature. The most prevalent phenotype is a defect in proliferation with gonad containing just a few germ cells (48.5 % n=70) (Figure 4.4.4.3B). Often, such gonads contain germ cells that display additional phenotypes like having highly decondensed chromatin configurations that do not resemble chromatin appearances of any wild-type germ cell stage (data not shown). Another defect observed apart from proliferation defect was germline survival defect, in which the gonad is completely devoid of germ cells (11.4 % n=70) (Figure 4.4.4.3C). Lastly animals with diplotene arrest were also observed (4.3 % n=70) (Figure 4.4.4.3D). Other rare phenotypes that were observed at very low frequency of less than 2 % included pachytene arrest, presence of heterochromatic oocytes and masculinization of the germline in which many male germ cells but no female germ cells were detected (data not shown). The distribution of these phenotypes at elevated temperature is in strong contrast to 20°C in which a significant number of sterile animals display *gld-2*-like diplotene arrest, although penetrance of sterility phenotype was low and hampered detailed analysis.

Together, ectopic expression of GRIF-1 causes several germ cell defects leading to a reduction or complete loss of fecundity.
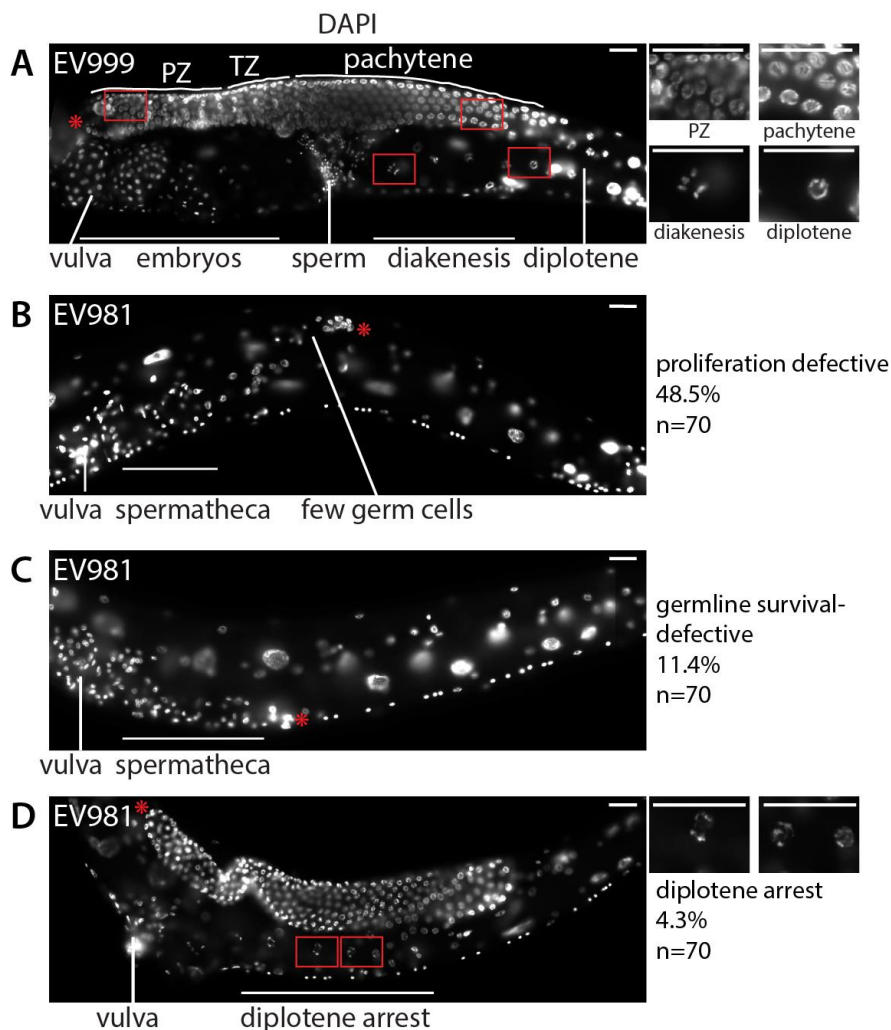
Figure 4.4.4.3. Ectopic expression of GRIF-1 causes germline defects.

Fluorescent DAPI images of transgenic animals ectopically expressing (A) GRIF-1[C43A]; EV999 and (B-D) GRIF-1[WT]; EV981. Asterisks (*) marks the distal end of germline. Blow ups on the right are germ cell nuclei at different stages of female meiosis. EV981 animals display several phenotypes including (B) germ cell proliferation defects, (C) germline survival phenotype, and (D) diplotene arrest (see blow up in right side of second image). Scale bar is 20 μM. The percentage of animals displaying this phenotype and the number analysed are also displayed on the right side of each phenotype.

The observed phenotypes may be a result of reduced GLD-2 levels or other potential GRIF-1 targets in animals ectopically expressing GRIF-1. Unfortunately, animals ectopically expressing GRIF-1 cannot be directly compared to animals that are either homozygous for *gld-2* null mutation, which completely lack GLD-2 protein, or animals that are heterozygous for *gld-2* null mutation, which may have only slight reduction in GLD-2 levels and thus display no obvious phenotypes at 20°C. This is because, unlike heterozygote or homozygote *gld-2* mutants, *grif-1* transgenes were most likely expressed at variable amounts among individual animals, causing a range of reduction in GLD-2 levels, from almost complete reduction in

some animals to very slight reduction in others, and hence appearance of varying phenotypes.

While the above scenario may explain appearance of *gld-2*-null phenotypes, neither proliferation defect nor germline survival phenotype had been linked to a reduction of *gld-2* activity. Therefore, to test if an intermediate reduction in GLD-2 levels may cause underproliferation and germline survival phenotypes either through maternal or zygotic activities that would otherwise be masked in *gld-2* null mutants, animals heterozygous for *gld-2(q497)* were maintained at elevated temperature for 2 to 3 generations. Interestingly, some of heterozygotes became sterile and possessed significantly under-proliferated germlines (data not shown). This argues that some of the under proliferative and germline survival phenotypes are due to a reduction of maternal GLD-2, presumably due to reduction in GLD-2 mRNA targets during embryogenesis as germline survival phenotype is often linked with embryogenesis.

In summary, together, these observations suggest that GRIF-1 is able to interact with GLD-2 regardless of the developmental stage of germ cells. The transgenes promoted only moderately robust expression levels of GRIF-1 in the germline, causing a partial reduction in GLD-2 levels in adults. To eventually achieve a complete or almost complete reduction of GLD-2 protein in the adult germline tissue through GRIF-1 activities, an alternative promoter or 3'UTR or a different approach that can drive higher expression levels of GRIF-1 protein may be required. It is noteworthy to mention that using constitutive promoter to achieve high level of expression will be a difficult task as animals expressing low levels of transgene will always survive better due to selective pressure. Therefore, using an inducible strong promoter may be the best strategy.

4.5. *grif-1* is under tight developmental control and its expression is regulated by its target in a feed forward loop

The highly restricted expression pattern of GRIF-1 protein suggests that GRIF-1 is under tight developmental control. This section describes all attempts made to delineate the molecular mechanisms that regulate the developmental expression of GRIF-1 protein.

4.5.1. *grif-1* is a maternally donated transcript

To begin to elucidate the gene expression mechanisms that control GRIF-1 protein expression pattern, the *grif-1* mRNA expression pattern was obtained from a publicly available nematode expression pattern database; Nextdb (see legend of Figure 4.5.1 for details). The database contains mRNA expression pattern of many *C. elegans* genes which were generated using *in situ* hybridization technique (ISH). ISH allows for detection of nucleic acid sequences within a tissue or histological section. Therefore, for a successful ISH procedure, the nucleic acids must be adequately preserved during preparation of biological sample. The localization of nucleic acids can be detected using nucleic acid probe that is complementary to target nucleic acid. A reporter molecule is attached to the probe which aids visualization of target RNA or DNA. Such molecules include radioactive isotopes and non-radioactive labelling molecules such as biotin, digoxigenin and fluorescent dyes.

The expression pattern of *grif-1* mRNA was then retrieved from the Nextdb database (Figure 4.5.1). In the available *in situ* hybridization images of *grif-1* transcript, a signal was not detected in either somatic or germ cells in all larvae stages. In young adults and adults, *grif-1* mRNA was also not detected in somatic cells, supporting developmental western blot that revealed that GRIF-1 protein is not expressed during larval development and somatic cells in adults (Figure 4.5.1). Intriguingly, a signal was detected in the gonad of adult animals, reaching from the bend region to the proximal region with no signal observed in the distal region (Figure 4.5.1). As no markers of germ cells are available in the images to identify the stages of cells in the germ lines, based on their position in the gonadal tube, transcription of *grif-1* mRNA is most likely initiated when germ cells are transitioning from pachytene into diplotene stage of meiosis program.

Moreover, a signal was also detected throughout the cytosol of 1-cell and 2-cell embryos indicating that the *grif*-1 transcript is an oocyte derived (maternally donated) mRNA (Figure 4.5.1). In embryos older than the 2-cell stage, *grif-1* mRNA was observed to disappear from somatic cells whereas, in contrast to somatic cells, the expression was continuously detected in germ cell precursors, which were identified based on their posterior position in the embryos (Figure 4.5.1). Furthermore, a robust signal was detectable in embryos that appeared to be between the 24-cell and 80-cell stage, and specifically in a cell that gastrulated from the posterior end into the middle of embryos (Figure 4.5.1). Based on

the earlier expression in germ cell precursors, the identity of this cell containing *grif-1* mRNA was judged to be the P4 germ cell primordium. In older embryos, a signal was detected in 2 centrally located cells which are likely the two PGCs, born from a symmetrical division of P4. Interestingly, *grif-1* mRNA was only detected robustly in nascent PGCs of embryos of approximately the 100-cell and 150-cell stage after which the signal was observed to disappear in PGC and no signal was detectable in embryos from embryos of 300-cell stage onward (Figure 4.5.1).
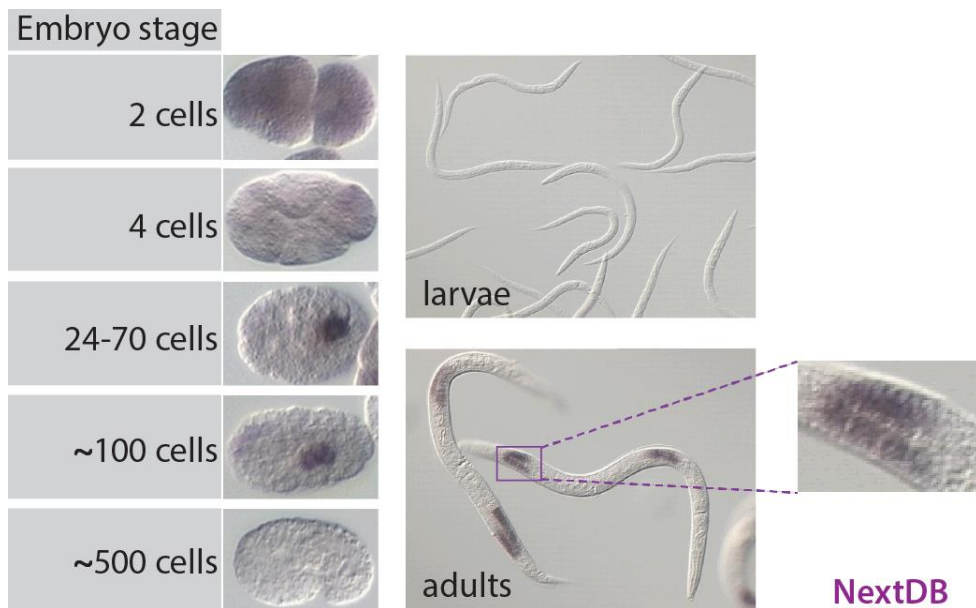
Figure 4.5.1. *grif-1* transcript is expressed in germ cells of adults and in embryonic germ cell lineage.

in situ hybridization images of different stage of development of wild-type animals showing *grif-1* mRNA expression. Images were obtained and adapted from nematode expression pattern database; NextDB version 4.0. (https://nematode.nig.ac.jp/db2/ShowCloneInfo.php?clone=666d1).

These data suggest that transcriptional regulation, presumably through *grif-1* promoter, contribute significantly to the developmental regulation of GRIF-1 protein expression by preventing expression of *grif-1* mRNA throughout larvae development and limiting *grif-1* transcripts mainly to oogenic cells thereby ensuring maternal load *grif-1* into early embryogenesis. In embryos, *grif-1* mRNA seems to be post-transcriptionally regulated with distinct timings of degradation in somatic cells and PGCs. Therefore, both transcriptional regulation and mRNA degradation contribute significantly to shaping GRIF-1 protein expression.

4.5.2. *grif-1 3'*UTR directs embryonic expression pattern of GRIF-1 protein

The *grif-1* mRNA expression pattern explains why GRIF-1 proteins was not detected throughout larval development. However, it does not explain a lack of robust GRIF-1 protein expression in oocytes or early germ cell precursors. The *grif-1* mRNA expression therefore

alludes to certain predictions. To begin with, it predicts that *grif-1* mRNA is transcribed during the last burst of transcription in oogenic diplotene. To prevent precocious expression of GRIF-1 protein, *grif-1* mRNA is kept translationally repressed until the birth of the germ cell primordium P4 during embryogenesis. Concomitantly with the birth of P4, the repression of *grif-1* mRNA may be lifted or *grif-1* mRNA may be translationally activated in P4, although the two mechanisms are not mutually exclusive. Furthermore, since oocytes and germ cell precursors are transcriptionally silent and cannot synthesize more of *grif-1* mRNA, this expression pattern predicts the existence of a germ cell-specific mechanism that is exerted by germ cell-enriched factors to prevent degradation of *grif-1* mRNA in oocytes and germ cell precursors during embryogenesis. An extension of this prediction is that the factors that stabilize *grif-1* mRNA must be turned over once PGCs are born to allow degradation of *grif-1* mRNA in PGCs. Alternatively, the default may be that *grif-1* mRNA is stable and that turnover is activated in somatic cells and PGCs of old embryos. In reality, competing mechanisms to degrade and to stabilize transcripts often take place in cells with the most dominant one, at a developmental stage, determining the fate of transcripts (Valencia-Sanchez, Liu et al. 2006, Parker and Sheth 2007, Huch and Nissan 2014).

During *C. elegans* germline development, the translational output of many transcripts is controlled by *cis*-acting regulatory elements in their 3'UTRs (Merritt, Rasoloson et al. 2008). Therefore, to test whether the *grif-1 3'*UTR contributes to developmental expression of GRIF-1 protein, and especially to the translational repression of *grif-1* mRNA in oocytes and germ cell precursors, a translational reporter was generated by creating a transgene containing the *mex-5* promoter, followed by an intronized green fluorescent protein fused to histone 2B as the open reading frame and the 3'UTR of the *grif-1* transcript; *mex-5:GFP::H2B:grif-1 3'UTR* (Figure 4.5.2.1).

Two 3'UTR sequences were fused to the translational reporter (Figure 4.5.2.1). Based on WormBase database analysis, the *grif-1* 3'UTR is 133 bases long. This was further confirmed by cDNA analysis; PCR amplification by combining a primer that binds to the last exon with oligo dT primer and the amplicon generated was subsequently analysed by sequencing (data not shown). However, this method of analysis does not exclude the presence and usage of a longer 3'UTR as PCR is always biased towards amplifying shorter amplicons. In fact, analysis of the genomic sequence revealed additional polyadenylation sequences downstream of the single one included in the annotated and later confirmed short 3'UTR; the first 133 bases after stop codon. Therefore, to capture all possible scenarios, two transgenes were generated (Figure 4.5.2.1). The first transgene contained the short annotated and later confirmed *grif-1* 3'UTR and the second transgene contained longer genomic sequence that captures all the downstream polyadenylation sequences which is hereafter referred to as long *grif-1* 3'UTR (Figure 4.5.2.1). The transgenes were

subsequently inserted and integrated into the genome using Mos-1-mediated Single Copy Insertion (MosSCI) genome engineering technique and two independent lines were generated and analyzed for each transgene (Zeiser, Frokjaer-Jensen et al. 2011).

Figure diagram showing:

LG II // ---- Promoter [mex-5] | ORF (genomic) [GFP::H2B] | 3'UTR [grif-1] ---- //
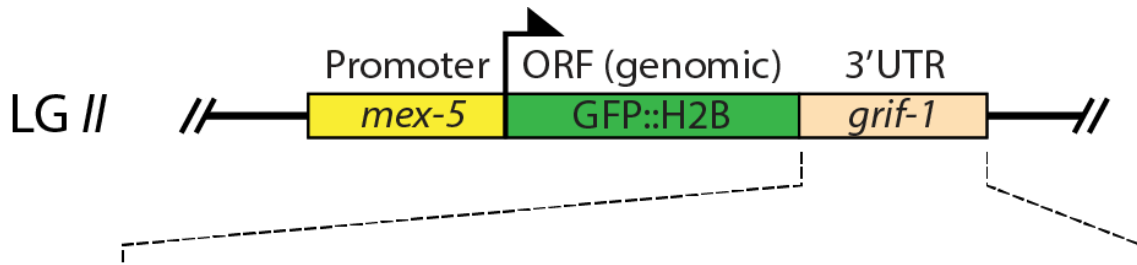
Short 3'UTR
1   TGAgcttttatatttttttttctcatcccaccaccacattaaaacagagtttttatatatacagtacccatt
73   attcgaacacaatttgttctaaaagagcccccaagaatcagatttaataaagaatgctctcacCaattacat
145 tttattgcaaagaaaagtatgaacatttacaggaaatgcgaaagaaaatgcggaagtgaaattgagatcg

Long 3'UTR
1   TGAgcttttatatttttttttctcatcccaccaccacattaaaacagagtttttatatatacagtacccatt
73   attcgaacacaatttgttctaaaagagcccccaagaatcagatttaataaagaatgctctcacCaattacat
145 tttattgcaaagaaaagtatgaacatttacaggaaatgcgaaagaaaatgcggaagtgaaattgagatcgtc
217 taagactcataaaaataaagtcgacgaaaaaggccttgtaggcaggtagataggcattttcgtgcctacgaa
289 gaaggggggaggatcagaaaatctatgtttaacttttcaaatactattgaaaagtgccataagtgccataatt
361 attaaaaatccaaattttgaaaatactccagaaaatttgaacatggtgcaacgtgaccaaaataacaaag
433 tgtgcaataaatatggcccgttttgccacttttaatagttttgatgggttaaacctagatttctgaat
505 tcagcatatatgaattacccgttttcaacaaatttagccgatgtttattttttgcccaaatcgttttttcag
577 ccatctaatgactgtcctttttttgggcaaaaaaagattattctgaaattgaacgaaactattaaattctaa
649 taaaggacattttttttagggttcggagataaatttagagtcctctagctacaaaattaaccattttagagg
721 agtttcaag

STOP codon   polyadenylation signal

Figure 4.5.2.1. Two *grif-1* 3'UTRs were used in translational reporter constructs.
Schematic diagram of the transgene used as *grif-1* 3'UTR translational reporter. *mex-5* promoter was fused to open reading frame (ORF) sequence containing a fusion of green fluorescent protein (GFP) with histone H2B and then fused to either short or long *grif-1* 3'UTR. Transgene was introduced as a single copy insertion using MosSCI protocol into chromosome II. Sequence in black is the annotated and confirmed 3'UTR of *grif-1* based on Wormbase and cDNA analysis, respectively. Additional sequences that were added to 3'UTR used to generate transgenes were depicted in faint black. Stop codon and polyadenylation sequences are coloured in red and green, respectively.

In the obtained strains, the translational reporter was observed through autofluorescence of GFP that localised to the chromatin of germ cells due to its fusion to histone H2B (Figure 4.5.2.2A). GFP signal was observed in the gonad of adult animals, beginning from the distal region to the proximal region (Figure 4.5.2.2A). An obvious drop in the expression levels was observed from pachytene exit to the proximal region with the most obvious reduction in expression level in oocytes (Figure 4.5.2.2A). In embryos, the GFP signal was detectable, at background levels, compared to the signal in oocytes, in early somatic cells with a gradual drop in signal until it was no longer detectable in the soma (Figure 4.5.2.2A and B). Similar observations were made in early germ cell precursors.

However, in contrast to somatic cells which lose the expression of GFP::H2B completely, GFP::H2B expression suddenly became abundantly detectable in P4 germ cell primordium and this level of expression was also observed in PGCs (Figure 4.5.2.2A and B). The identity of cells expressing GFP::H2B were further confirmed using a RFP-tagged PGL-1 transgene that was crossed into the animals expressing *grif-1* 3'UTR translational reporter (data not shown). GFP signal was also detectable in germ cells at all larvae stages. Identical results were obtained from strains expressing translational reporter transgene driven by long *grif-1* 3'UTR (data not shown). These data show that GFP::H2B is robustly expressed at all stages of germ cell development except in oocytes where a reduction in expression is observable and in germ cell precursors of early embryogenesis where background and almost undetectable levels of GFP signal was observed. Embryonic somatic cells, similar to germ cells precursors, only express an extremely weak background level of GFP::H2B. These observations suggest that short *grif-1* 3'UTR is sufficient to drive the embryonic expression pattern of GRIF-1 protein.
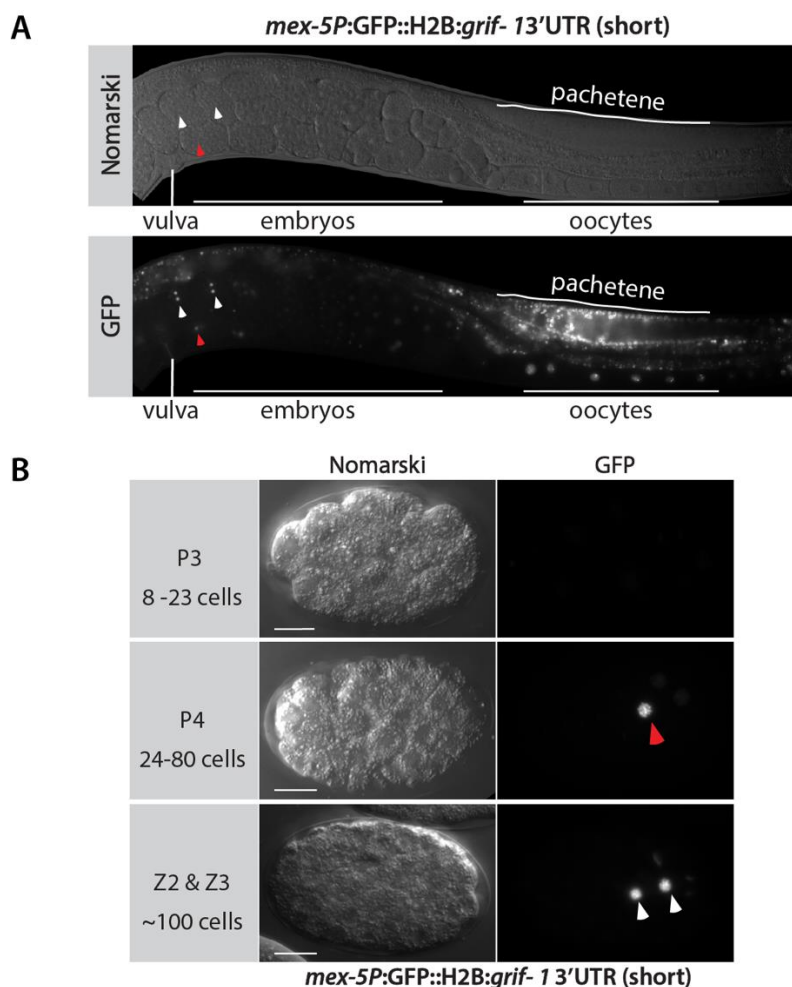
Figure 4.5.2.2. *grif-1* 3'UTR directs the embryonic expression pattern of translational reporter.

(A) Photomicrograph of adult animal expressing translational reporter transgene driven by short *grif-1* 3'UTR and observed with Nomarski (top) and fluorescent microscope (bottom). (B) Photomicrograph of different stages of embryos expressing same transgene in (A) observed with Nomarski (left column)

and fluorescence microscopy (right column). Red arrowheads point to P4 germ cell primordium while white arrowheads point to PGCs. Scale bar is 10 μM.

The expression of the translational reporter in larvae and adult germline was not surprising given the fact that *grif-1* mRNA is not expressed at these stages in wild-type larvae and the transcript is limited to oocyte in adult wild-type animals. However, unlike the promoter that drive transcription of *grif-1* transcripts beginning from diplotene, *mex-5* promoter is known to drive transcription in all stages of postembryonic germ cell development (Merritt, Rasoloson et al. 2008, Zeiser, Frokjaer-Jensen et al. 2011). This suggests that the *grif-1* 3'UTR is not sufficient to repress translation during larval development and in undifferentiated germ cells prior to region of pachytene exit of the adult gonadal tube without transcriptional regulation that limits the mRNA to certain region during adulthood. Only in oocytes, specific RNA-binding proteins that recognise and repress specific sequence in *grif-1* 3'UTR might be active. Upon maternal donation, they may also contribute to *grif-1* posttranscriptional regulation in early embryogenesis.

Nonetheless, unlike in early embryos with a significant reduction in levels of GFP::H2B, only a slight reduction of GFP::H2B signal was observed in oocytes and this may be due to different reasons. The most obvious and likely cause is the stability of the GFP::H2B protein. Even in the presence of a likely translational repression of the mRNA encoding the translational reporter, a robust signal of GFP::H2B from pachytene stage will still be detectable until it the protein is effectively degraded. This may explain the observed gradual reduction initiated in oogenic cells. Another cause, which might not contribute significantly, is the presence of endogenous wild-type copy of *grif-1* 3'UTR which may titrate repression activity. Together, the data suggest that *grif-1* 3'UTR contains information to drive the embryonic protein expression pattern of GRIF-1.

4.5.3. GLD-2 controls protein expression of GRIF-1

To achieve timely and highly restricted GRIF-1 expression, as earlier stipulated, certain factor(s) may exist that stabilizes *grif-1* mRNA in oocytes. The activity or expression of such a factor would be terminated in somatic cells but remain active in the germ cell lineage until the birth of PGCs where it is expected to be terminated again. A good candidate that satisfies these conditions is the cytoplasmic polyA polymerase, GLD-2, which is incidentally a target of GRIF-1 turnover activity. As a cytoPAP, GLD-2 may extend the polyA tail of *grif-1* 3'UTR to facilitate its stability and translatability. Moreover, GLD-2 is also germ cell enriched during early embryogenesis and it is turned over upon the birth of primordial germ cells.

To test a likely contribution of GLD-2 cytoPAP to regulating the expression of GRIF-1, an RNAi-mediated knockdown was performed to reduce *gld-2* expression during early

embryogenesis. *gld-2* is important for embryogenesis; embryos compromised for *gld-2* activities by RNAi-mediated knockdown are arrested at varying stages of embryogenesis. These embryos display several phenotypes including but not limited to polarity defects and multinuclear-cell defects suggesting that *gld-2* is important for cell division (Wang, Eckmann et al. 2002). Therefore, to allow *gld-2* compromised embryos to grow beyond the 24-cell stage in which P4 is born, a partial *gld-2* RNAi was performed in a time course experiment. To this end, young adults of strains expressing *grif-1* 3'UTR translational reporter were treated with either *gld-2* RNAi or control RNAi and the effect of knockdown was assessed after 15, 20 and 25 hours. Bacteria expressing dsRNA to *gld-2* were diluted with empty constructs to mitigate *gld-2* RNAi-mediated knockdown effects.

In control(RNAi) animals, GFP::H2B was detected at high levels and P4 during embryogenesis (100 %, n=30) (Figure 4.5.3). However, after 15 hours of *gld-2* RNAi knockdown, the expression of GFP::H2B was either reduced (34 % n=32) or almost undetectable (66 %, n=32) in embryos between 24-cell and 70-cell stage (Figure 4.5.3). At 20 hours of RNAi, the number of embryos that reached 24-cell stage was significantly reduced with almost all failing to express GFP::H2B. At 25 hours of *gld-2* RNAi-mediated knockdown, no single embryo developed to the 24-cell stage anymore, precluding further analysis. At this time point, however, a major observation made was that GFP signal was reduced in the gonad of fed mothers, especially affecting germ cells that are exiting pachytene stage and oocytes (data not shown). These results strongly suggest that GLD-2 is required for the post-transcipional control of the *grif-1* mRNA and importantly, it additionally suggest that GLD-2 is required for of stabilize this 3'UTR of its own turnover factor in oocytes and early embryogenesis.

mex-5P:GFP::H2B:*grif-1* 3'UTR (short)
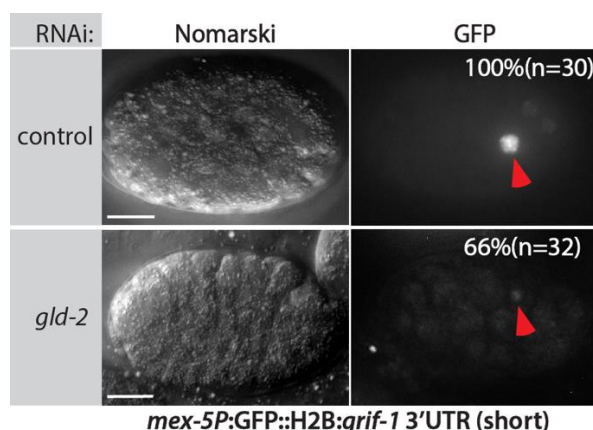
Figure 4.5.3. GLD-2 regulates expression of *grif-1* 3'UTR reporter

Photomicrograph of wild-type embryos treated with either control RNAi (top row) or *gld-2* RNAi (bottom row) observed with Nomarski (left column) and fluorescent microscope (right column). Percentages are a fraction of embryos analysed (n) that shows displayed phenotype. Red arrowheads point to P4 germ cell primordium.

In summary, all data show that several layers of regulations control the tight developmental expression pattern of GRIF-1 protein. This includes transcriptional and translational regulation; mRNA degradation in somatic cell, repression coupled with a likely maintenance of stability in oocytes and early germ cell precursors, translational activation in P4 and mRNA degradation in PGCs. Moreover, these data suggest that GLD-2 regulates the expression of its own turnover factor, generating a feed forward loop with the turnover of GRIF-1 protein through a yet-to-be identified protein degradation pathway closing this loop.

4.6. *grif-1* has mortal germline phenotype

GRIF-1 is a turnover factor that promotes the termination of expression of maternal proteins in PGCs. The continued expression of maternal proteins in primordial germ cells of *grif-1* mutants may interfere with germ cell development causing observable germ cell defects. This section describes experiments performed to analyse the biological role of GRIF-1 for germ cell development.

4.6.1. Animals devoid of *grif-1* activities lose fertility across generations

To determine the biological role of *grif-1*, the fertility of all *grif-1* mutants was analysed at 20°C (see Figure 4.2.2). As *grif-1* is a maternally expressed gene, second-generation descendants (F2) of heterozygote mothers were analysed. Surprisingly, these F2 *grif-1* animals were observed to be fertile with slightly a reduced brood size (data not shown). Occasionally, few sterile worms-ranging from one to ten percent, depending on the brood, were observed and appeared stochastically among F2 populations of *grif-1* animals. Regardless of harboured mutations, all analysed alleles of *grif-1* displayed this stochastic sterility phenotype.

In addition to F2 sterility that appeared stochastically, after careful monitoring over longer periods of time, several other tendencies were observed in all *grif-1* alleles, although the more so in *ef32, ok1610* and *ok1610ef40* than in *ef35* and *tm2559*. All broods of *grif-1* animals that were completely fertile in F2 generation eventually gave rise to a brood in which a small percentage of animals was sterile. This occurred in generations that ranges from the third (F3) to sometimes the thirtieth (F30) generation. Furthermore, regardless of the generation in which sterility showed up, once detected, the percentage of sterile worms increased in successive generations and even the fertile groups started to sire reduced numbers of progenies from generation to generation. This gradual reduction in fertility continued until all animals became sterile and this line could therefore not be maintained. These observations at 20°C suggest transgenerational sterility.

Additionally, the fecundity of *grif-1* mutants was also analysed at elevated temperature to test the effect of heat stress on transgenerational sterility. To this end, the total number of progenies sired by *grif-1* mutants were analysed for three successive generations at 25°C. In each generation, the total number of progenies sired was determined. Starting from synchronised L1 populations at 25°C, wild type or *grif-1* mutants were singled at L4 stage onto individual plates to determine their brood size. The singled L4 were allowed to lay all their progenies for the next 72 hours and to facilitate counting in these 72 hours, the animals were moved onto new plates every 24 hours. After the mother has been shifted to a new plate, the laid embryos were given additional 16 hours to complete embryogenesis. After 16 hours, hatched larvae were scored as living progenies and embryos

left on the plates were scored as dead embryos. The progenies of first-generation mothers were singled at L4 to become second-generation mothers and progenies of second-generation mothers became third-generation mothers (Figure 4.6.1.1).
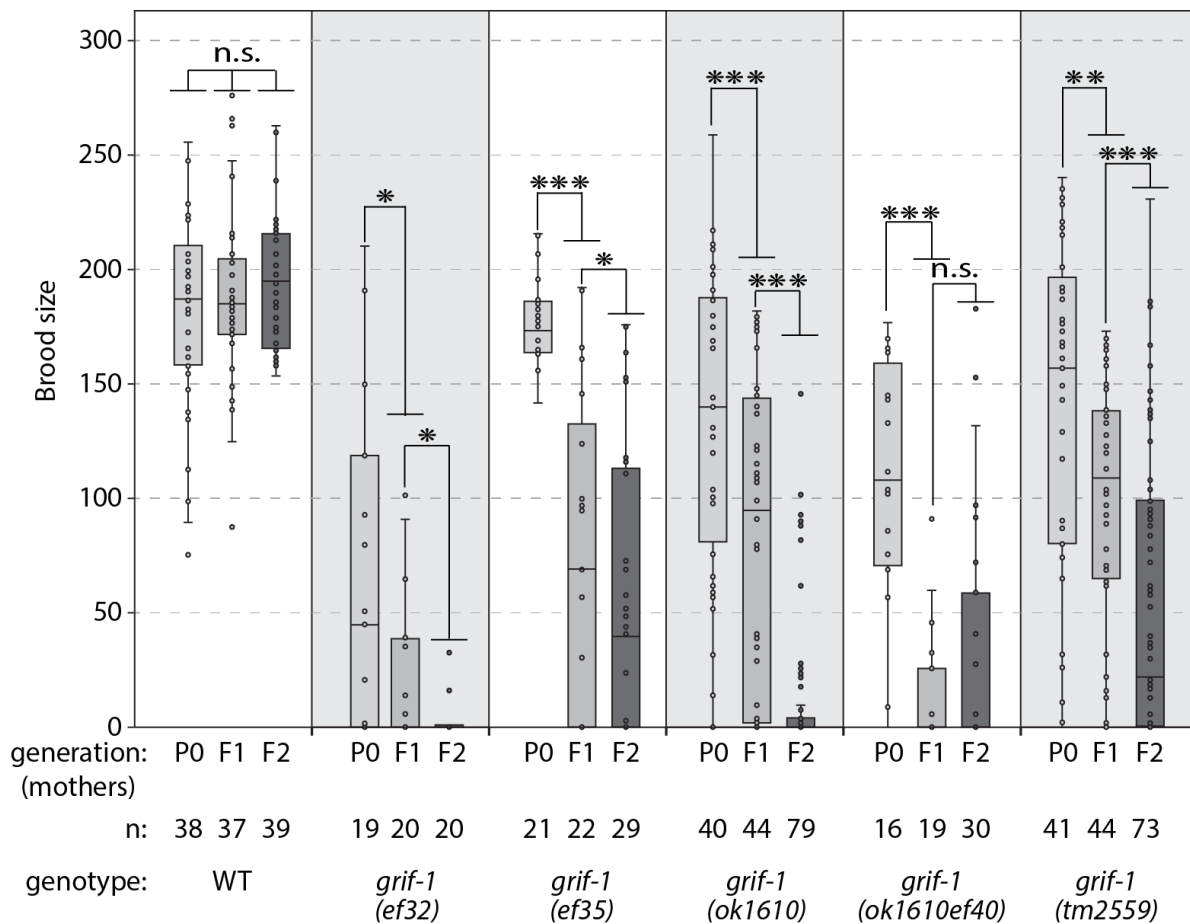
Figure 4.6.1.1. *grif-1* animals sired reduced number of progenies across generations.

Box plots showing the distribution and the number of progenies sired by wild type and different alleles of *grif-1* across three generations at 25°C. The number of mothers whose progenies were counted are shown as n. Significance was calculated by student's t-test. *= p<0.05, **= p<0.01, ***= p<0.001, n.s.= not significant.-

In the first or parental generation (P0) at 25°C, wild-type mothers sired approximately 190 total progenies on average and additionally, the total number of progenies on average sired by wild-type mothers in the two subsequent generation were not significantly different from first generation (Figure 4.6.1.1). All alleles of *grif-1,* except for *grif-1(ef35),* sired on average a reduced number of total progenies compared to wild type (Figure 4.6.1.1). Moreover, in contrast to wild type, all *grif-1* mutant mothers, including *ef35*, sired significantly reduced number of total progenies in the successive two generations compared to first-generation mothers. Additionally, third-generation *grif-1* mothers even sired more reduced total progenies compared to second-generation mothers (Figure 4.6.1.1). These results, like the 20°C observations, reveal that *grif-1* is important for transgenerational fertility and further

demonstrate the tendencies of *grif-1* mutant to lose fertility across generations suggesting that *grif-1* loss may cause mortal germline phenotype.

Mortal germline phenotype (*Mrt*) is a multigenerational defect in which a selfing lineage becomes progressively sterile (Ahmed and Hodgkin 2000). To make a firm conclusion that loss of any gene results in mortal germline phenotype, several observations have to be accounted for: (i) several generations must be analysed, and (ii) to account for high variations in brood size among siblings which may affect the outcome of experiment, an experiment which reflects the progressive sterility of population rather than individual mother is required. To put this in perspective, in Figure 4.6.1.1, on average, third generation *ok1610ef40* mothers sired more progenies than second generation mothers of the same genotype mostly due to high variation of a few mother that sired high numbers of progenies. Although these F3 mothers were outliers, the number of the total offspring is affected by their broods. However, by roughly gauging the fertility of all the brood on plates by under a dissecting microscope, it is evident that third generations mothers were less fertile when a higher number of worms were considered for both generations. Therefore, to confirm whether *grif-1* loss causes mortal germline phenotype, a standard experiment used to determine *Mrt* phenotype was carried out with slight adjustment (Ahmed and Hodgkin 2000).

To assay for *Mrt*, six L4 staged homozygote *grif-1* mutants, which were F1 progenies of heterozygotes, were randomly selected and shifted to 25°C. Then, six L4 progenies were randomly selected and passed every successive generation until complete sterility at 25°C (see scheme in Figure 4.6.1.2A). A line was regarded sterile at generation "n" when the total number of progenies sired by the six mothers were between zero and twelve. The original method passed six L1 at every successive generation (Ahmed and Hodgkin 2000), however, to avoid picking males which were occasionally produced at relatively higher rate than wild type by many mutants of genes displaying *Mrt* phenotype, L4 were randomly selected instead. Wild-type animals were treated the same way except the termination of experiment was defined mostly by sterility of gene under analysis.

All wild-type lines were fertile until the experiments lasted, which was up to 20 generations (Figure 4.6.1.2B). A careful observation of the plates containing wild type revealed that they constantly produced robust number of progenies although sterile wild-type animals were occasionally spotted at less than one percent of the entire population (just based on examination under a dissecting microscope). This suggests that populations of N2 animals (wild type) may be indefinitely fertile provided additional stressful conditions are not introduced into the population. In fact, in previous studies, N2 populations have been successfully maintained in this manner up to the fiftieth (50th) generation (Nigon and Felix 2017). By contrast, *grif-1* mutant populations became completely sterile at early generations, ranging from the third generation to the twelfth generations (Figure 4.6.1.2B). At 20°C,

although a small percentage of *grif-1* animals were sterile from second generation, it usually took more than 20 generations for the entire population to become completely sterile. Together, these results reveal that *grif-1* mutants have a mortal germline phenotype that is temperature sensitive.
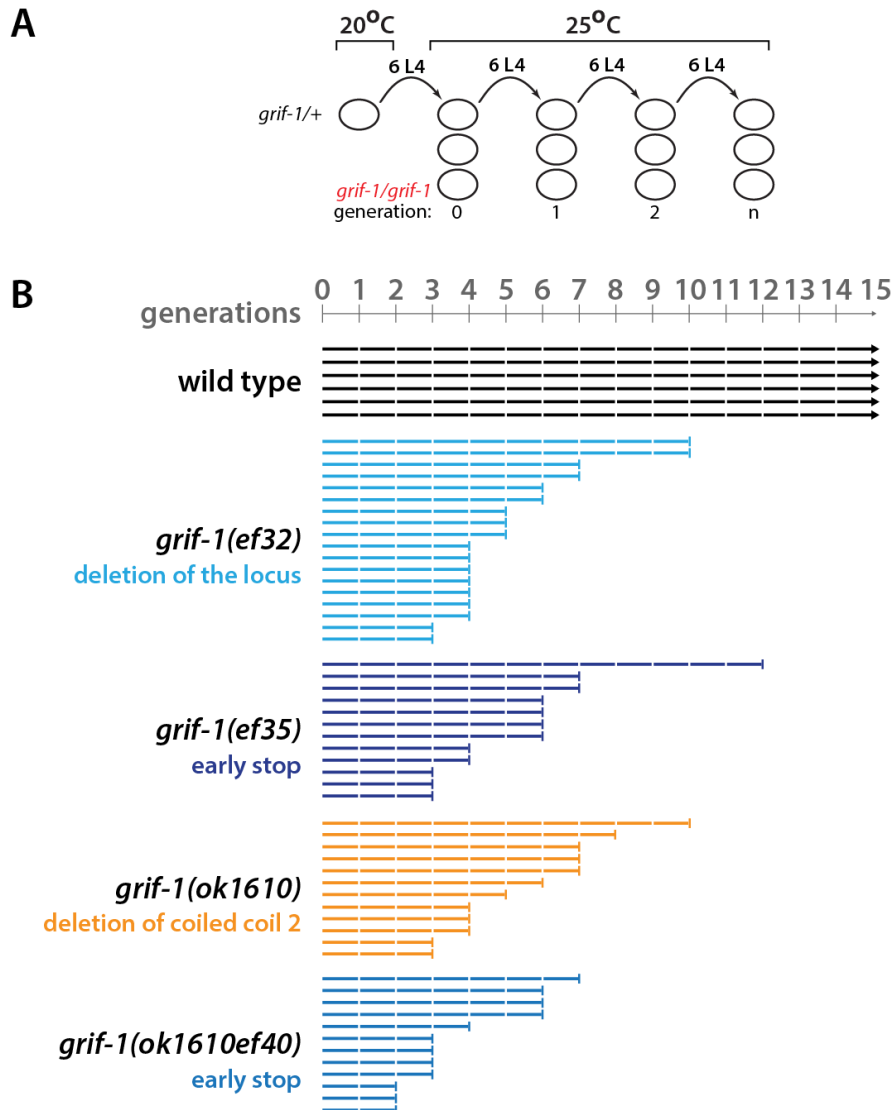
Figure 4.6.1.2. *grif-1* animals have mortal germline phenotype.

(A) Scheme of experimental workflow to determine whether *grif-1* loss causes a mortal germline phenotype. (B) A graphical display showing fertility of wild-type and *grif-1* mutant populations across generations corresponding to scheme in A (see main text for details).

4.6.2. *grif-1* mutants have degenerated germlines

The germline of either wild-type or *grif-1* adults were analysed using Nomarski microscopy to determine germline phenotype associated with *grif-1* loss. Gonads of wild-type adult animals appeared as a U-shaped tube-like structure, filled with germ cells, which are in a distal to proximal arrangement according to their differentiation. Undifferentiated cells were situated in its most distal end and mature oocytes were most proximal (see Figure 4.6.2.1A).

Further proximal to the oocytes is a sac-like spermatheca which stores sperms whose production is initiated during that last larvae stage of development (L4) and completed in young adults (Kimble and Hirsh 1979, Hubbard and Greenstein 2005, Kimble and Crittenden 2007). Signal from sperm induce ovulation of the most proximal oocytes which is subsequently fertilized inside the spermatheca. The resultant eggs are temporarily stored in the uterus of the mothers before they are eventually laid (Hubbard and Greenstein 2005, Kimble and Crittenden 2007).

To analyse germline defects associated with mortal germline phenotype of *grif-1,* sterile *grif-1* adults (L4+20hours) were analysed from populations containing significant number of sterile animals. This means that L4 larvae were picked from plates that were passed a generation or two before sterility. Since a prevalent number of mothers are sterile on these plates and fertile mothers lay significantly low number of eggs, the plates are preserved without starvation for a relatively long period and L4 can be recovered from such plates, a week later, for analysis. Sterile *grif-1* animals displayed several germline phenotypes which may reflect different levels of severities, emanating from a common cause. Regardless of the severity, all sterile *grif-1* animals have a small germ lines when compared to wild type which suggests germline proliferation defect (Figure 4.6.2.1B and C).

All additional phenotypes can be placed in four major categories. The first category of sterile animals had a normal organization of germ cells within their small germline tissue. This category often produces a few, small and most likely non-functional oocytes, although sperm were occasionally observed (images not shown). Their sterility implies defective gametogenesis. The second category had germline tissue containing a single row of very small and undifferentiated germ cells in the proximal region (images not shown). Lack of a single identifiable gamete in this category suggests that either no differentiation took place or the cells arrested during early stages of differentiation. The third category, which is shown in Figure 4.6.2.1B and C, had undifferentiated germ cells in the distal end of the gonad and no identifiable germ cells in the proximal end of the germline. These germ cell-lacking proximal ends always contained either few germ cell corpses (black arrowhead, Figure 4.6.2.1C) or structures that appeared like germline atrophy under microscope (red arrowheads, Figure 4.6.2.1B and C). These observations suggest that the proximal end of the germline tissue may be deteriorating or degenerating. The last category of animals had degenerated or deteriorated gonads that were completely devoid of germ cells. Occasionally, in less severe cases, up to ten germ cells may be observed inside the entire gonad of animals in this category (images not shown). Loss of germ cells and presence of germ cell corpses in the gonad suggest germ cells may be experiencing cell death and since almost all cells in the germline are lost, the last two categories may be displaying different severities of germline survival defect. Germline survival defects causes loss of germ line due to cell death after

several rounds of divisions during larvae development (Subramaniam and Seydoux 1999, Eckmann, Kraemer et al. 2002, Rybarska, Harterink et al. 2009). However, *grif-1* animals seem to have a delayed germline survival phenotype in which significant levels of germ cell death becomes noticeable during adulthood. The frequencies of all four mentioned categories of phenotypes were determined at 18 to 20 hours past L4 at 25°C and displayed in Figure 4.6.2.1D. Together, these results reveal that *grif-1* mutants have germline proliferation defect, differentiation defect and germline survival defect that seems to become noticeable in adults, although the fact that germ cell death may already started during larvae development cannot be excluded.
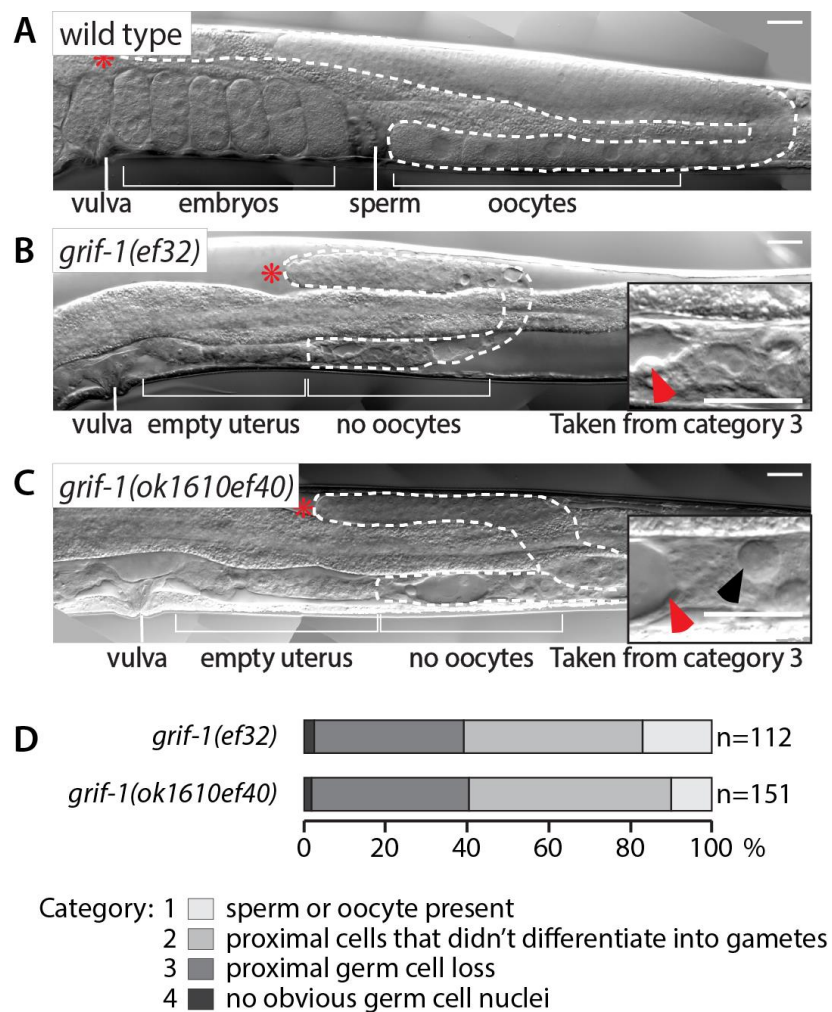
Figure 4.6.2.1. *grif-1* animals have degenerated germlines.

Nomarski images of (A) wild-type, (B) *grif-1(ef32)* and (C) *grif-1(ok1610ef40)* animals. *grif-1* animals have presence of germ cell corpses (black arrowhead in C) or atrophy (red arrowhead in B and C) in the gonad. Distal end of gonad indicated by asterisks (*). Scale bars of image and insets are 20 µM. (D) Analysis of all categories of germline phenotypes observed in gonad of sterile *grif-1* animals (see main text for detailed explanation).

During the course of analyses, it was observed that the frequency of severely affected gonads increased when animals aged and were analysed at later time points: 40

and 60 hours past L4, compared to those analysed at 18 to 20 hours past L4. This was also true for animals analysed from the same population. At 60 hours past L4, most animals could be assigned to the third or fourth category (data not shown). These additional observations suggest that once enough time had passed, the first three categories may culminate into a terminal phenotype, represented by the fourth category. However, a firm conclusion cannot be made since not exactly the same animals were checked at consecutive timepoints.
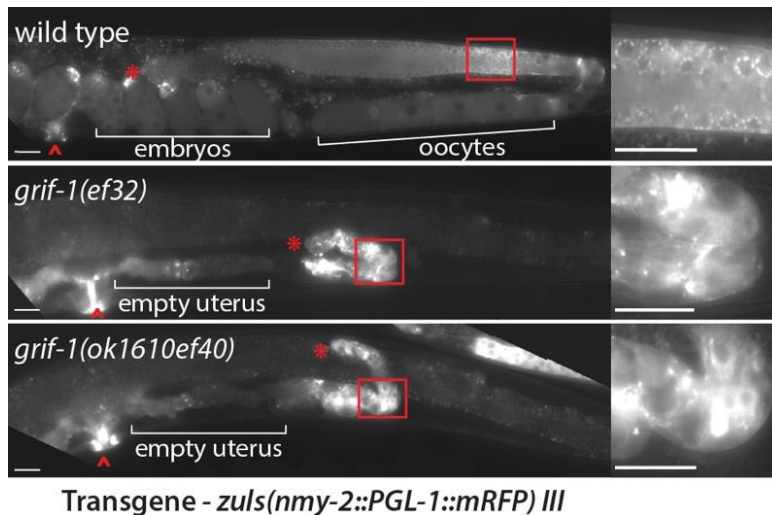
Figure 4.6.2.2. Aberrant expression of PGL-1::mRFP in *grif-1* germ lines.

Auto-fluorescent images of wild-type (top), *grif-1(ef32)* (middle) and *grif-1(ok1610ef40)* (bottom) animals expressing PGL-1::RFP transgene. Distal end of gonad is indicated by asterisks (*) and vulva is indicated by caret. Insets display a magnification of expected localization in wild type and aberrant expression and localization in *grif-1* animals. Scale bars of actual image and insets are 20 µM. Due to very weak expression, images of *grif-1* animals were taken at longer exposure time compared to wild type.

To determine whether germ cell death in *grif-1* mutants was a consequence of loss of germ cell identity, the expression of PGL-1 and by extension the presence of PGL-1-associated P granules were analysed by crossing PGL-1::RFP transgenes into *grif-1* mutants. PGL-1::RFP was detected throughout cytosol of wild-type germ lines and additionally observed to be enriched on P granules at the nuclear periphery of every immature germ cells with the highest signal at the region that appear to be the border of pachytene exit. By contrast, the expression of PGL-1::RFP was detected but reduced in adult germ line of most *grif-1* mutants (Figure 4.6.2.2. Note that to reveal the distribution of PGL-1::mRFP, images of *grif-1* animals were taken at a longer exposure time). Furthermore, the distribution of PGL-1::RFP was significantly altered in *grif-1* mutants and the following defects were observed. Adjacent germ cells expressed dissimilar levels of PGL-1::mRFP indicating differentiation problems (Figure 4.6.2.2). Enrichment of PGL-1 into P granules at the nuclear periphery was not observed in many of the germ lines indicating either loss of P granules or loss of association of PGL-1 with P granules (Figure 4.6.2.2). Lastly, highly concentrated mRFP signals were always observed in single spots in the gonad (Figure

4.6.2.2), indicating initiation of germ cell death, while loss of perinuclear PGL-1 protein occur in late stages of germ cell death (Sheth, Pitt et al. 2010). A recent study suggests that PGL-1 aggregates, which may appear as bright spots, are exported into the cytoplasmic core prior to the germ cell shrinkage during cell death, eventually leading to PGL-1 loss (Raiders, Eastwood et al. 2018). Together, these results reveal that since PGL-1 is still detectable in germ cells of *grif-1* mutants, they do not lose germ cell character completely until germ cell nuclei are removed by cell death. Also, initiation of trans-differentiation into a different fate cannot be excluded.

In summary, *grif-1* mutants have mortal germline phenotype with several associated germ cell defects. Furthermore, the results reveal that germ lines of *grif-1* mutants have proliferation and differentiation defects that seem to result into a completely degenerated germline by experiencing gradual germ cells death. Lastly, although germ cells lacking *grif-1* activities seems to lose P granules, they do not lose the expression of germ cell specific proteins. Importantly, when a line that is about to lose fertility completely, outcrossing several times with wild-type males was observed to restore fertility. However, the observed phenotypes return after several passage as homozygotes. This suggest that that *Mrt* phenotypes of *grif-1* may be a result of a molecular defects that accumulates over generation causing sterility phenotype when a threshold has been reached. Alternatively, it suggests that *grif-1* is involved in pathways whose efficiency is dependent on *grif-1* activity and other factors. These two possibilities are not mutually exclusive.

4.7. *nos-2* regulates PGC development redundantly with *grif-1*

      grif-1 is expressed in embryonic PGCs where it promotes the turnover of maternal GLD-2 cytoPAP. A highly possible scenario is that continued expression of GLD-2 and GLD-3 in PGCs of *grif-1* mutants causes a prolonged expression of GLD-2 target transcripts in PGCs thereby interfering, albeit inefficiently, with germ cell development maybe causing germline survival defects. The transgenerational phenotype of *grif-1* suggest that PGC development may be regulated by several redundant factors or pathways and removal of one aspect of this redundancy may take generations for effects to manifest. This section describes experiments carried out to identify additional players that regulate PGC development redundantly with *grif-1.*

4.7.1. *nos-2* but not *nos-1* is redundantly required with *grif-1* for fertility

      Two key factors that could potentially regulate PGC development redundantly with *grif-1* are *nos-1* and *nos-2.* While NOS-1 is a zygotically expressed protein that becomes detectable in PGCs just prior to hatching, NOS-2 is a maternally expressed protein that has almost has an identical expression pattern, if not exact, as GRIF-1 (Subramaniam and Seydoux 1999). NOS-1 and NOS-2 were recently shown to be redundantly required for the clearance of oocyte-derived transcripts in PGCs (Lee, Lu et al. 2017). Interestingly, although the fertility of animals compromised for either *nos-1* or *nos-2* remain largely unaffected, a significant percentage (around 70 %) of animals compromised for both *nos-1* and *nos-2* display a germline survival phenotype (Kraemer, Crittenden et al. 1999, Subramaniam and Seydoux 1999, Lee, Lu et al. 2017); a phenotype also observed in *grif-1* mutants. Therefore, experiments were carried out to determine whether *grif-1* potentially regulates PGC development redundantly with either *nos-1* or *nos-2* by generating double mutations with *grif-1.*

      The vast majority of *nos-1, nos-2,* or *grif-1* single mutant F1 adults were fertile with occasional sterility observed, especially in *grif-1* and *nos-2* mutants (Figure 4.7.1.1). Similar to single mutants, almost all of *grif-1; nos-1* double mutants were also fertile (Figure 4.7.1.1). By contrast, a significant number of *grif-1(ef32);nos-2(ax2033)* double mutant F1 animals were sterile (77 %, n=3090) (Figure 4.7.1.1).
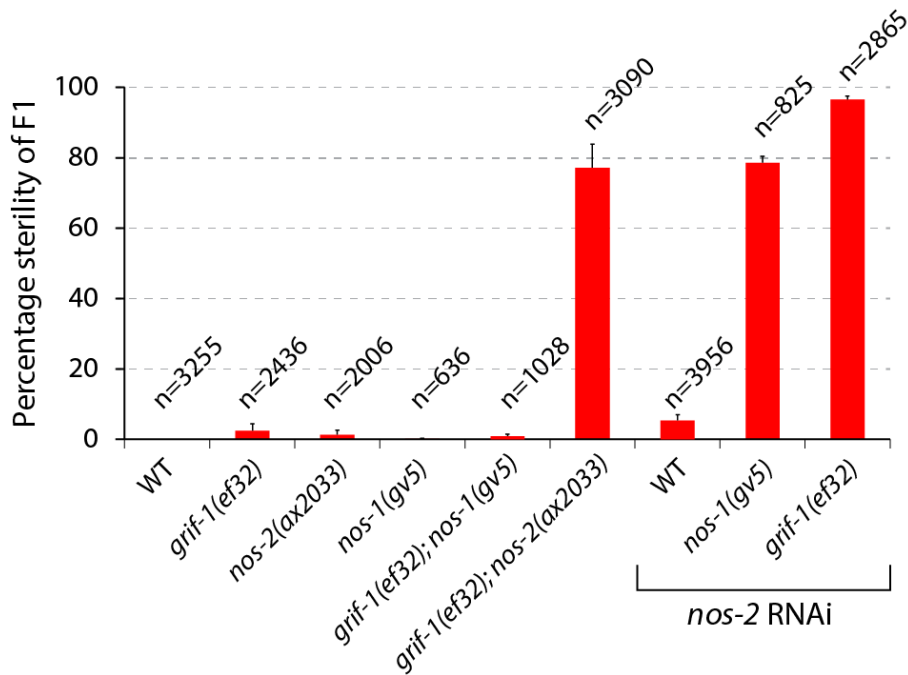
Figure 4.7.1.1. *nos-2* but not *nos-1* is redundantly required with *grif-1* for fertility.

Bar chart showing the average percentage sterility of indicated genotypes treated for either control or *nos-2* RNAi. F1 of P0 animals were analysed for sterility by checking for the presence of embryos in the uterus. Error bars shows SEM.

In addition to using mutants, *nos-2* expression was also compromised using RNAi-mediated knockdown. To this end, wild-type, *nos-1(gv5),* and *grif-1(ef32)* animals were treated with either control or *nos-2* RNAi beginning from L1; parental generation, and F1 progenies were analysed for sterility. Similar to *nos-2* single mutant, a vast majority of wild-type animals that experienced *nos-2* RNAi sired fertile progenies (Figure 4.7.1.1). In contrast to wild type but similar to previous studies (Subramaniam and Seydoux 1999, Lee, Lu et al. 2017), a considerable number of *nos-1* animals compromised for *nos-2* expression were sterile (79 % n=825) (Figure 4.7.1.1). Moreover, *grif-1* animals compromised for *nos-2* using RNAi-mediated knockdown produced sterile progenies (95 % n=2865) (Figure 4.7.1.1). Wild type, *grif-1(ef32),* and *nos-1(gv5)* that were treated with control RNAi were not different from untreated animals in anyway indicating that RNAi by itself does not contribute to observed phenotype (data not shown and see Figure 4.7.1.2). To further substantiate and confirm these observations, *nos-2* RNAi was performed in several *grif-1* mutant backgrounds. Regardless of the allele used, more than 80 % of progenies sired by *grif-1* mothers that experienced *nos-2* RNAi were sterile (Figure 4.7.1.2). Taken together, these results reveal that *nos-2* but not *nos-1* is redundantly required with *grif-1* for fertility.
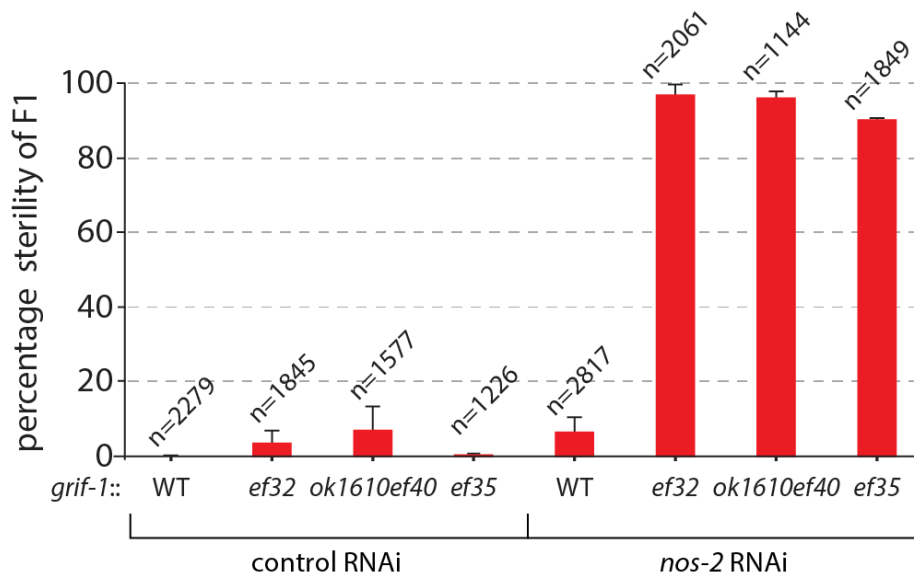
Figure 4.7.1.2. *grif-1* mutants that experience *nos-2* RNAi produced sterile progenies.
Bar chart showing the percentage sterility of indicated genotypes treated for either control or *nos-2* RNAi. F1 of P0 animals were analysed for sterility by checking for the presence of embryos in the uterus. Bar chart shows mean (± Std. Dev).

To determine the nature of sterility when the maternal expression of both *grif-1* and *nos-2* are compromised, germline defects of *grif-1(ef32); nos-2(RNAi)* and *grif-1(ok1610ef40); nos-2(RNAi)* F1 animals were analysed using Nomarski microscopy. Wild-type animals treated with control RNAi have adult germline tissue that were similar to wild type (see section 4.6.2 for detailed explanation of a wild-type gonad) (Figure 4.7.1.3A). By contrast, the few sterile *grif-1* mutants have pleiotropic germlines phenotypes that were similar to phenotypes observed during analysis of *grif-1* mortal germline phenotype at 25°C (see section 4.6.2 for detailed explanation). In contrast to wild type and similar to *grif-1* mutants, the few sterile *nos-2* single mutants that were analysed displayed several germline phenotypes including strong underproliferation, feminization, and others (images not shown). Furthermore, unlike wild type or either single mutant, a vast majority of sterile *grif-1(ef32); nos-2(RNAi)* animals have correctly formed somatic gonad but no obvious germline tissue (Figure 4.7.1.3 B and C). The majority of these animals had gonads with either less than 10 aberrant appearing germ cells or no germ cells at all and in addition, germ cell corpses were often observed (Figure 4.7.1.3 B, red arrowheads). Together, these observations show that germline tissue lacking the maternal activities of both *grif-1* and *nos-2* display a severe germline survival phenotype.

A wild type; control RNAi

vulva   embryos   sperm   oocytes

B *grif-1(ef32); nos-2* RNAi

vulva   empty uterus   empty oviduct

C
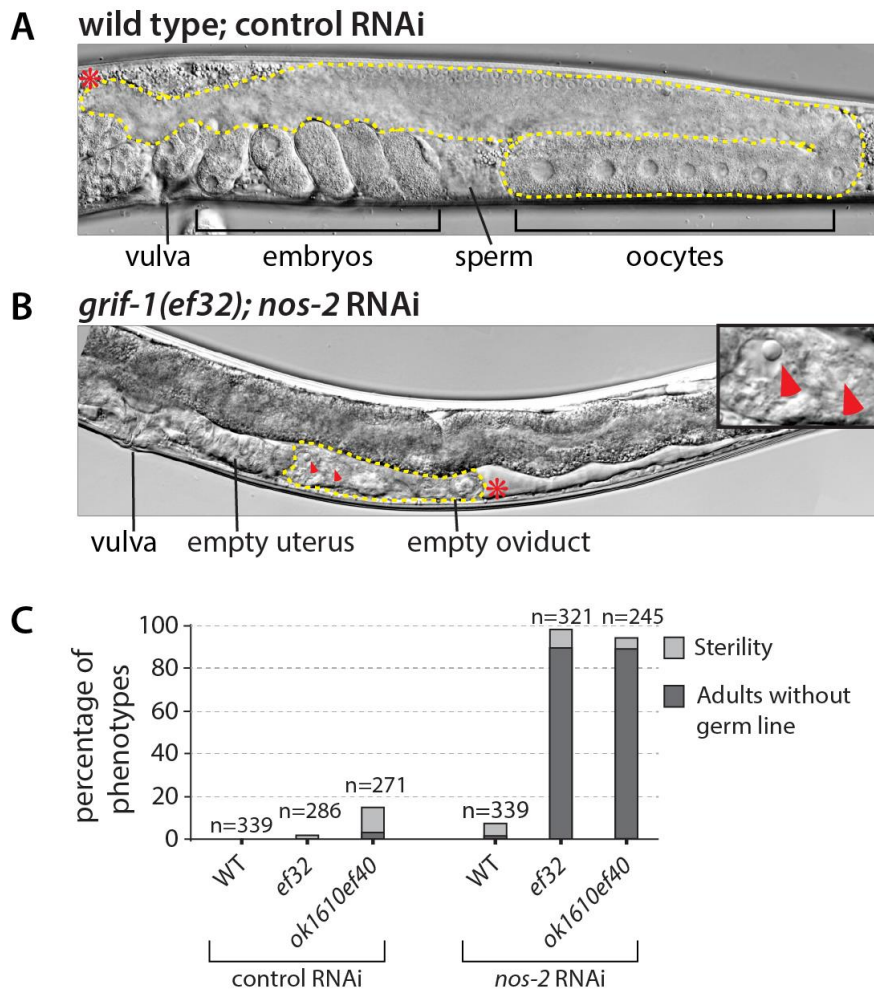
Figure 4.7.1.3. progenies of *grif-1(0); nos-2(RNAi)* animals have germline survival phenotype.

Nomarski images of (A) wild-type and (B) *grif-1(ef32); nos-2(RNAi)* animals. The distal end of gonad is marked by asterisk (*). *grif-1(ef32); nos-2(RNAi)* animals have germline survival phenotype. Red arrowheads highlight observed germ cell corpses (C) A bar chart showing the proportion of animals with sterility and germline survival phenotypes. Two replicate experiments were performed for analysis in C.

To determine the onset of germ cell death in animals lacking maternal contribution of both *grif-1* and *nos-2,* the presence and number of germ cells at every stage of larvae development were assessed. To this end, P0 wild-type and *grif-1(ef32)* animals were treated with control and *nos-2* RNAi, respectively. F1 embryos were collected and allowed to hatch overnight to have synchronised L1 animals, which were subsequently spotted on plate for feeding. Germ cell number was then analysed at different time points; 0, 22, 32, 38, 48 hours, past the initial time point of L1 feeding. These time points correspond to L1, L2, early L3, late L3 and L4, respectively. L1 to L3 were analysed using Nomarski microscopy and in addition to Nomarski, mid-L4 stage animals were stained with DAPI and analysed by fluorescent microscopy.

At time point zero, wild-type L1 whose mothers were treated with control RNAi contained two germ cells similar to wild type (n=15) (Figure 4.7.1.4). At 22 hours post feeding, control RNAi L2 animals have on average 16 cells (n=15). From L3 stage onward,

especially at Late L3 stage, the number of germ cells was observed to rise significantly compared to earlier stages in these animals. Therefore, in control RNAi, the average number of germ cells observed in early L3 (32 hours), late L3 (38 hours) and L4 (44 hours) were 36, 108 and 438 germ cells per larvae, respectively (Figure 4.7.1.4).

Similar to wild type; control(RNAi) animals, a vast majority of *grif-1(ef32); nos-2(RNAi)* animals contained two germ cells at time point zero of the experiment (n=12 of 15). However, unlike wild type; control(RNAi) animals, a limited number of animals contained three or four cells (n=3 of 15) (Figure 4.7.1.4A). The germ cell identity of the extra cells was verified by analysing PGL-1 expression. However, although PGL-1 was detected in all *grif-1(ef32); nos-2(RNAi)* L1 animals, the expression was often observed to be weaker than wild type (data not shown). At 22 hours post feeding, *grif-1(ef32); nos-2(RNAi)* L2 animals contained 12 cells on average which is quite comparable to wild type; control(RNAi) L2 animals which had 16 cells on average (Figure 4.7.1.4A). At 32 hour time point, in which wild type; control(RNAi) early L3 animals contained 36 cells on average, *grif-1(ef32); nos-2(RNAi)* F1 animals contained 14 germ cells, a significant reduction from wild type. A similar trend was observed in late L3 animals in which *grif-1(ef32); nos-2(RNAi)* F1 animals were observed to contain 32 cells on average which is in strong contrast to 108 cells observed in wild type; control(RNAi) animals. Additionally, from L2 stage onward, a vast majority of *grif-1(ef32); nos-2(RNAi)* animals contained germ cells whose nuclei appeared aberrant, occasionally multinucleated and obviously different from wild-type nuclei (Figure 4.7.1.4B and C). At the 44 hour time point, F1 *grif-1(ef32); nos-2(RNAi)* L4 animals was observed to contain 12 germ cells on average which is a significant difference compared to L3 stage animals of the same genotype and wild type; control (RNAi) animals of identical age.

Several inferences can be drawn from these results. (i) F1 *grif-1(0); nos-2(RNAi)* animals are born with germ cells, a few of the animals initiate precocious division of PGCs either during late stage embryogenesis or upon hatching even before food signal. (2) *grif-1(0); nos-2(RNAi)* postembryonic germ cells are able to initiate some rounds of division during the first two larvae stage. (3) *grif-1(0); nos-2(RNAi)* germ cell nuclei aberrations is observable from L2 stage and cell death seems to kick in from late L3 stage of development. Together these results reveal that F1 *grif-1(0); nos-2(RNAi)* animals begin to display germ cell phenotypes from L2 stage culminating in cell death beginning from L3 stage onwards.
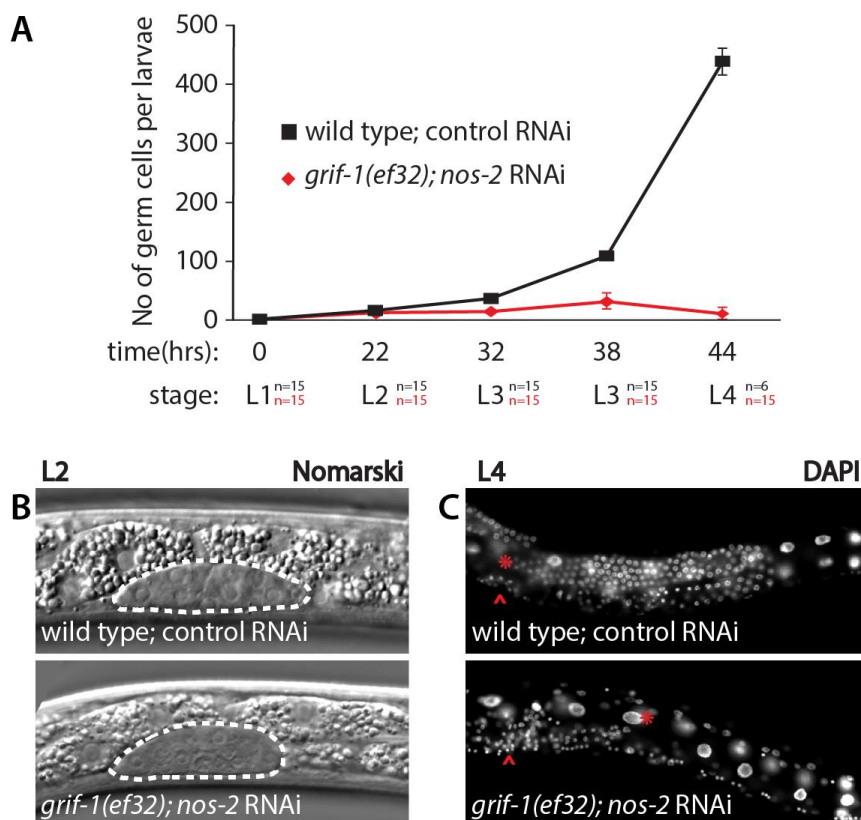
Figure 4.7.1.4. Germ cells of *grif-1(0); nos-2(RNAi)* animals begin to experience germ cell death during larvae development.

(A) A plot showing the number of germ cells in the gonad of wild type; control(RNAi) and *grif-1(ef32); nos-2(RNAi)* across larvae development. Error bars shows the standard deviation of germ cell number within analysed animals. (B) Nomarski images of L2 animals corresponding to A. *grif-1(ef32); nos-2(RNAi)* have aberrant nuclei from L2 onward. (C) Immunofluorescent images of L4 animals corresponding to (A). L4 *grif-1(ef32); nos-2(RNAi)* animals have either very few or no germ cells.

To determine whether germ cell death in *grif-1; nos-2* double mutants is due to abnormally induced apoptosis during larval development, the activities of *ced-3* and *ced-4*, which are proteases that are important for almost all, if not all, known apoptosis related events in *C. elegans*, are removed in *grif-1(0); nos-2(RNAi)* animals. To this end, *grif-1* mutants were crossed with either *ced-3* or *ced-4* animals. Resultant double mutants were treated with either control or *nos-2* RNAi. A vast majority of *grif-1(ok1610);* control(RNAi) *and grif-1(ok1610ef40); ced-4;* control(RNAi) animals were fertile (Figure 4.7.1.5). Contrary to control RNAi, *nos-2* RNAi Knockdown in *grif-1(ok1610ef40) and grif-1(ok1610ef40); ced-4* mothers led to comparable levels of sterility and appearance of the germline survival phenotype in a vast majority of F1 progenies of either strains (Figure 4.7.1.5). Similar results were obtained with *ced-3* removal (data not shown). Together, these data suggest that germ cell death or germline survival phenotype of *grif-1; nos-2* animals is largely independent of the *ced-3* and *ced-4* cell death machineries and most probably of the apoptotic program.

120
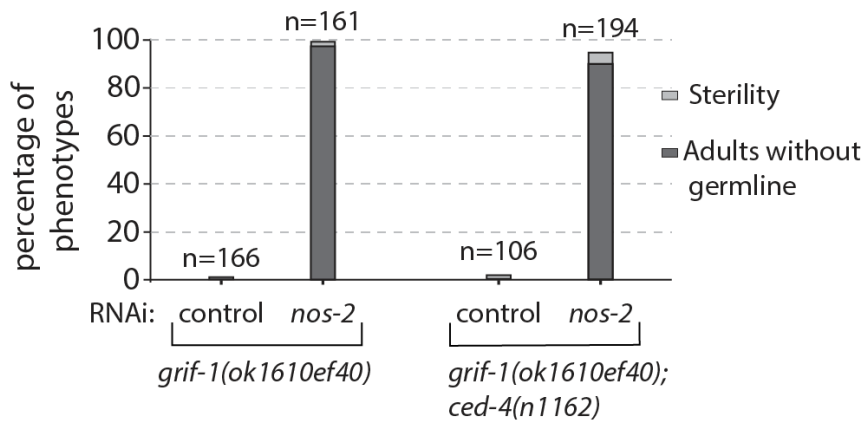
Figure 4.7.1.5. Germ cells death in *grif-1; nos-2* animals is *ced-4* independent.

A bar chart showing the percentage of sterility and germline survival phenotype of *grif-1(ok1610ef40)* and *grif-1(ok1610ef40); ced-4(n1162)* animals treated with either control or *nos-2* RNAi.

4.7.2. *nos-2* does not control GLD-2 expression

NOS-2 is important for the removal of maternal transcripts in primordial germ cells (Lee, Lu et al. 2017). Therefore, it is highly probable that NOS-2 also facilitates termination of GLD-2 expression, either by directly promoting *gld-2* transcripts turnover or indirectly promoting GLD-2 protein turnover. If either of these hypotheses were correct, germline survival phenotype due to simultaneous maternal loss of both *grif-1* and *nos-2* may be a consequence of more abundant expression of GLD-2 than in PGCs of either single mutants of both genes.

To determine whether *nos-2* regulates GLD-2 expression, GLD-2 protein expression was analysed by immunocytochemistry in PGCs of 100-cell to 150-cell stage wild-type embryos that experienced any of control RNAi, *nos-2* RNAi, *grif-1* RNAi and *grif-1; nos-2* double RNAi. Besides probing the treated embryos with GLD-2 antibodies, embryos were also probed with anti-PGL-1 antibodies to analyse PGL-1 expression and ultimately identify germ cells. Lastly, they were probed with anti-GRIF-1 antibodies to assess knockdown efficiency of *grif-1* RNAi. *nos-2* knockdown efficiency was assessed by analysing the sterility penetrance of resultant F1 adults.

Similar to wild type, PGL-1 protein was robustly detected in PGCs regardless of the RNAi conditions (Figure 4.7.2). Moreover, as observed in wild type, GRIF-1 protein was robustly detected in PGCs of analysed control(RNAi) embryos whereas GLD-2 protein was not detected (Figure 4.7.2). Similar to *grif-1* mutants discussed earlier but in contrast to control(RNAi) embryos, GRIF-1 protein was not detected in *grif-1(RNAi)* embryos while an extension of GLD-2 into PGCs was observed, indicating an efficient *grif-1* RNAi knockdown (Figure 4.7.2). In *nos-2(RNAi)* embryos, GRIF-1 but not GLD-2 was detected in PGCs of embryos; an observation similar to both control and wild-type embryos. Lastly, GRIF-1 was not detectable in *grif-1; nos-2* double RNAi condition, most probably due to *grif-1* RNAi, and GLD-2 expression levels were observed to be similar to *grif-1* single RNAi (Figure 4.7.2). A

121

vast majority of embryos that experienced *grif-1; nos-2* double RNAi became sterile as adults indicating that *nos-2* RNAi was efficient (90 % sterile, n=200). This experiment was repeated in different variations, including performing *grif-1* RNAi into *nos-2* mutants, *nos-2* RNAi into *grif-1* mutants, *grif-1; nos-2* double RNAi into a strain expressing FLAG tagged NOS-2 so that NOS-2 expression can be monitored using anti-FLAG antibodies to further judge the efficiency of *nos-2* knockdown and similar results were obtained in all conditions (data not shown). Together, these results reveal that *nos-2* most likely does not regulate GLD-2 protein expression and that synergistic biological interaction may be due to a function of *nos-2* that does not directly affect GLD-2 expression.
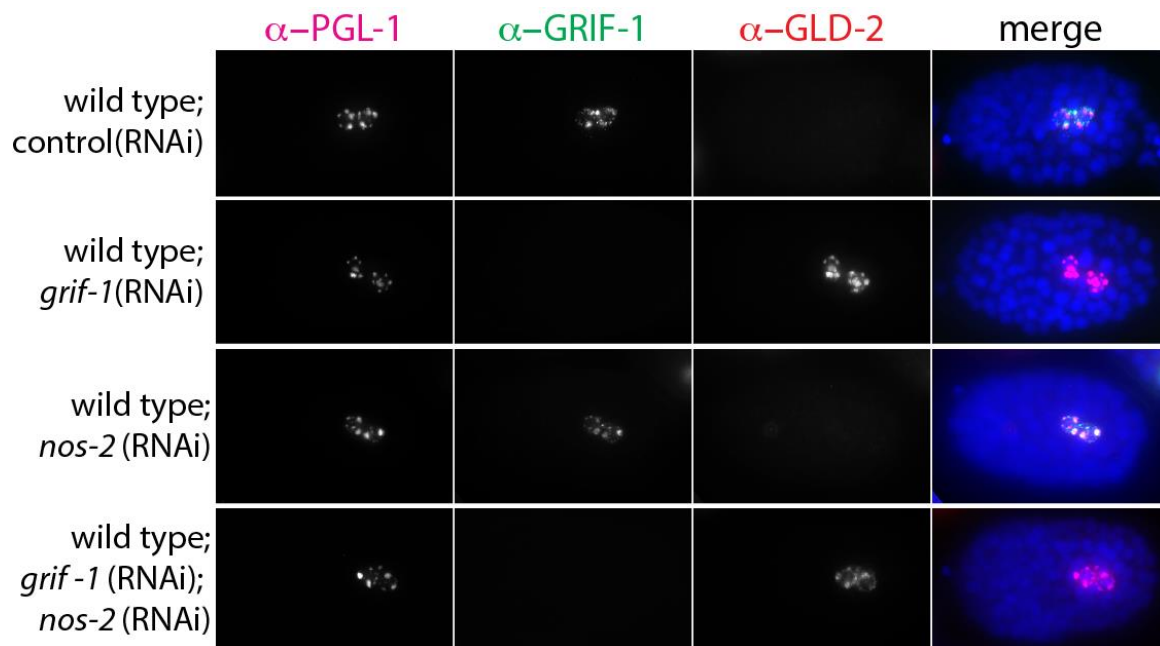
Figure 4.7.2. GLD-2 expression is unaffected by *nos-2* RNAi.

Immunofluorescent images of wild-type animals treated with, control, *grif-1* RNAi, *nos-2* RNAi, or *grif-1; nos-2* double RNAi probed with respective antibodies of PGL-1, GRIF-1 and GLD-2. Merge is a combination of all three channels and DAPI.

4.7.3. *grif-1* and *nos-2* redundantly promote turnover of oocyte derived transcripts in PGCs

grif-1 but not *nos-2* promotes turnover of GLD-2 cytoPAP, which is a factor that elongates polyA tails to stimulate stability of target transcripts. As such, *grif-1* may indirectly promote clearance of maternal transcripts by terminating the expression of their stability factor, GLD-2. Since *nos-2* has been shown to enhance clearance of maternal transcripts in PGCs, *grif-1* and *nos-2* may both be redundantly assisting the degradation of maternal transcripts in PGCs. To test this hypothesis, PGCs were isolated using fluorescence-activated cell sorting (FACS) (Sangaletti and Bianchi 2013).

To isolate PGCs, two transgenes were simultaneously used for cell sorting; PGL-1::RFP which is expressed in all embryonic germ cells and *grif-1* 3'UTR translational reporter

transgene which is mainly expressed in P4 and PGCs. Animals were raised at 25°C to increase transgene expression. Embryos were isolated from mothers and treated with chitinase to digest the chitinous embryonic shell. Dispersed cells were then sorted based on cell size and transgene expression to isolate PGCs only. All genotypes were sorted in triplicates (Figure 4.7.3.1 and see details in Materials and Methods).
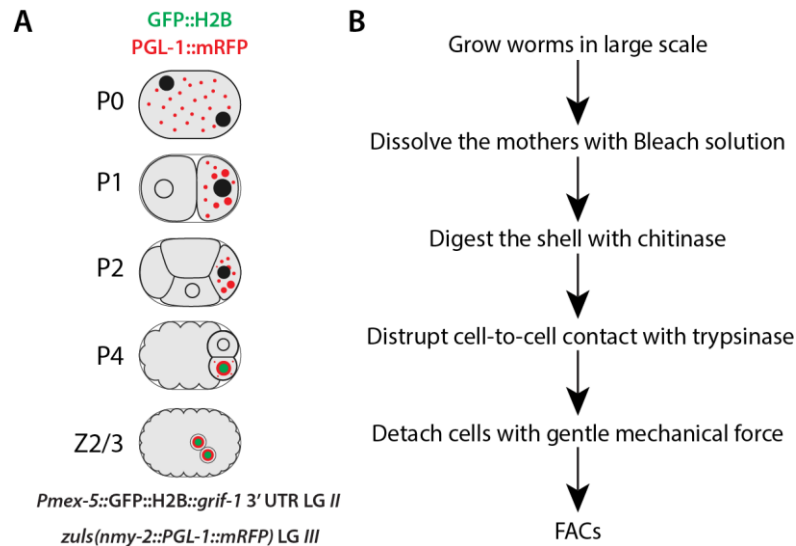
Figure 4.7.3.1. Experimental outline for PGC isolation using FACS.

(A) Cartoon images of different stages of embryogenesis showing the expression and localization of both transgenes used for PGC isolation. PGL-1::mRFP is expressed in all stages of embryonic germ cells development and enriched on P granule while GFP::H2B is predominantly expressed and localized to the nucleus of P4 and PGCs; Z2 and Z3. (B) Itemized protocol for PGC isolation.

These two transgenes were crossed into *grif-1(ef32)* and *nos-1(gv5)* mutant backgrounds. Subsequently, transgenic *grif-1(ef32)* and *nos-1(gv5)* alleles were treated with *nos-2* RNAi while transgenic wild type was treated with control RNAi. Thereafter, PGCs were isolated from any of wild-type; control(RNAi) embryos, *nos-1(gv5);* nos-2*(RNAi)* embryos, and *grif-1(ef32); nos-2(RNAi)* embryos. After isolation, the purity of isolated cells was assessed by determining the percentage of PGL-1::RFP-positive and GFP::H2B-positive cells by analysing a small sample of isolated cells with a fluorescent microscope. A vast majority of the isolated cells were observed to express both transgenes with correct localization of PGL-1::mRFP to P granules and GFP::H2B to histones in the nucleus and only a very few cells lacked the expression of both transgenes. Based on determination of the percentage of transgene expressing cells, the purity of all isolated samples was estimated to be 86.2 ± 6 % (Figure 4.7.3.2).

	Nomarski	mRFP+GFP
wild type; control RNAi		
grif-1(ef32); nos-2 RNAi		
nos-1(gv5); nos-2 RNAi		

Pmex-5::GFP::H2B::grif-1 3' UTR II

zuIs(nmy-2::PGL-1::mRFP) III
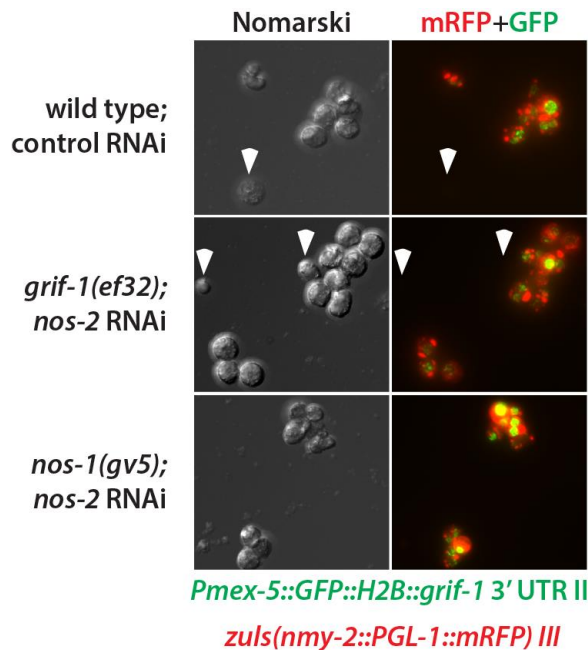
Figure 4.7.3.2. PGCs were successfully isolated with high purity.

Nomarski (left column) and fluorescent (right column) images of sorted PGCs corresponding to wild type; control(RNAi) (top), *grif-1(ef32); nos-2(RNAi)* (middle) and *nos-1(gv5); nos-2(RNAi)* (bottom). *Pmex-5*:GFP::H2B:*grif-1* 3'UTR transgene and *zuIs(nmy-2::PGL-1::mRFP) III* transgene were used for FACS sorting. The percentage purity of all isolated samples is 86.2±6 % (mean±SD). White arrowhead highlights contaminating cells that do not express either transgene.

Upon estimation of purity, total mRNA was extracted from isolated cells and transcripts were analysed using RT-qPCR and subsequently, next generation sequencing (see methods for details). GRIF-1 regulates the expression of polyA tail controlling factors and based on inferences of NANOS from studies in several other model systems (Suzuki, Igarashi et al. 2010, Weidmann, Qiu et al. 2016), NOS-2 may also recruit polyA tail controlling factors to mRNAs. Therefore, to avoid bias that may be introduced by polyA tail selection, random priming was used for reverse transcription reaction. Subsequently, in a pilot qPCR experiment performed prior to submitting samples for sequencing, the relative abundance of a few maternal transcripts was measured and normalised to *tbb-2* mRNA. Two of the tested transcripts; *oma-1* and *cpb-3,* were recovered to be significantly higher in PGCs of *nos-1(gv5); nos-2(RNAi)* embryos compared to wild-type embryos in a previous sequencing experiment (Lee, Lu et al. 2017).

After normalization to *tbb-2 (tubulin beta)* transcript, of the eight tested transcripts, the relative abundance of three transcripts; *oma-1, cpb-3,* and *gld-3L,* were observed to be significantly increased in both *grif-1(ef32); nos-2(RNAi)* and *nos-1(gv5); nos-2(RNAi)* animals compared to wild type. The observation that *oma-1* and *cpb-3* mRNAs were significantly increased in *nos-1(gv5); nos-2(RNAi)* is consistent with previous observations (Lee, Lu et al. 2017). It is noteworthy to mention that although both *cpb-3* and *gld-3L* transcript levels were statistically upregulated compared to wild type; control(RNAi), the fold increase for both

transcripts were only marginally above 1.5-fold compared to wild type; control(RNAi). Furthermore, the abundance of the *fbxc-50* transcript, was observed to be significantly increased in *grif-1(ef32); nos-2(RNAi)* PGCs but not in *nos-1(gv5); nos-2(RNAi)* PGCs. The remaining transcripts, except for *gld-1,* were observed to be comparable to wild type in both *grif-1(ef32); nos-2(RNAi)* and *nos-1(gv5); nos-2(RNAi)* PGCs. While *gld-1* is comparable to wild type; control(RNAi) in *grif-1(ef32); nos-2(RNAi),* it was observed to be significantly lower in *nos-1(gv5); nos-2(RNAi)* PGCs. These results reveal that although *grif-1(ef32); nos-2(RNAi)* and *nos-1(gv5); nos-2(RNAi)* PGCs seems to have defect in clearance of a subset of maternal mRNA and more importantly, while certain transcripts are upregulated in both genotype, others were selectively upregulated in one but not the other. To get a transcriptome-wide perspective, samples were submitted for RNA sequencing (see Materials and Methods for details).
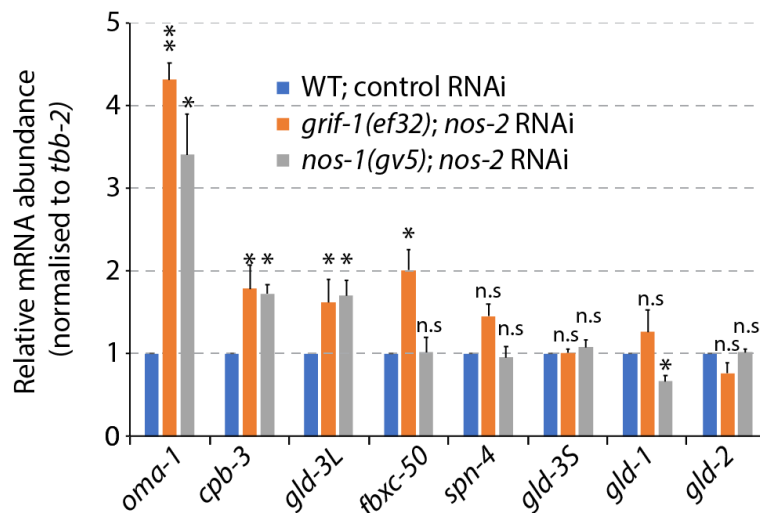
Figure 4.7.3.3. Several maternal transcripts are stabilized in PGCs of *grif-1; nos-2* animals.

Bar chart showing the relative mRNA levels, normalized to *tbb-2,* of maternal transcripts in PGCs of wild type (WT); control(RNAi) (blue), *grif-1(ef32); nos-2(RNAi)* (orange) and *nos-1(gv5); nos-2(RNAi)* (grey). Bar chart shows mean value (±S.E.M). Significance was calculated by Student's T-test by comparing *grif-1(ef32); nos-2(RNAi)* and *nos-1(gv5); nos-2(RNAi)* to WT; control(RNAi): *= $p < 0.05$, **= $P < 0.01$, n.s.= not significant.

After careful bioinformatic analysis of the sequencing results, based on cut-off of two-fold difference, several key observations were made. 308 transcripts were identified to be significantly overexpressed and 134 transcripts were significantly underexpressed in PGCs of *grif-1(ef32); nos-2(RNAi)* embryos. In comparison, 166 transcripts were overexpressed and only 29 genes were significantly underexpressed in PGCs of *nos-1(gv5); nos-2(RNAi)* embryos (Figure 4.7.3.4A and B).

The genes with significant changes were further analysed to determine to which gametogenic program they may belong; whether they are genes expressed in sperm, oocyte or they are gender neutral genes as defined by a previous study (Ortiz, Noble et al. 2014).

The majority of all analysed genes from wild type; control(RNAi) fell into the gender-neutral category (67 %, n=7525), while 20 % and 13 % fell into the oocyte and sperm expressed gene categories, respectively (Figure 4.7.3.4C). In contrast to wild type; control(RNAi) PGCs, oocyte expressed genes were observed to be over represented in genes upregulated in PGCs of *grif-1(ef32); nos-2(RNAi)* and *nos-1(gv5); nos-2(RNAi)* embryos. However, in contrast to upregulated genes, the distribution of each category appeared to be significantly unaffected in downregulated genes of both genotypes (Figure 4.7.3.4C). These data reveal that similar to *nos-1* and *nos-2, grif-1* and *nos-2* are redundantly required for clearance of maternally donated transcripts in PGCs.
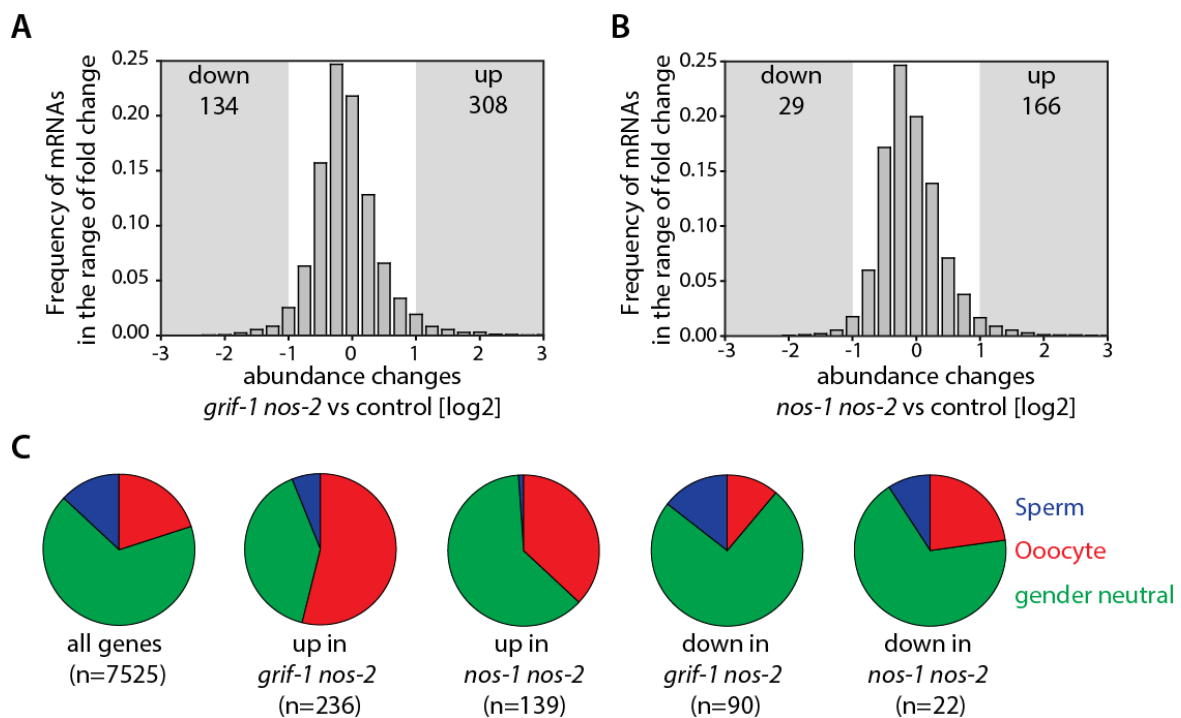
Figure 4.7.3.4. Many oocyte-derived transcripts are stabilized in PGCs of *grif-1(ef32); nos-2(RNAi)* and *nos-1(gv5); nos-2(RNAi)* embryos.

mRNA abundance changes in (A) *grif-1(ef32); nos-2(RNAi)* and (B) *nos-1(gv5); nos-2(RNAi)* PGCs. The histogram plots show the frequency of all detected transcript in range of fold change plotted against abundance changes of respective genotype compared to wild type; control(RNAi) PGC. Bars represent all detected mRNAs. Grey area marks region of at least two-fold change with the number of significantly upregulated and downregulated transcripts indicated at the top. (C) Pie charts showing the distribution of detected genes into different expression categories; sperm, oocyte and gender neutral according to the classification by Ortiz, Noble et al. 2014.

The majority of the transcripts overexpressed in PGCs of *nos-1(gv5); nos-2(RNAi)* embryos were also observed to be overexpressed in *grif-1(ef32); nos-2(RNAi)* embryos (63 %, n=105 of 166) (Figure 4.7.3.5A). However, many other transcripts were observed to be upregulated in *grif-1(ef32); nos-2(RNAi)* but not in *nos-1(gv5); nos-2(RNAi)* PGCs (Figure 4.7.3.5A). Moreover, the number of downregulated transcripts was smaller than that of upregulated genes in respective genotypes and additionally, a very weak overlap was

observed between genes that were downregulated in both genotypes compared to wild type (Figure 4.7.3.5A).

Analysis of mRNA cumulative changes measures the combined changes in distribution of a subset of transcripts compared to another subset or total transcript detected without a fold change restriction. Upregulated sets of transcripts will have a positive shift in distribution compared to the distribution of total transcripts while downregulated transcript will have a negative shift. A careful analysis of the cumulative changes without the 2-fold cut of restriction between both genotypes showed that although individual transcripts may be upregulated or downregulated to different extent in both genotypes, all genes have similar trends or pattern in both genotypes (Figure 4.7.3.5B). Moreover, the cumulative changes were also analysed for dataset from a previous study; Lee, Lu et al. 2017. Interestingly, a similar trend was also observed in that similar sets of genes tend to be upregulated in embryonic PGCs of *nos-1(gv5); nos-2(RNAi)* animals (Figure 4.7.3.5C).
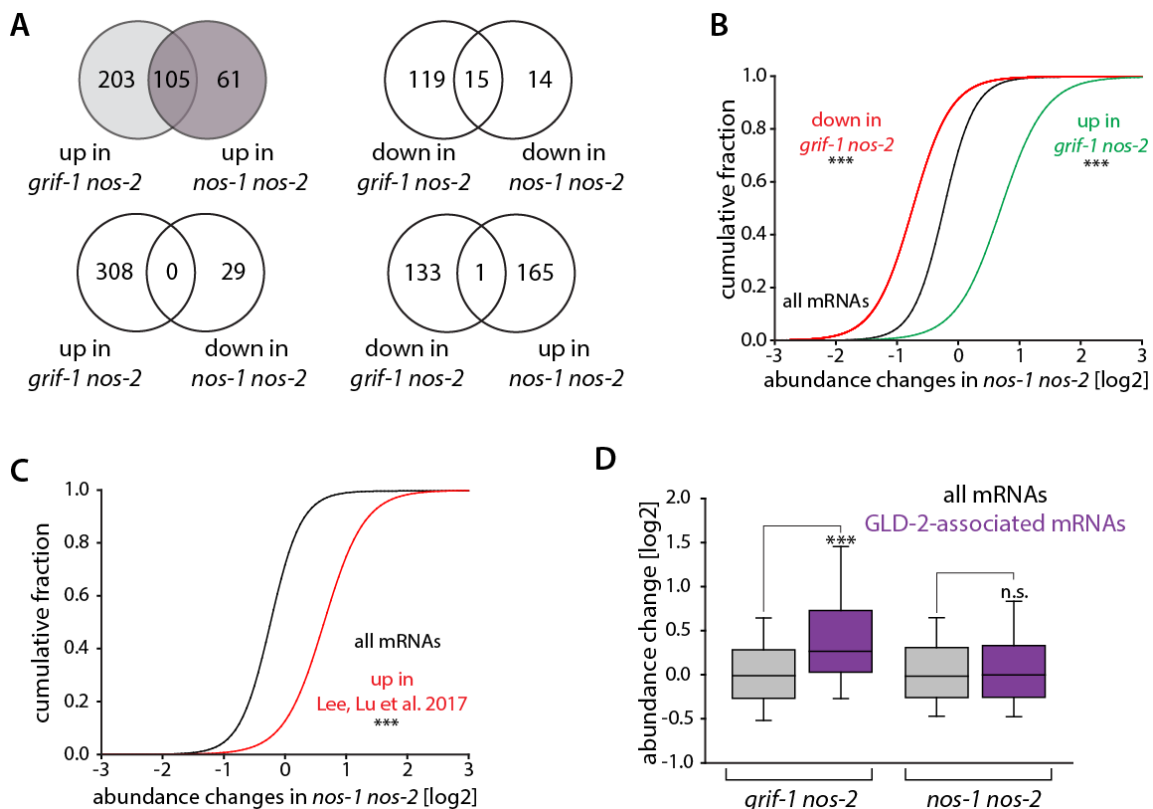
Figure 4.7.3.5. GLD-2-associated transcripts are stabilized in PGCs of *grif-1(ef32); nos-2(RNAi)* but not *nos-1(gv5); nos-2(RNAi)* embryos.

(A) Venn diagrams showing comparison of *grif-1(ef32); nos-2(RNAi)* and *nos-1(gv5); nos-2(RNAi)* transcripts that changed significantly compared to wild type; control(RNAi). (B-C) Cumulative fractions of mRNA abundance changes comparing all mRNA of *nos-1(gv5); nos-2(RNAi)* to (B) upregulated and downregulated genes in *grif-1(ef32); nos-2(RNAi)* PGCs, (C) upregulated genes from Lee, Lu et al. 2017. (D) Box plots comparing distribution of abundance change of all mRNA to GLD-2-associated mRNAs (Kim, Wilson et al. 2010) in the two genotypes.

Since a protein turnover defect of GLD-2 cytoPAP in embryonic PGCs of *grif-1* embryos might contribute significantly to mRNA turnover defects in PGCs of *grif-1(ef32); nos-2(RNAi)*, upregulated genes, changes of a GLD-2-associated mRNA dataset from a previous study were analysed (Kim, Wilson et al. 2010). GLD-2-associated transcripts were observed to be significantly upregulated in comparison to all detected transcripts in *grif-1(ef32); nos-2(RNAi)* but not in *nos-1(gv5); nos-2(RNAi)* (Figure 4.7.3.5C).

Together, the sequencing data reveal that just like *nos-1* and *nos-2, grif-1* and *nos-2* are redundantly required for the clearance of many maternal transcripts in embryonic PGCs, while downregulated transcripts were most likely an indirect effect, arising as a consequence of biological changes in the system. Additionally, the many transcripts that were significantly upregulated in *grif-1(ef32); nos-2(RNAi)* but not in *nos-1(gv5); nos-2(RNAi)* suggest that *grif-1* contribution to the activity of *nos-2* in promoting the clearance of maternal transcripts is unique and more encompassing compared to the contribution of *nos-1*. Lastly, the data predicts that many of the significantly upregulated transcripts in *grif-1(ef32); nos-2(RNAi)* but not in *nos-1(gv5); nos-2(RNAi)* or to put in simpler term, transcripts that were upregulated due to *grif-1*-specific activities were most likely upregulated due to extended GLD-2 expression, its association with target transcripts and hence its activity in *grif-1(ef32); nos-2(RNAi)* animals.

In summary, the experiments described in this section shows that *nos-2* but not *nos-1* is required redundantly with *grif-1* to promote survival of the germline. Therefore, germ cells lacking activities of both *grif-1* and *nos-2* might die during subsequent larvae development in a manner that seems to be independent of apoptosis. Tested germ cell death may be a consequence of turnover defects of maternal mRNAs in embryonic PGCs.

4.8. Prolonged GLD-2 expression in PGCs contributes to grif-1-dependent germline defects

grif-1 regulates GLD-2 turnover in PGCs. Based on sequencing data, many of the upregulated transcripts in grif-1; nos-2 but not nos-1; nos-2 PGCs are GLD-2-associated transcripts. Therefore, a likely possibility is that continued expression of GLD-2 may contributes to observed phenotypes in grif-1 animals and grif-1; nos-2 animals. This section describes experiments carried out to determine the biological consequence of GLD-2 stabilization in PGCs of grif-1 and grif-1; nos-2 embryos

4.8.1. The N-terminal IDR of GLD-2 is dispensable for GLD-2 germline activity

To determine the likely contribution of extended expression of GLD-2 in grif-1 mutants and grif-1; nos-2 embryos, the knowledge of interaction surface required by GLD-2 to bind to GRIF-1 was further explored to potentially cause prolonged GLD-2 expression in PGCs independently of GRIF-1 activity. To this end, gld-2 transgenes lacking the N-terminal intrinsically disordered region required for GRIF-1 interaction, as determined in Figure 4.3.2 were generated. Using the MosSCI transgenesis technique, several GLD-2 transgenes; aa1-1113, aa198-1113 and aa267-1113, driven by mex-5 promoter and gld-2 3'UTR were inserted into the genome (Figure 4.8.1.1).
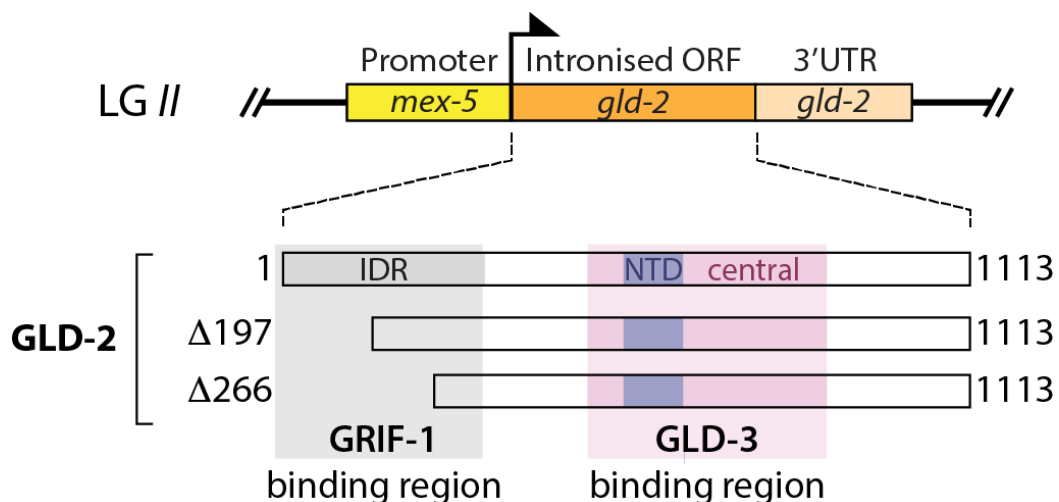
Figure 4.8.1.1. Several gld-2 transgenes were generated using MosSCI.

Cartoon images of gld-2 transgenes that were inserted into linkage group II using MosSCI transgenesis techniques (top, not to scale). Intronized gld-2 ORF is reengineered gld-2 locus optimized for easier cloning and transgenesis. cDNA sequence encoding for N terminal half of GLD-2 protein was fused with genomic sequence encoding for the C-terminal half of GLD-2 protein to generate a sequence that encodes for full-length GLD-2 protein (image of reengineered locus not shown). Using the construct that encodes for full-length GLD-2 protein as a template, two additional transgenes that truncate parts of GRIF-1 binding region were generated and inserted into the genome. Protein products of the three transgenes are displayed at the bottom.

The generated transgenes were subsequently crossed into a gld-2(q497) mutant background to assess the expression and function of the transgene independently of GLD-2

activity from wild-type locus. To eliminate effects that may accumulate over generations, *gld-2(q497)* mutation was maintained over a balancer chromosome even in the presence of the transgene. To determine whether GLD-2 transgenes were expressed, a western bot analysis of homozygote *gld-2(q497)* animals carrying GLD-2 transgenes was carried out, using wild type as control to compare the level of expression. To avoid bias in detection, a GLD-2 antibody that recognises the C-terminal portion of GLD-2 was used in the western blot analysis (Figure 4.8.1.2).
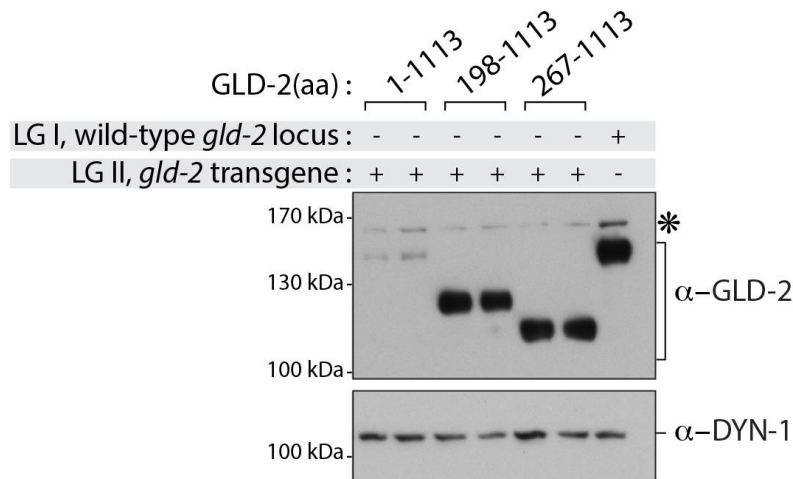
Figure 4.8.1.2. *gld-2 t*ransgenes are expressed in adult animals.

Immunoblots of wild type and transgenic strains expressing GLD-2 probed with anti-GLD-2 monoclonal antibody that binds the C-terminal end of GLD-2 (mAb a4-4) and anti-DYN-1 antibody as loading control. Asterisk (*) shows unspecific background signal. *gld-2* wild-type locus minus (-) = *gld-2(q497)* and *gld-2* wild-type locus plus (+) = wild type.

GLD-2 monoclonal antibody recognised full-length GLD-2 specifically and robustly in wild-type animals (Figure 4.8.1.2). In transgenic animals expressing full-length GLD-2, a band of identical size to wild-type GLD-2 protein was observed. However, unlike wild type, an extremely weak signal of full-length GLD-2 transgene was detected (Figure 4.8.1.2). In transgenic animals expressing N-terminally truncated GLD-2 variants (aa198-1113 and aa267-1113), bands of expected sizes were detected, with robust signals comparable to wild type (Figure 4.8.1.2). Importantly, full-length GLD-2 signal was not detected in animals expressing truncated GLD-2 protein. This is consistent with the genotyping experiment carried out to determine whether *gld-2(q497)* mutation was successfully crossed into transgenic animals expressing *gld-2* transgene (Figure 4.8.1.2). Together, the immunoblot analysis reveals that *gld-2* transgenes are successfully expressed. However, at different levels; the expressing full-length GLD-2 produces lower levels than wild type and its truncated counterparts.
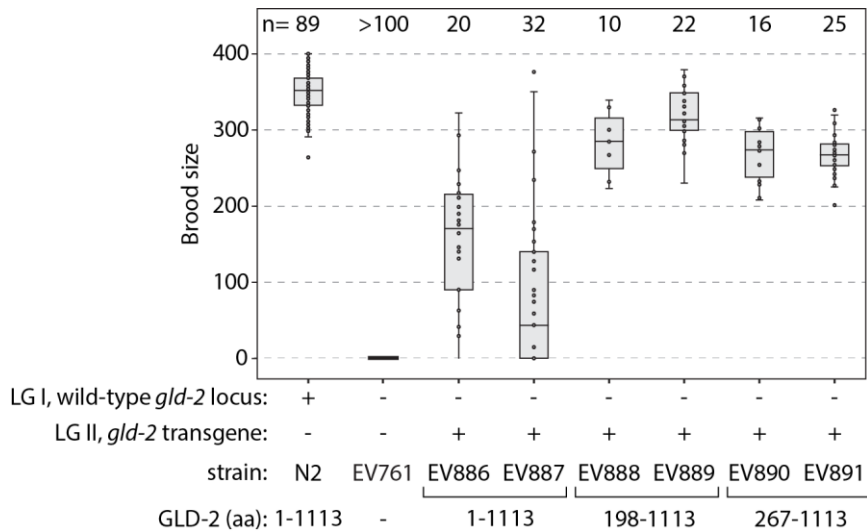
Figure 4.8.1.3. Rescue of postembryonic germ cell functions.
A box plot displaying the brood size of wild type (N2), *gld-2(q497)* mutant (EV761), and transgenic animals expressing GLD-2 in *gld-2(q497)* mutant background. n is the total number of mothers analysed. *gld-2* wild-type locus minus (-) = *gld-2(q497)* and *gld-2* wild-type locus plus (+) = wild type.

To determine whether removal of the N-terminal end affects GLD-2 activity and germline function, the capacity of the transgenes to rescue *gld-2(q497)* sterility was determined by comparing their fecundity to that of wild-type and *gld-2(q497)* animals. Two independent lines were analysed for each *gld-2* transgene to ensure reproducibility of results. On average, wild-type animals sired approximately 350 total progenies while homozygote *gld-2(q497)* were sterile and produced no progeny (Figure 4.8.1.3). The two independent lines of animals expressing full-length *gld-2* transgene in the background of *gld-2(q497)* mutation sired, on average, approximately 170 and 45 total progenies (n of mothers= 20 and 32, respectively) (Figure 4.8.1.3). Although the average total progenies were far apart in the two lines, the two lines have somewhat similar spread of variation from animal to animal to the extent that few animals had more than two hundred total progenies while others had very few total progenies. Given the high variation in the spread of total number of progenies sired by the animals expressing full-length transgene, the average will only be similar with a very high sample number. Additionally, the observation that the full-length transgene did not rescue *gld-2(q497)* sterility completely is not surprising given the extremely low level of protein expression detected during western blot analysis. The data also suggest that the full-length transgene may be expressed with high variation even within a single line with some animals presumably expressing the transgenes more robustly than others.

In contrast to transgenes expressing full-length GLD-2, which marginally rescues *gld-2(q497)* sterility with very high variation, the two transgenic lines expressing GLD-2 aa198-1113 produced, on average, 287 and 313 total progenies (n=10 and 22, respectively), which is almost a complete rescue of *gld-2(q497)* sterility (Figure 4.8.1.3). Moreover, just like the

aa198-1113 transgene, the two transgenic animals expressing GLD-2 aa267-1113 also produced, on average, 274 and 268 total progenies (n=16 and 25, respectively) (Figure 4.8.1.3)). Together, these results suggest that removal of the N-terminal part of GLD-2, at least the first 266 amino acids, may not drastically affect the enzymatic activity and germ cell function of GLD-2 during postembryonic germline development.

3.8.2. The N-terminal IDR of GLD-2 is important for GLD-2 turnover in embryonic PGCs

The removal of the first 266 amino acids of GLD-2 seems not to considerably affect GLD-2 germline function in adults. Hypothetically, the N-terminal region of GLD-2 may be a surface for protein-protein interaction. Alternatively, it could be used for modulation of GLD-2 embryonic or germline expression. These two possibilities are not mutually exclusive. Therefore, to determine whether removal of the N-terminal part of GLD-2 affects GLD-2 expression and turnover during embryogenesis, analysis of GLD-2 and GLD-3 expression was carried out by immunofluorescent analysis of wild-type embryos and transgenic embryos expressing truncated GLD-2 proteins. Again, to avoid bias in detection, a GLD-2 antibody that recognises the C-terminal end of GLD-2, mAb a4-4, was used in this study. The expression of PGL-1 served as penetration control and germ cell marker.

PGL-1 was robustly detected and enriched on P granules at all stages of embryonic germ cell development in wild type (see PGCs in Figure 4.8.2A). GLD-2 and GLD-3 expression is very similar, if not identical, during embryogenesis in wild type. Therefore, as observed before, the two proteins were robustly enriched in the germ cell precursors in early embryos, substantially reduced in somatic sisters and undetectable in other somatic cells (data not shown). GLD-2 and GLD-3 were not detected in PGCs of wild-type embryos (Figure 4.8.2A).

Transgenic embryos expressing full-length GLD-2 were observed to have highly variable and extremely weak expression of GLD-2 in early embryogenesis and in fact some embryos had to be exposed longer than others to detect GLD-2 signal. Several biological phenotypes were also observed to accompany low expression of the full-length GLD-2 (data not shown). This observation is consistent with the highly variable nature of the rescue of germline function of GLD-2, suggesting that the expression of this transgene is most likely highly variable in the germline as well. Since transgenically provided full-length GLD-2 is often not detectable even in early embryos, further analysis of GLD-2 in PGCs of these embryos was discontinued.
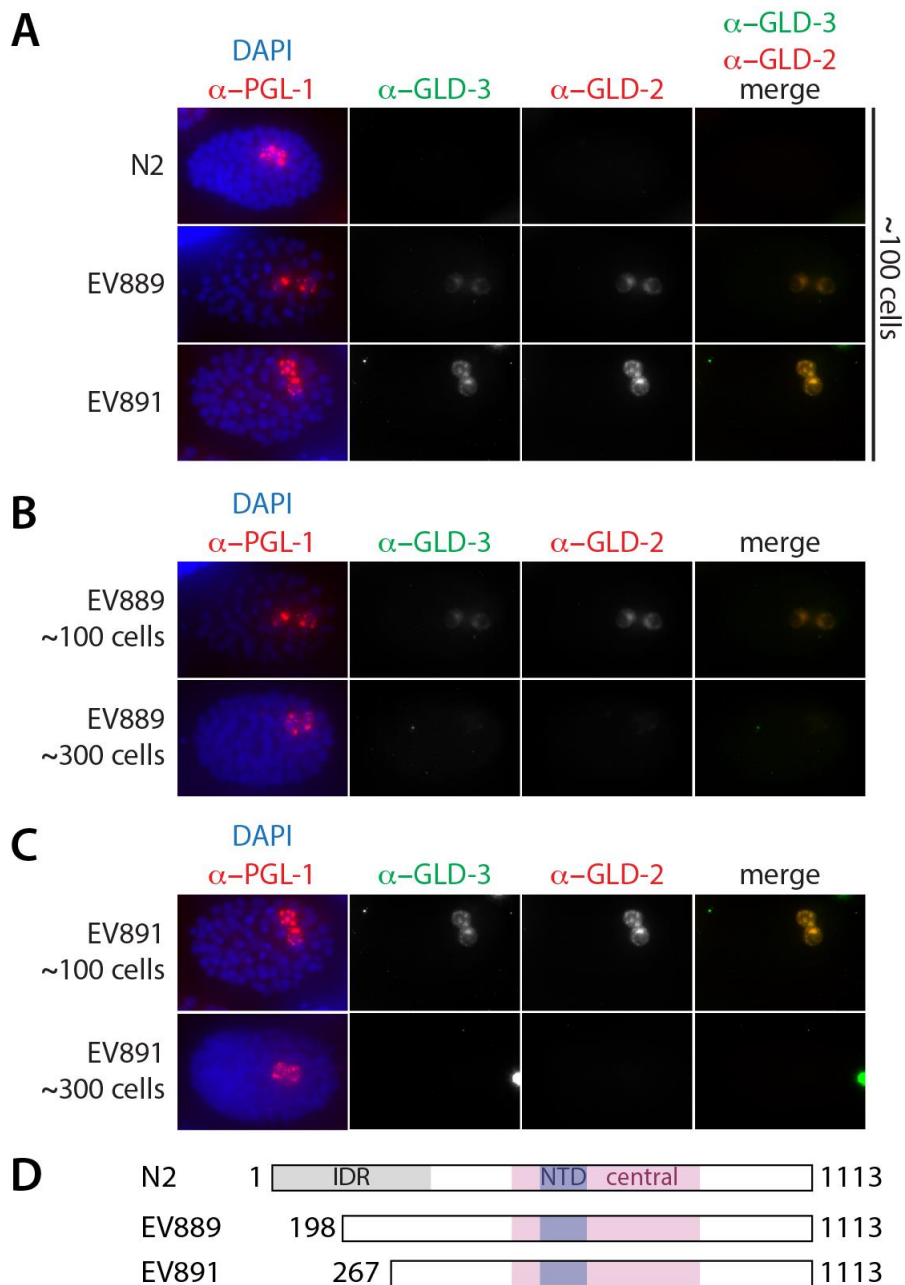
Figure 4.8.2. The N-terminal IDR of GLD-2 is important for turnover in embryonic PGCs.

(A) Immunofluorescent images of approximately 100-cell stage wild-type embryos (N2), and transgenic embryos expressing truncated GLD-2, in *gld-2(q497)* mutant background, EV889 and EV891. (B and C) Immunofluorescent images of approximately 100-cell stage (top) and approximately 300-cell stage embryos of EV889 and EV891, respectively. (A-C) All embryos were probed for chromatin and PGL-1 (left column), GLD-3 (middle-left column), and GLD-2 (middle-right column). Merge is a combination of GLD-3 and GLD-2 channels. (D) Cartoon images showing GLD-2 protein variants in all given strains.

In transgenic animals expressing truncated GLD-2 (aa198-1113 and aa267-1113), GLD-2 and GLD-3 expression were highly similar in pattern to GLD-2 expression in early embryogenesis of wild type. This suggests that removal of a N-terminal portion of GLD-2, at least the first 266 amino acids, may not affect GLD-2 expression in early embryos and its turnover in somatic cells (data no shown). However, in contrast to wild-type embryos whose expression of GLD-2 and GLD-3 began to diminish with the gastrulation of P4 germ cell

primordium, majority of P4 of transgenic embryos expressing N-terminal truncated GLD-2 proteins maintained relatively high levels of GLD-2 and GLD-3 proteins until gastrulation was completed and division was about to be initiated (data not shown). Upon completion of division, in approximately 100-cell stage embryos of animals expressing either GLD-2 truncation, both GLD-2 and GLD-3 were still detectable in nascent PGCs. However, unlike in *grif-1* mutants in which GLD-2 and GLD-3 expression continued to be robust and associated with P granules until relatively late stage of embryogenesis before they changed localization to become completely cytosolic and their expression begin to dwindle at these late stages, both GLD-2 and GLD-3 were no longer detectable by 300-cell stage in transgenic embryos expressing either truncated GLD-2 (Figure 4.8.2B and C).

To test whether, the rapid disappearance of GLD-2 in nascent PGCs of transgenic animals is due to GRIF-1 activity, transgenic animals expressing truncated GLD-2 were treated with control or *grif-1* RNAi. Control embryos expressed truncated GLD-2 transiently in PGCs as described above (data not shown). By contrast, *grif-1* RNAi treated embryos extended GLD-2 expression in PGCs throughout embryogenesis (data no shown), suggesting that although removal of the first 266 amino acids may have slightly impaired GLD-2 and GRIF-1 interaction, it did not completely abolish it. Together, these data suggest that the N-terminal end of GLD-2 may be important GLD-2 turnover in PGCs via interaction with GRIF-1. To make a firm conclusion, further studies are required in which the intrinsically disordered region is completely removed, which may abolish the GRIF-1 and GLD-2 interaction since Y2H tests suggest that the whole IDR is required for a robust interaction. More importantly, these data also suggest that stabilization of GLD-3 in *grif-1* animals is most likely not due to direct activity of GRIF-1 on GLD-3 but rather due to activity or presence of GLD-2 in PGCs. In all, the temporal stability of GLD-2 in PGCs of transgenic embryos is not to the same extent as in *grif-1(0)* null embryos.

4.8.3. Prolonged GLD-2 expression in PGCs contributes to germ cell defects in *grif-1* and *grif-1; nos-2* animals

grif-1 animals have transgenerational sterility or mortal germline phenotype which is temperature sensitive. A possible scenario is that continued expression of GLD-2 cytoPAP triggers the expression of certain maternal factors that promotes molecular events that accumulates over generations causing biological phenotypes upon reaching a threshold. Therefore, to determine whether prolonged GLD-2 expression is detrimental to germ cell development, transgenic animals that express full-length or N-terminal truncations of GLD-2 were tested for transgenerational sterility. One key fact was important to consider, as concluded from previous experiments (see Figure 4.8.2), GLD-2 is considerably transiently expressed in PGCs of transgenic embryos expressing truncated GLD-2 (GLD-2 expression is

terminated by 300-cell stage) compared to *grif-1(0)* embryos in which GLD-2 expression in prolonged in PGCs throughout embryogenesis. Therefore, if mortal germline phenotype in *grif-1* animals were a consequence of prolonged GLD-2 expression in PGCs, transgenic animals expressing truncated GLD-2 may have a less several transgenerational sterility phenotypes compare to *grif-1(0)* mutants.

To test transgenerational sterility, transgenic animals expressing GLD-2 in *gld-2(q497)/+* background were shifted to 25°C and allowed to lay progenies. Resultant homozygote *gld-2(q497)* transgenic F1 progenies, expressing GLD-2 were maintained for three generations at 25°C. The brood sizes of first-generation mothers were compared to those of third-generation mother to determine a likely reduction in total brood size across generations (see scheme in Figure 4.8.3.1A). As control for the experiment, wild type animals were treated similarly.

The F1 and F3 mothers of wild-type animals were observed to sire robust and comparable number of progenies at 25°C (Figure 4.8.3.1B). Surprisingly, although with high variation, F1 mothers of transgenic strains expressing full-length GLD-2 sired total number of progenies that were, on average, only slightly reduced compared to wild type (Figure 4.8.3.1B). This is in strong contrast to 20°C, at which transgenically provided full-length GLD-2 weakly rescued *gld-2* sterility phenotype (see Figure 4.8.1.3). More importantly, the F3 mothers of transgenic animals expressing the full-length GLD-2 sired comparable total number of progenies to F1 animals (Figure 4.8.3.1B).

Additional observations were made for transgenic animals expressing full-length GLD-2. (1) Surprisingly, similar to wild-type, a population of these strains can be indefinitely maintained at 25°C. In fact, the rescue capacity of transgenically provided full-length GLD-2 seems to improve across generations at 25°C. (2) During long term maintenance at 25°C, sterile animals were occasionally observed. (3) These rare sterile animals have extended gonads that accumulate small oocyte-like cells; a phenotype that is reminiscent of *gld-2(0)* phenotype (data not shown). These observations suggest that transgenically provided full-length GLD-2 rescues *gld-2(q497)* sterility phenotype better at 25°C when compared to 20°C. The results also suggest that occasionally, some of the transgenic animals may fail to express GLD-2, leading to rare appearance of *gld-2(q497)* phenotypes at 25°C. Lastly, wild-type and transgenic animals expressing full-length GLD-2 do not display transgenerational sterility.

Figure 4.8.3.1. Transgenerational passage led to lower brood size in transgenic animals expressing GLD-2 truncation while transgene protein expression remains unaffected.

(A) Scheme of experiments to determine transgenerational sterility in transgenic animals expressing GLD-2 at 25°C. *gld-2(TG)= gld-2* transgene (B) Box plot displaying the brood size of wild type and transgenic animals expressing GLD-2. Brood sizes were determined two generations apart, F1 and F3. n is the number of mothers whose brood sizes were determined. Differences were determined by student's t-test: *= p<0.05, **= p<0.01, ***= p<0.001, ****= p<0.0001, n.s= not significant. (C) Immunoblots of animals corresponding to (B) probed with anti-GLD-2 antibody to monitor GLD-2 levels and anti-DYN-1 antibody as loading control.

Similar to transgenic animals expressing full-length GLD-2, F1 mothers of transgenic animals expressing either truncated GLD-2 sired slightly reduced number of progenies compared to wild type (Figure 4.8.3.1B). However, unlike wild-type or transgenic animals expressing full-length GLD-2, F3 mothers of animals expressing truncated GLD-2 sired

136

significantly reduced number of progenies compared to respective F1 animals (Figure 4.8.3.1B).

The observed reduction in the brood size in the third generation compared to first generation may be a result of reduced levels of transgene expression across generations. To exclude this possibility, western blot analyses were carried out to compare the levels of GLD-2 expression in F1 and F3 mothers of wild-type and transgenic animals (Figure 4.8.3.1C). In wild-type animals, GLD-2 protein band was detected robustly with expected size. Similar to wild-type endogenous GLD-2 in size but with reduced intensities, full-length GLD-2 protein was also detected in corresponding transgenic animals and the level of expression is comparable between F1 and F3 animals (Figure 4.8.3.1C). Using endogenous full-length GLD-2 from wild-type as a basis, just by gauging the levels, it is quite apparent that there is an improvement in expression of transgenically provided full-length GLD-2 at 25°C over 20°C (compare Figure 4.8.1.2 and Figure 4.8.3.1C). This may explain better rescuing capacity of transgenically provided full-length GLD-2 at 25°C over 20°C (compare Figure 4.8.1.3 and Figure 4.8.3.1B). Moreover, the expression levels of truncated GLD-2 proteins were detected to comparable levels between F1 and F3 respective transgenic animals (Figure 4.8.3.1C). This argues that the reduced number of progenies sired by F3 transgenic animals expressing truncated GLD-2 compared to their respective F1 animals, is not due to decrease in expression levels of transgenically provided truncated GLD-2 across generations.

Several other observations were made in transgenic animals expressing truncated GLD-2 in addition to reduced brood size in the third generation: (1) similar to *grif-1(0)* animals, when a population is maintained at 25°C for many generations, some of the transgenic worms become sterile and the percentage of sterile worms increased from generation to generation, (2) unlike populations of *grif-1(0)* animals which become completely sterile between the third (F3) and the thirteenth (F13) generations at 25°C (see Figure 4.6.1.2), populations of transgenic animals expressing truncated GLD-2 can be maintained for more than twenty generations (F20), although most of the animals were sterile at these late generations, (3) The sterile worms displayed similar phenotypes as *grif-1(0)* animals. These phenotypes include underproliferation and germline survival phenotypes (data not shown). All the observed phenotypes, which are less severe form of transgenerational sterility of *grif-1,* were in strong contrast to transgenic animals expressing full-length transgene. The data suggest that transient expression of transgenically provided truncated GLD-2 causes transgenerational sterility. However, the sterility and germline phenotypes are less severe compared to *grif-1.* In fact, bearing in mind that GLD-2 is not prolonged to similar extent in embryonic PGCs of transgenic embryos expressing truncated GLD-2 compared to *grif-1,* a less severe phenotype is not surprising.

In the same manner, prolonged GLD-2 expression in PGCs of *grif-1* mutants may also contribute to germline survival phenotype displayed by *grif-1(0); nos-2(RNAi)* animals at 20°C. To test this, wild type, *grif-1(ef32)* and transgenic animals expressing truncated GLD-2 were treated with either control or *nos-2* RNAi. F2 homozygote descendant of a heterozygote animals of *grif-1(ef32)* or transgenic animals expressing truncated GLD-2 were treated with RNAI. These animals were treated with either control or *nos-2* RNAi from L1 to adulthood and their progenies were analysed for sterility at adulthood. For this experiment, transgenic strain expressing GLD-2 aa198-1113 was used. This strain is hereafter referred to as EV888.
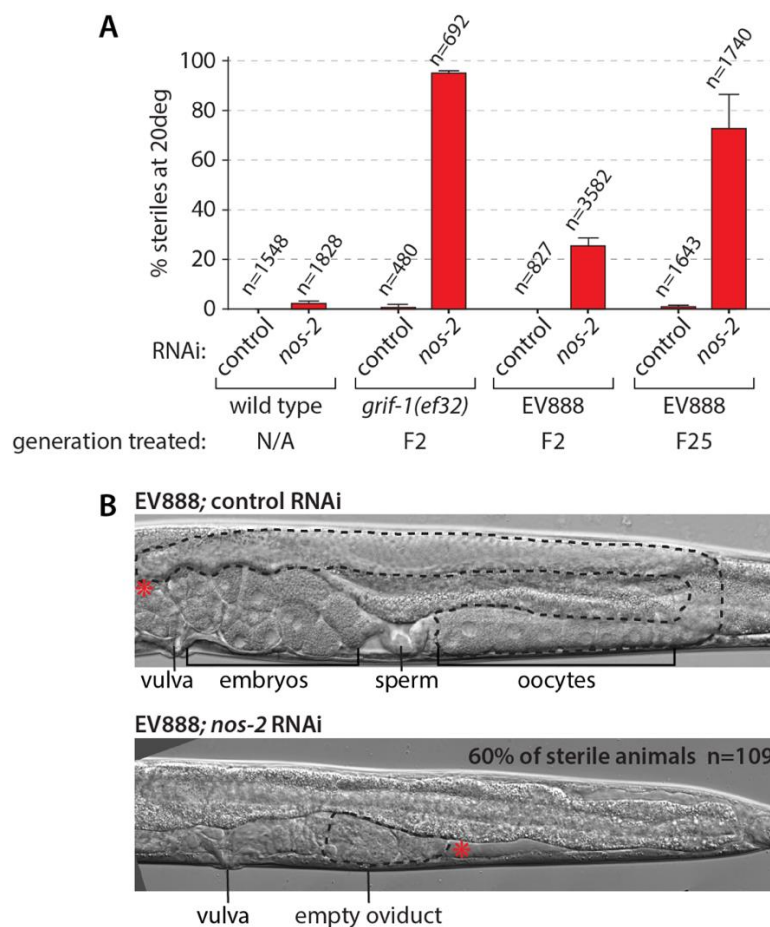
Figure 4.8.3.2. Sterility arises when *nos-2* activity is removed in transgenic animals expressing truncated GLD-2.

(A) Bar chart showing the percentage sterility of progenies of wild type, *grif-1(ef32)* and EV888 animals treated with either control or *nos-2* RNAi. F2 descendants of *grif-1/+* were treated. F2 and F25 homozygotes descendants of *gld-2(q497)/+* heterozygote were treated. N/A= not applicable. Bar chart shows mean (± Std. Dev). n is the number of analysed animals. (B) Nomarski images of EV888 animals treated with control (top) or *nos-2* RNAi (bottom). Asterisk (*) marks the distal end of germ line. 60% of sterile EV888; *nos-2(RNAi)* have no apparent germline.

All genotypes treated with control RNAi produced fertile progenies (Figure 4.8.3.2A). However, unlike control RNAi, *nos-2* RNAi led to sterility to of variable penetrance in all tested genotypes. Wild-type animals treated with *nos-2* RNAi produced background sterility (3 %, n =1828). By contrast, *grif-1(ef32); nos-2(RNAi)* animals predominantly produced

sterile progenies (95 %, n=692). Intriguingly, EV888 animals treated with *nos-2* RNAi also produced moderate number of sterile progenies (30 %, n=3582) (Figure 4.8.3.2A) and surprisingly, EV888 animals that have been maintained as homozygotes for many generations before *nos-2* RNAi produced significantly more sterile progenies compared to those that were only F2 homozygote descendant of a heterozygote animals (73 %, n=1740) (Figure 4.8.3.2A). These data suggest that transient expression of transgenically provided truncated GLD-2 In embryonic PGCs leads to moderate sterility at 20°C when *nos-2* activity is removed. The moderate sterility of EV888; *nos-2(RNAi)* animals is not comparable to the considerable sterility seen in *grif-1; nos-2* animals due to varying degree of prolonged GLD-2 expression; GLD-2 is prolonged at best to 300-cell stage in EV888 while it is prolonged throughout embryogenesis in *grif-1* animals. Therefore, the less severe phenotype seen in F1 EV888 compared to F1 *grif-1* animals, when *nos-2* activity is removed, is expected.

Furthermore, a higher level of sterility observed when *nos-2* is removed after EV888 had been maintained at 20°C for many generations is reminiscent of behaviour of *grif-1* mutants. At 20°C, *grif-1* animals become sterile after many generations and this sterility increases in successive generations. Similarly, EV888 may accumulate the same molecular phenotypes which causes GLD-2-dependent mortal germline phenotype in *grif-1* animals. However, unlike *grif-1* animals, the molecular signature may not reach a threshold to independently induce sterility but only revealed as biological phenotype with the removal of *nos-2* after EV888 had been maintained for many generations.

Additionally, the gonad of sterile EV888; *nos-2(RNAi)* animals were analysed using Nomarski microscopy to determine whether they have germline survival phenotype associated with their sterility, similar to *grif-1; nos-2(RNAi)* animals. Approximately 60 % of analysed animals have extremely small gonad with either less than 10 germ cell nuclei or no germ cell at all. The remaining 40 % of sterile animals have gonads with many germ cells whose germline phenotypes were not analysed in details (Figure 4.8.3.2B and C). These data reveal that performing *nos-2* RNAi into transgenic animals expressing truncated GLD-2 produces phenotypes that are reminiscent of *grif-1; nos-2* double mutants. This suggests that extended GLD-2 expression contributes towards *grif-1; nos-2* germline phenotypes.

In summary, transgenically provided truncated GLD-2 rescues *gld-2(q497)* phenotypes suggesting that N-terminal end of GLD-2 is not important for catalytic activities and adult germline functions of GLD-2. Furthermore, removal of the N-terminal portion of GLD-2 leads to transient extended expression of GLD-2 in embryonic PGCs. The relevance of GLD-2 turnover in PGCs was tested by analysing the impact of transient expression of truncated GLD-2 in PGCs. In all tested scenarios, transient expression of transgenically provided truncated GLD-2 leads to less severe phenotypes compared to *grif-1* animals. This is not surprising, due to the fact that truncated GLD-2 is removed before 300-cell stage while

GLD-2 expression is prolonged in embryonic PGCs throughout embryogenesis in *grif-1* animals. Taken together, all the data suggest that GLD-2 turnover in PGCs is important for germ cell development.

5. Discussion

Regulatory proteins are required to execute accurate gene expression programs across development. Therefore, developmental expression of regulatory proteins must be tightly controlled for the best possible output. Most of these regulations occur predominantly at the level of transcription. However, during gametogenesis and early embryogenesis, when transcription is globally repressed, complex biological tasks are regulated predominantly at posttranscriptional levels. At these stages, to developmentally regulate the abundance and spatiotemporal expression of proteins, timely control of proteins synthesis and protein turn over becomes critical. To this end, maternal RNA regulators such as RBPs and RNA-modifying enzymes bind and control the fate of maternally provided transcripts. Especially, developmentally regulated protein degradation is expected to limit the activity of maternal RNA regulators to facilitate the switch from maternal-to-zygotic gene expression programs. But the involved molecular mechanisms remain largely unclear.

In an attempt to identify and characterize molecular mechanisms that control posttranscriptional gene expression machinery during embryonic primordial germ cell development, this thesis investigated the regulated turnover of maternal cytoplasmic polyA polymerase GLD-2. Specifically, this thesis examined the requirement of ubiquitin proteasome system (UPS) in regulating the spatiotemporal expression of GLD-2 cytoPAP in primordial germ cells (PGCs). Additionally, it also addressed the relationship between GLD-2 turnover and maternal gene expression during embryonic PGC development.

5.1. Proteasome is indispensable to germ cell development in *C. elegans*

Similar to other biological systems, the proteasome is important for multiple aspects of development in *C. elegans* including germline development (Takahashi, Iwasaki et al. 2002, Kisielnicka, Minasaki et al. 2018). Either mutations in, or a knockdown of genes encoding majority of core and regulatory proteasome factors affects fertility (Kipreos 2005). Systematic approaches to identify proteins degraded by the proteasome to promote aspects of germline development revealed to date roles in only four contexts: the mitosis-to-meiosis transition (Macdonald, Knox et al. 2008, Gupta, Leahul et al. 2015), sex determination (Starostina, Lim et al. 2007), pachytene-to-diplotene progression (Kisielnicka, Minasaki et al. 2018), and the oocyte-to-embryo transition (Pintard, Willis et al. 2003, Xu, Wei et al. 2003, Peel, Dougherty et al. 2012, Beard, Smit et al. 2016). In all above-mentioned contexts, cullin-based ubiquitin E3 ligases have been implicated. Hence, cullin-based multi-subunit ubiquitin ligases contribute significantly to regulation of germline development via proteasome-mediated degradation of germ cell proteins.

Although, the mitosis-to-meiosis decision is majorly regulated by Notch signaling and the network of RNA regulators including GLD-1, GLD-2, GLD-3, GLD-4 and NOS-3, the

proteasome contributes through protein degradation to achieve a fine-tuned balance of cell fates in the proliferative region. To facilitate proliferation (or mitosis), the proteasome promotes turnover of a cyclin-dependent kinase inhibitor 1 (CKI-1) and him-three paralogue 3 (HTP-3), a meiosis promoting factor, through the activity of Cul-2-based ubiquitin ligase (Merlet, Burger et al. 2010, Starostina, Simpliciano et al. 2010, Burger, Merlet et al. 2013). The proteasome also promotes degradation of the RNA regulator GLD-1 in proliferative cells through a yet to be identified ligase (Jeong, Verheyden et al. 2011). In contrast to promoting proliferation, the proteasome enhances a transition to meiosis by promoting the turnover of mortality factor-related gene 1 (MRG-1) (Gupta, Leahul et al. 2015). Therefore, through the activity of different regulatory ubiquitin ligase recognizing different protein targets, proteasome contributes to both proliferation and transition into meiosis.

The proteasome also regulates progression of germ cells from pachytene to diplotene during meiosis. A recent study demystified how the turnover of two translational regulators, GLD-1 and CPB-3, is coupled to meiotic progression. MPK-1 phosphorylates GLD-1 and CPB-3 at the pachytene-diplotene border. SEL-10, a substrate recognition subunit (SRS) of the CUL-1 ubiquitin ligase, binds phosphorylated forms of these RNA regulators and promote their proteasome-mediated degradation (Kisielnicka, Minasaki et al. 2018).

Furthermore, the proteasome also promotes oocyte-to-embryo transition. Two studies have shown the sequential requirement of proteasome for this transition. Once female meiosis is completed, the CUL-3-based ubiquitin ligase uses MEL-26 as its SRS to promote the turnover of MEI-1, which is essential for the formation of a meiotic spindle in an oocyte but compromises the formation of a mitotic spindle in a 1-cell embryo (Pintard, Willis et al. 2003, Xu, Wei et al. 2003, Beard, Smit et al. 2016). Also, the Polo-like kinase 4, ZYG-1, a factor regulating centrosome number must be removed. Here, the two F-box proteins, LIN-23 and SEL-10, act as SRS to reduce ZYG-1 levels, as part of CUL-1-based ligase complexes (Peel, Dougherty et al. 2012).

The contributions of the proteasome to embryonic germ cell development remain largely unexplored. So far, only one study showed that it contributes to embryonic germ cell specification during early embryogenesis, albeit, indirectly. The proteasome targets several germline determining factors in somatic blastomeres. To this end, ZIF-1, a SRS of a CUL-1 ubiquitin ligase binds several zinc-finger domain-containing proteins, including POS-1, PIE-1, MEX-1, MEX-5 and MEX-6 and promotes their turnover in soma (DeRenzo, Reese et al. 2003). This assist the exclusion of germ plasm from somatic lineages (DeRenzo, Reese et al. 2003). Therefore, proteasome indirectly contribute to embryonic germ cell development by terminating the expression of germline-enriched proteins in somatic blastomeres. In contrast to postembryonic stages of germline development, no single ubiquitin ligase or its protein target has been identified in *C. elegans* germ cell precursors and PGCs to regulate

embryonic germline formation. Therefore, the contribution of proteasome to PGC development remain completely elusive.

The requirement of proteasome for early stages in embryogenesis may have precluded a discovery of its potential contribution to PGC development. This is because relatively late stage phenotypes are often masked by earlier ones and early embryonic defects may lead to embryonic arrest. To circumvent its requirement for larval development and allow analysis of proteasome specifically in adult germline, an *in vivo* study successfully inhibited proteasome in young adult animals using the chemical inhibitor, MG132 (Orsborn, Li et al. 2007). However, since *C. elegans* embryos are a physically closed system with a chitinous shell, delivery of MG132 is a very difficult option. Therefore, this thesis used a partial RNA-mediated knockdown approach to analyze the importance of the proteasome in PGC development.

Several new aspects of proteasome functions were discovered: (i) the proteasome regulates the number of specified primordial germ cells (Figure 4.1.2A and C); (ii) it terminates the expression maternal proteins in PGCs including GLD-2 and GLD-3 (Figure 4.1.2A and B), limiting the activity of the GLD-2 cytoPAP complex to germ cell precursors; (iii) the proteasome promotes postembryonic germline development (most embryos that experience partial knockdown of proteasome developed into sterile adults even when returned to regular OP50 bacteria during postembryonic development) (Figure 4.1.1C); (iv) GRIF-1 was identified as a TRIM32-related ubiquitin ligase that promotes proteasomal degradation of GLD-2 protein. Together, the evidence presented in this thesis suggests that proteasome-mediated GLD-2 turnover may assist degradation of maternal transcripts during MZT in PGCs.

5.2. GRIF-1 is a novel E3 ligase that promotes GLD-2 turnover in *C. elegans* PGCs

The birth of PGCs coincides with many molecular and biological turning points. One of the key changes in nascent PGCs is the turnover of maternal proteins whose activities may be required earlier in germ cell precursors. So far, the molecular pathways that remove maternal proteins in *C. elegans* PGCs remained elusive. One implication of the finding that the proteasome regulates GLD-2 and GLD-3 in PGCs is that an E3 ubiquitin ligase(s) or ligase complex(es) may exist that links GLD-2 cytoPAP to the proteasome. Using GLD-2 as bait, a Y2H screen recovered GRIF-1, a TRIM32-related RING domain containing putative ubiquitin ligase, as a likely turnover factor of GLD-2.

In *C. elegans,* the functions of single subunit RING domain E3 ubiquitin ligases during germline development are not well characterized. This is in strong contrast to multisubunit RING domain ubiquitin ligases. As illustrated earlier, almost all described germline functions of proteasome have been linked to multimeric cullin-based ubiquitin ligases. There are over

152 single subunit RING domain-containing putative E3 ligases encoded by *C. elegans* genome. While some are TRIM proteins others are not. In either case, only a handful of these single subunit putative E3 ligases have been revealed to have specific functions in germ cell development (Boulton, Martin et al. 2004, Moore and Boyd 2004, Boulton 2006, Tocchini, Keusch et al. 2014, Gupta, Leahul et al. 2015). The individual disruptions of the genes encoding these single subunit RING domain ligases often reveal soma-specific but not germline-specific phenotypes, suggesting that while they are individually required in soma, a great deal of redundancies may exist for their germline functions (Jongeward, Clandinin et al. 1995, Hsieh, Liu et al. 1999, Gonczy, Echeverri et al. 2000, Schaefer, Hadwiger et al. 2000, Jones, Crowe et al. 2002, Kamath, Fraser et al. 2003, Simmer, Moorman et al. 2003, Moore and Boyd 2004). Alternatively, they may be involved only in germ cell-independent functions. This later possibility is quite unlikely given the unique spatiotemporal expression of many regulatory proteins, especially RNA regulators, that are critical for germ cell development.

GLD-2 interacting RING finger protein 1 (GRIF-1) is the first TRIM-type E3 ligase that is known to both demonstrate protein turnover role and regulate germline development. So far, at least three TRIM proteins have been demonstrated to be important for germline development. LIN-41 is a TRIM-NHL protein required for larval and oocyte development. However, mutation in RING finger domain of LIN-41 does not affect larvae and oocyte development, suggesting that its ligase activity is dispensable for LIN-41 functions and rather its RNA-regulatory NHL domains are important for larval and germline development (Spike, Coetzee et al. 2014, Tocchini, Keusch et al. 2014). Similarly, NCL-1, another TRIM-NHL protein, is a translational regulator that control nucleolar and germ cell size by binding and inhibiting the translation of the pre-rRNA processing factor, FIB-1/fibrillarin. (Yi, Ma et al. 2015). Lastly, NHL-2 is yet another TRIM-NHL protein in *C. elegans* important for germline development. Loss of *nhl-2* results in significant reduction in brood size. In molecular terms, NHL-2 binds RNAs with its NHL domain and modulates small RNA pathways (Davis, Tu et al. 2018). Several observations are common to these three described TRIM proteins. (1) They are expressed and exert their activities during postembryonic germ cell development. (2) They all regulate gene expression through RNA-binding activities. (3) The NHL repeats are implicated in RNA binding. (4) The expression levels of proteins known to interact with these TRIM proteins are not controlled by these three proteins. The identified interaction partners of these TRIM-NHL proteins are regulators that modulate expression and activities of the three TRIM proteins.

In contrast of the above-mentioned TRIM proteins, GRIF-1 binds GLD-2 and regulates the turnover of GLD-2 protein in PGCs. Several evidence and observations suggest that GRIF-1 regulates GLD-2 expression as a E3 ligase that connects GLD-2 to proteasome-mediated degradation (Figure 5.2). (1) GRIF-1 directly binds GLD-2 protein in

Y2H tests. (2) *In vivo* protein interaction was detected from embryos extract and when GRIF-1 was ectopically expressed, protein interaction was recapitulated in the germline in an RNA-independent manner. (3) GRIF-1 is specifically expressed at the time of GLD-2 turnover in PGCs. (4) GLD-2 expression is extended in *grif-1* compromised PGCs. (5) Partial removal of GRIF-1 binding site in GLD-2 protein led to a transient extended expression of GLD-2 in PGCs. (6) Ectopic expression of GRIF-1 led to lower levels of GLD-2 in adult germline. (7) GLD-2 degradation products accumulate in highly concentrated extracts of animals ectopically expressing functional GRIF-1. (8) The capacity of GRIF-1 to interact with and degrade GLD-2 is dependent on the RING domain; when ectopically expressed, a point mutation in its RING domain affects activity and interaction. (9) GRIF-1 lacks C-terminal NHL repeats required by TRIM-NHL proteins for RNA regulation. (10) GLD-2 protein expression but not *gld-2* mRNA level is regulated in PGCs by GRIF-1; *gld-2* mRNA levels remain unchanged in PGCs of *grif-1; nos-2* embryos. Together, these findings suggest that GRIF-1 may not be directly involved in RNA regulation. Instead, GRIF acts through its RING domain and may be a E3 ubiquitin ligase.
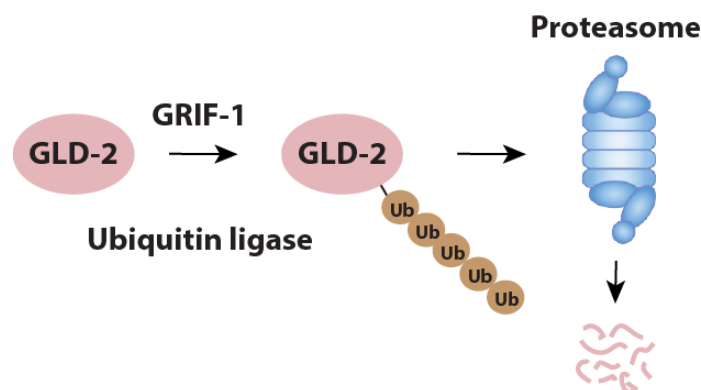
Figure 5.2. A model for GRIF-1-mediated proteasomal degradation of GLD-2 in PGCs
GRIF-1 binds GLD-2 and promote its proteasomal degradation in of GLD-2 protein in PGCs presumably through polyubiquitination.

In several ways, GRIF-1 is unique among TRIM32 protein family members. In addition to the loss of NHL domains, both the RING domain and the B-Box harbor a novel loop that is not observed in other TRIM32 family members (Figure 4.2.1B and C). It would be interesting to study the structure of these domains to determine whether GRIF-1 evolved this loop for a distinctive interaction with its targets or E2 proteins. Additionally, it is the first turnover factor described for cytoPAPs in any system. Furthermore, it is the first described E3 ligase and TRIM protein with expression and activity during PGC development. In all, several aspects of GRIF-1 protein are novel and GRIF-1 opens a distinct opportunity to study TRIM ubiquitin ligase during *C. elegans* germline development.

5.2.1. GRIF-1 is highly developmentally regulated

GRIF-1 protein has an intriguing and highly developmentally regulated expression pattern. Its expression is limited to the time of GLD-2 turnover in primordial germ cells. Upon birth of the germ cell precursor, P4, GRIF-1 protein is expressed and localizes to P granules. A strong correlation was observed between the presence of GLD-2 on P granules and recruitment of GRIF-1 to P granules. Once GLD-2 is terminated in PGCs, GRIF-1 dissociates from P granules and becomes entirely cytosolic until its expression is terminated by protein degradation in PGCs during late embryogenesis. But how is this intriguing and highly restricted expression pattern achieved?

Several layers of regulations may work to achieve this highly restricted expression pattern. Transcriptional regulation may preclude *grif-1* transcript expression in larvae (see Figure 4.5.1). Translational regulation of protein synthesis most likely prevents protein expression in oocytes and germ cell precursors, P1-P3. Furthermore, mRNA degradation terminates *grif-1* mRNA expression in somatic embryonic cells. This shows that several layers of regulations ensure that GRIF-1 protein is not prematurely produced from *grif-1* mRNA.

A very insignificant amount of GRIF-1 is detected during immunoblotting experiments using adult samples. Further analysis revealed that this signal may be due to both *in utero* embryos and background expression in oocytes. Incomplete translational repression of *grif-1* mRNA may result in residual or leaked GRIF-1 expression at an insignificant rate. This is consistent with inability of *grif-1's* 3'UTR to drive complete repression of a translation reporter in germ cells (Figure 4.5.2.2). Several studies have suggested that repression of translation is often incomplete and results in residual expression that may be insignificant for gene expression, although, residual expression may occasionally contribute to noise in gene expression (Komorowski, Miekisz et al. 2009, Hand and Bazzini 2017, Westbrook and Lucks 2017). The identity of RNA-binding proteins that repress *grif-1* 3'UTR remains to be determined.

Posttranslational modifications are known to trigger formation and localization of proteins to RNP granules including P granules. Once translated in P4, GRIF-1 protein localizes almost exclusively to P granules. Details of how GRIF-1 localizes to P granules is unknown. One particular modification that promote association with P granules is phosphorylation. During early embryogenesis, P granules are highly dynamic and undergo series of asymmetric partitioning into germ cell precursors. MBK-2 phosphorylate MEG-3/4 proteins to promote their association with and formation of P granules while PP2A pptr-1/-2 phosphatase dephosphorylate them to facilitate their dissociation (Wang, Smith et al. 2014, Chen, Cipriani et al. 2016, Smith, Calidas et al. 2016, Seydoux 2018). It is likely that a kinase phosphorylates GRIF-1 to facilitate its association with P granules. However, regulation of

146

protein localization to P granules in P4 when P granules are exclusively perinuclear and not highly dynamic, compared to early embryogenesis, has not been documented.

Another important mechanism that promotes P granule association is protein-protein interaction. For example, GLH-1 recruits PGL-1 to P granules (Kawasaki, Shim et al. 1998, Spike, Meyer et al. 2008) and similarly, IFET-1 recruits both RNA regulators, CGH-1 and CAR-1, to P granules (Sengupta, Low et al. 2013). Therefore, GRIF-1 may be dragged to P granules by other proteins, presumably, via its ubiquitination targets such as GLD-2. Consistent with this later possibility, upon PGC birth, at approximately 150-cell stage onwards, GRIF-1 protein begins to dissociate from P granules. This time correlates with complete removal of proteins that are degraded in nascent PGCs. By 500-cell stage, GRIF-1 is completely dissociated from P granules (see Figure 4.2.8). This observation suggests that localization of GRIF-1 to P granules may be primarily triggered by protein-protein interaction and recruitment rather than phosphorylation. However, contribution of phosphorylation cannot be excluded as both mechanisms are not mutually exclusive.

Lastly, the intriguing developmental regulation of GRIF-1 protein expression is terminated in PGCs by protein degradation. Upon complete dissociation from P granules, GRIF-1 forms small but distinct puncta in the cytoplasm which is the predominant form of GRIF-1 from 500-cell stage onward. GRIF-1 protein is completely degraded in PGCs prior to 3-fold stage of embryogenesis. The molecular pathways that promotes GRIF-1 protein turnover in PGCs during late embryogenesis remains to be determined. TRIM proteins, including TRIM32, have been observed to trigger self-ubiquitination *in vitro* and promote self-degradation *in vivo* (Yang, Fang et al. 2000, Kudryashova, Kudryashov et al. 2005, Wada and Kamitani 2006, Ichimura, Taoka et al. 2013). Similar to GRIF-1, human TRIM32 self-associates in the cytoplasm forming visible puncta. TRIM32 forms these puncta, named as cytoplasmic bodies (CBs), in the absence of target substrates to regulate its cytoplasmic levels (Albor, El-Hizawi et al. 2006, Locke, Tinsley et al. 2009, Ichimura, Taoka et al. 2013). Therefore, it is highly possible that GRIF-1 forms these cytoplasmic puncta after degradation of its targets and promotes self-degradation to complete the loop of its developmental regulation. Knowledge of GRIF-1 protein turnover mechanisms in late PGCs will give a vital insight into the intriguing developmental regulation of GRIF-1 protein expression.

Developmentally regulated activity of E3 ligase can be achieved through other mechanisms. In the case of GRIF-1, the expression was restricted to the time point of GLD-2 turnover. An alternative mechanism may be to synchronize protein degradation with biological events by post-translational modifications. Many E3 ubiquitin ligases such F-box proteins recognize only phosphorylated target substrates (Skaar, Pagan et al. 2013, Kisielnicka, Minasaki et al. 2018). This way, developmentally regulated protein turnover is

triggered by the activity of a kinase that phosphorylates the target protein at a specific time in development.

Spatial regulation can also allow developmental regulation of protein turnover. An E3 ligase can be spatially separated from its target proteins in the cell during development. In this manner, a nuclear target may be prevented at a particular developmental timepoint by sequestering the E3 ligase in the cytoplasm. Although used for developmental regulation across phyla, this mode of regulation is prevalent in by plants that undergo cycles of hot and cold weather during development. Heat triggers the translocation of E3 ligase into the nucleus to promote turnover of transcription factors (Qin, Sakuma et al. 2008, Yoshida, Sakuma et al. 2008, Lim, Cho et al. 2013).

In these two regulatory modes, the expression of the E3 ligases do not have to be restricted to a particular developmental stage. F-box proteins and several other SRS obligately recognize phosphorylated substrates. While substrate phosphorylation has been demonstrated as a requirement for recognition for a few TRIM ubiquitin ligases (Jain, Allton et al. 2014), substrate phosphorylation is not required for many, further strengthening the argument that recognition of GLD-2 and recruitment of GRIF-1 protein to P granules may not require phosphorylation. Therefore, similar to most TRIM E3 ligases, a highly restricted expression pattern may be necessitated for GRIF-1 to prevent a precocious degradation of target proteins. As evident by ectopic expression of GRIF-1, activity of GRIF-1 in the adult germline tissue led to developmental defects. Therefore, the tight developmental regulation of GRIF-1 expression is crucial to germ cell development.

5.2.2. Each domain of GRIF-1 appears crucial for GLD-2 interaction and turnover

GRIF-1 possesses at least four protein-protein interaction domains including a RING finger, a B-box and two coiled coil domains, any of which may be important for interaction and function. Using Y2H interaction tests, attempts were made to determine which part of GRIF-1 is required for binding to GLD-2. Although not without its limitations, Y2H assay is a common and versatile method used to map binding domains of two interacting proteins. However, it is important to keep in mind that β-gal reporter assays represent an indirect readout of robust interactions. It does not measure the amount of gene expression products as a result of transcription triggered by constituted transcription factor. Nonetheless, a robust β-gal signal indicates a likely robust interaction. This was the case when full-length GRIF-1 was co-expressed with full-length GLD-2. By contrast, perturbation of any of GRIF-1 domain significantly affected this interaction. Granted, removal of domains may affect overall fold of the protein without necessarily removing the interaction surface and thus affecting the conclusion of this experiment. However, point mutations that replaces either of the conserved cysteine 155 and 158 in the B-Box domain gave similar results (data not shown). This excludes that a domain deletion unnaturally changes the overall fold and consequently

affecting the interaction between GRIF-1 and GLD-2. These observations suggest that several domains including the B-Box are required for an optimal interaction with GLD-2. Overall, all domains of GRIF-1 protein may contribute either directly or indirectly to GLD-2 interaction. Therefore, a perturbation of any GRIF-1 domain affect interaction with GLD-2. Further structural studies may be required to address this problem.

How does each domain contribute to substrate recognition and ultimately to protein turnover in other TRIM proteins compared to GRIF-1? The RING domain of TRIM proteins is often required for interaction with the ubiquitin conjugating enzyme, E2, and for the transfer of ubiquitin from E2 to its target substrate. Other domains that are positioned in the C-terminal end of the RING domain including B-Box, coiled coil domain and the highly variable C-terminal domains have been described as critical for substrate recognition (Lorick, Jensen et al. 1999, Li, Song et al. 2007). In some cases, the highly variable C-terminal domain does not contribute to substrate recognition and ubiquitination. For example, C-terminal SPRY domain of TRIM25 and TRIM5alpha contributes to substrate recognition (Sanchez, Okreglicka et al. 2014, Yudina, Roa et al. 2015). However, RBCC domain of TRIM32 performs E3 ligase activity independently of its NHL repeats (Streich, Ronchi et al. 2013). Instead, the NHL repeats bind microRNA-loaded Ago-1 and regulate microRNAs independently of the ubiquitination function of RBCC domain (Neumuller, Betschinger et al. 2008, Schwamborn, Berezikov et al. 2009). Therefore, the observation that all domains, including the RING domain, are required for GLD-2 interaction is not exactly consistent with the canonical view of TRIM proteins.

Similar to GRIF-1, recent data on other TRIM proteins are challenging the canonical view that TRIM proteins act mostly as single proteins in which each domain function can be clearly separated from those of the other domain (Li, Yeung et al. 2011, Streich, Ronchi et al. 2013, Li, Wu et al. 2014, Sanchez, Okreglicka et al. 2014, Yudina, Roa et al. 2015, Koliopoulos, Esposito et al. 2016, Watanabe and Hatakeyama 2017). While RING domain is still viewed as indispensable for ubiquitin transfer, a more complex relationship and interactions have been recently shown to exist among TRIM protein domains (Li, Yeung et al. 2011, Streich, Ronchi et al. 2013, Li, Wu et al. 2014, Sanchez, Okreglicka et al. 2014, Yudina, Roa et al. 2015, Koliopoulos, Esposito et al. 2016, Watanabe and Hatakeyama 2017).

Most recent studies suggest that TRIM E3 ubiquitin ligases may form homomeric dimer to perform ubiquitination (Li, Wu et al. 2014, Yudina, Roa et al. 2015, Koliopoulos, Esposito et al. 2016, Dawidziak, Sanchez et al. 2017, Watanabe and Hatakeyama 2017). Higher order forms including oligomerization (up to heptamers) and multimerization have been also observed (Mische, Javanbakht et al. 2005, Javanbakht, Yuan et al. 2006, Napolitano and Meroni 2012, Yudina, Roa et al. 2015, Koliopoulos, Esposito et al. 2016).

While the oligomerization has been proposed to significantly improve ubiquitination (Sanchez, Okreglicka et al. 2014, Yudina, Roa et al. 2015, Koliopoulos, Esposito et al. 2016, Dawidziak, Sanchez et al. 2017), the implication of multimerization for E3 ligase activity remains speculative (Napolitano and Meroni 2012). Similar to TRIM32, several TRIMs have been shown to form cytoplasmic bodies (Reymond, Meroni et al. 2001, Campbell, Dodding et al. 2007). Cytoplasmic bodies may reflect the ability of TRIM proteins to self-associate or multimerize. Additionally, they may control local concentration of TRIM proteins in the cytoplasm by sequestering available cytoplasmic proteins (Ichimura, Taoka et al. 2013) but may also promote self-ubiquitination and degradation (Diaz-Griffero, Li et al. 2006).

In both TRIM25 and TRIM32, oligomerization facilitates interaction with substrates but also facilitate dimerization of RING domains (Koliopoulos, Esposito et al. 2016) RING dimerization has been proposed to be the critical factor that significantly improves ubiquitination activities (Yudina, Roa et al. 2015, Koliopoulos, Esposito et al. 2016, Dawidziak, Sanchez et al. 2017). Occasionally, TRIM proteins form a heteromeric dimer with other TRIM proteins. Heterodimerization has been proposed to occur only between highly related or similar TRIM proteins and not in a promiscuous manner (Goldstone, Walker et al. 2014, Sanchez, Okreglicka et al. 2014, Watanabe and Hatakeyama 2017).

Regardless of homomeric or heteromeric association, the overall 3-dimensional fold of the dimer contributes to ubiquitination of target proteins. Homo or hetero-dimer formation is often promoted by antiparallel interaction between coiled coil domains of the two monomers (Sanchez, Okreglicka et al. 2014, Koliopoulos, Esposito et al. 2016). The remaining available surface in the C-terminal end contribute to substrate recognition. Additionally, while the RING domains of the dimer interact with E2 enzymes, B-Box domains may facilitate the function of RING domains or contribute to substrate recognition. In this manner, perturbation of any part of the RBCC domain may affect both substrate recognition and ubiquitination reaction (Sanchez, Okreglicka et al. 2014, Koliopoulos, Esposito et al. 2016). Therefore, it is likely that full-length GRIF-1 may self-associate to form a dimer before an optimal interaction with GLD-2 is possible and removal of any of the domains may either affect self-association or GLD-2 interaction, or both. Since GRIF-1 has two predicted coiled coil domains, one may be involved in dimerization while the other participate as part of substrate interaction module. It would be interesting to study the 3D structure of GRIF-1 in the nearest future to determine how its structure contribute to GLD-2 interaction and a likely dimer formation. Together, GRIF-1 domains seem to work cooperatively for GLD-2 interaction.

If GRIF-1 domains were to work cooperatively, perturbation of any of the domains will significantly affect GRIF-1's *in vivo* functions. Interestingly, *grif-1(ok1610)* contains a deletion that predominantly affects the second coiled coil domain (CC2); it removes eleven amino

acids in CC1, and almost the entire CC2 domain. The truncated protein containing the RING, B-Box, and almost intact CC1 domains is expressed at a comparable level to wild-type GRIF-1 protein. However, *grif-1(ok1610)* displayed molecular and biological phenotypes that were very similar to null mutants such as *grif-1(ok1610ef40)* and *grif-1(ef32)*: (i) GLD-2 is stabilized to a similar extent throughout embryogenesis in all the three mutant strains, and (ii) either mutant displays transgenerational sterility at 25°C to similar extents. These shows that CC2 domain is crucial to *in vivo* functions

Furthermore, an interaction between GRIF-1[ok1610] and full-length GLD-2 was tested in Y2H test. The obtained result, which is consistent with those obtained when only the CC2 domain was removed, shows that a likely interaction with GLD-2 is significantly affected (data not shown). This shows that the CC2 domain may contribute significantly to GLD-2 interaction. Similarly, when ectopically expressed, a point mutation in the RING domain significantly abrogated GRIF-1 activity in the adult germline and compromised its interaction with GLD-2. In conclusion, contrary to canonical views, all domains of TRIM proteins seem to have coevolved to behave as an integrated module and not as independent units. Similarly, all GRIF-1 domains may contribute synergistically to interaction with substrate and ultimately, to GRIF-1 function.

5.2.3. N-terminal IDR connects GLD-2 to developmentally regulated turnover in PGCs

Intrinsically disordered regions (IDRs) in proteins serve as regulatory and protein-protein interaction platforms in many proteins. In GLD-2, the function of the N-terminal IDR remains elusive. Intriguingly, there are at least two splice form of the *gld-2* transcript; the germline-specific full-length *gld-2* transcript and the soma-specific shorter transcripts that lacks the GLD-2 IDR (Wang, Eckmann et al. 2002). This suggests that the N-terminal GLD-2 IDR may not contribute to catalytic activity. Instead, in germ cells, GLD-2 IDR may be an interaction surface that serves a regulatory function to control either the GLD-2 cytoPAP activity or developmental expression or both. Consistent with these hypotheses, GLD-2's IDR provides a likely GRIF-1 binding surface. Although further experiments are required, accumulating evidence from this work suggest that the N-terminal IDR is not significantly required for GLD-2 postembryonic germline function. Instead, it may be required in PGCs for regulation of GLD-2 developmental expression.

To date, this study connects for the first time any cytoPAP to proteasome degradation. Therefore, limited knowledge on how cytoPAPs are recognized by E3 ligases and submitted to proteasome-mediated degradation exists. Nonetheless, accumulating evidence suggest that IDR may be required in many proteins for ubiquitin-dependent and ubiquitin-independent proteasome degradation (This is reviewed here (Suskiewicz, Sussman et al. 2011, Erales and Coffino 2014)). One paradigm is that their disordered nature allows

for IDRs to adopt multiple folds and conformations (Johnson, Xue et al. 2012, Van Roey, Uyar et al. 2014, Guharoy, Bhowmick et al. 2016, Guharoy, Bhowmick et al. 2016, Niemeyer, Moreno Castillo et al. 2020). This in turn permits them to interact with a vast array of proteins, including E3 ligases. IDRs often immediately adopts 3D folds upon binding to ligases (Van Roey, Uyar et al. 2014, Guharoy, Bhowmick et al. 2016, Guharoy, Bhowmick et al. 2016, Niemeyer, Moreno Castillo et al. 2020). Additionally, IDRs tend to have easily accessible sites containing amino acids that can be modified. Therefore, most E3 ligases that bind IDRs also often have ubiquitination site in the proximity of their binding sites (Guharoy, Bhowmick et al. 2016, Guharoy, Bhowmick et al. 2016, Niemeyer, Moreno Castillo et al. 2020).

IDRs may also facilitate ubiquitin-independent protein turnover. Several proteins have been shown to be targeted to proteasome through direct binding of IDR of target proteins to proteasome without ubiquitin attachment. Examples of proteins degraded in this manner include p53 (Asher, Lotem et al. 2002, Asher, Tsvetkov et al. 2005, Tsvetkov, Reuven et al. 2010), p21 (Chen, Barton et al. 2007), p73 (Asher, Tsvetkov et al. 2005), c-Jun (Jariel-Encontre, Pariat et al. 1995), alpha-synuclein (Tofaris, Layfield et al. 2001), HIF-alpha (Kong, Alvarez-Castelao et al. 2007), eIF3 and eIF4 (Baugh and Pilipenko 2004). In rare cases, proteasome degradation of proteins bearing IDRs may be ligase-dependent but ubiquitin-independent (Jin, Lee et al. 2003, Kalejta, Bechtel et al. 2003, Kalejta and Shenk 2003, Sdek, Ying et al. 2005). In short, ubiquitin-independent proteasome degradation seems to be a common feature of IDPs.

Furthermore, IDRs have also been shown to predispose IDPs to attack by proteases *in vitro* (Fontana, de Laureto et al. 2004). However, presence of IDRs in proteins may only significantly increase unregulated decay rate *in vivo* when IDRs are not sequestered by other proteins (Suskiewicz, Sussman et al. 2011). GLD-2 IDR connects GLD-2 to proteasome by interacting with GRIF-1, presumably through ubiquitination. Whether ubiquitin-independent turnover and cytosolic protease attacks also contribute to the gradual decay of GLD-2 protein observed in late-stage PGCs of *grif-1* mutant embryos is unknown.

5.2.4. Additional E3 ubiquitin ligases promote proteasome degradation of GLD-2 cytoPAP

GLD-2 expression is terminated both in soma and PGCs. Similar to PGCs, analysis of early embryos revealed that knockdown of proteasome factors also led to prolonged expression of GLD-2 cytoPAP complex in somatic blastomeres. Several observations suggest that proteasome-mediated turnover in soma is GRIF-1-independent. (1) It is envisaged that elevated, mis-regulated or that continued GLD-2 cytoPAP expression in soma during early embryogenesis may affects somatic development or embryogenesis (Elewa,

Shirayama et al. 2015). *grif-1* loss does not affect somatic development. (2) Perturbation of *grif-1* led to extended expression of GLD-2 cytoPAP in PGCs but not in soma. (3) Most importantly, immunofluorescent analysis shows that GRIF-1 protein is specifically expressed in embryonic germ cell lineage; P4 and PGCs but not in soma. These suggest that a yet to be identified E3 ubiquitin ligase(s) target residual GLD-2 protein that is detected in somatic sister for proteasome degradation. Alternatively, similar to other P granule components (Zhang, Yan et al. 2009, Kaushik and Cuervo 2012), GLD-2 may also be degraded by autophagy in somatic cells.

In PGCs, GRIF-1 promotes GLD-2 turnover. However, a gradual reduction in GLD-2 levels is still noticeable in *grif-1* null mutants. In *grif-1* embryos, GLD-2 levels and localization in nascent PGCs is comparable to P4. By 500-cell stage, GLD-2 levels stay high and GLD-2 is completely dissociated from P granules and entirely cytosolic. The reason for this change in localization remain elusive. A possibility is that proteins or modifications that recruit GLD-2 cytoPAP to P granules may be removed at this stage in these PGCs in a *grif-1*-independent manner. Alternatively, this observation may reflect changes in mRNA regulation dynamics or a switch from maternal to zygotic program. All these possibilities are not mutually exclusive. However, from 500-cell stage onward, levels of cytosolic GLD-2 was observed to diminish gradually. At hatching, only extremely low levels of cytosolic GLD-2 are visible. These observations suggest that a residual degradation of GLD-2 still occurs in *grif-1* null mutants. It is possible that GLD-2 may be inefficiently targeted for degradation in *grif-1* mutants by another E3 ligase that may or may not be a heterodimeric complex member. Alternatively, the gradual reduction may reflect the natural decay rate of GLD-2 protein at all stages of development that may not require developmental regulation. Possibly, GLD-2 production ceases at this stage and background decay catches up without additional protein production. Nonetheless, the data suggest that proteasome regulates the expression of GLD-2 in both soma and germ cells. While GRIF-1 is the key GLD-2 turnover factor in PGCs, a different E3 ligases may link GLD-2 to the proteasome in soma.

5.3. *grif-1* regulates germ cell development

What is the biological contribution of GRIF-1 protein to germ cell development? To explore the biological role of GRIF-1 during germ cell development for fertility, the brood size sired by *grif-1* animals were assessed at different temperatures. At both 20°C and 25°C, fertility of *grif-1* animals decreases across generation. However, *grif-1* animals reached complete sterility faster or at earlier generations at 25°C compared to 20°C. The germline phenotypes associated with *grif-1* loss include proliferation defect, differentiation defect and germline survival phenotype. This shows *grif-1* loss causes a mortal germline phenotype that kicks in earlier at elevated temperature.

Germ cell immortality and germline survival are two highly related terms but with distinct meanings. Mutations affecting germline immortality cause a progressive loss of fertility across generation which eventually terminates with complete sterility; a phenotype referred to as mortal germline phenotype. This implies that germ cells, which are by nature immortal; they are able to support fertility across an infinite number of generations, now become "mortal" (Ahmed and Hodgkin 2000, Buckley, Burkhart et al. 2012, Svendsen, Reed et al. 2019, Weiser and Kim 2019). By contrast, mutations affecting germline survival cause postembryonic germ cells to experience cell death in a manner that is independent of the *ced-3* and *ced-4* apoptotic pathways. Therefore, while mortal germline phenotype describes fertility defects which may be accompanied by varying germline defects, germline survival describes germline/germ cell defects (Subramaniam and Seydoux 1999, Eckmann, Kraemer et al. 2002, Leacock and Reinke 2008, Kapelle and Reinke 2011, Mainpal, Nance et al. 2015, Lee, Lu et al. 2017).

Reaching complete sterility faster at elevated temperature is fairly common in mutant animals that display mortal germline phenotype. Several reasons may cause this temperature sensitivity. Increase in temperature may be an additional source of stress that tilts the whole system leading to earlier downstream molecular phenotypes that may cause early sterility. It is known that germ cell development is inherently sensitive to increasing temperature in many systems including *C. elegans*. The reproductive capacity of *C. elegans* decreases with increasing temperature. Therefore, in certain single mutants, heat stress may affect redundant pathways that may protect germ cells in these single mutants at 20°C (lower temperature). Alternatively, molecular processes regulated either directly or indirectly by genes that maintain germ cell immortality may be sensitive to temperature. These two possibilities are not mutually exclusive. For example, in *grif-1* embryos, it is possible that maternal transcripts may be stabilized to equal extents at both temperature but more protein is produced from these maternal transcripts at elevated temperature. Consistent with this possibility, the number of embryos transiently expressing POS-1 and PIE-1 in *grif-1* PGCs increases at 25°C compared to 20°C (see Figure 4.3.7).

Several observations suggest that an increase in the number of *grif-1* with extended PIE-1 and POS-1 expression at elevated temperature may be directly due to prolonged GLD-2 in *grif-1* PGCs. (1) PIE-1 does not co-purify with GRIF-1 in co-IP experiments, demonstrating that prolonged expression of PIE-1 is not due to direct GRIF-1-mediated protein turnover of PIE-1; (2) In the sequencing data, *pie-1* expression is upregulated (1.8 times more) in PGCs of *grif-1; nos-2* compared to wild type; control(RNAi) but in not *nos-1; nos-2,* suggesting that upregulation of *pie-1* transcript is due to *grif-1* but not *nos-2*. Unfortunately, *pos-1* transcript was not detected in all samples precluding the analysis of *pos-1* mRNA. *pos-1* mRNA may be expressed at low levels to the extent that it is not

captured in either tests or control samples   (3) Both *pie-1* and *pos-1* transcripts are dependent on GLD-2 for stability in the adult germline (Nousch, Yeroslaviz et al. 2014). Therefore, it is envisaged that prolonged GLD-2 leads to prolonged expression of maternal transcripts including *pie-1* and *pos-1*. An increase in temperature may further delay the turnover of many maternal transcripts or increase their translation leading to more maternal proteins. Therefore, the event controlled by any or multiple of these maternal proteins may reach a threshold required to cause sterility earlier at 25°C degrees compared to 20°C.

5.3.1. GRIF-1 is a novel regulator of germ cell immortality

Factors that regulates germ cell immortality can be categorized into three gene categories. These include factors that regulate epigenetics, factors that regulate small RNAs, and factors that maintain checkpoints and genome integrity (Ahmed and Hodgkin 2000, Katz, Edwards et al. 2009, Buckley, Burkhart et al. 2012). The molecular mechanisms via which they regulate germ cell immortality involve a complex interplay between these three gene categories. For example, the *set-25/32* chromatin regulators act downstream of small RNAs (siRNAs and piRNAs) to establish a heritable memory leading to transgenerational regulation of gene expression (Ashe, Sapetschnig et al. 2012).

At least two genes that do not belong to these three categories have been identified to regulate germ cell immortality. SUP-46 is required to prevent temperature-dependent sperm-mediated transgenerational sterility in hermaphrodites (Johnston, Krizus et al. 2017). The molecular mechanism via which it regulates germ cell immortality is not completely understood. SUP-46 is a RBP that belong to the hnRNPM family (Johnston, Krizus et al. 2017). SUP-46 is ubiquitously expressed during germline development. Human homologues of SUP-46 associates with multiple proteins that regulate non-coding RNAs. Since many proteins that regulate small RNAs have sperm-specific transgenerational phenotypes, it is highly likely that SUP-46 associate with these factors to regulate germ cell immortality (Johnston, Krizus et al. 2017).

Another gene family that does not belong to previously listed three gene category that was recently shown to regulate germ cell immortality is polyU polymerase family (Li and Maine 2018). Animals devoid of both *pup-1* and *pup-2* lose fertility across generation in a temperature-dependent manner. Again, details of the pathways regulated by PUPs remain elusive (Li and Maine 2018). Since PUPs in other model systems have been shown to regulate microRNA biogenesis and expression (Shen and Goodman 2004, Heo, Joo et al. 2009, Thornton, Du et al. 2014, Kim, Ha et al. 2015, Faehnle, Walleshauser et al. 2017), It is likely that PUPs may regulate germ cell immortality by regulating the levels of small RNAs. Alternatively, *C. elegans* PUPs may target mRNAs (Morgan, Much et al. 2017, Morgan,

Kabayama et al. 2019) encoding epigenetic factors causing transgenerational heritable memory that results in sterility. Therefore, similar to SUP-46, PUPs may indirectly regulate germ cell immortality in either small RNA-dependent or small RNA-independent manner or both. Asides from these two instances outside those three gene categories, GRIF-1 is the first E3 ligase implicated in regulating germ cell immortality. Therefore, it presents a new layer to our understanding of germ cell immortality.

5.3.2. *grif-1* and *nos-2* redundantly promote PGC development

Nanos/Pumilio complex regulates numerous aspect of germ cell development in several systems (Kraemer, Crittenden et al. 1999, Koprunner, Thisse et al. 2001, Jaruzelska, Kotecki et al. 2003, Weidmann, Qiu et al. 2016). In worms, fruit fly, zebrafish, and frog, Nanos regulates almost identical aspects of primoridial germ cell development. These include PGC division, incorporation of PGCs into somatic gonads, epigenetic regulation, and survival of PGCs (Subramaniam and Seydoux 1999, Koprunner, Thisse et al. 2001, Schaner, Deshpande et al. 2003, Lai, Singh et al. 2012). Nanos and Pumilio bind to mRNAs and promote mRNA repression and degradation. To achieve this, the complex recruits CCR4-Not deadenylase complex which trims polyA tail of target transcripts (Kadyrova, Habara et al. 2007, Suzuki, Igarashi et al. 2010).

C. elegans Nanos proteins, NOS-1 and NOS-2, are expressed specifically in embryonic PGCs and are maternally required to promote postembryonic germ cell development. Germ cells devoid of both maternal NOS-1 and NOS-2 experience cell death during larval development (Subramaniam and Seydoux 1999). These NOS proteins were recently shown to promote clearance of oocyte-derived transcripts in PGCs (Lee, Lu et al. 2017). Similar to NOS proteins, GRIF-1 is also expressed in PGCs and is maternally required to promote germline immortality and postembryonic survival of germ cells. Therefore, a likely synergism or interaction among *grif-1*, *nos-1* and/or *nos-2* was tested genetically. Intriguingly, *grif-1* promotes postembryonic germ cell development redundantly with *nos-2* but not *nos-1.* This observation suggests that *grif-1* and *nos-2* function in redundant pathways controlling PGC development.

Several probable causes may account for lack of interaction with *nos-1*: (i) the lack of interaction between *grif-1* and *nos-1* and their mutual synergistic interaction with *nos-2* suggest that *grif-1* and *nos-1* may function in the same genetic pathway having overlapping but not necessarily identical functions with *nos-2;* (ii) *nos-1* and *nos-2* may have distinct but synergistic roles in maternal mRNA turnover, providing the likelihood of differential interaction with either gene. The sterility penetrance of *grif-1; nos-2* animals is higher than those of *nos-*

1; nos-2 animals, suggesting that *grif-1* rather has more encompassing function with *nos-2*. Interestingly, and consistent with the later hypothesis, a further removal of *nos-1* in *grif-1; nos-2(RNAi)* animals increases the sterility penetrance to almost 100 %; >99 %, fertile worms are rarely observed. This suggests that these three genes may have distinct and redundant roles in PGC development.

A possibility of distinct roles for these redundant genes is highly feasible. In molecular terms, that *nos-1* and *nos-2* do not simultaneously promote maternal transcript clearance as they are sequentially expressed. It is highly possible that NOS-2 may initiate transcript clearance and "handover" to NOS-1 for completion. Alternatively, despite the sequential expression, *nos-1* and *nos-2* may regulate distinct sets of maternal transcripts with some overlap. In both scenarios, a synergism is possible with one of the factors without the other.

Differential interaction with *nos-1* and *nos-2* is not peculiar to *grif-1.* X̲ chromosome n̲o̲n̲d̲isjunction factor 1 (*xnd-1*) is chromatin associated and abundantly expressed during post embryonic germline development. It is zygotically required to regulate global recombination landscape during meiosis (Wagner, Kuervers et al. 2010) and maternally required for PGC development (Mainpal, Nance et al. 2015). Analogous to *grif-1, xnd-1* regulates postembryonic germline survival in combination with *nos-2* but not *nos-1;* <10 %, 57 % and 98 % sterility were observed in progenies of *xnd-1* single mutant, *xnd-1; nos-2* double mutants and *nos-1; nos-2; xnd-1* triple mutants, respectively (Mainpal, Nance et al. 2015)*.* Therefore, comparable to the *grif-1* scenario, *xnd-1* and *nos-1* have unique roles which overlap with *nos-2.*

Similar to GRIF-1 and NOS-2*,* the expression of maternal XND-1 protein is activated in germ cell precursor, P4, from a maternally donated mRNA. However, unlike GRIF-1 and NOS-2 which are cytosolic proteins, XND-1 has nuclear localization and is chromatin-associated. Therefore, XND-1 may directly regulate transcriptional program in nascent PGCs. This transcriptional program may distinctively interact with *nos-1* and *nos-2* due to their differential effect or activity for mRNA turnover. since NOS-2 expression precedes NOS-1, NOS-2 may be the major player while NOS-1 may be an accessory protein required in order to increase efficiency of NOS-2 maternal transcript clearance turnover by degrading leftover maternal transcripts. GRIF-1 may indirectly promote the turnover of maternal transcript by promoting the turnover of RNA-stability factor, GLD-2.

What is the molecular mechanism via which GRIF-1 promotes PGC development and what is the relationship with the NOS proteins? One key potential molecular mechanism is that GRIF-1 may indirectly enhance maternal transcript clearance by promoting GLD-2 turnover. In this scenario, prolonged GLD-2 expression may cause continued expression of GLD-2 maternal target mRNAs in PGCs of *grif-1*; *nos-2* embryos. Therefore, maternal mRNAs may be stabilized due to both *nos-2* activity and GLD-2 stability effects. To test this

hypothesis, mRNA abundance were analyzed in PGCs of wildtype; control(RNAi), *nos-1; nos-2(RNAi),* and *grif-1; nos-2(RNAi)* embryos. Consistent with previous study (Lee, Lu et al. 2017), this work observed upregulation of many maternal transcripts in *nos-1; nos-2(RNAi)* compared to wildtype; control(RNAi). Additionally, almost twice as much transcripts were upregulated in *grif-1; nos-2(RNAi).* Fewer gene were downregulated in PGCs of both *nos-1; nos-2(RNAi)* embryos and *grif-1; nos-2(RNAi)* embryos compared to respective upregulated genes, suggesting that downregulation of these genes may be due to indirect effects. Therefore, similar to *nos-1* but with more encompassing effects, *grif-1* promotes maternal mRNA turnover in PGCs

Interestingly, there is a strong overlap between maternal transcripts that are upregulated in *nos-1; nos-2* PGCs and *grif-1; nos-2* PGCs (see Figure 4.7.3.4)*.* These observations show that a reasonable overlap may exist in the transcripts regulated by *grif-1* and *nos-1.* Based on the higher number of maternal transcripts stabilized in *grif-1; nos-2* PGCs compared to *nos-1; nos-2* PGCs, *grif-1* seems to have a broader impact on maternal transcripts compared to *nos-1.* This is consistent with more penetrant and expressive sterility and phenotypes observed in the progenies of *grif-1; nos-2* animals compared to those of *nos-1; nos-2* animals. Importantly, the correlation of the number of stabilized transcripts to the penetrance of sterility and phenotypes suggest that expression of several of these transcripts, rather than a single transcript, lead to germline survival phenotype.

Is the upregulation of some of the maternal transcripts in *grif-1; nos-2* embryos due to extended GLD-2 expression? A simple approach to solve this problem is to induce the degradation of GLD-2 protein specifically in the PGCs of *grif-1; nos-2* embryos. However, this is a technically challenging experiment in *C. elegans* embryo. Therefore, the behavior of previously-identified GLD-2-associated transcripts were analyzed (Kim, Wilson et al. 2010). While GLD-2-associated transcripts are not significantly affected in *nos-1; nos-2* PGCs, they are significantly upregulated in *grif-1; nos-2* PGCs, which strongly suggest that maternal transcripts may be stabilized due to prolonged GLD-2 cytoPAP expression. Therefore, *grif-1* may regulate maternal transcripts and germ cell immortality and survival through GLD-2 turnover.

Delayed maternal program may indirectly affect zygotic genome activation (ZGA) causing either significant reduction in amount of transcripts produced (Siddiqui, Li et al. 2012, Lee, Lu et al. 2017). Further analyses were performed to determine whether the downregulated transcripts of *grif-1; nos-2* PGCs belong to either oocyte-expressed, sperm-expressed or neutral gene category (Figure 4.7.3.4). These analyses revealed that, unlike upregulated transcripts which were significantly enriched for oocyte-expressed genes, oocyte-expressed genes were underrepresented in genes that are downregulated in PGCs of *grif-1; nos-2* embryos, suggesting that the downregulated genes are not maternal mRNAs.

Since embryonic PGCs undergo a minor wave of zygotic transcription upon their birth, a good number of these transcripts may be zygotically produced in wild-type PGCs (Kawasaki, Shim et al. 1998, Spencer, Zeller et al. 2011, Mainpal, Nance et al. 2015). Therefore, their downregulation in *grif-1; nos-2* PGCs may be an indirect effect of delayed maternal program on zygotic genome activation. More proteins may be produced from upregulated maternal transcripts which may interfere with zygotic program.

Several gene families are represented in the downregulated transcripts. Whereas many of the downregulated genes are unknown and uncharacterized, several of them are known for either direct or indirect epigenetic regulation or small RNA biogenesis, regulation and maintenance: at least 5 of the 134 downregulated transcripts are known to be involved in small RNA and epigenetic regulation. Interestingly, lowering the cut-off from 2.5-fold change to 1.5-fold adds another 7 transcripts, making a total of 13. These include *prg-2, prde-1, nrde-2, wago-2, set-32, mes-2, parn-1, set-5, set-23, prmt-7, glh-1, glh-4, pgl-2.* This indicates that the expression of genes that regulate either small RNA or epigenetics, or both, is affected in PGCs of *grif-1; nos-2* embryos.

Remarkably, several genes itemized above have been linked with either transgenerational sterility including *glh-1, set-32,* and *nrde-2* (Spracklin, Fields et al. 2017, Woodhouse, Buchmann et al. 2018) or germline survival phenotype such as *mes-2* (Garvin, Holdeman et al. 1998, Holdeman, Nehrt et al. 1998). Other genes that do not belong to the categories of genes that regulate either small RNA or epigenetics but whose loss have been demonstrated to contribute to either mortal germline phenotype or germline survival phenotype, such as *rfs-1* (a paralogue of the genome integrity regulator, *rad-51*) (Yanowitz 2008) and *puf-8* (Subramaniam and Seydoux 1999), were also downregulated. Therefore, although due to indirect consequence, the reduction of any or all of these transcripts may contribute to mortal germline phenotype in *grif-1* animals and germline survival phenotypes in *grif-1; nos-2* animals. Together, similar to previous studies ((Siddiqui, Li et al. 2012, Lee, Lu et al. 2017)), the data suggest that delay in maternal transcript turnover in *grif-1; nos-2* PGCs may affect zygotic genome activation. This may be further explored in the future to definitively determine the impact of delayed maternal program on zygotic transcription.

5.4. Prolonged GLD-2 expression in PGCs contributes to phenotype in *grif-1* and *grif-1; nos-2* animals

The upregulation of GLD-2-associated mRNAs in *grif-1; nos-2* but not *nos-1; nos-2* PGCs strongly suggests that their upregulation: (i) is mostly due to *grif-1* and not *nos-2,* (ii) may be largely due to prolonged GLD-2 expression. If these were true, then it is expected that prolonged GLD-2 expression in *grif-1* mutants contributes significantly to both sterility and other germline phenotypes in both *grif-1* and *grif-1; nos-2* animals. To test this

hypothesis, transgenic animals either lacking the first 197 or 266 amino acid of GLD-2 were generated. Deletion of the first 197 or 266 amino acids of GLD-2 proteins removes part of the IDR that is required and sufficient for GRIF-1 interaction in Y2H tests. Transgenic strains expressing these N-terminally truncated GLD-2 proteins are fertile but produce slightly lower number of progenies compared to wild type. This suggest that this N-terminal part of GLD-2 only marginally contributes to and is largely dispensable for postembryonic germline roles of GLD-2 cytoPAP.

The rescue of *gld-2(null)* phenotypes by these transgenically provided N-terminally truncated GLD-2 protein is consistent with a recent study that proposed that the primary aspect of GLD-2 function is polyadenylation which is largely dependent on the central catalytic domain and GLD-3 interaction (Nousch, Minasaki et al. 2017). Nonetheless, a slight reduction in brood size suggest that this N-terminal part may serve regulatory function in the germ line. For example, a yet to be identified or described RBPs may bind the N-terminal end to recruit GLD-2 cytoPAP to specific mRNAs during germline development. Future studies may reveal novel RBPs or regulatory proteins that control the postembryonic germline function of GLD-2 cytoPAP.

Intriguingly, the expression of transgenic N-terminally truncated GLD-2 is transiently extended in PGCs. However, unlike in *grif-1* embryos in which GLD-2 is extended throughout embryogenesis, transgenic N-terminally truncated GLD-2 is degraded in PGCs prior to 300-cell stage. Y2H experiments suggest that the entire GLD-2 IDR is required for optimal interaction with GRIF-1. Since the deletion of first 266 amino acids does not remove the entire IDR, it is likely that the interaction between the transgenic N-terminally truncated GLD-2 protein and GRIF-1 is perturbed but not completely abolished. Consistent with this hypothesis, knockdown of *grif-1* in these transgenic animals leads to additional extension of transgenic truncated GLD-2 protein (data not shown), demonstrating that the eventual turnover of truncated GLD-2 is still GRIF-1-dependent.

Given that at least a transient extended expression in PGCs was achieved, these strains were analyzed for transgenerational sterility. Interestingly, transgenic animals expressing truncated GLD-2 sired reduced progenies across generations and displayed germline phenotypes similar to those displayed by *grif-1* mutants. Noteworthy, transgenic animals expressing N-terminally truncated GLD-2 do not display the same levels of severity as *grif-1* mutants. This less severe mortal germline phenotype correlates with the very transient nature of extended GLD-2 expression in PGCs of transgenic animals expressing truncated GLD-2 compared to *grif-1* mutants in which GLD-2 is extended in PGCs throughout embryogenesis. Further truncations of GLD-2 will be analyzed in future. Regardless, these data suggest that prolonged GLD-2 expression in PGCs contributes significantly to mortal germline phenotypes displayed by *grif-1* mutants. Again, this is the first study that links

dysregulation of polyA tail controlling factors directly to mortal germline phenotype in *C. elegans.* Prolonged GLD-2 expression may also contribute to germline survival phenotype in *grif-1; nos-2* animals. RNAi-mediated knockdown of *nos-2* into transgenic animals expressing truncated GLD-2 led to sterility and germline survival phenotype in offspring of treated animals. Therefore, similar to mortal germline phenotype, extended GLD-2 expression contributes significantly to germline survival phenotype in *grif-1; nos-2* animals.

GLD-2 may regulate epigenetic or small RNA pathways prior to PGC birth and continued expression may lead to overexpression of those epigenetics regulators or small RNA regulators. Alternatively, extended GLD-2 might cause a delay in maternal programs, which in turn may indirectly affect ZGA causing perturbation or reduction in the expression levels of epigenetic regulators or small RNA regulators. Therefore, extended GLD-2 expression in PGCs of *grif-1* embryos may affect small RNA pathways or epigenetic landscape leading to transgenerational defects in *grif-1* and contributes to germline survival defects in *grif-1; nos-2*. Since several transcripts encoding components of small RNA pathways and epigenetics are dysregulated in *grif-1; nos-2* PGCs, the effect of this dysregulation and contribution towards sterility of *grif-1; nos-2* animals will be examined in future experiments.

In wild type, SPR-5 removes the H3K4me2 mark upon PGC birth. Loss of *spr-5* leads to mortal germline phenotypes (Katz, Edwards et al. 2009). Therefore, GLD-2 may promote the expression of factors that inhibit the activities of *spr-5* in germ cell precursors. In this scenario, prolonged GLD-2 expression may limit SPR-5 activities in PGCs leading mortal germline phenotype. This possibility is also true for *mrg-1* that is required for regulation of H3K4me2 and H4K16ac in PGCs (Takasaki, Liu et al. 2007, Miwa, Inoue et al. 2019). Consistent with this hypothesis, H3K4me2 accumulates in PGCs of *nos-2, xnd-1, nos-1; nos-2* and *xnd-1; nos-2* mutants. Importantly, this accumulation strongly corelates with penetrance sterility in these animals. Time constraint and tool availability did not permit analysis H3K4me2 accumulation in the PGCs of *grif-1* and *grif-1; nos-2* animals. Together, all observations show that GLD-2 cytoPAP is the primary target that links GRIF-1 to germ cell immortality and germline survival phenotype.

5.5. GLD-2 cytoPAP directly promotes the maternal gene expression program.

5.5.1 GLD-2 promotes the maternal program gene expression during early embryogenesis

The time-resolved nature of maternal gene expression program is critical for both somatic and germ cell development. This implies that maternal program must be initially promoted by certain factors. The observation that many maternal mRNAs may be stabilized in a GLD-2-

dependent manner in *grif-1; nos-2* PGCs alludes to the fact that GLD-2 may drive maternal gene program prior to zygotic transcription.

Intriguingly, several findings in this study support the fact that the GLD-2/GLD-3 cytoPAP complex may promote maternal gene program during early embryogenesis in both germ cell lineage and soma. Knockdown of *gld-2* or *gld-3* leads to embryonic arrest and lethality (Eckmann, Kraemer et al. 2002, Wang, Eckmann et al. 2002). Depending on RNAi-mediated knockdown conditions, embryonic arrest happens either at the 1-cell stage or later (Wang, Eckmann et al. 2002), suggesting that GLD-2/GLD-3 cytoPAP is continuously required in many embryonic blastomeres during early embryogenesis.

A partial knockdown of *gld-2* produces following pleiotropic phenotypes (Agata Rybarska (PhD thesis), this work (data not shown)). (1) Transformation of somatic sisters to germ cells. Depending on when *gld-2* knockdown is felt by the system, any of the four somatic sister blastomeres (AB, EMS, C, and D) were transformed into germ cell-like blastomeres, as judged by the analyses of germ cell markers. (2) Loss of association of PGL-1 and GLH-1/2 proteins with P granules. Upon *gld-2* RNAi, PGL-1 and GLH-1/2 become predominantly cytosolic and fail to enrich on P granules. Occasionally, PGL-1 expression is completely lost, suggesting that GLD-2 may be required for PGL-1 expression and loss of association of PGL-1 and GLHs with P granules may be a secondary effect due to reduction of local protein concentration. (3) Gastrulation defects. some *gld-2* RNAi embryos grow beyond the 24-cell stage before arrest and P4 often fails to be internalized into the center of these embryos. Two possible scenarios might account for this defect: either (i) GLD-2 may be required to stimulate association of P4 to somatic blastomeres by promoting expression of factors required for this association, such as E-cadherin (Chihara and Nance 2012) or (ii) transiently expressed GLD-2 in somatic sister blastomere may promote the expression of factors required by somatic sisters for gastrulation. (4) GLD-2 is required for division of P4. In embryos that experience a later effect of *gld-2* RNAi, a single germ cell is occasionally seen in the center of approximately 500-cell stage embryos. This suggest that, in these embryos, P4 gastrulated but it failed to divide. Alternatively, one of the specified PGCs potentially underwent cell death. However, due to the formation of a germ cell primordium, this is less likely. Maternal *xnd-1* mRNA is translated in P4 and is required for the division of P4 into PGCs. Therefore, the stability of the *xnd-1* mRNA may be dependent on GLD-2. Regardless, these observations suggest that GLD-2 may be required for several aspects of somatic and germ cell development.

Interestingly, the germline abundance of many maternally donated mRNA including *xnd-1* is GLD-2 dependent (Nousch, Yeroslaviz et al. 2014). While some of the GLD-2 dependent mRNAs are required for both germline and embryonic development, many others are largely required for embryogenesis but not adult germline development. Examples of these include

pos-1, spn-4, nos-2, xnd-1, meg-1, zif-1, and *mex-6.* This implies that GLD-2 primarily protects these transcripts in adult's germline to ensure that they are abundantly donated into the embryos.

All findings suggest that GLD-2 begins to protect maternal transcripts in the adult germline and continue into early embryogenesis. Hence, regulated GLD-2 turnover may be required for a successful termination of maternal program both in soma and germ cells. Interestingly, consistent with this idea, GLD-2 expression strongly correlates with maternal gene program in both soma and germ cells. As an extension of this observations, prolongation of maternal gene program in germ cells, compared to soma, until PGC birth may be facilitated by differential continued GLD-2 expression in germ cell lineage.

5.5.2. GLD-2-type cytoPAPs may regulate maternal program in many systems

CytoPAPs may protect maternal transcripts in many systems. GLD-2 has been demonstrated in multiple organisms to be important for polyA tail extension just prior to fertilization and in some cases for soma during early embryogenesis. These include worm, fruit fly, and frog (Barnard, Ryan et al. 2004, Nakanishi, Kubota et al. 2006, Cui, Sackton et al. 2008, Cui, Sartain et al. 2013). However, the impact of GLD-2 on maternal transcripts in germ cell lineage during early embryogenesis has not been demonstrated in other systems. Only in a gene-specific manner, a very recent study in *Drosophila* demonstrated GLD-2 promote the expression of maternal *nanos* mRNA in germ cell lineage (Dufourt, Bontonou et al. 2017). Smaug forms complex with piRNA-loaded Aubergine to enhance maternal transcript clearance in soma. However, in germ cell lineage, Aubergine acts as a molecular switch to protect the *nanos* transcript from both Smaug-mediated transcript turnover which act in soma. Furthermore, to enhance stability, it recruits Wispy to *nanos* mRNA. As a consequence, Wispy stabilizes *nanos* mRNA by extending its polyA tail (Dufourt, Bontonou et al. 2017).

5.6. GLD-2 cytoPAP contributes to the termination of the maternal gene expression program.

5.6.1. GLD-2 contribute indirectly to its own turnover

GLD-2 promotes the expression of its turnover factor. *grif-1* mRNA is detectable in oocytes and in germ cell precursors of early embryos but not translated into proteins. This suggest that *grif-1* mRNA is maternally donated into the embryos and is repressed until it is translated into GRIF-1 protein in P4. Several observations suggest that GLD-2 regulates *grif-1* mRNA expression: (i) GLD-2 promotes the abundance of *grif-1* mRNA in the adult germline (Nousch, Yeroslaviz et al. 2014), (ii) *gld-2(RNAi)* embryos of 24-cell stage and beyond do not express GRIF-1 protein, and (iii) *gld-2* is required for the expression of a translational

reporter driven by *grif-1* 3'UTR. Together, these observations suggest that GLD-2 contributes to expression of its turnover factor, GRIF-1 protein. The regulation of the *grif-1* 3'UTR translational reporter by *gld-2* suggest that GLD-2 regulates *grif-1* mRNA expression through its 3'UTR. A scenario is envisaged in which GLD-2 promotes the abundance/or stability of *grif-1* mRNA by promoting its polyA tail extension. The implication of this regulation is that GLD-2 cytoPAP activity indirectly contributes to its own regulated protein turnover in PGCs, in a feed forward loop.
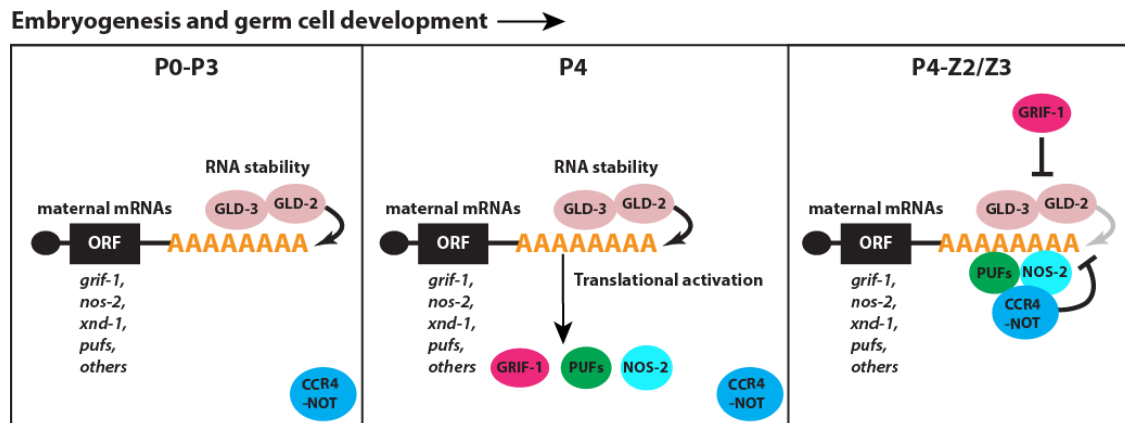
Figure 5.6. Proposed model for GLD-2-mediated establishment and termination of maternal program

GLD-2 and GLD-3 protects maternal transcripts from P0 to P4. Upon P4 birth, GRIF-1 and NOS-2 proteins are expressed from maternal transcripts. GRIF-1 and NOS-2 promotes maternal transcript clearance. *grif-1* indirectly promote mRNA turnover through GLD-2 degradation while NOS-2 may recruit the CCR4-Not deadenylase complex for polyA tail trimming.

5.6.2. GLD-2 cytoPAP may indirectly contribute to maternal transcript clearance and postembryonic germline survival

In several systems, termination of maternal program is achieved, at least in part, by maternal factors (De Renzis, Elemento et al. 2007, Tadros and Lipshitz 2009). GLD-2 promotes maternal gene expression program but may also contribute to its termination. Intriguingly, besides *grif-1,* GLD-2 also promotes mRNA abundance of factors that are required for maternal transcript clearance including several Nanos and Pumilio genes (i.e *nos-1, nos-2, puf-5, puf-6,* and *puf-7*) (Nousch, Yeroslaviz et al. 2014). This suggest that GLD-2 contributes to maternal transcript clearance in the following ways. (1) By indirectly promoting its own turnover. (2) By promoting the expression of other turnover factors. (3) A combination of both mechanisms. These observations suggest that GLD-2 indirectly promotes termination of the maternal program in PGCs (Figure 5.6).

Furthermore, GLD-2 also promotes the expression of other genes that do not directly affect maternal transcript clearance but whose loss lead to either changes epigenetic landscape or cause germline survival phenotypes (Figure 5.6). These include *meg-1, xnd-1, lsd-1,* and *set-25* (Nousch, Yeroslaviz et al. 2014). *meg-1* and *xnd-1* genetically interact with

nos-2 to regulate postembryonic germline survival (Leacock and Reinke 2008, Kapelle and Reinke 2011, Mainpal, Nance et al. 2015) while *lsd-1* and *set-25* modify chromatin (Ashe, Sapetschnig et al. 2012).

From the above, GLD-2 may indirectly promote postembryonic germline survival in three possible ways: either (i) by promoting the expression of factors required for maternal transcripts clearance, or (ii) by promoting the expression of other factors required for postembryonic germline development, or (iii) a combination of both. Therefore, it would be expected that loss of maternal GLD-2 leads to postembryonic germline survival phenotype. Unfortunately, removal or knockdown of *gld-2* leads to highly penetrant embryonic arrest which precludes this analysis. The germline survival phenotype observed in transgenic animals ectopically expressing GRIF-1^{WT} may therefore be as a result of GRIF-1-meditaed turnover of GLD-2 resulting in low levels of GLD-2 (but not complete loss) during embryonic germ cell development.

Together, GLD-2 may promotes the stability or abundance of maternal transcripts prior to MZT. At MZT, maternal proteins required for termination of maternal transripts and proteins are expressed including GRIF-1 and NOS-2. NOS-2 promotes maternal mRNA turnover in PGCs presumably by reruiting the CCR4-Not complex to trim polyA tail of maternal mRNAs. At the same time, GRIF-1 also promotes the turnover of GLD-2, a factor that extends polyA. Therefore, combined activity of GRIF-1 and NOS-2 synergestically lead to mRNA turnover in PGCs leading to termination of maternal gene expression program (Figure 5.6).

5.6.3. The mechanisms of maternal transcript clearance are conserved with some unique details

Are molecular mechanisms of MZT exactly conserved across systems? Particularly in germ cell lineage, the study of MZT mechanisms is at its infancy. Therefore, knowledge of these molecular mechanisms still needs to accumulate before a robust comparison is possible. Despite this, certain predictions and analyses can be made based on currently available data.

While conservation is highly expected to exist across phyla, several aspects appear unique to individual organisms. For example, in *C. elegans,* a direct orthologue of Smaug has not been identified and likley does not exist. In addition, no single piRNA specific Argonautes equivalent to Aubergine has been identified to be important for embryonic germ cell development. Single mutants of *prg-1,* an orthologue of aubergine, and other argonautes do not display any severe embryonic germ cell phenotype; defects of Argonaute mutants mostly affect sperms (Wang and Reinke 2008, Conine, Moresco et al. 2013). This argues that a single Argonaute that performs Aubergine-type function to recruit GLD-2 to maternal

mRNA does not exist in *C. elegans*. Alternatively, several worm Argonautes (WAGOs) likely recruit GLD-2 to maternal transcripts. Where exact orthologs may not exist, functional orthologs may act to exert the same molecular mechanisms or principles. Therefore, while the larger picture of molecular mechanisms that regulate MZT in germ cells may be similar across phyla, molecular details may differ.

5.6.4. GLD-2 turnover may be a universal mechanims to promote MZT in both soma and germ cells.

GLD-2 turnover may be linked with termination of maternal program in many systems. Similar to *ce*GLD-2, Wispy may also be degraded concomitantly with PGC specification. Consistent with this hypothesis, similar to *C. elegans,* in *Drosophila,* Wispy expression is terminated in soma at 2 to 4 hours into embryogenesis, a time that coincide with MZT in soma (Benoit, Papin et al. 2008, Lee, Choi et al. 2014). By contrast, Wispy expression is prolonged in pole cells which experience delayed maternal program (Dufourt, Bontonou et al. 2017). Around 7 hours into embryogenesis, maternal transcripts with SRE sequence become sensitive to Smaug-mediated transcript turnover. This suggests that, similar to *C. elegans,* protective mechanisms are time resolved in *Drosophila* (Bashirullah, Halsell et al. 1999, Dahanukar, Walker et al. 1999, Lecuyer, Yoshida et al. 2007, Siddiqui, Li et al. 2012). For example, it is highly likely that Wispy expression is terminated at this point in PGCs to allow maternal transcript turnover.

Furthermore, to further enhance this maternal transcript turnover, other components may also be activated in a germ cell-specific manner to facilitate maternal transcript degradation in the absence of Wispy. Consistent with this idea, of all the trancripts that are stable in developing PGCs but degraded later after 7 hours, only 34 % are dependent on Smaug for degradation (Siddiqui, Li et al. 2012). This suggests that other maternal and/or zygotic components exist to facilitate transcript turnover redundantly with Smaug in PGCs. In fact, many of these transcripts bear Pumilio binding site, suggesting that, similar to *C. elegans,* Pumilio/Nanos complex may also be critical to maternal transcript turnover specifically in PGCs in *Drosophila* (Siddiqui, Li et al. 2012). This suggest that GLD-2 cytoPAP-mediated protective mechanisms and Nanos/Pumilio-mediated turnover of maternal transcripts in germs cells seem to be highly likely in *D. melanogaster* and *C. elegans* and even potentially many other organisms.

Together, this work identified a developmenatlly regulated molecular pathway that promote the turnover of maternal GLD-2 protein in *C. elegans* PGCs. Evidence presented suggest that a novel TRIM32-related ubiquitin ligase, GRIF-1, interact with and promotes proteasomal degradation of GLD-2 protein in PGCs. Therefore, protein degradation limits the activities of GLD-2 cytoPAP to germ cell precursors. By promoting the turnover of GLD-2 and

presumably other maternal proteins, the proteasome promotes the reprograming of PGCs allowing a termination of maternal program and estabilishment of a clean zygotic program. In essence, this work illuminates the importance of maternal protein turnover during primordial germ cell development.

6. References

Abdu, Y., C. Maniscalco, J. M. Heddleston, T. L. Chew and J. Nance (2016). "Developmentally programmed germ cell remodelling by endodermal cell cannibalism." Nat Cell Biol **18**(12): 1302-1310.

Ahmed, S. and J. Hodgkin (2000). "MRT-2 checkpoint protein is required for germline immortality and telomere replication in C. elegans." Nature **403**(6766): 159-164.

Alberts, B. (2008). Molecular biology of the cell. New York, Garland Science.

Albor, A., S. El-Hizawi, E. J. Horn, M. Laederich, P. Frosk, K. Wrogemann and M. Kulesz-Martin (2006). "The interaction of Piasy with Trim32, an E3-ubiquitin ligase mutated in limb-girdle muscular dystrophy type 2H, promotes Piasy degradation and regulates UVB-induced keratinocyte apoptosis through NFkappaB." J Biol Chem **281**(35): 25850-25866.

Asaoka-Taguchi, M., M. Yamada, A. Nakamura, K. Hanyu and S. Kobayashi (1999). "Maternal Pumilio acts together with Nanos in germline development in Drosophila embryos." Nat Cell Biol **1**(7): 431-437.

Ashe, A., A. Sapetschnig, E. M. Weick, J. Mitchell, M. P. Bagijn, A. C. Cording, A. L. Doebley, L. D. Goldstein, N. J. Lehrbach, J. Le Pen, G. Pintacuda, A. Sakaguchi, P. Sarkies, S. Ahmed and E. A. Miska (2012). "piRNAs can trigger a multigenerational epigenetic memory in the germline of C. elegans." Cell **150**(1): 88-99.

Asher, G., J. Lotem, L. Sachs, C. Kahana and Y. Shaul (2002). "Mdm-2 and ubiquitin-independent p53 proteasomal degradation regulated by NQO1." Proc Natl Acad Sci U S A **99**(20): 13125-13130.

Asher, G., P. Tsvetkov, C. Kahana and Y. Shaul (2005). "A mechanism of ubiquitin-independent proteasomal degradation of the tumor suppressors p53 and p73." Genes Dev **19**(3): 316-321.

Barnard, D. C., K. Ryan, J. L. Manley and J. D. Richter (2004). "Symplekin and xGLD-2 are required for CPEB-mediated cytoplasmic polyadenylation." Cell **119**(5): 641-651.

Bashirullah, A., R. L. Cooperstock and H. D. Lipshitz (2001). "Spatial and temporal control of RNA stability." Proc Natl Acad Sci U S A **98**(13): 7025-7028.

Bashirullah, A., S. R. Halsell, R. L. Cooperstock, M. Kloc, A. Karaiskakis, W. W. Fisher, W. Fu, J. K. Hamilton, L. D. Etkin and H. D. Lipshitz (1999). "Joint action of two RNA degradation pathways controls the timing of maternal transcript elimination at the midblastula transition in Drosophila melanogaster." The EMBO journal **18**(9): 2610-2620.

Batchelder, C., M. A. Dunn, B. Choy, Y. Suh, C. Cassie, E. Y. Shim, T. H. Shin, C. Mello, G. Seydoux and T. K. Blackwell (1999). "Transcriptional repression by the Caenorhabditis elegans germ-line protein PIE-1." Genes Dev **13**(2): 202-212.

Baugh, J. M. and E. V. Pilipenko (2004). "20S proteasome differentially alters translation of different mRNAs via the cleavage of eIF4F and eIF3." Mol Cell **16**(4): 575-586.

Baugh, L. R., A. A. Hill, D. K. Slonim, E. L. Brown and C. P. Hunter (2003). "Composition and dynamics of the Caenorhabditis elegans early embryonic transcriptome." Development **130**(5): 889-900.

Bazzini, A. A., M. T. Lee and A. J. Giraldez (2012). "Ribosome profiling shows that miR-430 reduces translation before causing mRNA decay in zebrafish." Science **336**(6078): 233-237.

Beard, S. M., R. B. Smit, B. G. Chan and P. E. Mains (2016). "Regulation of the MEI-1/MEI-2 Microtubule-Severing Katanin Complex in Early Caenorhabditis elegans Development." G3 (Bethesda) **6**(10): 3257-3268.

Bender, L. B., R. Cao, Y. Zhang and S. Strome (2004). "The MES-2/MES-3/MES-6 complex and regulation of histone H3 methylation in C. elegans." Curr Biol **14**(18): 1639-1643.

Benoit, B., C. H. He, F. Zhang, S. M. Votruba, W. Tadros, J. T. Westwood, C. A. Smibert, H. D. Lipshitz and W. E. Theurkauf (2009). "An essential role for the RNA-binding protein Smaug during the Drosophila maternal-to-zygotic transition." Development **136**(6): 923-932.

Benoit, P., C. Papin, J. E. Kwak, M. Wickens and M. Simonelig (2008). "PAP- and GLD-2-type poly(A) polymerases are required sequentially in cytoplasmic polyadenylation and oogenesis in Drosophila." Development **135**(11): 1969-1979.

Bergsten, S. E. and E. R. Gavis (1999). "Role for mRNA localization in translational activation but not spatial restriction of nanos RNA." Development **126**(4): 659-669.

Berndsen, C. E. and C. Wolberger (2014). "New insights into ubiquitin E3 ligase mechanism." Nat Struct Mol Biol **21**(4): 301-307.

Blackwell, T. K. (2004). "Germ cells: finding programs of mass repression." Curr Biol **14**(6): R229-230.

Bontems, F., A. Stein, F. Marlow, J. Lyautey, T. Gupta, M. C. Mullins and R. Dosch (2009). "Bucky ball organizes germ plasm assembly in zebrafish." Curr Biol **19**(5): 414-422.

Borlepawar, A., A. Y. Rangrez, A. Bernt, L. Christen, S. Sossalla, D. Frank and N. Frey (2017). "TRIM24 protein promotes and TRIM32 protein inhibits cardiomyocyte hypertrophy via regulation of dysbindin protein levels." J Biol Chem **292**(24): 10180-10196.

Boulton, S. J. (2006). "Cellular functions of the BRCA tumour-suppressor proteins." Biochem Soc Trans **34**(Pt 5): 633-645.

Boulton, S. J., J. S. Martin, J. Polanowska, D. E. Hill, A. Gartner and M. Vidal (2004). "BRCA1/BARD1 orthologs required for DNA repair in Caenorhabditis elegans." Curr Biol **14**(1): 33-39.

Brangwynne, C. P., C. R. Eckmann, D. S. Courson, A. Rybarska, C. Hoege, J. Gharakhani, F. Julicher and A. A. Hyman (2009). "Germline P granules are liquid droplets that localize by controlled dissolution/condensation." Science **324**(5935): 1729-1732.

Brenner, S. (1974). "The genetics of Caenorhabditis elegans." Genetics **77**(1): 71-94.

Buckley, B. A., K. B. Burkhart, S. G. Gu, G. Spracklin, A. Kershner, H. Fritz, J. Kimble, A. Fire and S. Kennedy (2012). "A nuclear Argonaute promotes multigenerational epigenetic inheritance and germline immortality." Nature **489**(7416): 447-451.

Burger, J., J. Merlet, N. Tavernier, B. Richaudeau, A. Arnold, R. Ciosk, B. Bowerman and L. Pintard (2013). "CRL2(LRR-1) E3-ligase regulates proliferation and progression through meiosis in the Caenorhabditis elegans germline." PLoS Genet **9**(3): e1003375.

Bushati, N., A. Stark, J. Brennecke and S. M. Cohen (2008). "Temporal reciprocity of miRNAs and their targets during the maternal-to-zygotic transition in Drosophila." Current biology : CB **18**(7): 501-506.

Campbell, E. M., M. P. Dodding, M. W. Yap, X. Wu, S. Gallois-Montbrun, M. H. Malim, J. P. Stoye and T. J. Hope (2007). "TRIM5 alpha cytoplasmic bodies are highly dynamic structures." Mol Biol Cell **18**(6): 2102-2111.

Capowski, E. E., P. Martin, C. Garvin and S. Strome (1991). "Identification of grandchildless loci whose products are required for normal germ-line development in the nematode Caenorhabditis elegans." Genetics **129**(4): 1061-1072.

Chen, J. X., P. G. Cipriani, D. Mecenas, J. Polanowska, F. Piano, K. C. Gunsalus and M. Selbach (2016). "In Vivo Interaction Proteomics in Caenorhabditis elegans Embryos Provides New Insights into P Granule Dynamics." Mol Cell Proteomics **15**(5): 1642-1657.

Chen, X., L. F. Barton, Y. Chi, B. E. Clurman and J. M. Roberts (2007). "Ubiquitin-independent degradation of cell-cycle inhibitors by the REGgamma proteasome." Mol Cell **26**(6): 843-852.

Chihara, D. and J. Nance (2012). "An E-cadherin-mediated hitchhiking mechanism for C. elegans germ cell internalization during gastrulation." Development **139**(14): 2547-2556.

Ciosk, R., M. DePalma and J. R. Priess (2006). "Translational regulators maintain totipotency in the Caenorhabditis elegans germline." Science **311**(5762): 851-853.

Conine, C. C., J. J. Moresco, W. Gu, M. Shirayama, D. Conte, Jr., J. R. Yates, 3rd and C. C. Mello (2013). "Argonautes promote male fertility and provide a paternal memory of germline gene expression in C. elegans." Cell **155**(7): 1532-1544.

Cui, J., K. L. Sackton, V. L. Horner, K. E. Kumar and M. F. Wolfner (2008). "Wispy, the Drosophila homolog of GLD-2, is required during oogenesis and egg activation." Genetics **178**(4): 2017-2029.

Cui, J., C. V. Sartain, J. A. Pleiss and M. F. Wolfner (2013). "Cytoplasmic polyadenylation is a major mRNA regulator during oogenesis and egg activation in Drosophila." Dev Biol **383**(1): 121-131.

Dahanukar, A., J. A. Walker and R. P. Wharton (1999). "Smaug, a novel RNA-binding protein that operates a translational switch in Drosophila." Mol Cell **4**(2): 209-218.

Davis, G. M., S. Tu, J. W. Anderson, R. N. Colson, M. J. Gunzburg, M. A. Francisco, D. Ray, S. P. Shrubsole, J. A. Sobotka, U. Seroussi, R. X. Lao, T. Maity, M. Z. Wu, K. McJunkin, Q. D. Morris, T. R. Hughes, J. A. Wilce, J. M. Claycomb, Z. Weng and P. R. Boag (2018). "The TRIM-NHL protein NHL-2 is a co-factor in the nuclear and somatic RNAi pathways in C. elegans." Elife **7**.

Dawidziak, D. M., J. G. Sanchez, J. M. Wagner, B. K. Ganser-Pornillos and O. Pornillos (2017). "Structure and catalytic activation of the TRIM23 RING E3 ubiquitin ligase." Proteins **85**(10): 1957-1961.

De Renzis, S., O. Elemento, S. Tavazoie and E. F. Wieschaus (2007). "Unmasking activation of the zygotic genome using chromosomal deletions in the Drosophila embryo." PLoS Biol **5**(5): e117.

Decker, C. J. and R. Parker (1993). "A turnover pathway for both stable and unstable mRNAs in yeast: evidence for a requirement for deadenylation." Genes & development **7**(8): 1632-1643.

DeRenzo, C., K. J. Reese and G. Seydoux (2003). "Exclusion of germ plasm proteins from somatic lineages by cullin-dependent degradation." Nature **424**(6949): 685-689.

Detivaud, L., G. Pascreau, A. Karaiskou, H. B. Osborne and J. Z. Kubiak (2003). "Regulation of EDEN-dependent deadenylation of Aurora A/Eg2-derived mRNA via phosphorylation and dephosphorylation in Xenopus laevis egg extracts." J Cell Sci **116**(Pt 13): 2697-2705.

Diaz-Griffero, F., X. Li, H. Javanbakht, B. Song, S. Welikala, M. Stremlau and J. Sodroski (2006). "Rapid turnover and polyubiquitylation of the retroviral restriction factor TRIM5." Virology **349**(2): 300-315.

Duerr, J. S. (2013). "Antibody staining in C. elegans using "freeze-cracking"." J Vis Exp(80).

Dufourt, J., G. Bontonou, A. Chartier, C. Jahan, A. C. Meunier, S. Pierson, P. F. Harrison, C. Papin, T. H. Beilharz and M. Simonelig (2017). "piRNAs and Aubergine cooperate with Wispy poly(A) polymerase to stabilize mRNAs in the germ plasm." Nat Commun **8**(1): 1305.

Eckmann, C. R., S. L. Crittenden, N. Suh and J. Kimble (2004). "GLD-3 and control of the mitosis/meiosis decision in the germline of Caenorhabditis elegans." Genetics **168**(1): 147-160.

Eckmann, C. R., B. Kraemer, M. Wickens and J. Kimble (2002). "GLD-3, a bicaudal-C homolog that inhibits FBF to control germline sex determination in C. elegans." Dev Cell **3**(5): 697-710.

Eckmann, C. R., B. Kraemer, M. Wickens and J. Kimble (2002). "GLD-3, a bicaudal-C homolog that inhibits FBF to control germline sex determination in C. elegans." Developmental cell **3**(5): 697-710.

Eckmann, C. R., C. Rammelt and E. Wahle (2011). "Control of poly(A) tail length." Wiley interdisciplinary reviews. RNA **2**(3): 348-361.

Eddy, E. M. (1975). "Germ plasm and the differentiation of the germ cell line." Int Rev Cytol **43**: 229-280.

Elewa, A., M. Shirayama, E. Kaymak, P. F. Harrison, D. R. Powell, Z. Du, C. D. Chute, H. Woolf, D. Yi, T. Ishidate, J. Srinivasan, Z. Bao, T. H. Beilharz, S. P. Ryder and C. C. Mello (2015). "POS-1 Promotes Endo-mesoderm Development by Inhibiting the Cytoplasmic Polyadenylation of neg-1 mRNA." Dev Cell **34**(1): 108-118.

Ephrussi, A. and R. Lehmann (1992). "Induction of germ cell formation by oskar." Nature **358**(6385): 387-392.

Erales, J. and P. Coffino (2014). "Ubiquitin-independent proteasomal degradation." Biochim Biophys Acta **1843**(1): 216-221.

Ewen-Campen, B., S. Donoughe, D. N. Clarke and C. G. Extavour (2013). "Germ cell specification requires zygotic mechanisms rather than germ plasm in a basally branching insect." Curr Biol **23**(10): 835-842.

Extavour, C. G. and M. Akam (2003). "Mechanisms of germ cell specification across the metazoans: epigenesis and preformation." Development **130**(24): 5869-5884.

Faehnle, C. R., J. Walleshauser and L. Joshua-Tor (2017). "Multi-domain utilization by TUT4 and TUT7 in control of let-7 biogenesis." Nat Struct Mol Biol **24**(8): 658-665.

Fay, D. S., E. Large, M. Han and M. Darland (2003). "lin-35/Rb and ubc-18, an E2 ubiquitin-conjugating enzyme, function redundantly to control pharyngeal morphogenesis in C. elegans." Development **130**(14): 3319-3330.

Feng, H., W. Zhong, G. Punkosdy, S. Gu, L. Zhou, E. K. Seabolt and E. T. Kipreos (1999). "CUL-2 is required for the G1-to-S-phase transition and mitotic chromosome condensation in Caenorhabditis elegans." Nat Cell Biol **1**(8): 486-492.

Ferg, M., R. Sanges, J. Gehrig, J. Kiss, M. Bauer, A. Lovas, M. Szabo, L. Yang, U. Straehle, M. J. Pankratz, F. Olasz, E. Stupka and F. Muller (2007). "The TATA-binding protein regulates maternal mRNA degradation and differential zygotic transcription in zebrafish." EMBO J **26**(17): 3945-3956.

Fontana, A., P. P. de Laureto, B. Spolaore, E. Frare, P. Picotti and M. Zambonin (2004). "Probing protein structure by limited proteolysis." Acta Biochim Pol **51**(2): 299-321.

Fox, P. M., V. E. Vought, M. Hanazawa, M. H. Lee, E. M. Maine and T. Schedl (2011). "Cyclin E and CDK-2 regulate proliferative cell fate and cell cycle progression in the C. elegans germline." Development **138**(11): 2223-2234.

Frokjaer-Jensen, C., M. W. Davis, M. Ailion and E. M. Jorgensen (2012). "Improved Mos1-mediated transgenesis in C. elegans." Nat Methods **9**(2): 117-118.

Gack, M. U., Y. C. Shin, C. H. Joo, T. Urano, C. Liang, L. Sun, O. Takeuchi, S. Akira, Z. Chen, S. Inoue and J. U. Jung (2007). "TRIM25 RING-finger E3 ubiquitin ligase is essential for RIG-I-mediated antiviral activity." Nature **446**(7138): 916-920.

Gallo, C. M., E. Munro, D. Rasoloson, C. Merritt and G. Seydoux (2008). "Processing bodies and germ granules are distinct RNA granules that interact in C. elegans embryos." Dev Biol **323**(1): 76-87.

Gallo, C. M., J. T. Wang, F. Motegi and G. Seydoux (2010). "Cytoplasmic partitioning of P granule components is not required to specify the germline in C. elegans." Science **330**(6011): 1685-1689.

Gartner, A., S. Milstein, S. Ahmed, J. Hodgkin and M. O. Hengartner (2000). "A conserved checkpoint pathway mediates DNA damage--induced apoptosis and cell cycle arrest in C. elegans." Mol Cell **5**(3): 435-443.

Garvin, C., R. Holdeman and S. Strome (1998). "The phenotype of mes-2, mes-3, mes-4 and mes-6, maternal-effect genes required for survival of the germline in Caenorhabditis elegans, is sensitive to chromosome dosage." Genetics **148**(1): 167-185.

Ghosh, D. and G. Seydoux (2008). "Inhibition of transcription by the Caenorhabditis elegans germline protein PIE-1: genetic evidence for distinct mechanisms targeting initiation and elongation." Genetics **178**(1): 235-243.

Gietz, R. D. and R. A. Woods (2002). "Transformation of yeast by lithium acetate/single-stranded carrier DNA/polyethylene glycol method." Methods Enzymol **350**: 87-96.

Giraldez, A. J., Y. Mishima, J. Rihel, R. J. Grocock, S. Van Dongen, K. Inoue, A. J. Enright and A. F. Schier (2006). "Zebrafish MiR-430 promotes deadenylation and clearance of maternal mRNAs." Science **312**(5770): 75-79.

Goldstone, D. C., P. A. Walker, L. J. Calder, P. J. Coombs, J. Kirkpatrick, N. J. Ball, L. Hilditch, M. W. Yap, P. B. Rosenthal, J. P. Stoye and I. A. Taylor (2014). "Structural studies of postentry restriction factors reveal antiparallel dimers that enable avid binding to the HIV-1 capsid lattice." Proc Natl Acad Sci U S A **111**(26): 9609-9614.

Goldstrohm, A. C. and M. Wickens (2008). "Multifunctional deadenylase complexes diversify mRNA control." Nat Rev Mol Cell Biol **9**(4): 337-344.

Gonczy, P., C. Echeverri, K. Oegema, A. Coulson, S. J. Jones, R. R. Copley, J. Duperon, J. Oegema, M. Brehm, E. Cassin, E. Hannak, M. Kirkham, S. Pichler, K. Flohrs, A. Goessen, S. Leidel, A. M. Alleaume, C. Martin, N. Ozlu, P. Bork and A. A. Hyman (2000). "Functional genomic analysis of cell division in C. elegans using RNAi of genes on chromosome III." Nature **408**(6810): 331-336.

Grabowski, M. M., N. Svrzikapa and H. A. Tissenbaum (2005). "Bloom syndrome ortholog HIM-6 maintains genomic stability in C. elegans." Mech Ageing Dev **126**(12): 1314-1321.

Graindorge, A., O. Le Tonqueze, R. Thuret, N. Pollet, H. B. Osborne and Y. Audic (2008). "Identification of CUG-BP1/EDEN-BP target mRNAs in Xenopus tropicalis." Nucleic Acids Res **36**(6): 1861-1870.

Gruidl, M. E., P. A. Smith, K. A. Kuznicki, J. S. McCrone, J. Kirchner, D. L. Roussell, S. Strome and K. L. Bennett (1996). "Multiple potential germ-line helicases are components of the germ-line-specific P granules of Caenorhabditis elegans." Proceedings of the National Academy of Sciences of the United States of America **93**(24): 13837-13842.

Guharoy, M., P. Bhowmick, M. Sallam and P. Tompa (2016). "Tripartite degrons confer diversity and specificity on regulated protein degradation in the ubiquitin-proteasome system." Nat Commun **7**: 10239.

Guharoy, M., P. Bhowmick and P. Tompa (2016). "Design Principles Involving Protein Disorder Facilitate Specific Substrate Selection and Degradation by the Ubiquitin-Proteasome System." J Biol Chem **291**(13): 6723-6731.

Gumienny, T. L., E. Lambie, E. Hartwieg, H. R. Horvitz and M. O. Hengartner (1999). "Genetic control of programmed cell death in the Caenorhabditis elegans hermaphrodite germline." Development **126**(5): 1011-1022.

Gupta, P., L. Leahul, X. Wang, C. Wang, B. Bakos, K. Jasper and D. Hansen (2015). "Proteasome regulation of the chromodomain protein MRG-1 controls the balance between proliferative fate and differentiation in the C. elegans germ line." Development **142**(2): 291-302.

Guraya, S. S. (1979). "Recent advances in the morphology, cytochemistry, and function of Balbiani's vitelline body in animal oocytes." Int Rev Cytol **59**: 249-321.

Guven-Ozkan, T., Y. Nishi, S. M. Robertson and R. Lin (2008). "Global transcriptional repression in C. elegans germline precursors by regulated sequestration of TAF-4." Cell **135**(1): 149-160.

Guven-Ozkan, T., S. M. Robertson, Y. Nishi and R. Lin (2010). "zif-1 translational repression defines a second, mutually exclusive OMA function in germline transcriptional repression." Development **137**(20): 3373-3382.

Hamatani, T., M. G. Carter, A. A. Sharov and M. S. Ko (2004). "Dynamics of global gene expression changes during mouse preimplantation development." Dev Cell **6**(1): 117-131.

Hand, J. M. and A. A. Bazzini (2017). "When LIN41 Comes to a Fork in the Road, It Takes BOTH Paths: Translational Repression OR mRNA Decay, Depending on the Target Site Position." Mol Cell **65**(3): 375-377.

Hanna, J., A. Guerra-Moreno, J. Ang and Y. Micoogullari (2019). "Protein Degradation and the Pathologic Basis of Disease." Am J Pathol **189**(1): 94-103.

Hansen, D., L. Wilson-Berry, T. Dang and T. Schedl (2004). "Control of the proliferation versus meiotic development decision in the C. elegans germline through regulation of GLD-1 protein accumulation." Development **131**(1): 93-104.

Hanyu-Nakamura, K., H. Sonobe-Nojima, A. Tanigawa, P. Lasko and A. Nakamura (2008). "Drosophila Pgc protein inhibits P-TEFb recruitment to chromatin in primordial germ cells." Nature **451**(7179): 730-733.

Hatakeyama, S. (2017). "TRIM Family Proteins: Roles in Autophagy, Immunity, and Carcinogenesis." Trends Biochem Sci **42**(4): 297-311.

Heo, I., C. Joo, Y. K. Kim, M. Ha, M. J. Yoon, J. Cho, K. H. Yeom, J. Han and V. N. Kim (2009). "TUT4 in concert with Lin28 suppresses microRNA biogenesis through pre-microRNA uridylation." Cell **138**(4): 696-708.

Hipp, M. S., S. H. Park and F. U. Hartl (2014). "Proteostasis impairment in protein-misfolding and -aggregation diseases." Trends Cell Biol **24**(9): 506-514.

Hird, S. N., J. E. Paulsen and S. Strome (1996). "Segregation of germ granules in living Caenorhabditis elegans embryos: cell-type-specific mechanisms for cytoplasmic localisation." Development **122**(4): 1303-1312.

Hirsh, D., D. Oppenheim and M. Klass (1976). "Development of the reproductive system of Caenorhabditis elegans." Developmental biology **49**(1): 200-219.

Hochstrasser, M. (1995). "Ubiquitin, proteasomes, and the regulation of intracellular protein degradation." Curr Opin Cell Biol **7**(2): 215-223.

Hofmann, E. R., S. Milstein, S. J. Boulton, M. Ye, J. J. Hofmann, L. Stergiou, A. Gartner, M. Vidal and M. O. Hengartner (2002). "Caenorhabditis elegans HUS-1 is a DNA damage checkpoint protein required for genome stability and EGL-1-mediated apoptosis." Curr Biol **12**(22): 1908-1918.

Holdeman, R., S. Nehrt and S. Strome (1998). "MES-2, a maternal protein essential for viability of the germline in Caenorhabditis elegans, is homologous to a Drosophila Polycomb group protein." Development **125**(13): 2457-2467.

Hsieh, J., J. Liu, S. A. Kostas, C. Chang, P. W. Sternberg and A. Fire (1999). "The RING finger/B-box factor TAM-1 and a retinoblastoma-like protein LIN-35 modulate context-dependent gene silencing in Caenorhabditis elegans." Genes Dev **13**(22): 2958-2970.

Hubbard, E. J. and D. Greenstein (2005). "Introduction to the germ line." WormBook: 1-4.

Huch, S. and T. Nissan (2014). "Interrelations between translation and general mRNA degradation in yeast." Wiley Interdiscip Rev RNA **5**(6): 747-763.

Hwang, W. Y., Y. Fu, D. Reyon, M. L. Maeder, S. Q. Tsai, J. D. Sander, R. T. Peterson, J. R. Yeh and J. K. Joung (2013). "Efficient genome editing in zebrafish using a CRISPR-Cas system." Nat Biotechnol **31**(3): 227-229.

Ichimura, T., M. Taoka, I. Shoji, H. Kato, T. Sato, S. Hatakeyama, T. Isobe and N. Hachiya (2013). "14-3-3 proteins sequester a pool of soluble TRIM32 ubiquitin ligase to repress autoubiquitylation and cytoplasmic body formation." J Cell Sci **126**(Pt 9): 2014-2026.

Illmensee, K. and A. P. Mahowald (1974). "Transplantation of posterior polar plasm in Drosophila. Induction of germ cells at the anterior pole of the egg." Proc Natl Acad Sci U S A **71**(4): 1016-1020.

Jain, A. K., K. Allton, A. D. Duncan and M. C. Barton (2014). "TRIM24 is a p53-induced E3-ubiquitin ligase that undergoes ATM-mediated phosphorylation and autodegradation during DNA damage." Mol Cell Biol **34**(14): 2695-2709.

Jariel-Encontre, I., M. Pariat, F. Martin, S. Carillo, C. Salvat and M. Piechaczyk (1995). "Ubiquitinylation is not an absolute requirement for degradation of c-Jun protein by the 26 S proteasome." J Biol Chem **270**(19): 11623-11627.

Jaruzelska, J., M. Kotecki, K. Kusz, A. Spik, M. Firpo and R. A. Reijo Pera (2003). "Conservation of a Pumilio-Nanos complex from Drosophila germ plasm to human germ cells." Dev Genes Evol **213**(3): 120-126.

Javanbakht, H., W. Yuan, D. F. Yeung, B. Song, F. Diaz-Griffero, Y. Li, X. Li, M. Stremlau and J. Sodroski (2006). "Characterization of TRIM5alpha trimerization and its contribution to human immunodeficiency virus capsid binding." Virology **353**(1): 234-246.

Jaworska, A. M., N. A. Wlodarczyk, A. Mackiewicz and P. Czerwinska (2020). "The role of TRIM family proteins in the regulation of cancer stem cell self-renewal." Stem Cells **38**(2): 165-173.

Jedamzik, B. and C. R. Eckmann (2009). "Analysis of in vivo protein complexes by coimmunoprecipitation from Caenorhabditis elegans." Cold Spring Harb Protoc **2009**(10): pdb prot5299.

Jeong, J., J. M. Verheyden and J. Kimble (2011). "Cyclin E and Cdk2 control GLD-1, the mitosis/meiosis decision, and germline stem cells in Caenorhabditis elegans." PLoS genetics **7**(3): e1001348.

Jin, Y., H. Lee, S. X. Zeng, M. S. Dai and H. Lu (2003). "MDM2 promotes p21waf1/cip1 proteasomal turnover independently of ubiquitylation." EMBO J **22**(23): 6365-6377.

Jo, B. S. and S. S. Choi (2015). "Introns: The Functional Benefits of Introns in Genomes." Genomics Inform **13**(4): 112-118.

Johnson, D. E., B. Xue, M. D. Sickmeier, J. Meng, M. S. Cortese, C. J. Oldfield, T. Le Gall, A. K. Dunker and V. N. Uversky (2012). "High-throughput characterization of intrinsic disorder in proteins from the Protein Structure Initiative." J Struct Biol **180**(1): 201-215.

Johnston, W. L., A. Krizus, A. K. Ramani, W. Dunham, J. Y. Youn, A. G. Fraser, A. C. Gingras and J. W. Dennis (2017). "C. elegans SUP-46, an HNRNPM family RNA-binding protein that prevents paternally-mediated epigenetic sterility." BMC Biol **15**(1): 61.

Johnstone, O. and P. Lasko (2001). "Translational regulation and RNA localization in Drosophila oocytes and embryos." Annu Rev Genet **35**: 365-406.

Jones, D., E. Crowe, T. A. Stevens and E. P. Candido (2002). "Functional and phylogenetic analysis of the ubiquitylation system in Caenorhabditis elegans: ubiquitin-conjugating enzymes, ubiquitin-activating enzymes, and ubiquitin-like proteins." Genome Biol **3**(1): RESEARCH0002.

Jongeward, G. D., T. R. Clandinin and P. W. Sternberg (1995). "sli-1, a negative regulator of let-23-mediated signaling in C. elegans." Genetics **139**(4): 1553-1566.

Jukam, D., S. A. M. Shariati and J. M. Skotheim (2017). "Zygotic Genome Activation in Vertebrates." Dev Cell **42**(4): 316-332.

Kadyrova, L. Y., Y. Habara, T. H. Lee and R. P. Wharton (2007). "Translational control of maternal Cyclin B mRNA by Nanos in the Drosophila germline." Development **134**(8): 1519-1527.

Kahn, N. W., S. L. Rea, S. Moyle, A. Kell and T. E. Johnson (2008). "Proteasomal dysfunction activates the transcription factor SKN-1 and produces a selective oxidative-stress response in Caenorhabditis elegans." Biochem J **409**(1): 205-213.

Kalejta, R. F., J. T. Bechtel and T. Shenk (2003). "Human cytomegalovirus pp71 stimulates cell cycle progression by inducing the proteasome-dependent degradation of the retinoblastoma family of tumor suppressors." Mol Cell Biol **23**(6): 1885-1895.

Kalejta, R. F. and T. Shenk (2003). "Proteasome-dependent, ubiquitin-independent degradation of the Rb family of tumor suppressors by the human cytomegalovirus pp71 protein." Proc Natl Acad Sci U S A **100**(6): 3263-3268.

Kamath, R. S., A. G. Fraser, Y. Dong, G. Poulin, R. Durbin, M. Gotta, A. Kanapin, N. Le Bot, S. Moreno, M. Sohrmann, D. P. Welchman, P. Zipperlen and J. Ahringer (2003). "Systematic functional analysis of the Caenorhabditis elegans genome using RNAi." Nature **421**(6920): 231-237.

Kano, S., N. Miyajima, S. Fukuda and S. Hatakeyama (2008). "Tripartite motif protein 32 facilitates cell growth and migration via degradation of Abl-interactor 2." Cancer Res **68**(14): 5572-5580.

Kapelle, W. S. and V. Reinke (2011). "C. elegans meg-1 and meg-2 differentially interact with nanos family members to either promote or inhibit germ cell proliferation and survival." Genesis **49**(5): 380-391.

Katz, D. J., T. M. Edwards, V. Reinke and W. G. Kelly (2009). "A C. elegans LSD1 demethylase contributes to germline immortality by reprogramming epigenetic memory." Cell **137**(2): 308-320.

Kaushik, S. and A. M. Cuervo (2012). "Chaperone-mediated autophagy: a unique way to enter the lysosome world." Trends Cell Biol **22**(8): 407-417.

Kawasaki, I., A. Amiri, Y. Fan, N. Meyer, S. Dunkelbarger, T. Motohashi, T. Karashima, O. Bossinger and S. Strome (2004). "The PGL family proteins associate with germ granules and function redundantly in Caenorhabditis elegans germline development." Genetics **167**(2): 645-661.

Kawasaki, I., Y. H. Shim, J. Kirchner, J. Kaminker, W. B. Wood and S. Strome (1998). "PGL-1, a predicted RNA-binding component of germ granules, is essential for fertility in C. elegans." Cell **94**(5): 635-645.

Kim, B., M. Ha, L. Loeff, H. Chang, D. K. Simanshu, S. Li, M. Fareh, D. J. Patel, C. Joo and V. N. Kim (2015). "TUT7 controls the fate of precursor microRNAs by using three different uridylation mechanisms." EMBO J **34**(13): 1801-1815.

Kim, J. H. and J. D. Richter (2006). "Opposing polymerase-deadenylase activities regulate cytoplasmic polyadenylation." Mol Cell **24**(2): 173-183.

Kim, K. W., T. L. Wilson and J. Kimble (2010). "GLD-2/RNP-8 cytoplasmic poly(A) polymerase is a broad-spectrum regulator of the oogenesis program." Proc Natl Acad Sci U S A **107**(40): 17445-17450.

Kimble, J. and S. L. Crittenden (2007). "Controls of germline stem cells, entry into meiosis, and the sperm/oocyte decision in Caenorhabditis elegans." Annual review of cell and developmental biology **23**: 405-433.

Kimble, J. and D. Hirsh (1979). "The postembryonic cell lineages of the hermaphrodite and male gonads in Caenorhabditis elegans." Developmental biology **70**(2): 396-417.

Kimble, J. E. and J. G. White (1981). "On the control of germ cell development in Caenorhabditis elegans." Developmental biology **81**(2): 208-219.

Kinzler, K. W., M. C. Nilbert, L. K. Su, B. Vogelstein, T. M. Bryan, D. B. Levy, K. J. Smith, A. C. Preisinger, P. Hedge, D. McKechnie and et al. (1991). "Identification of FAP locus genes from chromosome 5q21." Science **253**(5020): 661-665.

Kipreos, E. T. (2005). "Ubiquitin-mediated pathways in C. elegans." WormBook: 1-24.

Kisielnicka, E., R. Minasaki and C. R. Eckmann (2018). "MAPK signaling couples SCF-mediated degradation of translational regulators to oocyte meiotic progression." Proc Natl Acad Sci U S A **115**(12): E2772-E2781.

Kisselev, A. F., T. N. Akopian and A. L. Goldberg (1998). "Range of sizes of peptide products generated during degradation of different proteins by archaeal proteasomes." J Biol Chem **273**(4): 1982-1989.

Koegl, M., T. Hoppe, S. Schlenker, H. D. Ulrich, T. U. Mayer and S. Jentsch (1999). "A novel ubiquitination factor, E4, is involved in multiubiquitin chain assembly." Cell **96**(5): 635-644.

Koliopoulos, M. G., D. Esposito, E. Christodoulou, I. A. Taylor and K. Rittinger (2016). "Functional role of TRIM E3 ligase oligomerization and regulation of catalytic activity." EMBO J **35**(11): 1204-1218.

Komander, D. (2009). "The emerging complexity of protein ubiquitination." Biochem Soc Trans **37**(Pt 5): 937-953.

Komorowski, M., J. Miekisz and A. M. Kierzek (2009). "Translational repression contributes greater noise to gene expression than transcriptional repression." Biophys J **96**(2): 372-384.

Kong, X., B. Alvarez-Castelao, Z. Lin, J. G. Castano and J. Caro (2007). "Constitutive/hypoxic degradation of HIF-alpha proteins by the proteasome is independent of von Hippel Lindau protein ubiquitylation and the transactivation activity of the protein." J Biol Chem **282**(21): 15498-15505.

Koprunner, M., C. Thisse, B. Thisse and E. Raz (2001). "A zebrafish nanos-related gene is essential for the development of primordial germ cells." Genes & development **15**(21): 2877-2885.

Korf, I., Y. Fan and S. Strome (1998). "The Polycomb group in Caenorhabditis elegans and maternal control of germline development." Development **125**(13): 2469-2478.

Kraemer, B., S. Crittenden, M. Gallegos, G. Moulder, R. Barstead, J. Kimble and M. Wickens (1999). "NANOS-3 and FBF proteins physically interact to control the sperm-oocyte switch in Caenorhabditis elegans." Current biology : CB **9**(18): 1009-1018.

Kudryashova, E., D. Kudryashov, I. Kramerova and M. J. Spencer (2005). "Trim32 is a ubiquitin ligase mutated in limb girdle muscular dystrophy type 2H that binds to skeletal muscle myosin and ubiquitinates actin." J Mol Biol **354**(2): 413-424.

Kudryashova, E., J. Wu, L. A. Havton and M. J. Spencer (2009). "Deficiency of the E3 ubiquitin ligase TRIM32 in mice leads to a myopathy with a neurogenic component." Hum Mol Genet **18**(7): 1353-1367.

Kuznicki, K. A., P. A. Smith, W. M. Leung-Chiu, A. O. Estevez, H. C. Scott and K. L. Bennett (2000). "Combinatorial RNA interference indicates GLH-4 can compensate for GLH-1; these two P granule components are critical for fertility in C. elegans." Development **127**(13): 2907-2916.

Kwak, J. E., E. Drier, S. A. Barbee, M. Ramaswami, J. C. Yin and M. Wickens (2008). "GLD2 poly(A) polymerase is required for long-term memory." Proc Natl Acad Sci U S A **105**(38): 14644-14649.

Labbadia, J. and R. I. Morimoto (2015). "The biology of proteostasis in aging and disease." Annu Rev Biochem **84**: 435-464.

Lai, F., A. Singh and M. L. King (2012). "Xenopus Nanos1 is required to prevent endoderm gene expression and apoptosis in primordial germ cells." Development **139**(8): 1476-1486.

Leacock, S. W. and V. Reinke (2008). "MEG-1 and MEG-2 are embryo-specific P-granule components required for germline development in Caenorhabditis elegans." Genetics **178**(1): 295-306.

Lecuyer, E., H. Yoshida, N. Parthasarathy, C. Alm, T. Babak, T. Cerovina, T. R. Hughes, P. Tomancak and H. M. Krause (2007). "Global analysis of mRNA localization reveals a prominent role in organizing cellular architecture and function." Cell **131**(1): 174-187.

Lee, C. S., T. Lu and G. Seydoux (2017). "Nanos promotes epigenetic reprograming of the germline by down-regulation of the THAP transcription factor LIN-15B." Elife **6**.

Lee, M., Y. Choi, K. Kim, H. Jin, J. Lim, T. A. Nguyen, J. Yang, M. Jeong, A. J. Giraldez, H. Yang, D. J. Patel and V. N. Kim (2014). "Adenylation of maternally inherited microRNAs by Wispy." Mol Cell **56**(5): 696-707.

Lehmann, R. (2012). "Germline stem cells: origin and destiny." Cell stem cell **10**(6): 729-739.

Lesch, B. J. and D. C. Page (2012). "Genetics of germ cell development." Nat Rev Genet **13**(11): 781-794.

Lev, I., U. Seroussi, H. Gingold, R. Bril, S. Anava and O. Rechavi (2017). "MET-2-Dependent H3K9 Methylation Suppresses Transgenerational Small RNA Inheritance." Curr Biol **27**(8): 1138-1147.

Li, X., B. Song, S. H. Xiang and J. Sodroski (2007). "Functional interplay between the B-box 2 and the B30.2(SPRY) domains of TRIM5alpha." Virology **366**(2): 234-244.

Li, X., D. F. Yeung, A. M. Fiegen and J. Sodroski (2011). "Determinants of the higher order association of the restriction factor TRIM5alpha and other tripartite motif (TRIM) proteins." J Biol Chem **286**(32): 27959-27970.

Li, Y. and E. M. Maine (2018). "The balance of poly(U) polymerase activity ensures germline identity, survival and development in Caenorhabditis elegans." Development **145**(19).

Li, Y., H. Wu, W. Wu, W. Zhuo, W. Liu, Y. Zhang, M. Cheng, Y. G. Chen, N. Gao, H. Yu, L. Wang, W. Li and M. Yang (2014). "Structural insights into the TRIM family of ubiquitin E3 ligases." Cell Res **24**(6): 762-765.

Lim, S. D., H. Y. Cho, Y. C. Park, D. J. Ham, J. K. Lee and C. S. Jang (2013). "The rice RING finger E3 ligase, OsHCI1, drives nuclear export of multiple substrate proteins and its heterogeneous overexpression enhances acquired thermotolerance." J Exp Bot **64**(10): 2899-2914.

Liu, J., S. Vasudevan and E. T. Kipreos (2004). "CUL-2 and ZYG-11 promote meiotic anaphase II and the proper placement of the anterior-posterior axis in C. elegans." Development **131**(15): 3513-3525.

Locke, M., C. L. Tinsley, M. A. Benson and D. J. Blake (2009). "TRIM32 is an E3 ubiquitin ligase for dysbindin." Hum Mol Genet **18**(13): 2344-2358.

Lorick, K. L., J. P. Jensen, S. Fang, A. M. Ong, S. Hatakeyama and A. M. Weissman (1999). "RING fingers mediate ubiquitin-conjugating enzyme (E2)-dependent ubiquitination." Proc Natl Acad Sci U S A **96**(20): 11364-11369.

Lund, E., M. Liu, R. S. Hartley, M. D. Sheets and J. E. Dahlberg (2009). "Deadenylation of maternal mRNAs mediated by miR-427 in Xenopus laevis embryos." RNA **15**(12): 2351-2363.

Macdonald, L. D., A. Knox and D. Hansen (2008). "Proteasomal regulation of the proliferation vs. meiotic entry decision in the Caenorhabditis elegans germ line." Genetics **180**(2): 905-920.

Magnusdottir, E. and M. A. Surani (2014). "How to make a primordial germ cell." Development **141**(2): 245-252.

Mainpal, R., J. Nance and J. L. Yanowitz (2015). "A germ cell determinant reveals parallel pathways for germ line development in Caenorhabditis elegans." Development **142**(20): 3571-3582.

Marlow, F. (2015). "Primordial Germ Cell Specification and Migration." F1000Res **4**.

McIntyre, D. C. and J. Nance (2020). "Niche Cell Wrapping Ensures Primordial Germ Cell Quiescence and Protection from Intercellular Cannibalism." Curr Biol **30**(4): 708-714 e704.

Mello, C. C., B. W. Draper, M. Krause, H. Weintraub and J. R. Priess (1992). "The pie-1 and mex-1 genes and maternal control of blastomere identity in early C. elegans embryos." Cell **70**(1): 163-176.

Mello, C. C., C. Schubert, B. Draper, W. Zhang, R. Lobel and J. R. Priess (1996). "The PIE-1 protein and germline specification in C. elegans embryos." Nature **382**(6593): 710-712.

Merlet, J., J. Burger, N. Tavernier, B. Richaudeau, J. E. Gomes and L. Pintard (2010). "The CRL2LRR-1 ubiquitin ligase regulates cell cycle progression during C. elegans development." Development **137**(22): 3857-3866.

Merritt, C., D. Rasoloson, D. Ko and G. Seydoux (2008). "3' UTRs are the primary regulators of gene expression in the C. elegans germline." Curr Biol **18**(19): 1476-1482.

Metzger, M. B., V. A. Hristova and A. M. Weissman (2012). "HECT and RING finger families of E3 ubiquitin ligases at a glance." J Cell Sci **125**(Pt 3): 531-537.

Metzger, M. B., J. N. Pruneda, R. E. Klevit and A. M. Weissman (2014). "RING-type E3 ligases: master manipulators of E2 ubiquitin-conjugating enzymes and ubiquitination." Biochim Biophys Acta **1843**(1): 47-60.

Millonigg, S., R. Minasaki, M. Nousch, J. Novak and C. R. Eckmann (2014). "GLD-4-mediated translational activation regulates the size of the proliferative germ cell pool in the adult C. elegans germ line." PLoS Genet **10**(9): e1004647.

Mische, C. C., H. Javanbakht, B. Song, F. Diaz-Griffero, M. Stremlau, B. Strack, Z. Si and J. Sodroski (2005). "Retroviral restriction factor TRIM5alpha is a trimer." J Virol **79**(22): 14446-14450.

Miwa, T., K. Inoue and H. Sakamoto (2019). "MRG-1 is required for both chromatin-based transcriptional silencing and genomic integrity of primordial germ cells in Caenorhabditis elegans." Genes Cells **24**(5): 377-389.

Mokhonova, E. I., N. K. Avliyakulov, I. Kramerova, E. Kudryashova, M. J. Haykinson and M. J. Spencer (2015). "The E3 ubiquitin ligase TRIM32 regulates myoblast proliferation by controlling turnover of NDRG2." Hum Mol Genet **24**(10): 2873-2883.

Moore, L. A., H. T. Broihier, M. Van Doren, L. B. Lunsford and R. Lehmann (1998). "Identification of genes controlling germ cell migration and embryonic gonad formation in Drosophila." Development **125**(4): 667-678.

Moore, R. and L. Boyd (2004). "Analysis of RING finger genes required for embryogenesis in C. elegans." Genesis **38**(1): 1-12.

Morgan, M., Y. Kabayama, C. Much, I. Ivanova, M. Di Giacomo, T. Auchynnikava, J. M. Monahan, D. M. Vitsios, L. Vasiliauskaite, S. Comazzetto, J. Rappsilber, R. C. Allshire, B. T. Porse, A. J. Enright and D. O'Carroll (2019). "A programmed wave of uridylation-primed mRNA degradation is essential for meiotic progression and mammalian spermatogenesis." Cell Res **29**(3): 221-232.

Morgan, M., C. Much, M. DiGiacomo, C. Azzi, I. Ivanova, D. M. Vitsios, J. Pistolic, P. Collier, P. N. Moreira, V. Benes, A. J. Enright and D. O'Carroll (2017). "mRNA 3' uridylation and poly(A) tail length sculpt the mammalian maternal transcriptome." Nature **548**(7667): 347-351.

Munemitsu, S., I. Albert, B. Souza, B. Rubinfeld and P. Polakis (1995). "Regulation of intracellular beta-catenin levels by the adenomatous polyposis coli (APC) tumor-suppressor protein." Proc Natl Acad Sci U S A **92**(7): 3046-3050.

Nakamura, A. and G. Seydoux (2008). "Less is more: specification of the germline by transcriptional repression." Development **135**(23): 3817-3827.

Nakanishi, T., H. Kubota, N. Ishibashi, S. Kumagai, H. Watanabe, M. Yamashita, S. Kashiwabara, K. Miyado and T. Baba (2006). "Possible role of mouse poly(A) polymerase mGLD-2 during oocyte maturation." Developmental biology **289**(1): 115-126.

Nakatogawa, H. (2007). "[Mechanisms of membrane biogenesis in autophagy]." Seikagaku **79**(11): 1065-1068.

Nakatogawa, H., Y. Ichimura and Y. Ohsumi (2007). "Atg8, a ubiquitin-like protein required for autophagosome formation, mediates membrane tethering and hemifusion." Cell **130**(1): 165-178.

Nakel, K., F. Bonneau, C. R. Eckmann and E. Conti (2015). "Structural basis for the activation of the C. elegans noncanonical cytoplasmic poly(A)-polymerase GLD-2 by GLD-3." Proc Natl Acad Sci U S A **112**(28): 8614-8619.

Napolitano, L. M. and G. Meroni (2012). "TRIM family: Pleiotropy and diversification through homomultimer and heteromultimer formation." IUBMB Life **64**(1): 64-71.

Navarro, R. E., E. Y. Shim, Y. Kohara, A. Singson and T. K. Blackwell (2001). "cgh-1, a conserved predicted RNA helicase required for gametogenesis and protection from physiological germline apoptosis in C. elegans." Development **128**(17): 3221-3232.

Neumuller, R. A., J. Betschinger, A. Fischer, N. Bushati, I. Poernbacher, K. Mechtler, S. M. Cohen and J. A. Knoblich (2008). "Mei-P26 regulates microRNAs and cell growth in the Drosophila ovarian stem cell lineage." Nature **454**(7201): 241-245.

Niemeyer, M., E. Moreno Castillo, C. H. Ihling, C. Iacobucci, V. Wilde, A. Hellmuth, W. Hoehenwarter, S. L. Samodelov, M. D. Zurbriggen, P. L. Kastritis, A. Sinz and L. I. A. Calderon Villalobos (2020). "Flexibility of intrinsically disordered degrons in AUX/IAA proteins reinforces auxin co-receptor assemblies." Nat Commun **11**(1): 2277.

Nigon, V. M. and M. A. Felix (2017). "History of research on C. elegans and other free-living nematodes as model organisms." WormBook **2017**: 1-84.

Nishida, K. M., K. Saito, T. Mori, Y. Kawamura, T. Nagami-Okada, S. Inagaki, H. Siomi and M. C. Siomi (2007). "Gene silencing mechanisms mediated by Aubergine piRNA complexes in Drosophila male gonad." RNA **13**(11): 1911-1922.

Nousch, M., R. Minasaki and C. R. Eckmann (2017). "Polyadenylation is the key aspect of GLD-2 function in C. elegans." RNA **23**(8): 1180-1187.

Nousch, M., N. Techritz, D. Hampel, S. Millonigg and C. R. Eckmann (2013). "The Ccr4-Not deadenylase complex constitutes the main poly(A) removal activity in C. elegans." J Cell Sci **126**(Pt 18): 4274-4285.

Nousch, M., A. Yeroslaviz, B. Habermann and C. R. Eckmann (2014). "The cytoplasmic poly(A) polymerases GLD-2 and GLD-4 promote general gene expression via distinct mechanisms." Nucleic Acids Res **42**(18): 11622-11633.

Orsborn, A. M., W. Li, T. J. McEwen, T. Mizuno, E. Kuzmin, K. Matsumoto and K. L. Bennett (2007). "GLH-1, the C. elegans P granule protein, is controlled by the JNK KGB-1 and by the COP9 subunit CSN-5." Development **134**(18): 3383-3392.

Ortiz, M. A., D. Noble, E. P. Sorokin and J. Kimble (2014). "A new dataset of spermatogenic vs. oogenic transcriptomes in the nematode Caenorhabditis elegans." G3 (Bethesda) **4**(9): 1765-1772.

Osborne Nishimura, E., J. C. Zhang, A. D. Werts, B. Goldstein and J. D. Lieb (2015). "Asymmetric transcript discovery by RNA-seq in C. elegans blastomeres identifies neg-1, a gene important for anterior morphogenesis." PLoS Genet **11**(4): e1005117.

Ozato, K., D. M. Shin, T. H. Chang and H. C. Morse, 3rd (2008). "TRIM family proteins and their emerging roles in innate immunity." Nat Rev Immunol **8**(11): 849-860.

Paillard, L., F. Omilli, V. Legagneux, T. Bassez, D. Maniey and H. B. Osborne (1998). "EDEN and EDEN-BP, a cis element and an associated factor that mediate sequence-specific mRNA deadenylation in Xenopus embryos." EMBO J **17**(1): 278-287.

Paix, A., Y. Wang, H. E. Smith, C. Y. Lee, D. Calidas, T. Lu, J. Smith, H. Schmidt, M. W. Krause and G. Seydoux (2014). "Scalable and versatile genome editing using linear DNAs with microhomology to Cas9 Sites in Caenorhabditis elegans." Genetics **198**(4): 1347-1356.

Palmisano, N. J. and A. Melendez (2016). "Detection of Autophagy in Caenorhabditis elegans Using GFP::LGG-1 as an Autophagy Marker." Cold Spring Harb Protoc **2016**(1): pdb prot086496.

Papaevgeniou, N. and N. Chondrogianni (2014). "The ubiquitin proteasome system in Caenorhabditis elegans and its regulation." Redox Biol **2**: 333-347.

Parker, R. and U. Sheth (2007). "P bodies and the control of mRNA translation and degradation." Molecular cell **25**(5): 635-646.

Passmore, L. A. and D. Barford (2004). "Getting into position: the catalytic mechanisms of protein ubiquitylation." Biochem J **379**(Pt 3): 513-525.

Paulsen, J. E., E. E. Capowski and S. Strome (1995). "Phenotypic and molecular analysis of mes-3, a maternal-effect gene required for proliferation and viability of the germ line in C. elegans." Genetics **141**(4): 1383-1398.

Peel, N., M. Dougherty, J. Goeres, Y. Liu and K. F. O'Connell (2012). "The C. elegans F-box proteins LIN-23 and SEL-10 antagonize centrosome duplication by regulating ZYG-1 levels." J Cell Sci **125**(Pt 15): 3535-3544.

Pickart, C. M. (1997). "Targeting of substrates to the 26S proteasome." FASEB J **11**(13): 1055-1066.

Pickart, C. M. and R. E. Cohen (2004). "Proteasomes and their kin: proteases in the machine age." Nat Rev Mol Cell Biol **5**(3): 177-187.

Pintard, L., J. H. Willis, A. Willems, J. L. Johnson, M. Srayko, T. Kurz, S. Glaser, P. E. Mains, M. Tyers, B. Bowerman and M. Peter (2003). "The BTB protein MEL-26 is a substrate-specific adaptor of the CUL-3 ubiquitin-ligase." Nature **425**(6955): 311-316.

Qin, F., Y. Sakuma, L. S. Tran, K. Maruyama, S. Kidokoro, Y. Fujita, M. Fujita, T. Umezawa, Y. Sawano, K. Miyazono, M. Tanokura, K. Shinozaki and K. Yamaguchi-Shinozaki (2008). "Arabidopsis DREB2A-interacting proteins function as RING E3 ligases and negatively regulate plant drought stress-responsive gene expression." Plant Cell **20**(6): 1693-1707.

Raiders, S. A., M. D. Eastwood, M. Bacher and J. R. Priess (2018). "Binucleate germ cells in Caenorhabditis elegans are removed by physiological apoptosis." PLoS Genet **14**(7): e1007417.

Ran, F. A., P. D. Hsu, J. Wright, V. Agarwala, D. A. Scott and F. Zhang (2013). "Genome engineering using the CRISPR-Cas9 system." Nat Protoc **8**(11): 2281-2308.

Reymond, A., G. Meroni, A. Fantozzi, G. Merla, S. Cairo, L. Luzi, D. Riganelli, E. Zanaria, S. Messali, S. Cainarca, A. Guffanti, S. Minucci, P. G. Pelicci and A. Ballabio (2001). "The tripartite motif family identifies cell compartments." EMBO J **20**(9): 2140-2151.

Richardson, B. E. and R. Lehmann (2010). "Mechanisms guiding primordial germ cell migration: strategies from different organisms." Nat Rev Mol Cell Biol **11**(1): 37-49.

Rouget, C., C. Papin, A. Boureux, A. C. Meunier, B. Franco, N. Robine, E. C. Lai, A. Pelisson and M. Simonelig (2010). "Maternal mRNA deadenylation and decay by the piRNA pathway in the early Drosophila embryo." Nature **467**(7319): 1128-1132.

Rouhana, L., L. Wang, N. Buter, J. E. Kwak, C. A. Schiltz, T. Gonzalez, A. E. Kelley, C. F. Landry and M. Wickens (2005). "Vertebrate GLD2 poly(A) polymerases in the germline and the brain." RNA **11**(7): 1117-1130.

Rudolph, T., M. Yonezawa, S. Lein, K. Heidrich, S. Kubicek, C. Schafer, S. Phalke, M. Walther, A. Schmidt, T. Jenuwein and G. Reuter (2007). "Heterochromatin formation in Drosophila is initiated through active removal of H3K4 methylation by the LSD1 homolog SU(VAR)3-3." Mol Cell **26**(1): 103-115.

Rybarska, A., M. Harterink, B. Jedamzik, A. P. Kupinski, M. Schmid and C. R. Eckmann (2009). "GLS-1, a novel P granule component, modulates a network of conserved RNA regulators to influence germ cell fate decisions." PLoS genetics **5**(5): e1000494.

Saitou, M. and M. Yamaji (2012). "Primordial germ cells in mice." Cold Spring Harbor perspectives in biology **4**(11).

Sakaguchi, A., P. Sarkies, M. Simon, A. L. Doebley, L. D. Goldstein, A. Hedges, K. Ikegami, S. M. Alvares, L. Yang, J. R. LaRocque, J. Hall, E. A. Miska and S. Ahmed (2014). "Caenorhabditis elegans RSD-2 and RSD-6 promote germ cell immortality by maintaining small interfering RNA populations." Proc Natl Acad Sci U S A **111**(41): E4323-4331.

Sanchez, J. G., K. Okreglicka, V. Chandrasekaran, J. M. Welker, W. I. Sundquist and O. Pornillos (2014). "The tripartite motif coiled-coil is an elongated antiparallel hairpin dimer." Proc Natl Acad Sci U S A **111**(7): 2494-2499.

Sanchez-Lanzas, R. and J. G. Castano (2014). "Proteins directly interacting with mammalian 20S proteasomal subunits and ubiquitin-independent proteasomal degradation." Biomolecules **4**(4): 1140-1154.

Sangaletti, R. and L. Bianchi (2013). "A method for culturing embryonic C. elegans cells." J Vis Exp(79): e50649.

Santos, A. C. and R. Lehmann (2004). "Germ cell specification and migration in Drosophila and beyond." Curr Biol **14**(14): R578-589.

Saric, T., C. I. Graef and A. L. Goldberg (2004). "Pathway for degradation of peptides generated by proteasomes: a key role for thimet oligopeptidase and other metallopeptidases." J Biol Chem **279**(45): 46723-46732.

Sartain, C. V., J. Cui, R. P. Meisel and M. F. Wolfner (2011). "The poly(A) polymerase GLD2 is required for spermatogenesis in Drosophila melanogaster." Development **138**(8): 1619-1629.

Schaefer, A. M., G. D. Hadwiger and M. L. Nonet (2000). "rpm-1, a conserved neuronal gene that regulates targeting and synaptogenesis in C. elegans." Neuron **26**(2): 345-356.

Schaner, C. E., G. Deshpande, P. D. Schedl and W. G. Kelly (2003). "A conserved chromatin architecture marks and maintains the restricted germ cell lineage in worms and flies." Dev Cell **5**(5): 747-757.

Schierenberg, E. (1988). "Localization and segregation of lineage-specific cleavage potential in embryos of Caenorhabditis elegans." Roux Arch Dev Biol **197**(5): 282-293.

Schisa, J. A. (2019). "Germ Cell Responses to Stress: The Role of RNP Granules." Front Cell Dev Biol **7**: 220.

Schmid, M. (2008). GLD-4, a novel poly(A) polymerase affecting germ cell development in *C. elegans.* Dissertation, Technical University Dresden.

Schmid, M., B. Kuchler and C. R. Eckmann (2009). "Two conserved regulatory cytoplasmic poly(A) polymerases, GLD-4 and GLD-2, regulate meiotic progression in C. elegans." Genes & development **23**(7): 824-836.

Schubert, C. M., R. Lin, C. J. de Vries, R. H. Plasterk and J. R. Priess (2000). "MEX-5 and MEX-6 function to establish soma/germline asymmetry in early C. elegans embryos." Mol Cell **5**(4): 671-682.

Schulz, K. N. and M. M. Harrison (2019). "Mechanisms regulating zygotic genome activation." Nat Rev Genet **20**(4): 221-234.

Schulze, E., M. E. Altmann, I. M. Adham, B. Schulze, S. Frode and W. Engel (2003). "The maintenance of neuromuscular function requires UBC-25 in Caenorhabditis elegans." Biochem Biophys Res Commun **305**(3): 691-699.

Schwamborn, J. C., E. Berezikov and J. A. Knoblich (2009). "The TRIM-NHL protein TRIM32 activates microRNAs and prevents self-renewal in mouse neural progenitors." Cell **136**(5): 913-925.

Sdek, P., H. Ying, D. L. Chang, W. Qiu, H. Zheng, R. Touitou, M. J. Allday and Z. X. Xiao (2005). "MDM2 promotes proteasome-dependent ubiquitin-independent degradation of retinoblastoma protein." Mol Cell **20**(5): 699-708.

Semotok, J. L., R. L. Cooperstock, B. D. Pinder, H. K. Vari, H. D. Lipshitz and C. A. Smibert (2005). "Smaug recruits the CCR4/POP2/NOT deadenylase complex to trigger maternal transcript localization in the early Drosophila embryo." Curr Biol **15**(4): 284-294.

Sengupta, M. S., W. Y. Low, J. R. Patterson, H. M. Kim, A. Traven, T. H. Beilharz, M. P. Colaiacovo, J. A. Schisa and P. R. Boag (2013). "ifet-1 is a broad-scale translational repressor required for normal P granule formation in C. elegans." J Cell Sci **126**(Pt 3): 850-859.

Seshagiri, S. and L. K. Miller (1997). "Caenorhabditis elegans CED-4 stimulates CED-3 processing and CED-3-induced apoptosis." Curr Biol **7**(7): 455-460.

Seydoux, G. (2018). "The P Granules of C. elegans: A Genetic Model for the Study of RNA-Protein Condensates." J Mol Biol **430**(23): 4702-4710.

Seydoux, G. and A. Fire (1994). "Soma-germline asymmetry in the distributions of embryonic RNAs in Caenorhabditis elegans." Development **120**(10): 2823-2834.

Shabek, N., Y. Herman-Bachinsky, S. Buchsbaum, O. Lewinson, M. Haj-Yahya, M. Hejjaoui, H. A. Lashuel, T. Sommer, A. Brik and A. Ciechanover (2012). "The size of the proteasomal substrate determines whether its degradation will be mediated by mono- or polyubiquitylation." Mol Cell **48**(1): 87-97.

Shaul, O. (2017). "How introns enhance gene expression." Int J Biochem Cell Biol **91**(Pt B): 145-155.

Shen, B. and H. M. Goodman (2004). "Uridine addition after microRNA-directed cleavage." Science **306**(5698): 997.

Sheth, U., J. Pitt, S. Dennis and J. R. Priess (2010). "Perinuclear P granules are the principal sites of mRNA export in adult C. elegans germ cells." Development **137**(8): 1305-1314.

Siddiqui, N. U., X. Li, H. Luo, A. Karaiskakis, H. Hou, T. Kislinger, J. T. Westwood, Q. Morris and H. D. Lipshitz (2012). "Genome-wide analysis of the maternal-to-zygotic transition in Drosophila primordial germ cells." Genome Biol **13**(2): R11.

Simmer, F., C. Moorman, A. M. van der Linden, E. Kuijk, P. V. van den Berghe, R. S. Kamath, A. G. Fraser, J. Ahringer and R. H. Plasterk (2003). "Genome-wide RNAi of C. elegans using the hypersensitive rrf-3 strain reveals novel gene functions." PLoS Biol **1**(1): E12.

Simonelig, M. (2012). "Maternal-to-zygotic transition: soma versus germline." Genome biology **13**(2): 145.

Skaar, J. R., J. K. Pagan and M. Pagano (2013). "Mechanisms and function of substrate recruitment by F-box proteins." Nat Rev Mol Cell Biol **14**(6): 369-381.

Smelick, C. and S. Ahmed (2005). "Achieving immortality in the C. elegans germline." Ageing Res Rev **4**(1): 67-82.

Smith, J., D. Calidas, H. Schmidt, T. Lu, D. Rasoloson and G. Seydoux (2016). "Spatial patterning of P granules by RNA-induced phase separation of the intrinsically-disordered protein MEG-3." Elife **5**.

Sonneville, R. and P. Gonczy (2004). "Zyg-11 and cul-2 regulate progression through meiosis II and polarity establishment in C. elegans." Development **131**(15): 3527-3543.

Sparks, A. B., P. J. Morin, B. Vogelstein and K. W. Kinzler (1998). "Mutational analysis of the APC/beta-catenin/Tcf pathway in colorectal cancer." Cancer Res **58**(6): 1130-1134.

Sparrer, K. M. J., S. Gableske, M. A. Zurenski, Z. M. Parker, F. Full, G. J. Baumgart, J. Kato, G. Pacheco-Rodriguez, C. Liang, O. Pornillos, J. Moss, M. Vaughan and M. U. Gack (2017). "TRIM23 mediates virus-induced autophagy via activation of TBK1." Nat Microbiol **2**(11): 1543-1557.

Sparrer, K. M. J. and M. U. Gack (2018). "TRIM proteins: New players in virus-induced autophagy." PLoS Pathog **14**(2): e1006787.

Spector, M. S., S. Desnoyers, D. J. Hoeppner and M. O. Hengartner (1997). "Interaction between the C. elegans cell-death regulators CED-9 and CED-4." Nature **385**(6617): 653-656.

Spencer, W. C., G. Zeller, J. D. Watson, S. R. Henz, K. L. Watkins, R. D. McWhirter, S. Petersen, V. T. Sreedharan, C. Widmer, J. Jo, V. Reinke, L. Petrella, S. Strome, S. E. Von Stetina, M. Katz, S. Shaham, G. Ratsch and D. M. Miller, 3rd (2011). "A spatial and temporal map of C. elegans gene expression." Genome Res **21**(2): 325-341.

Spike, C., N. Meyer, E. Racen, A. Orsborn, J. Kirchner, K. Kuznicki, C. Yee, K. Bennett and S. Strome (2008). "Genetic analysis of the Caenorhabditis elegans GLH family of P-granule proteins." Genetics **178**(4): 1973-1987.

Spike, C. A., D. Coetzee, C. Eichten, X. Wang, D. Hansen and D. Greenstein (2014). "The TRIM-NHL protein LIN-41 and the OMA RNA-binding proteins antagonistically control the prophase-to-metaphase transition and growth of Caenorhabditis elegans oocytes." Genetics **198**(4): 1535-1558.

Spracklin, G., B. Fields, G. Wan, D. Becker, A. Wallig, A. Shukla and S. Kennedy (2017). "The RNAi Inheritance Machinery of Caenorhabditis elegans." Genetics **206**(3): 1403-1416.

Starostina, N. G., J. M. Lim, M. Schvarzstein, L. Wells, A. M. Spence and E. T. Kipreos (2007). "A CUL-2 ubiquitin ligase containing three FEM proteins degrades TRA-1 to regulate C. elegans sex determination." Dev Cell **13**(1): 127-139.

Starostina, N. G., J. M. Simpliciano, M. A. McGuirk and E. T. Kipreos (2010). "CRL2(LRR-1) targets a CDK inhibitor for cell cycle control in C. elegans and actin-based motility regulation in human cells." Dev Cell **19**(5): 753-764.

Starz-Gaiano, M. and R. Lehmann (2001). "Moving towards the next generation." Mech Dev **105**(1-2): 5-18.

Streich, F. C., Jr., V. P. Ronchi, J. P. Connick and A. L. Haas (2013). "Tripartite motif ligases catalyze polyubiquitin chain formation through a cooperative allosteric mechanism." J Biol Chem **288**(12): 8209-8221.

Strome, S., J. Powers, M. Dunn, K. Reese, C. J. Malone, J. White, G. Seydoux and W. Saxton (2001). "Spindle dynamics and the role of gamma-tubulin in early Caenorhabditis elegans embryos." Mol Biol Cell **12**(6): 1751-1764.

Strome, S. and D. Updike (2015). "Specifying and protecting germ cell fate." Nat Rev Mol Cell Biol **16**(7): 406-416.

Strome, S. and W. B. Wood (1982). "Immunofluorescence visualization of germ-line-specific cytoplasmic granules in embryos, larvae, and adults of Caenorhabditis elegans." Proc Natl Acad Sci U S A **79**(5): 1558-1562.

Subramaniam, K. and G. Seydoux (1999). "nos-1 and nos-2, two genes related to Drosophila nanos, regulate primordial germ cell development and survival in Caenorhabditis elegans." Development **126**(21): 4861-4871.

Suh, N., B. Jedamzik, C. R. Eckmann, M. Wickens and J. Kimble (2006). "The GLD-2 poly(A) polymerase activates gld-1 mRNA in the Caenorhabditis elegans germ line." Proc Natl Acad Sci U S A **103**(41): 15108-15112.

Sulston, J. E., E. Schierenberg, J. G. White and J. N. Thomson (1983). "The embryonic cell lineage of the nematode Caenorhabditis elegans." Developmental biology **100**(1): 64-119.

Suskiewicz, M. J., J. L. Sussman, I. Silman and Y. Shaul (2011). "Context-dependent resistance to proteolysis of intrinsically disordered proteins." Protein Sci **20**(8): 1285-1297.

Suzuki, A., K. Igarashi, K. Aisaki, J. Kanno and Y. Saga (2010). "NANOS2 interacts with the CCR4-NOT deadenylation complex and leads to suppression of specific RNAs." Proc Natl Acad Sci U S A **107**(8): 3594-3599.

Svendsen, J. M., K. J. Reed, T. Vijayasarathy, B. E. Montgomery, R. M. Tucci, K. C. Brown, T. N. Marks, D. A. H. Nguyen, C. M. Phillips and T. A. Montgomery (2019). "henn-1/HEN1 Promotes Germline Immortality in Caenorhabditis elegans." Cell Rep **29**(10): 3187-3199 e3184.

Tabara, H., R. J. Hill, C. C. Mello, J. R. Priess and Y. Kohara (1999). "pos-1 encodes a cytoplasmic zinc-finger protein essential for germline specification in C. elegans." Development **126**(1): 1-11.

Tadros, W., A. L. Goldman, T. Babak, F. Menzies, L. Vardy, T. Orr-Weaver, T. R. Hughes, J. T. Westwood, C. A. Smibert and H. D. Lipshitz (2007). "SMAUG is a major regulator of maternal mRNA destabilization in Drosophila and its translation is activated by the PAN GU kinase." Dev Cell **12**(1): 143-155.

Tadros, W., S. A. Houston, A. Bashirullah, R. L. Cooperstock, J. L. Semotok, B. H. Reed and H. D. Lipshitz (2003). "Regulation of maternal transcript destabilization during egg activation in Drosophila." Genetics **164**(3): 989-1001.

Tadros, W. and H. D. Lipshitz (2009). "The maternal-to-zygotic transition: a play in two acts." Development **136**(18): 3033-3042.

Takahashi, M., H. Iwasaki, H. Inoue and K. Takahashi (2002). "Reverse genetic analysis of the Caenorhabditis elegans 26S proteasome subunits by RNA interference." Biol Chem **383**(7-8): 1263-1266.

Takasaki, T., Z. Liu, Y. Habara, K. Nishiwaki, J. Nakayama, K. Inoue, H. Sakamoto and S. Strome (2007). "MRG-1, an autosome-associated protein, silences X-linked genes and protects germline immortality in Caenorhabditis elegans." Development **134**(4): 757-767.

Thomsen, S., S. Anders, S. C. Janga, W. Huber and C. R. Alonso (2010). "Genome-wide analysis of mRNA decay patterns during early Drosophila development." Genome Biol **11**(9): R93.

Thornton, J. E., P. Du, L. Jing, L. Sjekloca, S. Lin, E. Grossi, P. Sliz, L. I. Zon and R. I. Gregory (2014). "Selective microRNA uridylation by Zcchc6 (TUT7) and Zcchc11 (TUT4)." Nucleic Acids Res **42**(18): 11777-11791.

Thrower, J. S., L. Hoffman, M. Rechsteiner and C. M. Pickart (2000). "Recognition of the polyubiquitin proteolytic signal." EMBO J **19**(1): 94-102.

Tocchini, C., J. J. Keusch, S. B. Miller, S. Finger, H. Gut, M. B. Stadler and R. Ciosk (2014). "The TRIM-NHL protein LIN-41 controls the onset of developmental plasticity in Caenorhabditis elegans." PLoS Genet **10**(8): e1004533.

Tofaris, G. K., R. Layfield and M. G. Spillantini (2001). "alpha-synuclein metabolism and aggregation is linked to ubiquitin-independent degradation by the proteasome." FEBS Lett **509**(1): 22-26.

Tsuda, M., Y. Sasaoka, M. Kiso, K. Abe, S. Haraguchi, S. Kobayashi and Y. Saga (2003). "Conserved role of nanos proteins in germ cell development." Science **301**(5637): 1239-1241.

Tsvetkov, P., N. Reuven and Y. Shaul (2010). "Ubiquitin-independent p53 proteasomal degradation." Cell Death Differ **17**(1): 103-108.

Updike, D. L., A. K. Knutson, T. A. Egelhofer, A. C. Campbell and S. Strome (2014). "Germ-granule components prevent somatic development in the C. elegans germline." Curr Biol **24**(9): 970-975.

Valencia-Sanchez, M. A., J. Liu, G. J. Hannon and R. Parker (2006). "Control of translation and mRNA degradation by miRNAs and siRNAs." Genes Dev **20**(5): 515-524.

van Gent, M., K. M. J. Sparrer and M. U. Gack (2018). "TRIM Proteins and Their Roles in Antiviral Host Defenses." Annu Rev Virol **5**(1): 385-405.

Van Roey, K., B. Uyar, R. J. Weatheritt, H. Dinkel, M. Seiler, A. Budd, T. J. Gibson and N. E. Davey (2014). "Short linear motifs: ubiquitous and functionally diverse protein interaction modules directing cell regulation." Chem Rev **114**(13): 6733-6778.

Van Wynsberghe, P. M. and E. M. Maine (2013). "Epigenetic control of germline development." Adv Exp Med Biol **757**: 373-403.

Verdecia, M. A., C. A. Joazeiro, N. J. Wells, J. L. Ferrer, M. E. Bowman, T. Hunter and J. P. Noel (2003). "Conformational flexibility underlies ubiquitin ligation mediated by the WWP1 HECT domain E3 ligase." Mol Cell **11**(1): 249-259.

Vicens, Q., J. S. Kieft and O. S. Rissland (2018). "Revisiting the Closed-Loop Model and the Nature of mRNA 5'-3' Communication." Mol Cell **72**(5): 805-812.

Voronina, E., G. Seydoux, P. Sassone-Corsi and I. Nagamori (2011). "RNA granules in germ cells." Cold Spring Harb Perspect Biol **3**(12).

Wada, K. and T. Kamitani (2006). "Autoantigen Ro52 is an E3 ubiquitin ligase." Biochem Biophys Res Commun **339**(1): 415-421.

Wagner, C. R., L. Kuervers, D. L. Baillie and J. L. Yanowitz (2010). "xnd-1 regulates the global recombination landscape in Caenorhabditis elegans." Nature **467**(7317): 839-843.

Walker, A. K., J. H. Rothman, Y. Shi and T. K. Blackwell (2001). "Distinct requirements for C.elegans TAF(II)s in early embryonic transcription." EMBO J **20**(18): 5269-5279.

Wang, G. and V. Reinke (2008). "A C. elegans Piwi, PRG-1, regulates 21U-RNAs during spermatogenesis." Curr Biol **18**(12): 861-867.

Wang, J. T. and G. Seydoux (2013). "Germ cell specification." Adv Exp Med Biol **757**: 17-39.

Wang, J. T., J. Smith, B. C. Chen, H. Schmidt, D. Rasoloson, A. Paix, B. G. Lambrus, D. Calidas, E. Betzig and G. Seydoux (2014). "Regulation of RNA granule dynamics by phosphorylation of serine-rich, intrinsically disordered proteins in C. elegans." Elife **3**: e04591.

Wang, L., C. R. Eckmann, L. C. Kadyk, M. Wickens and J. Kimble (2002). "A regulatory cytoplasmic poly(A) polymerase in Caenorhabditis elegans." Nature **419**(6904): 312-316.

Ward, C. L., S. Omura and R. R. Kopito (1995). "Degradation of CFTR by the ubiquitin-proteasome pathway." Cell **83**(1): 121-127.

Warrior, R. (1994). "Primordial germ cell migration and the assembly of the Drosophila embryonic gonad." Dev Biol **166**(1): 180-194.

Watanabe, M. and S. Hatakeyama (2017). "TRIM proteins and diseases." J Biochem **161**(2): 135-144.

Weber, J., S. Polo and E. Maspero (2019). "HECT E3 Ligases: A Tale With Multiple Facets." Front Physiol **10**: 370.

Weidinger, G., U. Wolke, M. Koprunner, C. Thisse, B. Thisse and E. Raz (2002). "Regulation of zebrafish primordial germ cell migration by attraction towards an intermediate target." Development **129**(1): 25-36.

Weidmann, C. A., C. Qiu, R. M. Arvola, T. F. Lou, J. Killingsworth, Z. T. Campbell, T. M. Tanaka Hall and A. C. Goldstrohm (2016). "Drosophila Nanos acts as a molecular clamp that modulates the RNA-binding and repression activities of Pumilio." Elife **5**.

Weiser, N. E. and J. K. Kim (2019). "Multigenerational Regulation of the Caenorhabditis elegans Chromatin Landscape by Germline Small RNAs." Annu Rev Genet **53**: 289-311.

Westbrook, A. M. and J. B. Lucks (2017). "Achieving large dynamic range control of gene expression with a compact RNA transcription-translation regulator." Nucleic Acids Res **45**(9): 5614-5624.

Whittle, C. A. and C. G. Extavour (2017). "Causes and evolutionary consequences of primordial germ-cell specification mode in metazoans." Proc Natl Acad Sci U S A **114**(23): 5784-5791.

Woodhouse, R. M., G. Buchmann, M. Hoe, D. J. Harney, J. K. K. Low, M. Larance, P. R. Boag and A. Ashe (2018). "Chromatin Modifiers SET-25 and SET-32 Are Required for Establishment but Not Long-Term Maintenance of Transgenerational Epigenetic Inheritance." Cell Rep **25**(8): 2259-2272 e2255.

Xu, L., Y. Wei, J. Reboul, P. Vaglio, T. H. Shin, M. Vidal, S. J. Elledge and J. W. Harper (2003). "BTB proteins are substrate-specific adaptors in an SCF-like modular ubiquitin ligase containing CUL-3." Nature **425**(6955): 316-321.

Yang, Y., S. Fang, J. P. Jensen, A. M. Weissman and J. D. Ashwell (2000). "Ubiquitin protein ligase activity of IAPs and their degradation in proteasomes in response to apoptotic stimuli." Science **288**(5467): 874-877.

Yanowitz, J. L. (2008). "Genome integrity is regulated by the Caenorhabditis elegans Rad51D homolog rfs-1." Genetics **179**(1): 249-262.

Yi, Y. H., T. H. Ma, L. W. Lee, P. T. Chiou, P. H. Chen, C. M. Lee, Y. D. Chu, H. Yu, K. C. Hsiung, Y. T. Tsai, C. C. Lee, Y. S. Chang, S. P. Chan, B. C. Tan and S. J. Lo (2015). "A Genetic Cascade of let-7-ncl-1-fib-1 Modulates Nucleolar Size and rRNA Pool in Caenorhabditis elegans." PLoS Genet **11**(10): e1005580.

Ying, M., X. Huang, H. Zhao, Y. Wu, F. Wan, C. Huang and K. Jie (2011). "Comprehensively surveying structure and function of RING domains from Drosophila melanogaster." PLoS One **6**(9): e23863.

Yoshida, T., Y. Sakuma, D. Todaka, K. Maruyama, F. Qin, J. Mizoi, S. Kidokoro, Y. Fujita, K. Shinozaki and K. Yamaguchi-Shinozaki (2008). "Functional analysis of an Arabidopsis heat-shock transcription factor HsfA3 in the transcriptional cascade downstream of the DREB2A stress-regulatory system." Biochem Biophys Res Commun **368**(3): 515-521.

Yudina, Z., A. Roa, R. Johnson, N. Biris, D. A. de Souza Aranha Vieira, V. Tsiperson, N. Reszka, A. B. Taylor, P. J. Hart, B. Demeler, F. Diaz-Griffero and D. N. Ivanov (2015). "RING Dimerization Links Higher-Order Assembly of TRIM5alpha to Synthesis of K63-Linked Polyubiquitin." Cell Rep **12**(5): 788-797.

Zeiser, E., C. Frokjaer-Jensen, E. Jorgensen and J. Ahringer (2011). "MosSCI and gateway compatible plasmid toolkit for constitutive and inducible expression of transgenes in the C. elegans germline." PLoS One **6**(5): e20082.

Zhang, Y., L. Yan, Z. Zhou, P. Yang, E. Tian, K. Zhang, Y. Zhao, Z. Li, B. Song, J. Han, L. Miao and H. Zhang (2009). "SEPA-1 mediates the specific recognition and degradation of P granule components by autophagy in C. elegans." Cell **136**(2): 308-321.

Zhao, B. S., X. Wang, A. V. Beadell, Z. Lu, H. Shi, A. Kuuspalu, R. K. Ho and C. He (2017). "m(6)A-dependent maternal mRNA clearance facilitates zebrafish maternal-to-zygotic transition." Nature **542**(7642): 475-478.

7. Appendix

7.1. List of primary antibodies used for immunodetection

Antibody[1]	Species	Dilution[2]	Reference
αGRIF-1 (mAb CU35)	mouse	Sup. 1:20	This study
αGRIF-1 (mAb CV44)	mouse	Sup. 1:20	This study
αGRIF-1 (mAb CV85)	mouse	Sup. 1:20	This study
αGRIF-1 (mAb CV24)*	mouse	Sup. 1:20	This study
αGRIF-1 (mAb CU33)*	mouse	Sup. 1:20	This study
αGRIF-1 (mAb CV26)*	mouse	Sup. 1:20	This study
αGRIF-1 (mAb CV28)*	mouse	Sup. 1:20	This study
αGRIF-1 (mAb CV30)*	mouse	Sup. 1:20	This study
αGRIF-1 (mAb CV31)*	mouse	Sup. 1:20	This study
αCCF-1 (G25-1)	mouse	1:1000	Nousch, Techritz et al. 2013
αCCR-4 (B55-1)	mouse	1:1000	Nousch, Techritz et al. 2013
αLAF-1 (BW-75)	mouse	1:1000	Eckmannlab
αGLD-2 (A4-4)	mouse	1:1000	Millonigg, Minasaki et al. 2014
αGLD-3 (A23-1)	mouse	1:1000	Eckmannlab
αLexA (2-12)	mouse	1:2000	Santa Cruz, #Sc-7544
αHA	mouse	1.1000	Developmental studies Hybridoma bank
αDYN-1(dynamin)	mouse	1:1000	Developmental studies Hybridoma bank
αtubulin (B-5-1-2)	mouse	1:50000	Sigma-Adrich, Cat. #T5168
αNOS-3 (6DE5)	rabbit	1:2000	Eckmannlab
αPIE-1	goat	1:1000	Santa Cruz, (cN19): sc-9245

1) * - in western blot, antibody recognizes recombinant GRIF-1 but not GRIF-1 from worm

2) Sup- supernatant of hybridoma cell culture

7.2. List of primers used in this study

Application	gene or allele	CE number	Sequence (5' – 3')	For/Rev	Inner/outer
Genotyping					
	grif-1(tm2559)	4605	TGTGTTCGACGTGTCTCCTC	forward	N/A
	grif-1(tm2559)	4569	CCGATCTTCAACGCACCATCTC	reverse	N/A
	grif-1(ef35)	5499	ctaggcctaatctcaattttaactg	forward	N/A
	grif-1(ef35)	5191	ACGGGTGTAAGATCGGAGTG	reverse	N/A
	grif-1(ef36)	5198	TTGAGTCTAATGAAGCAATCCG	forward	N/A
	grif-1(ef36)	4554	ctgattcttgggggtctttagaacaaattg	reverse	N/A
	grif-1(ef38)	5499	ctaggcctaatctcaattttaactg	forward	N/A
	grif-1(ef38)	5191	ACGGGTGTAAGATCGGAGTG	reverse	N/A
	grif-1(ef32)	6548	GGAAGCTTCTTAGTGGCTTATACGTC	forward	N/A
	grif-1(ef32)	6550	GCCTATCTACCTGCCTACAAGGCC	reverse	N/A
	grif-1(ok1610)	4571	TTCTGATCCTCCCCCTTCTT	forward	outer
	grif-1(ok1610)	4572	AAAACTGGCGGTATTGATGC	reverse	outer
	grif-1(ok1610)	4567	ATGCTCATCCCACTGAACTC	forward	inner
	grif-1(ok1610)	4568	AAATAGTAGGCGACGGAGTTG	reverse	inner
	gld-2(q497)	1956	aagtcatcttgccgagctgt	forward	outer
	gld-2(q497)	46	TGGACGAACctcgagTGCAGCCCTTTC	reverse	outer
	gld-2(q497)	72	CTTCTTTCggatccACTCTCTAGGATGG	forward	inner
	gld-2(q497)	47	CGAATCGAGATGGCctcgagATCATAATTG	reverse	inner
	nos-1(gv5)	5880	ATGTTGATTTTCAGGACTTCTCC	forward	N/A
	nos-1(gv5)	5883	caacatgtcaacagtgttcgc	reverse	N/A
	nos-2(ax2033)	5876	AGAGTTCAACCAGCTCGAAAC	forward	N/A
	nos-2(ax2033)	5878	AAGTGATGGATCCGATGGATC	reverse	N/A
	nos-2(ax2049)	5876	AGAGTTCAACCAGCTCGAAAC	forward	N/A
	nos-2(ax2049)	5878	AAGTGATGGATCCGATGGATC	reverse	N/A
	parn-1(tm869)	3286	AAACTTCCTGGATGCTGCAGG	forward	N/A
	parn-1(tm869)	3287	TCTTCGAGTGGGTTCATCCATG	reverse	N/A
	ccr-4(tm1312)	1313	GTCGCTTTCTGTGAGCGGTC	forward	outer
	ccr-4(tm1312)	1314	GCTACATGTGGATGAGGGAA	reverse	outer
	ccr-4(tm1312)	1315	GGGGACGACGACATCTCTG	forward	inner
	ccr-4(tm1312)	1316	CCACTGTGGGTCAAATGGTC	reverse	inner
	ced-3(n717)	1016	TCTTGGATTCTGTCGACGGAG	forward	N/A
	ced-3(n717)	1017	TGTCTGAAATCCACAAGCGACC	reverse	N/A
	ced-4(n1162)	1019	TCCACGACTTTGAACCACGTG	forward	N/A
	ced-4(n1162)	1020	ACTGATTTTCCGGATCCAGCTC	reverse	N/A
	fog-1(q785)	5281	GCGGATTTTTAAATTTTTCG	forward	N/A
	fog-1(q785)	5282	AAACTTCGGAACGAGAAATG	reverse	N/A
	pup-1/-2(om129)	6050	gagcgtgatatgacaatggaag	forward	N/A
	pup-1/-2(om129)	6052	ctcctggataccgttcttcg	reverse	N/A
	MosSCI	3376	ccagctttcttgtacaaagtgg	forward	outer
	MosSCI	2640	cgtgttctcccattcttcac	forward	outer
	MosSCI	2634	atcgggaggcgaacctaactg	reverse	inner
	MosSCI	4314	ataattcactggccgtcgttttaca	reverse	inner
RNAi clones					
	grif-1	4249	atatccatggctTACAGTTTCAAAAGCAGCACCGA	forward	N/A
	grif-1	4250	atatctcgagAAATTGGTGCTCAAAATAGTAGGC	reverse	N/A
	nos-2	5771	cgatgaattcgagctccaccgCCGACTTCGACTCTCGAATC	forward	N/A
	nos-2	5772	cctcgaggtcgacggtatcgcttCTAGAAAGAATCTTCGGATG	reverse	N/A
Gateway construct					
	grif-1 short 3'UTR	5065	ggggacagctttcttgtacaaagtggCACCATTCGACAACTCCG	forward	N/A
	grif-1 short 3'UTR	5066	ggggacaactttgtataataaagttgCGATCTCAATTTCACTTCCG	reverse	N/A
	grif-1 long 3'UTR	5065	ggggacagctttcttgtacaaagtggCACCATTCGACAACTCCG	forward	N/A
	grif-1 long 3'UTR	5067	ggggacaactttgtataataaagttgCTTGAAACTCCTCTAAAATGG	reverse	N/A
	grif-1(WT) ectopic expression	5059	ggggacaagtttgtacaaaaaagcaggctggATGTACAGTTTCAAAAGCAGCACC	forward	N/A
	grif-1(WT) ectopic expression	5072	ggggaccactttgtacaagaaagctgggtgTCAAAATTGGTGCTCAAAATAGTAGG	reverse	N/A
	grif-1C43A) ectopic exp.	5731	GCCGAGAGATGCATCGGTTTGCTCG	forward	N/A
	grif-1C43A) ectopic exp.	5733	GACCGTGTGGGCACATTGCAG	reverse	N/A
	gld-2 aa1-1113 (FL)	5478	ggggacaagtttgtacaaaaaagcaggctggATGGTTATGGCTCAACAGCAGAAAAATG	forward	N/A
	gld-2 aa1-1113 (FL)	5477	ggggaccactttgtacaagaaagctgggtgTCATTGAGATACATTTGATGATGCCATC	reverse	N/A
	gld-2 aa198-1113	5473	ggggacaagtttgtacaaaaaagcaggctggATGAATCATGATCCTAAAATTCATTTGTAC	forward	N/A
	gld-2 aa198-1113	5477	ggggaccactttgtacaagaaagctgggtgTCATTGAGATACATTTGATGATGCCATC	reverse	N/A
	gld-2 aa267-1113	5474	ggggacaagtttgtacaaaaaagcaggctggATGCCAGCCTCAATAGAGCTCC	forward	N/A
	gld-2 aa267-1113	5477	ggggaccactttgtacaagaaagctgggtgTCATTGAGATACATTTGATGATGCCATC	reverse	N/A
qPCR					
	oma-1	2757	GCGGCTAAATTGCCACTAGG	forward	N/A
	oma-1	2759	AGCGAGACGGTGGATAGGTC	reverse	N/A
	cpb-3	1890	CATTTCGCAACCTCAGCAAC	forward	N/A
	cpb-3	1891	cagaactacgagcgacggaac	reverse	N/A
	fbxc-50	1947	CAAGTGTTCGCGTTGTCTGAG	forward	N/A
	fbxc-50	1948	TTTCTCGGGGCTCTTCTTTTC	reverse	N/A
	spn-4	5858	ACAGTGCGAATCCTTCCAAC	forward	N/A
	spn-4	5859	TCACGAAACGAGAAGGGAAT	reverse	N/A
	gld-3s	5385	GCCACATTTTGCACCACCAA	forward	N/A
	gld-3s	5386	CGCACCAAAGGATCCATCGA	reverse	N/A
	gld-3l	5381	CAGCAACATCAGCAAGCTCA	forward	N/A
	gld-3l	5382	CAAATGGCAGAGCAGACACA	reverse	N/A
	gld-1	1892	TGCAGTTCCTCTGCTCTCTCC	forward	N/A
	gld-1	1893	CGTTAGATCCGAGAAGGTTGG	reverse	N/A
	gld-2	1878	GGAGAACGTGGCAAGTACGA	forward	N/A
	gld-2	1879	TTTAGCTGGTTCTGGTGATTGC	reverse	N/A
	tbb-2	3973	CCAACCCAACCTACGGTGAT	forward	N/A
	tbb-2	3974	TGGGAATGGAACCATGTTGA	reverse	N/A
DNA sequencing					
	M13 forward (-20)	N/A	gtaaaacgacggccagt	N/A	N/A
	gld-2	79	GATCCATGTCAGATGAGTTGT	N/A	N/A

7.3. List of strains used in this study and methods by which they were generated

Strain name	Allele/genotype	Methods applied	Reference / source
EV902	*grif-1(ef32)/hT2g I*	CRISPR/Cas9 and Crossing	This study
EV899	*grif-1(ef35)/hT2g I*	CRISPR/Cas9 and Crossing	This study
EV648	*grif-1(tm2559)/hT2g I*	Crossing	This study
EV647	*grif-1(ok1610)/hT2g I*	Crossing	This study
EV896	*grif-1(ok1610ef40)/hT2g I*	CRISPR/Cas9 and Crossing	This study
EV866	*grif-1(ef36) I*	CRISPR/Cas9	This study
EV868	*grif-1(ef38) I*	CRISPR/Cas9	This study
JK2077	*glp-4(bn2ts) I*	N/A	Kimble Lab
JK3743	*fog-1(q785) I*	N/A	Kimble Lab
EV761	*gld-2(q497)/hT2g I*	N/A	Eckmann Lab
JH1270	*nos-1(gv5)*	N/A	Subramaniam and Seydoux 1999
JH3193	*nos-2(ax2049[3XFLAG::nos-2]) II*	N/A	Paix, Wang et al. 2014
JH3180	*nos-2(ax2033) II*	N/A	Paix, Wang et al. 2014
EV1017	*grif-1(ef32)/hT2g I; nos-1(gv5) II*	CRISPR/Cas9 and Crossing	This study
EV1007	*grif-1(ef32)/hT2g I; nos-2(ax2033) II*	CRISPR/Cas9 and Crossing	This study
MT2550	*unc-79(e1068) III; ced-4(n1162) III*	N/A	Eckmann Lab
EV971	*grif-1(ok1610ef40)/hT2g I; ced-4(n1162)/hT2g III*	CRISPR/Cas9 and Crossing	This study
EV448	*parn-1(tm869) V*	N/A	Nousch, Techritz et al. 2013
EV995	*grif-1(ef32)/hT2g I; parn-1(tm869) V*	CRISPR/Cas9 and Crossing	This study
EV960	*ccr-4(tm1312) IV/ nT1g (IV;V)*	N/A	Nousch, Techritz et al. 2013
EV994	*grif-1(ef32)/hT2g I; ccr-4 (tm1312) IV*	CRISPR/Cas9 and Crossing	This study
EL622	*pup-1(tm1021)/qC1 gfp III*	N/A	Li and Maine 2018
EL623	*pup-2(tm4344)/qC1 gfp III*	N/A	Li and Maine 2018
EL602	*pup-1/-2(om129)/qC1 gfp III*	N/A	Li and Maine 2018
EV981/EV982	*efIs207/209[Cbr-unc-119(+) + Pmex-5::GRIF-1 genomic::tbb-2 3UTR] II; unc-119(ed3) III*	MosSCI	This study
EV999/EV1006	*efIs217/218[Cbr-unc-119(+) + Pmex-5::grif-1 C43A genomic::tbb-2 3'UTR] II; unc 119(ed3) III*	MosSCI	This study
EV886/EV887	*gld-2(q497) I; efIs158[Cbr-unc-119(+) + Pmex-5::intronized GLD-2 aa1-1113::gld-2 3UTR] II*	MosSCI and Crossing	This study
EV888/EV889	*gld-2(q497) I; efIs160[Cbr-unc-119(+) + Pmex-5::intronized GLD-2 aa198-1113::gld-2 3UTR] II*	MosSCI and Crossing	This study
EV890/EV891	*gld-2(q497) I; efIs162[Cbr-unc-119(+) + Pmex-5::intronized GLD-2 aa267-1113::gld-2 3UTR] II*	MosSCI and Crossing	This study
EV802	*efIs134[Cbr-unc-119(+) + Pmex-5::PEST::GFP::H2B::grif-1 short 3UTR] II 1A*	MosSCI	This study
EV805	*efIs137[Cbr-unc-119(+) + Pmex-5::PEST::GFP::H2B::grif-1 long 3'UTR] II 2B*		
EV549	*bsIs2(unc-119(+) + pie-1p::GFP::SPD-2); zuIs?(nmy-2::PGL-1::mRFP-1 line 24-1) III*	N/A	Eckmannlab
EV942	*grif-1(ef32)/hT2g I; zuIs(nmy-2::PGL-1::mRFP-1 line 24-1) III*	CRISPR/Cas9 and Crossing	This study
EV943	*grif-1(ok1610ef40)/hT2g I; zuIs(nmy-2::PGL-1::mRFP-1 line 24-1) III*	CRISPR/Cas9 and Crossing	This study
EV1016	*grif-1(ef32)/hT2g I; efIs134[Cbr-unc-119(+) + Pmex-5::PEST::GFP::H2B::grif-1 short 3'UTR] II; zuIs?(nmy-2::PGL-1::mRFP-1 line 24-1) III*	CRISPR/Cas9, MosSCI and Crossing	This study
EV1018	*efIs134[Cbr-unc-119(+) + Pmex-5::PEST::GFP::H2B::grif-1 short 3'UTR] II; unc-119(ed3) III; bsIs2(unc-119(+) + pie-1p::GFP::SPD-2); zuIs?(nmy-2::PGL-1::mRFP-1 line 24-1) III*	CRISPR/Cas9, MosSCI and Crossing	This study
EV1029	*nos-1(gv5) II; efIs134[Cbr-unc-119(+) + Pmex-5::PEST::GFP::H2B::grif-1 short 3'UTR] II; zuIs?(nmy-2::PGL-1::mRFP-1 line 24-1) III*	CRISPR/Cas9, MosSCI and Crossing	This study
EV1020/EV1021	*grif-1(ef32) / hT2g I; efIs215[Cbr-unc-119(+) + Pmex-5::grif-1 genomic::grif-1 3'UTR] II*	CRISPR/Cas9, MosSCI and Crossing	This study
MT1522	*ced-3(n717) IV*	N/A	Eckmann Lab
EV1022	*grif-1(ef32)/hT2g I, ced-3(n717) IV*	CRISPR/Cas9 and Crossing	This study
EV1027/EV1028	*nos-1(gv5) II; pup-1/-2(om129)/qC1 gfp III*	Crossing	This study

N/A- strains were either already generated in our lab or obtained from external sources. External sources include *C. elegans* deletion consortia and other laboratories.

7.4. Identity of sgRNAs and repair templates used to modify *grif-1* locus

sgRNA (Sequence 5'-3')	Single stranded RNA repair template (Sequence 5'-3')	Type of modification	*grif-1* alleles generated
CE04921(dpy10gRNA) (5'-gctaccataggcaccacgag-3')	CE4922(dpy10_HR) (acttcaatacggcaagatgagaatgactggaaaccgtaccgcatgcggtgcctatggtagcggagcttcacatggcttcagaccaac)	dpy-10 - co-CRISPR	N/A
CE4709(fpgrif_sgE) (5'-aagacatatccggcacgacg-3')	CE5505(grf_D/Estop) (caaaagcagcaccgacgtgaagacttatatcagcacaccgtgaagcttcgtgccagatatgtcttgagccatttggttagtgagttttttg)	Stop codon (exon 1)	*ef35, ok1610ef40*
CE04770(fPgrf_sgN) (5'-gctgatataagtcttcacgt-3')	CE05507(grf_N2flag) (ctgtggacaaaaatgtacagtttcaaaagcagcactgacgactataaagatcatgacattgactacaaggatgacgacgacaaggtgaagacttatatcagcaccccgtcgtgccggat)	2xFLAG (exon 1)	*ef38*
CE04771(fpgrf_sgM) (5'-gcgacggagttgtcgaatgg-3')	CE05503(grf_M2flag2) tgccacgtagctcaactccagcgccagcactaccagactataaagatcatgacattgactacaaggatgacgacgacaagttcgacaactccgtcgcctactattttgagcacca	2xFLAG (exon 1)	*ef36*
CE04770(fPgrf_sgN) and CE04771(fpgrf_sgM)	None	Deletion	*ef32*

Desired genomic modifications are colored in red.

7.5. List of antibodies used in Immunofluorescent experiment

Antibody	Species	Dilution	Reference
αGRIF-1 (mAb CU35)	mouse	Sup-1:20, purified-100 ng/µl	This study
αGRIF-1 (333043)	rabbit	Aff. Purified 1:20	This study
αPIE-1	mouse	1.50	Mello, Schubert et al. 1996
αGLD-2 (317)	rat	1:100	Eckmann Lab
αGLD-2 (184)	rabbit	1:100	Nousch, Minasaki et al. 2017
αGLD-3 (a23-1)	mouse	1:100	Eckmannlab
αGLD-3 (237)	rat	1:100	Eckmannlab
αCCF-1 (G25-1)	mouse	1:100	Nousch, Techritz et al. 2013
αCCR-4 (B77-1)	mouse	1:100	Nousch, Techritz et al. 2013
αFLAG (M2)	mouse	1:500	Sigma-Adrich, #F3165
αPOS-1	rat	1:100	Eckmannlab
αPGL-1	guinea pig	1:100	Kawasaki, Shim et al. 1998
αGLH-1/2	guinea pig	1:100	Eckmannlab

Aff. Purified- affinity purified.

Sup- supernatant of hybridoma cell culture.

7.6. List of antibodies used for co-immunoprecipitation (co-IP) experiments

antibody	Application	Reference
moGLD-2 (A4-4)	GLD-2 pulldown	Millonigg, Minasaki et al. 2014
moRFP (125B42-4)	Background control	Developmental studies Hybridoma bank
moHA	Background control	Developmental studies Hybridoma bank
moGRIF-1 (mAb CU33, mAb CU35, mAb CV31, mAb CV44)	GRIF-1 pulldown	This study

8. Acknowledgement

First and foremost, I would like to say a huge thank you to Prof. Christian R. Eckmann for giving me the opportunity to undertake this project in his laboratory. I highly appreciate his support, supervision, and mentorship. He was always available for discussion about scientific problems and experimental ideas. His availability was really helpful throughout my thesis work. Importantly, he gave me words of encouragements and motivation during rough times. Thank you Christian, I am indebted in gratitude to you.

Special thanks go to my thesis reviewers for taking the time to peruse my thesis.

I wish to thank all members of the Eckmann group for creating conducive research atmosphere and environment. I also want to thank you all for introducing me to worm works, for sharing reagents, protocols, and worm strains when necessary. Particularly, I want to thank Ryuji and Marco for taking time to diligently answer my never-ending questions, especially in the beginning of my thesis work. Lastly, I wish to say big thank you to Krzysztof, my colleague that became a friend. Your friendship was one of those things that kept me going.

I would like to greatly thank my family and friends, whose encouraging words have always been my support system. Specifically, I thank my parents, Mr and Mrs Oyewale. You are the best parents anyone can ask for. Thanks for your support. To my wife and daughter and son, I say thank you for a loving home. I love you all dearly

9. Eidesstattliche Erklärung

Hiermit erkläre ich, dass ich die vorliegende wissenschaftliche Arbeit selbständig und ohne fremde Hilfe verfasst habe. Ich erkläre weiterhin, dass andere als die von mir angegebene Quellen und Hilfsmittel nicht benutzt und die den benutzten Werken wörtlich oder inhaltlich entnommenen Stellen als solche kenntlich gemacht wurden.

Mit dieser Arbeit bewerbe ich mich erstmals um die Erlangung des Doktorgrades.

Halle (Saale), den ……………….

Tosin Oyewale

10. Curriculum vitae

Personal details

Name:	Tosin Oyewale
Sex:	Male
Date of birth:	12th August 1987
Place of birth:	Odeomu, Osun State, Nigeria
Nationality:	Nigerian

Education

University of Westminster, London. 2012 to 2013

Medical Molecular Biology (MSc)_Distinction Obtained

University of Agriculture, Abeokuta, Nigeria. 2005 to 2010

Biochemistry (BSc)_First Class Obtained

School of Science, Imesi-Ile Osun State, Nigeria. 2001 to 2004

Secondary School Leaving Certificate (8 Distinctions).

Work experience

Research assistant- Since January 2015

Division of Developmental Genetics, Martin Luther University, Halle, Germany.

Junior Research Fellow- August 2011- March 2013.

Department of Biochemistry, University of Agriculture, Abeokuta.

Chemistry Teacher. July 2010 – July 2011

Uzere Senior Secondary school, Uzere, Delta state, Nigeria (National Youth Service)

Scholarships, awards and prizes

- PhD fellowship (GRK 1591) in posttranscription gene expression mechanisms-2014
- The Caparo award for best graduating student in the faculty of Life Sciences, University of Westminster, UK- 2013
- Tertiary Education Trust Fund, Nigeria- Scholarship for postgraduate study in the UK- 2012
- University of Agriculture, Abeokuta- Senate prize for first class student in Biochemistry, College of Natural Sciences- 2008/2009.
- Senator Isiaka Adetunji award for outstanding student from Osun state, Nigeria. 2008

- Professor Ishola Adamson prize for the best Student in Biochemistry with a minimum cGPA of 4.0/5.0 -2008/2009
- Late Dr. Apampa prize for the best graduating student in Biochemistry-2008/2009
- Award of Best Student in Biochemistry from College of Natural Sciences Student Association– 2008/2009.

………………….…………